Complement component 5 (C5)-dependent and -independent susceptibility to eukaryotic pathogens in mouse models

Irena Radovanovic

Department of Biochemistry
McGill University
Montreal, Quebec, Canada

December 2014

A thesis submitted to the Faculty of Graduate Studies and Research in partial fulfillment of the requirements of the degree of Doctor of Philosophy.

ABSTRACT

The complement system is an intricate immune surveillance system that plays an integrative role in host defense and homeostasis. The dominant protective effect of the fifth complement component (C5) was firmly established in the mouse model of disseminated *Candida albicans* infection, where C5 deficiency results in increased mortality and high fungal burden. Using a cohort of 23 inbred mouse strains, we have uncovered several putative genetic associations by GWAS, in addition to *C5*, that control replication of *C. albicans* in the host, and identified two discordant strains, namely AKR/J and SM/J. C5-deficient AKR/J strain displays a reduced fungal burden in target organs and increased survival, concomitant with high levels of serum IFNγ. Subsequent genetic linkage analysis in informative F2 progeny derived from susceptible A/J and resistant AKR/J mice validated loci on chromosome 8 (*Carg3*, *Candida albicans resistance gene 3*; LOD=3.95) and chromosome 11 (*Carg4*; LOD=4.59) as modulating susceptibility to *C. albicans* infection in the context of C5-deficiency. Furthermore, we ascribed the genetic basis of increased susceptibility in C5-sufficient SM/J mice to distal chromosome 15 (*Carg5*; LOD=6.09) by performing genetic linkage analysis in [B6xSM/J]F2 animals fixed for functional C5 alleles. Detailed scrutiny of the innate immune compartment revealed a complex myeloid defect in SM/J mice, regulated in part by *Carg5* and exemplified by decreased Ly6G expression, aberrant reactive oxygen species generation, decreased recruitment of inflammatory monocytes, and increased serum CCL2. Finally, by combining haplotype association mapping in 34 AcB/BcA recombinant congenic strains (RCS) and linkage analysis in informative F2 progeny derived from permissive DBA/2J and restrictive AcB55 strains, we demonstrate that *C5* underlies the *Tccr1* locus on chromosome 2 (*Taenia crassiceps cysticercosis restrictive locus 1*; LOD=4.76) and modulates the outcome to *Taenia crassiceps* infection in mice. Therefore, the work in this thesis *bona fide* identified the complement system in the early protective inflammatory response to infection with diametrically divergent pathogens *C. albicans* and *T. crassiceps*, and uncovered novel C5-independent loci involved in the host response to *C. albicans*.

RÉSUMÉ

Le système du complément est un système de surveillance immunitaire élaboré qui joue un rôle intégrant dans la défense de l'hôte et de l'homéostasie. L'effet dominant protecteur du cinquième composant du complément (C5) a été fermement établi dans le modèle murin d'infection systémique à *Candida albicans*, où le déficit en C5 cause une mortalité accrue et une charge fongique élevée. En utilisant une cohorte de 23 lignées pures de souris, nous avons découvert plusieurs associations génétiques putatives, en plus de *C5*, qui contrôlent la réplication de *C. albicans* dans l'hôte, et identifié deux lignées discordantes, soit AKR/J et SM/J. La lignée C5-déficiante AKR/J affiche une charge fongique réduite dans les organes cibles et une survie améliorée, concomitamment avec des niveaux élevés d'IFNγ dans le sérum. Une analyse de liaison génétique par balayage du génome entier dans la progéniture F2 dérivée de la lignée susceptible A/J et résistante AKR/J a validé les locus sur le chromosome 8 (*Carg3*, *Candida albicans resistance gene 3*; LOD=3.95) et le chromosome 11 (*Carg4*; LOD=4.59) modulant la susceptibilité à l'infection à *C. albicans* dans le contexte de déficit en C5. De plus, nous avons attribué la base génétique de la susceptibilité accrue des souris C5-suffisantes SM/J au segment distal sur le chromosome 15 (*Carg5*; LOD=6.09) en effectuant une analyse de liaison génétique dans les animaux [B6xSM/J]F2 fixés pour les allèles *C5* fonctionnels. Une inspection détaillée du compartiment immunitaire inné a révélé un défaut myéloïde complexe chez la lignée SM/J, régulé en partie par *Carg5* et caractérisé par l'expression abaissée de Ly6G, la production aberrante d'espèces réactives de l'oxygène, le recrutement réduit des monocytes inflammatoires, et les niveaux circulatoires de CCL2 augmentés. Finalement, en combinant la cartographie de l'association des haplotypes dans 34 lignées de souris AcB/BcA recombinantes et l'analyse de liaison génétique dans la progéniture F2 informative dérivée de la lignée permissive DBA/2J et restrictive AcB55, nous avons démontré que *C5* est à la base du locus *Tccr1* (*Taenia crassiceps cysticercosis restrictive locus 1*; LOD=4.76) et module l'issue de l'infection à *Taenia crassiceps* chez la souris. Donc, le travail dans cette thèse met en évidence le besoin commun pour le système du complément dans

la réponse inflammatoire protectrice durant les débuts de l'infection par des pathogènes diamétralement distincts, *C. albicans* et T. *crassiceps*, et dévoile des nouveaux locus indépendants du C5 impliqués dans la réponse de l'hôte à *C. albicans*.

PREFACE

The work described in Chapters 2, 3 and 4 of this thesis have been published as follows:

Chapter 2: Radovanovic I, Mullick A, Gros P. 2011. "Genetic control of susceptibility to infection with *Candida albicans* in mice." *PLoS One*. 6(4): e18957.

Chapter 3: Radovanovic I, Leung V, Iliescu A, Bongfen SE, Mullick A, Langlais D, Gros P. 2014. "Genetic control of susceptibility to *Candida albicans* in SM/J mice." *J Immunol.* 193(3): 1290-1300. Reprinted with permission, © The American Association of Immunologists, 2010.

Chapter 4: Ramirez-Aquino R*, Radovanovic I*, Fortin A, Sciutto-Conde E, Fragoso-Gonzalez G, Gros P, Aguilar-Delfin I. 2011. "Identification of loci controlling restriction of parasite growth in experimental *Taenia crassiceps* cysticercosis." *PLoS Negl Trop Dis*. 5(12): e1435. *Equal authorship.

CONTRIBUTION OF AUTHORS

Chapter 2: The work presented in Chapter 2 is essentially my own, with helpful technical assistance as follows: Zully Leon and I performed the phenotyping of 23 inbred mouse strains together, sacrificing animals, collecting blood, and determining the renal fungal load (Figure 1). I genotyped inbred strains for C5 status and performed the genome-wide association mapping using EMMA (Figures 2 and S1, Tables 1 and S1). I assessed the fungal burden in the heart, kidney, and brain of AKR/J and A/J mice, performed kidney histology, as well as the survival study (Figure 3 and Figure 4C). Zully Leon carried out the additional infection with different doses of *C. albicans*, assessed blood urea nitrogen and cytokine levels (Figure 4A-B and Figure 5). I phenotyped the [AKR/JxA/J] cross, prepared DNA from tail clips, genotyped additional microsatellite markers, and performed linkage analysis (Figures 6 and 7). I also analyzed the published ChIP-Seq dataset for positional candidates underlying *Carg3* and *Carg4* (Tables S2 and S3). I prepared all figures and tables and wrote the initial draft of the manuscript. Dr. Alaka Mullick provided feedback on experimental designs and did a critical reading of the manuscript.

Chapter 3: The work presented in this chapter was mainly performed by myself, in collaboration with our colleagues as follows: I assessed the fungal burden in the heart, kidney and brain of B6 and SM/J mice, and performed kidney histology (Figures 1 and S1). I also phenotyped the [B6xSM/J] cross, prepared DNA from tail clips, genotyped additional markers, and conducted all linkage analyses (Figure 2). Dr. Silayuv Bongfen taught me the flow cytometric procedure, while I carried out detailed immunophenotyping of neutrophils in parental and [B6xSM/J]F2 animals, as well as all functional studies with purified neutrophils (Figures 3, 4, S2, and S3A). Vicki Leung processed kidneys, performed immunofluorescent staining on cryosections, and acquired images (data not shown). I am responsible for immunophenotyping of monocytes and BMDM functional studies (Figures 5 and 6A), whereas Alexandra Iliescu acquired images for BMDM phagocytosis (Figure

5B). I performed the CCL2 ELISAs and the subsequent correlation studies (Figure 6B-D). Dr. David Langlais computed the myeloid inflammatory scores for all candidate genes in the *Carg5* interval (Figure 6E and Table S1) and provided valuable advice. I constructed all figures and wrote the first draft of the manuscript. Dr. Alaka Mullick did a critical reading of the manuscript.

Chapter 4: The studies presented in Chapter 4 have been produced in collaboration with our colleagues as follows: Photographs of *Taenia crassiceps* and infected mice were kindly provided by Dr. Carlos Larralde (Figure 1). Ruben Ramirez-Aquino performed the phenotyping of AcB/BcA recombinant congenic strains, [AcB55xDBA/2] and [AcB55xA/J] crosses (Figures 2, 4A, S2). I conducted the genome-wide association mapping using EMMA (Figures 3 and S1), genotyping of additional markers, all linkage analyses (Figures 4B-C, 5, S3) and tabulation of C5 status in AcB/BcA strains (Table 1). I constructed all figures and tables, and wrote the first draft of the manuscript. Drs. Anny Fortin and Irma Aguilar-Delfin provided extensive feedback on experimental designs and did a critical reading of the manuscript.

My supervisor, Dr Philippe Gros, examined the results, provided crucial guidance and advice throughout all of the abovementioned studies, and edited all final versions of the manuscripts.

TABLE OF CONTENTS

LIST OF FIGURES

Chapter 1

Chapter 2

Chapter 3

Chapter 4

Appendix

LIST OF TABLES

ACKNOWLEDGEMENTS

First and foremost, I would like to thank my supervisor, Philippe Gros, for providing an unprecedented research environment during all these years, and instilling in me a scientific curiosity and perseverance that are critical for my future endeavors. I am most grateful for the creative freedom and independence that I was accorded, allowing me to explore, fail, and succeed. I would like to thank our collaborator Dr. Alaka Mullick for welcoming me to her lab at the BRI on numerous occasions. I would also like to extend my gratitude to the entire group from UNAM (Mexico City), especially Irma Aguilar-Delfin and Ruben Ramirez-Aquino for allowing me to partake on their project and inviting me to Puebla. Over the years, I was fortunate to have crossed path with exceptional individuals, and would like to distinguish several who have left an unforgettable print in my life. Silayuv, thank you for your spirituality, beautiful personality, and for teaching me flow cytometry! Alex and Vicki, I cannot thank you enough for your friendship, encouragements, and laughter! David, an outstanding scientist and mentor, thank you for all your advice and early morning chats! I would like to thank Norm and Sooz, the people that I consider the backbone of the Gros laboratory, for their devoted work throughout these years. To the many past and present members of the Gros lab and the Complex Traits Group, thank you for sharing scientific insight, protocols, and laughs, whether it was for a few weeks or a few years. On the non-scientific side, I want to thank my great friends Marina, Guillermo, and Yibin for uplifting my spirits and keeping me sane! To Pablo, thank you for standing by my side through this roller coaster ride, for sharing my despair and joy, and for always being proud of me! A big thank you to my little sister Bojana, and Niall, for the many wonderful moments shared in the family! Last but not least, I dedicate this thesis to my parents, Nada Stupar and Veliša Radovanović, who left ex-Yugoslavia in 1995 to build a better life for my sister and myself, allowing us to pursue our dreams; for that, I will never be able to thank them enough. Finally, I would like to acknowledge the Team Grant in Fungal Pathogenesis from the Canadian Institutes of Health Research (CIHR) for providing financial support.

OBJECTIVES AND RATIONALE

Invasive candidiasis remains a persistent public health problem associated with high morbidity and mortality, along with considerable economic encumbrance. Difficulties in diagnosis, and thereby delays of suitable antifungal therapy, are known to decrease patient survival (*1*). While the risk factors associated with candidemia and invasive candidiasis are well documented in several epidemiological reports (*2*-*5*), the genetic component of susceptibility to systemic *C. albicans* infection in humans has only recently begun to be elucidated (*6*). Meanwhile, genetic studies in inbred and mutant mouse strains have uncovered an imperative role of the complement system in early innate defenses against systemic *C. albicans* infection (*7*, *8*). The fifth complement component C5, in particular, exerts a dominant protective effect on fungal burden in target organs and overall survival (*7*, *9*, *10*). The notion that host response to *C. albicans* infection is rather complex, entailing the contribution of additional C5-independent genetic modifiers, is advocated by observations in AcB/BcA RCS (*7*) and the uncovering of two *Carg* loci (*11*, *12*). Therefore, work in this thesis aimed to identify and characterize novel host genetic factors modulating response to disseminated *C. albicans* infection, independently of C5.

The objectives of the study presented in Chapter 2 were to phenotype a genetically diversified cohort of inbred mouse strains and uncover novel host genetic loci controlling susceptibility to disseminated *C. albicans* infection. We approached this by conducting GWAS in 23 phylogenetically distinct inbred mouse strains, ultimately discovering several highly significant associations controlling fungal replication in the host, and two previously undisclosed discordant strains: AKR/J (C5-deficient, resistant) and SM/J (C5-sufficient, susceptible). Linkage analysis in the informative [A/JxAKR/J]F2 progeny ascertained two *in silico* associations in the context of C5-deficiency, mapping to chromosomes 8 (*Carg3*) and 11 (*Carg4*). In Chapter 3, we sought to characterize the genetic basis and phenotypic expression of susceptibility to *C. albicans* infection in the C5-sufficient SM/J strain. Linkage analysis in the [B6xSM/J]F2 population established distal chromosome 15 (*Carg5*) as a novel locus controlling the immune response to *C. albicans*, independently of

functional C5. Meticulous assessment of innate immune cell effectors uncovered a pleiotropic myeloid defect in SM/J, typified by altered expression of Ly6G and decreased ROS production. Finally, Chapter 4 aimed to dissect the genetic component underlying differential permissiveness to a distinct pathogen, the cestode *T. crassiceps*, in B6 and A/J mice. We applied an analogous strategy to that utilized in Chapter 2, combining haplotype association mapping in 34 AcB/BcA RCS with linkage analysis in informative crosses. A major locus designated *Tccr1* was identified on proximal chromosome 2, corresponding to *C5*, where deficiency correlates with permissiveness to *T. crassiceps* cysticercosis.

The overall objective of these studies was to utilize a hypothesis free genetic approach for the identification of novel loci that contribute to the pathogenesis of two antipodal pathogens, *C. albicans* and *T. crassiceps*. These newly described C5-dependent and –independent modifiers should improve our understanding of the intricate host-pathogen relationship, and ultimately guide the development of novel therapeutic strategies for these infections.

Chapter 1:

Introduction and Literature Review

1.1 *Candida albicans*

Our estimates of the number of eukaryotic species on Earth have recently been amended. Some 8.7 million eukaryotic species exist, with fungi comprising approximately 7% (611,000 species) of that number (*13*), a conservative underestimate from the perspective of mycologists (*14-16*). Of all fungi, only a relatively small group of ~300 species are human pathogens (*17*), and encompass fungi causing superficial cutaneous infections, such as dermatophytes and *Malassezia* species, as well as fungi capable of causing life-threatening systemic infections, notably *Aspergillus fumigatus*, *Cryptococcus neoformans*, *Histoplasma capsulatum*, and *Candida albicans* (*18*).

For over thirty years, *Candida* species have deservedly held the title of the most important cause of opportunistic mycoses worldwide. While the genus *Candida* comprises 150 heterogeneous species (*19*, *20*), clinical reports from the last two-three decades indicate that in 95% of infections, *C. albicans*, *C. glabrata*, *C. parapsilosis*, *C. tropicalis*, and *C. krusei* constitute the most common isolates (*2*, *21-23*). Despite the rise in the emergence of non-*albicans Candida* species, *C. albicans* remains the predominant cause of invasive candidiasis (*24*, *25*). Paradoxically, *Candida albicans* is a benign denizen of the oral mucosa, the gastrointestinal and genitourinary tracts, and the skin of most healthy individuals (*26-29*). In the setting of severe underlying disease and compromised immune system, however, *C. albicans* is capable of causing disease ranging from benign to disseminated infection with important repercussions on morbidity and mortality.

1.1.1 Types of infection

C. albicans is a resilient pathogen that is ubiquitously present in virtually all environmental niches, and has been recovered from a range of animal and bird hosts (*19*). In humans, *C. albicans* causes a wide range of diseases that can be broadly classified into two major categories: superficial and systemic candidiasis.

1.1.1.1 Superficial (mucocutaneous)

Superficial candidiasis involves colonization of the skin and mucosal surfaces, and encompasses oropharyngeal, vulvovaginal, and onycho-cutaneous infections (*19*, *30*). Recurrent or persistent mucocutaneous infections simultaneously affecting multiple superficial sites are referred to as chronic mucocutaneous candidiasis (CMC), and occur in the setting of impaired IL-17 immunity (*19*, *31*). Severe oropharyngeal candidiasis commonly occurs in HIV-positive individuals, while patients with severe combined immunodeficiencies (SCID), combined immunodeficiencies (CID), or undergoing immunosuppressive therapies are prone to develop CMC (*32*, *33*), collectively underscoring the importance of T cell mediated adaptive immunity. Despite their frequency and concomitant morbidity, superficial *C. albicans* infections are non-lethal.

1.1.1.2 Systemic

In contrast to superficial candidiasis, systemic candidiasis is markedly more debilitating and associated with a high crude mortality rate, even following initiation of antifungal therapy (*2*). The spectrum of systemic candidiasis comprises severe and invasive disorders, such as candidemia, endocarditis, disseminated infection, central nervous system infection, endophthalmitis, osteomyelitis, and other forms of visceral candidiasis (*19*, *21*). It still remains unclear whether *Candida* originates from an endogenous source such as the gastrointestinal tract (*34*), or whether entry of exogenous *Candida* is facilitated by means of a mechanical device (eg. catheter) (*2*, *35*). Nonetheless, dissemination to one or multiple organs arises upon breach of the normally impenetrable epithelial layer leading to bloodstream invasion. Systemic infections occur most frequently in patients with underlying hematologic malignancies or those undergoing myeloablative therapy, although invasive candidiasis in critically ill non-immunosuppressed individuals is becoming a growing concern (*2*, *21*).

1.2 Invasive *C. albicans* infection in humans

1.2.1 Epidemiology

The epidemiology of opportunistic or nosocomial *Candida* infections during the past three decades followed global health and demographic trends. From 1980 to the mid-1990s, the onset of the HIV epidemic resulted in a dramatic increase of incidence rates and crude mortality (from 0.7 to 4.2 deaths per 100,000 population in 1989) associated with all opportunistic mycoses, promoting them from the 10th to the 7th rank of underlying causes of infectious disease mortality in the United States in 1997 compared to 1980 (*36*). Mortality rates specifically attributed to candidiasis have mirrored this tendency, and incidence rates of invasive candidiasis have increased both in Europe and the US from the 1970s to the early 1990s, after which they remained constant (*2*, *35*, *37*). *Candida* species are one of the most common causative agents of nosocomial bloodstream infections (BSI) in the US and Europe, and isolated from ~9% of all BSI cases, with higher occurrence in intensive care units (ICU) (*38*, *39*). The crude mortality associated with *Candida* infections can range anywhere between 19% to 75%, depending on the geographical location, species, and the type of population surveyed (*2*, *3*, *37*), while it has been estimated that attributable mortality is as high as 47% (*21*). Wenzel and colleagues have estimated the death toll associated with nosocomial *Candida* to range from 2 800 to 11 200 each year in US alone (*40*). *C. albicans* is recovered from roughly half of BSI patients, remaining the most common *Candida* isolate in nosocomial infection (*2*, *3*, *35*). The risk factors associated with candidemia and invasive candidiasis were described by several epidemiological reports (*2-5*), (Table 1). When two or more of these risk factors are present, the probability of infection increases in an exponential manner (*4*). While the risk factors remained essentially the same for the past two decades, the focus has shifted from immunocompromised and neutropenic individuals to critically ill, non-immunocompromised patients (*2*, *3*, *22*). Among these patients, the single most important risk factor is the length of stay in the ICU, with the peak incidence of invasive candidiasis occurring around day 10 (*21*). This implies that fortitude of invasive candidiasis is largely a result of medical progress. Despite major

Table 1. Risk factors associated with invasive candidiasis for adults and children

Hematological or solid malignancies
Neutropenia
Renal failure
Severe acute pancreatitis
Organ transplantation
Long hospitalization period in the intensive care unit
High APACHE II (Acute Physiology and Chronic Health Evaluation) score
Hemodialysis
Usage of antibiotics with broad spectrum
Usage of antifungal agents
Presence of central venous catheters
Mechanical ventilation
Total parenteral nutrition
Usage of immunosuppressive agents
Colonization with *Candida* species
Surgical procedures
For neonates and children, in addition to adults
Prematurity
Low birth weight
Low APGAR (American Pediatric Gross Assessment) score
Congenital malformations

The table is reproduced from *(5)*.

advances in the field of antifungal therapy, unchanged incidence and mortality rates associated with this infection illustrate that invasive candidiasis is a persistent public health problem associated with high incurred healthcare costs.

1.2.2 Genetic predisposing factors

In 1988, Odds postulated that "There is no evidence of any substance so far to indicate major racial or other genetic variations in susceptibility to *Candida* infections" (*19*). Some 25 years later, improved diagnostic tools and surveillance programs led to the identification of large familial pedigrees and sporadic cases of chronic mucocutaneous candidiasis (CMC) and invasive candidiasis. This facilitated the elucidation of genetic variants governing susceptibility to *Candida* infection. In recent years, several genetic polymorphisms underlying CMC have been characterized (Table 2). Detailed portrayal of inherited, syndromic, and isolated CMC is beyond the scope of this thesis, but has been the focus of several excellent reviews (*30*, *32*, *41*, *42*). While adaptive immunity is critical for CMC, invasive candidiasis often occurs in the setting of impaired neutrophil responses like chronic granulomatous disease (CGD) and MPO deficiency.

1.2.2.1 MPO deficiency

Myeloperoxidase (MPO) deficiency is the most common phagocyte disorder with prevalence of one in 2000-4000 individuals in Europe and North America (*43-45*). MPO deficiency is inherited in an autosomal recessive manner and caused by assorted mutations in the *MPO* gene. These are often present in the compound heterozygous state and can lead to a range of molecular abnormalities giving rise to partial or complete MPO deficiency (*44*, *46-52*). Myeloperoxidase is produced in neutrophils and monocytes (*53*) and catalyzes the production of hypochlorous acid during respiratory burst. More recently, it was revealed that MPO is required for making neutrophil extracellular traps (NETs), whose defective formation may undermine host defense in MPO-deficient patients (*54*). Human neutrophils lacking MPO are capable of

Table 2. Genetic mutations associated with superficial candidiasis in humans

Gene	Mutation	Mode of inheritance[a]	Phenotype[b]	Disease[c]
AIRE	R257X	AD	Ab against IL-17 and IL-22	CMC
CARD9	Q295X	AR	↓ TNFα and Th17	CMC
CD25	Deletion (60–64)	AR	↓ number of $CD4^+$ cells	*Candida* esophagitis
DOCK8	Multiple deletions and point mutations	AR	↓ Th17 cells	HIES
IL-12Rb1	Multiple point mutations	AR	↓ IFNγ	Mucosal candidiasis
IL-17RA	Q284X	AR	× IL-6 and CXCL1	CMC
IL-17F	S65L	AD	↓ IL-6 and CXCL1	CMC
STAT1	R274W A267V	AD	↓ IL-17, IL-22 and IFNγ	CMC
STAT3	Multiple point mutations	AD	↓ IL-17	HIES
TYK2	Deletion (550–553)	AR	↓Th1 and Type I IFN responses	HIES

[a]AD-Autosomal dominant; AR-Autosomal recessive
[b]Ab-autoantibodies; ↓ reduced; × absent
[c]CMC-Chronic mucocutaneous candidiasis; HIES-Hyper IgE syndrome
The table is adapted from *(40)*.

phagocytosing *C. albicans* and various bacteria as efficiently as normal neutrophils. However they exhibit impaired in *Candida* killing in vitro and exhibit a significant delay in bactericidal activity (*55-58*). In line with these observations, MPO-deficient mice present an increased susceptibility to intratracheal and intraperitoneal (i.p.) *C. albicans* infection, whereas the clearance of i.p. *S. aureus* is normal (*59*, *60*). Paradoxically, rather than suffering from recurrent or severe fungal infections, the vast majority of MPO-deficient patients are asymptomatic unless also affected by an underlying disease, such as diabetes mellitus (*43*, *44*, *57*, *61*, *62*). Although MPO-deficiency is not regarded as a predisposing genetic factor to invasive *C. albicans* infection *per se*, it constitutes a concomitant condition adversely affecting neutrophil function.

1.2.2.2 Chronic granulomatous disease

Chronic granulomatous disease (CGD) is a rare primary immunodeficiency encompassing a compilation of mutations affecting the nicotinamide adenine dinucleotide phosphate-oxidase (NADPH oxidase) complex with an incidence rate of ~1/200,000 (*63*). The first clinical diagnoses in boys suggested an X-linked recessive mode of inheritance (*64-66*); however, it quickly became apparent that CGD is also inherited in autosomal recessive manner (*67*). In the 1960s, classic studies established CGD as a phagocytic disorder, characterized by the inability of neutrophils and monocytes to kill several bacterial and fungal species by producing reactive oxygen species (*55*, *65-68*). It is now understood that more than two thirds of CGD cases are X-linked and result from defects in the *CYBB* gene encoding $gp91^{phox}$; whereas the remaining cases are autosomal recessive and caused by defects in *CYBA*, *NCF-1*, *NCF-4*, *NCF-2*, which encode NADPH oxidase subunits $p22^{phox}$, $p40^{phox}$, $p47^{phox}$, and $p67^{phox}$, respectively (reviewed in (*69-72*)). 95% of CGD mutations completely abolish protein expression or result in greatly diminished levels of protein (*70*). NADPH oxidase assembly is required for generation of microbicidal oxygen radicals and consequently, CGD patients are highly susceptible to severe, and sometimes fatal bacterial and fungal infections (*63*). Accordingly, *Aspergillus* species are the most prominent fungal infectious agents in CGD patients, although *Candida* species rank

as the most common cause of meningitis in these individuals (*32*, *63*). The importance of intact NADPH oxidase is reflected in X-CGD mice ($gp91^{phox}$ knockout), which display increased mortality compared to controls upon intraperitoneal infection with *C. albicans*, even more so than $Mpo^{-/-}$ (*60*).

1.2.2.3 CARD9 deficiency

Deficiency of CARD9 (caspase recruitment domain-containing protein 9) is a recently described autosomal-recessive primary immunodeficiency and the first genetic defect that was causally linked to susceptibility to candidiasis in humans (*6*). CARD9 is an adaptor molecule mediating intracellular signaling downstream of Dectin-1, involved in antifungal immunity as illustrated by the increased susceptibility of $Dectin\text{-}1^{-/-}$ (*73*) and $Card9^{-/-}$ (*74*) mice to invasive *C. albicans* infection. Although mucocutaneous disease may occur in afflicted patients (*6*), the staple feature is the recurrent community-acquired central nervous system (CNS) infection, involving either brain parenchyma and/or meninges, which may be fatal (*6*, *75*, *76*). The cutting-edge report by Glocker *et al.* identified a homozygous null CARD9 mutation (Q295X) by genetic linkage analysis in a large consanguineous Iranian pedigree, out of which at least three members died from invasive candidiasis (*6*). The null allele resulted in the loss of CARD9 expression, accompanied by reduced Th17 cell numbers *ex vivo* and abolished Dectin-1-mediated TNFα responses (*6*). Furthermore, a recent report by Drewniak and colleagues described a compound heterozygous mutation (G72S, R37P) in an Asian female patient with relapsing meningoencephalitis caused by a non-*albicans* species *C. dubliniensis* (*75*). The protein expression was abolished and the null allele characterized by a selective neutrophil killing defect (*75*). Most recently, Gavino *et al.* describe a novel hypomorphic mutation (Y91H) in a French-Canadian male patient with relapsing *C. albicans* meningoencephalitis (*76*). In contrast to previously reported CARD9 mutations, Y91H did not result in loss of protein expression, nor defective Th17 responses; rather, patient peripheral blood marrow cells (PBMC) produced significantly less granulocyte-macrophage colony-stimulating factor (GM-CSF) when stimulated with zymosan (*76*), suggesting that CARD9/GM-CSF axis is implicated in

invasive candidiasis. Finally, the finding that a syndrome of deep dermatophytosis is associated with recessive CARD9 deficiency (*77*) further corroborates the importance of CARD9-dependent pathways and commands their deciphering in both myeloid and lymphoid cells in humans.

1.2.2.4 IL-12Rβ1 deficiency

IL-12Rβ1 deficiency is the most common genetic etiology of Mendelian susceptibility to mycobacterial diseases (MSMD), a rare genetic immunodeficiency that affects 156 individuals to date, characterized by a predisposition to infection by mycobacteria and *Salmonella*, and mild forms of chronic mucocutaneous candidiasis (CMC) in approximately 25% of cases (*78*-*80*). *IL12RB1* encodes the dual subunit of interleukin-12 (IL-12) and interleukin-23 (IL-23) receptors (*81*), whose deficiency is inherited in an autosomal recessive fashion and engendered by diverse transcriptional alterations typically resulting in complete absence of surface protein (*78*, *79*, *82*). The broad infectious phenotype in these patients is unsurprising, as IL-12 is an important cytokine for the development of IFNγ-producing T cells and IFNγ production (*81*), while IL-23 is required for expansion and maintenance of IL-17-producing T cells (*83*, *84*). Recently, Ouederni and colleagues reported the clinical signs of candidiasis in 35 patients with IL-12Rβ1 deficiency, four out of which exhibited invasive or disseminated candidiasis episodes (*80*). While three episodes could be ascribed to nosocomial factors, at least one of these episodes was community-acquired candidiasis that manifested in endocarditis characteristic for non-*albicans* species of *Candida* (*80*). Although the patient in question was designated as IL-12Rβ1-deficient, his genetic status was not evaluated, and the underlying cellular and/or functional deficiencies remain elusive. Hence, whether IL-12Rβ1-deficiency truly constitutes a predisposing genetic factor for invasive candidiasis in humans remains to be ascertained.

1.3 Immunity to systemic candidiasis

The host response to systemic *C. albicans* infection entails finely concerted action of *Candida* recognition by complement and innate immune cells through PRRs, cellular effector functions to contain the infection, and antigen presentation to polarize naïve T cells into an appropriate effector subset to resolve the infection.

1.3.1 *Candida* recognition and signaling

The *C. albicans* cell wall is composed of an inner pillar layer containing the skeletal chitin and β-glucan, which is decorated with an outer lattice of mannans and proteins (Figure 1) (*85*). In response to the elaborate alterations in cell wall architecture during infection (*86*, *87*), the leukocytes of the mammalian host have evolved an array of PRRs (Figure 2) acting in an orchestrated manner to elicit an appropriate immune response, ultimately leading to pathogen eradication.

1.3.1.1 C-type lectin receptors

C-type lectin receptors (CLRs) belong to the C-type lectin-like domain (CTLD) superfamily, which encompasses more than 1000 proteins classified into 17 subgroups (I-XVII) according to domain architecture and phylogeny (*88*). Although not absolute, the most common CTLD function in vertebrates is Ca^{2+}-dependent carbohydrate binding, in which case the CTLD is branded a carbohydrate recognition domain (CRD). The specificity of carbohydrate binding is dictated by the CRD, where residues with carbonyl side chains coordinate Ca^{2+} and are directly involved in monosaccharide binding (*88*).

Herein, the emphasis is placed on CLRs that are involved in the recognition of *C. albicans* and subsequent downstream signaling, notably Dectin-1, Dectin-2, Dectin-3, Mincle, MR, DC-SIGN, and MBL (reviewed in (*89*, *90*)).

Dectin-1

Dectin-1 (encoded by *Clec7a*) belongs to the group V of C-type lectins,

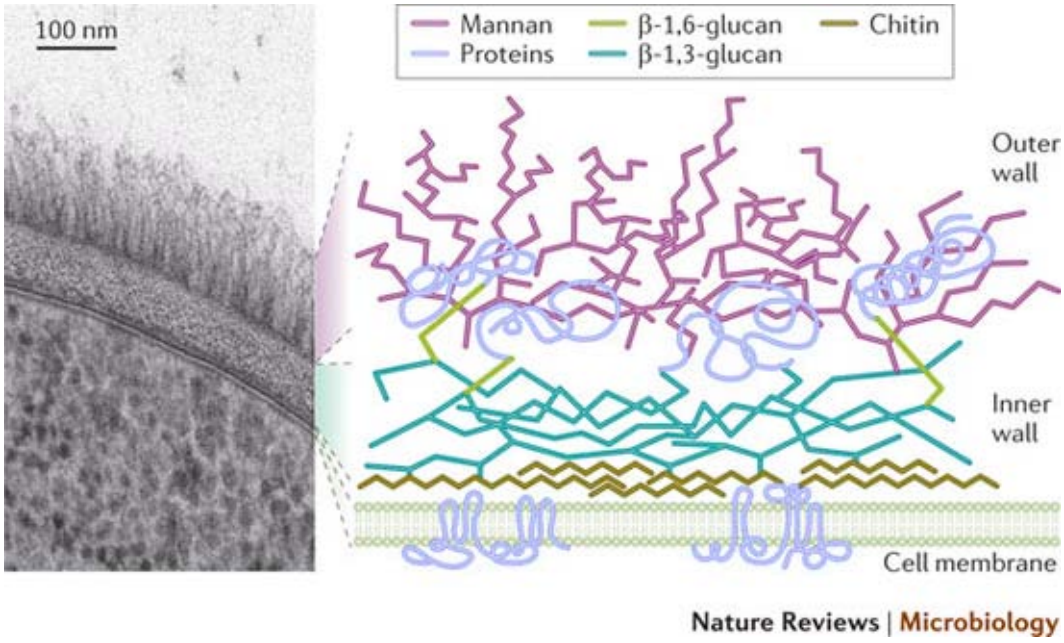

Figure 1. Components of the *Candida albicans* cell wall

The *C. albicans* cell wall is composed of an inner scaffold layer containing the polysaccharides chitin and β-1,3-glucan, maintaining rigidity and cell shape. The outer wall is enriched with mannans and proteins, and is linked to the inner framework through a more flexible β-1,6-glucan. The figure is reproduced, with permission, from *(87)*.

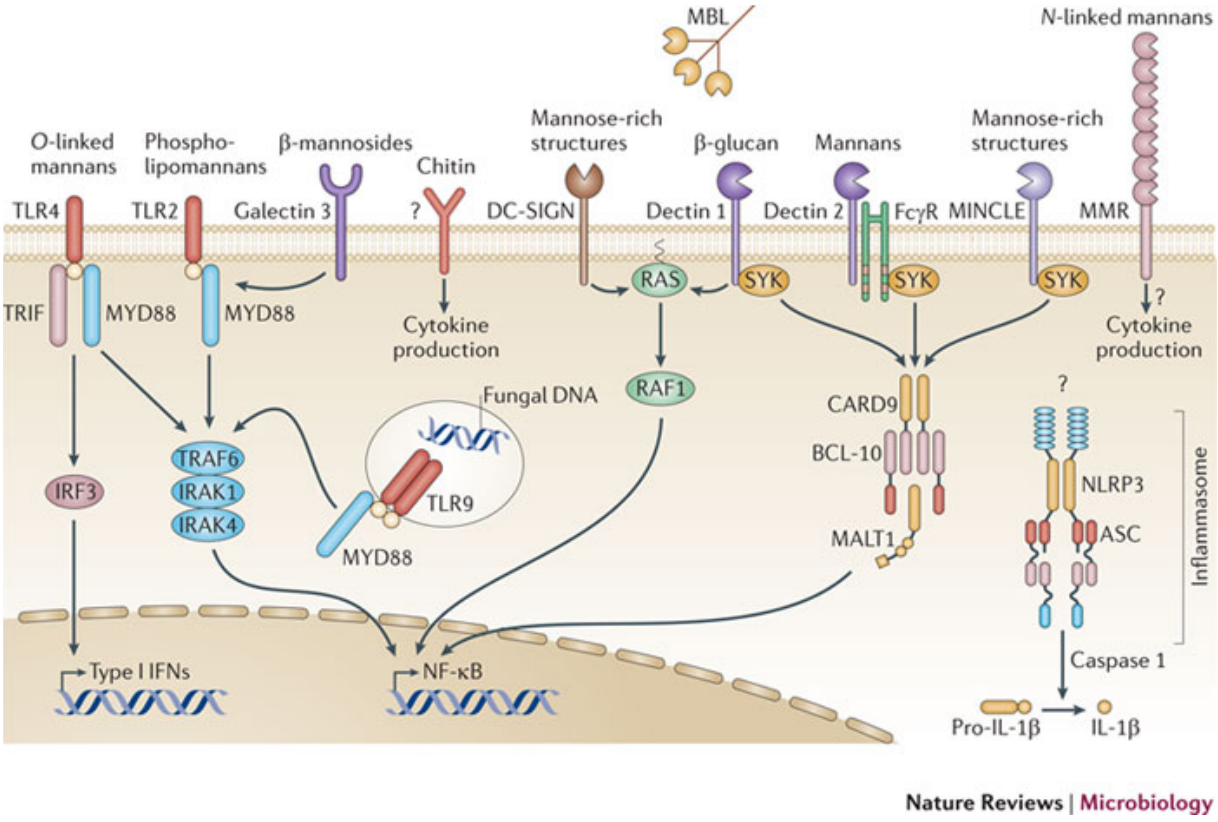

Figure 2. Major pattern-recognition receptors (PRRs) involved in the recognition of *C. albicans*

The mammalian host has evolved a range of PRRs that can recognize various carbohydrate moieties that decorate the *C. albicans* surface and elicit cytokine production via downstream signaling events. Note that not all PRRs or signaling events are depicted. The figure was reproduced, with permission, from *(85)*.

characterized by an atypical CRD, and binds β -1,3-linked glucan moieties on unopsonized zymosan, *C. albicans*, and *Saccharomyces cerevisiae* independently of Ca^{2+} (*91-95*). Murine Dectin-1 is broadly expressed by all myeloid cells (*96*) and γδ T cells (*97*), while the human orthologue is additionally detected on eosinophils and B cells (*98*). The expression of Dectin-1 in murine macrophages was enhanced by GM-CSF, IL-4, and IL-13, whereas IL-10, LPS, and dexamethasone had the opposite effect, directly correlating with zymosan binding and TNFα production (*99*). Dectin-1 is furnished with a hemiITAM in its cytoplasmic tail (*91*) that mediates signal transduction by recruiting and activating Syk upon binding of agonist ligands. Indeed, several groups showed that induction of TNFα, IL-10, and IL-2 by yeasts is triggered by the mere engagement of Dectin-1 via Syk kinase, without any requirement for internalization (*100*, *101*).

Furthermore, engagement of Dectin-1 by zymosan or *Candida* elicited ROS production in macrophages (*73*, *102*, *103*), neutrophils (*73*, *104*), and DCs (*105*, *106*), whereas β -glucan-induced production of proinflammatory cytokines (IL-12, IFNγ, IL-10, and TNFα) or ROS are abolished in Dectin-1-deficient DCs (*106*). Despite the aberrant cytokine profile, Saijo *et al*. claimed that Dectin-1 KO mice were not more susceptible to intravenous *C. albicans* challenge (*106*). In contrast, Taylor and colleagues reported significantly impaired survival of *Dectin-1*$^{-/-}$ mice following systemic *C. albicans* infection, concomitant with increased fungal load in mucosal organs, but not in kidneys (*73*). Results obtained from a peritoneal infection model implied that the increase in susceptibility is due to an abnormal antifungal inflammatory response, consisting of reduced leukocyte recruitment and decreased cytokine levels in the peritoneal exudate (*73*).

Moreover, an elegant study by Gross *et al.* identified Card9 as a key transducer of Dectin-1 signaling (*74*). Accordingly, Card9$^{-/-}$ mice were highly susceptible to systemic *C. albicans* infection, succumbing rapidly and displaying elevated fungal outgrowth in deep seeded organs (*74*). Card9$^{-/-}$ BMDCs had severely impaired zymosan- or *C. albicans*-induced cytokine production, as well as defective Dectin-1/Syk-dependent IL-10 production. Additionally, Card9 signaling required

Bcl10 and Malt1 to induce the canonical activation of NF-κB (*74*). DC maturation and cytokine production, which promoted differentiation of $CD4^+$ T cells towards the Th17 lineage, relied on the Dectin-1/Syk/Card9 signaling (*107*). In addition, restimulation of *C. albicans*-infected splenocytes with heat-killed yeasts elicited IFNγ and IL-17 production, in a Card9-dependent manner (*107*). Independent of Card9, Dectin-1/Syk modulated the activation of NIK and the non-canonical RelB pathway (*108*). Alternatively, Dectin-1 engagement recruits Raf-1, which antagonized Syk-induced RelB activation, ultimately skewing T cell differentiation toward Th1 (*108*). Moreover, PKCδ (encoded by *Prkcd*) was specifically required to induce Card9-Bcl10 complex assembly, for subsequent TAK1 activation and canonical NF-κB control (*109*). Consequently, *C. albicans*-induced cytokine production was abolished in $Prkcd^{-/-}$ BMDCs and PKCδ was found to be critical for antifungal host defense (*109*). In addition to NF-κB activation, Dectin-1 signaling resulted in the activation of p38, ERK, JNK cascades (*107*) and the NFAT pathway (*110*, *111*).

Transcription and synthesis of pro-IL-1β following *C. albicans* challenge also depended on the Dectin-1/Syk/Card9 axis, while the Nlrp3 inflammasome mediated Caspase-1-dependent pro-IL-1β processing (*112*, *113*). Recruitment of Malt1, caspase-8, and ASC into this scaffold proved crucial for processing of pro-IL-1β by caspase-8 (*114*). Unlike the canonical caspase-1 inflammasome, which needed additional cytosolic PRRs, such as Nlrp3, activation of the noncanonical caspase-8 inflammasome was independent of pathogen internalization (*114*).

Furthermore, immune sensing of *C. albicans* compels concerted recognition of mannans and glucans by CLRs and TLRs. Dectin-1 synergizes with TLR2 and TLR4 (*115*, *116*) or Galectin-3 (*117*) to elicit proinflammatory responses by monocytes or macrophages to pathogenic fungi. The role of Dectin-1, however, extends beyond mere triggering of cytokine production. Immediately after onset of *C. albicans* phagocytosis, Dectin-1 accumulated at the phagocytic cup, possibly collaborating with CR3 (*118*). BTK and Vav1 formed complexes with Dectin-1 at the phagocytic cup enriched for $PI(3,4,5)P_3$, where BTK controls diacylglycerol production and subsequent PKC signaling (*119*). BTK- and Vav1-deficient mice

succumbed more rapidly to systemic *C. albicans* infection than their wild type counterparts, attributable to a reduced uptake of *C. albicans* by BMDM of these animals (*119*). In neutrophils, Vav1 recruitment upon Dectin-1 engagement activated the integrin Mac-1 (CR3) to induce phagocytosis and respiratory burst (*120*). Congruently, Mac-$1^{-/-}$ and Vav1,$3^{-/-}$ mice displayed impaired survival and elevated renal fungal burden, arising from aberrant neutrophil killing rather than defective recruitment (*120*). Using a signaling incompetent Dectin-1, Mansour *et al.* further demonstrated defective phagolysosomal maturation in macrophages, as evidenced by failure to acquire LAMP-1 and diminished acidification (*121*). Recruitment of the autophagy factor LC3 to the phagosome relied on the activation of Dectin-1 and Syk, but not Card9, resulting in enhanced macrophage fungicidal activity (*122*).

The relevance of DECTIN-1 and CARD9 is underscored by the identification of human patients bearing rare loss of function mutations in these genes, suffering from fungal infections ranging from recurrent mucocutaneous candidiasis to the severe invasive fungal disease, respectively (*6*, *123*). The mutated Dectin-1 failed to bind β-glucan, therefore leading to a defective production of IL-17, TNFα, and IL-6 by monocytes (*123*). Consistent with its adaptor role downstream of several PRRs, CARD9 deficiency resulted in a more severe disease phenotype, attributed to impaired signaling from Dectin-1 and defective Th17 polarization (*6*).

Dectin-2

Dectin-2 (encoded by *Clec4n*) is another member of the group V C-type lectin family, sharing several features with Dectin-1 meanwhile displaying a relatively low degree of sequence homology (*124*). Predominantly myeloid-restricted, the expression of Dectin-2 was detected in several DC subsets, inflammatory monocytes, and a wide variety of tissue macrophages (*124*, *125*). The CRD of Dectin-2 displays high affinity for high-mannose structures and binds α-mannans (*126*, *127*), thereby recognizing several fungal species including *C. albicans*, *Microsporum audouinii*, *Trichophyton rubrum, Histoplasma capsulatum,* and capsule-deficient *Cryptococcus neoformans*, albeit with varying avidity (*126*, *128*). Unlike Dectin-1, Dectin-2 lacks

the ITAM signaling motif and thus couples with the ITAM-bearing common γ-chain of the Fc receptors (FcRγ) (*128*), permitting an efficient downstream signaling cascade, and functional surface expression of Dectin-2 (*129*). Hyphal stimulation in RAW264.7 macrophages transfected with Dectin-2 induced protein tyrosine phosphorylation by Src kinases, NF-κB activation, and secretion of TNFα and IL-1ra (*128*). In mouse BMDCs and BMDM, Dectin-2 signaling triggered CARD9-Bcl10-dependent activation of NF-κB via recruitment of Syk to phosphorylated FcRγ, as well as activation of ERK, JNK and p38 MAPK pathways (*129*, *130*). In fact, NF-κB activation occurs as a coordinated effort by Syk-dependent IκBα kinase phosphorylation, whereas CARD9 mediates IκBα kinase-NEMO ubiquitination (*130*). As abovementioned, Card9-Bcl10 complex assembly was contingent upon PKCδ, which constituted a common adaptor relaying signaling from Dectin-1, Dectin-2, and Mincle (*109*). Gorjestani *et al.* showed that PLCγ2 is a key component in Dectin-2 signaling (*131*). Hence, PLCγ2 knock out mice display defective MAPK and NF-κB activation, leading to impaired BMDM cytokine and ROS production upon hyphal *C. albicans* stimulation. As a result, PLCγ2$^{-/-}$ mice were highly susceptible to systemic *C. albicans* infection (*131*).

In the context of genetic deficiency of Dectin-1, blockade of Dectin-2 in DCs led to a profound reduction in IL-2, IL-10, and TNF levels in response to challenge with either zymosan or *C. albi*cans (*129*). Similarly, in *Dectin-2*$^{-/-}$ DCs, the production of IL-6, TNF, IL-1β, IL-10, IL-23, and IL-12p70 was virtually absent upon stimulation with *C. albicans* yeasts, while the hyphal form induced limited amounts of these cytokines (*127*). Studies in DCs using an antagonistic mAb against Dectin-2 (*129*) and genetically deficient mice (*127*) illustrated that Dectin-2, rather then Dectin-1, is the predominant Syk-coupled receptor involved in the induction of Th17-based immunity upon *C. albicans* exposure. Robinson *et al.* and Saijo *et al.* unanimously concluded that while Dectin-2 is the sole PRR responsible for IL-17 induction by *C. albicans*, both Dectin-1 and Dectin-2 contribute to Th1 cell differentiation (*127*, *129*). In addition, Dectin-2 KO mice exhibited increased mortality and higher renal fungal counts compared to WT counterparts during systemic *C. albicans* infection (*127*). This susceptibility was attributed to a defective

Th17 polarization, as *IL-17a*$^{-/-}$ mice also display a reduced survival phenotype during infection (*127*).

Dectin-3

Dectin-3 (originally named murine macrophage C-type lectin (MCL); encoded by *Clec4d*) constitutes the least characterized member of the group II C-type lectins (*132*, *133*). First identified by differential display in macrophage cell lines, it was found to be highly expressed in human and murine bone marrow, peripheral blood leukocytes, spleen and, within the hematopoietic lineage, in monocytes and macrophages (*132-134*). The expression of Dectin-3 in monocytes was upregulated by IL-6, TNFα, IL-10, and IFNγ, with opposing effects of LPS (*133*). Similar to Mincle, Dectin-3 has a short cytoplasmic tail without any signaling motifs, and the rapid internalization following antibody ligation suggested that it might associate with a partner mediating its endocytosis (*133*). Although reports indicate that Dectin-3 does not associate with DAP10, DAP12, or FcRγ adaptors in transfected cells (*134*), Dectin-3 induced Syk phosphorylation and NF-κB activation in response to hyphal α-mannans (*134*, *135*). Similarly, *Clec4d*$^{-/-}$ BMDM failed to induce NF-κB activation upon hyphae exposure, concomitant with reduced production of proinflammatory cytokines such as TNFα, IL-6, and IL-12 (*135*). Antibody-mediated blockade or genetic deletion of Dectin-3 rendered mice highly susceptible to *C. albicans* infection, with respect to abridged survival and increased renal fungal burden, concomitant with a decreased renal proinflammatory cytokine profile. Lastly, Zhu and colleagues demonstrated that Dectin-3 formed heterodimers with Dectin-2, binding α-mannans more effectively than their respective homodimers, and leading to a more potent inflammatory response against fungal infection (*135*).

Mincle

Mincle (macrophage-inducible C-type lectin; encoded by *Clec4e*) was first identified on the basis of high homology to the group II C-type lectins and as a transcriptional target of NF-IL6 (C/EBPβ) in response to LPS in macrophages (*136*).

Similarly to Dectin-2, Mincle was classified as an ITAM-coupled receptor, whose arginine residue in the transmembrane domain permits direct association with FcγR (*137*). It was later demonstrated that both human and mouse Mincle bind *C. albicans* (*138*, *139*) probably via mannose-rich structures (*138*) and not chitin (*140*). While Mincle is enriched at the nascent phagocytic cup of macrophages exposed to *C. albicans* yeasts, it was not required for phagocytosis to occur (*139*). Rather, it was shown to play a non-redundant role in the induction of inflammatory (i.e. TNF) response to *C. albicans* infection, which translated to protection against disseminated candidiasis (*139*). In thioglycollate-elicited peritoneal macrophages, activation of Mincle leads to phosphorylation of Syk and ERK kinases, and subsequent production of TNF, MIP-2 (CXCL2), KC (CXCL1), and IL-6 (*137*), suggesting that Mincle may share a common signaling axis with Dectin-1 and Dectin-2. Indeed, in the absence of PKCδ, Dectin-1-, Dectin-2-, or Mincle-induced IL-10 and TNF production was severely abrogated (*109*). Finally, Vijayan *et al*. reported reciprocal patterns of Mincle expression on human monocytes and neutrophils, for which they postulated that functional dichotomy provides a manner to orchestrate early responses to infection (*141*).

MR

MR (mannose receptor; encoded by *CD206*) belongs to the group VI of C-type lectins and bears a cysteine-rich domain and eight CRDs, with CRDs 4-8 mediating recognition of mannose, fucose, and N-acetylglucosamine residues (*142*, *143*). Although initially thought to be restricted to tissue macrophages, MR presence was since detected on DCs (*144-146*) and various non-myeloid cells (*147*). In peritoneal macrophages, MR transcription is induced by IL-4 or IL-13, and abrogated by IFNγ stimulation (*148*, *149*). Coste *et al.* demonstrated that IL-13 promoted yeast-triggered ROS production in a MR-dependent fashion (*149*). The functional characterization of MR is impeded by the fact that mannose is redundantly recognized by a number of PRRs (Mincle, Dectin-2, and DC-SIGN). Indeed, MR proved to be dispensable for host defense against intraperitoneal *C. albicans* infection or for uptake of *Candida* by primary macrophages (*150*). Therefore, conclusions

stemming from earlier studies utilizing mannose or mannan as a specific MR inhibitor are unreliable (*151-155*).

The MR cytoplasmic tail possesses a diaromatic motif involved in endosomal sorting and an adjacent tyrosine-based internalization motif (*156*). MR-blocking antibodies interfered with *C. albicans* or zymosan internalization by DCs, supporting the role of MR as a phagocytic receptor (*105*). Additionally, reduced cell surface expression of mannose-binding receptors, MR and DC-SIGN, during *Candida* uptake reflected their internalization (*105*). J774-E macrophages expressing elevated levels of MR (*157*) and transfection of non-phagocytic COS-1 cell line with MR (*158*) partially mediated phagocytosis of *C. albicans*. Furthermore, MR is present in mature phagosomes, as indicated by the presence of flotillin-1 (*157*) and IF of *Candida*-containing phagosomes (*159*). However, Le Cabec *et al.* disputed the phagocytic role of MR, as CHO cells transfected with hMR failed to phagocytose classical MR particulate ligands, yet retained an efficient binding and endocytic capacity (*160*). As such, MR may require association with other cell surface receptors to elicit particle uptake in some cells. Notably, while Dectin-1 and CR3 accumulated at the nascent phagocytic cup, MR accumulation on *C. albicans* phagosomes at later stages implied a role in phagosomal sampling (*118*). MR is also the generative receptor for the formation of dorsal pseudopodial protrusions, the "fungipod", formed by DC after contact with yeast cell wall (*161*). Moreover, Martínez-Pomares and colleagues detected a functional soluble form of MR (sMR) in naive mouse serum and in the supernatant of IL-4-stimulated macrophages (*162*). The authors postulated that sMR could interact with native antigens through CRDs and hitchhike on APCs via the cysteine-rich domain for subsequent delivery to spleen and lymph node follicular zones (*162*, *163*). MR cleavage in response to *C. albicans* or β-glucan requires expression of dectin-1, thereby increasing the magnitude of TNFα production (*164*). Knock down of MR in peritoneal macrophages significantly hampered production of IL-1β, IL-6, and GM-CSF upon exposure to *C. albicans* (*165*). Also, MR blockade in human MNCs (*115*) or MR deficiency in murine macrophages (*118*) decreased TNFα production. Most recently, van de Veerdonk *et al.* revealed that *Candida* mannan was capable of triggering IL-17 production in human PBMCs in the absence of additional

stimuli (*166*). Blockade of MR by an antibody or with an siRNA at the transcriptional level abolished the bulk of IL-17 production, while the Dectin-1 contribution was minor (*166*). The IL-17 production induced by *C. albicans* and mannan was dependent on inflammatory monocytes, as they expressed higher levels of MR and more potently induced a Th17 response in T cells than patrolling monocytes (*166*, *167*).

DC-SIGN

DC-SIGN (DC-specific ICAM-3 grabbing non-integrin; encoded by *CD209*) was isolated in human monocyte-derived DCs as a high affinity binding partner for ICAM-3, mediating primary immune responses through transient adhesion with T cells (*168*). DC-SIGN is a type II C-type lectin with a single CRD comprising a highly conserved Glu-Pro-Asn (EPN) motif that recognizes high-mannose and fucose oligosaccharides (*169*, *170*), ligands that are present on a plethora of pathogens including *C. albicans* (*170*, *171*). The presence of various internalization motifs (di-leucine, acidic triad, and tyrosine-based) in its cytoplasmic tail enables DC-SIGN to endocytose soluble cargo for antigen presentation (*172*). In addition, Cambi *et al.* demonstrated through colocalization of DC-SIGN, phagosomes, and *Candida* blastospores, that DC-SIGN also participated in the binding and uptake of various *Candida* species (*159*, *171*). Studies employing *C. albicans* glycosylation mutants helped delineate N-linked mannan, but not O-linked or phosphomannan, as the specific carbohydrate structure on the fungal cell wall recognized by both DC-SIGN and mannose receptor on human DCs, directly modulating production of IL-6 (*159*). The signaling cascade ensuing recognition of *C. albicans* by DC-SIGN could be inferred from engagement of DC-SIGN by specific antibodies. Using this methodology, Caparrós *et al.* demonstrated that DC-SIGN engagement on DCs did not drive their maturation, but rather induced phosphorylation of ERK and Akt (*173*). Consistent with its role in signaling, DC-SIGN was present in lipid rafts in association with Syk and Lyn kinases, and subsequently led to enhanced IL-10 release through synergism with TNFα-initiated signals (*173*).

The mouse counterpart of human (h)DC-SIGN consists of five homologues comprised in a gene cluster (*174*), out of which only SIGNR1 has been considered to share properties of polysaccharide recognition with hDC-SIGN (*175*). Indeed, SIGNR1 was found to be expressed by most peritoneal $CD11b^+$ cells, while SIGNR1-transfected non-phagocytic cells exhibited the capacity to bind and uptake dextran, zymosan, ovalbumin, heat-killed *C. albicans*, and Gram-negative bacteria (*175*). Moreover, Taylor *et al.* have identified SIGNR1 as a major mannose receptor on resident peritoneal macrophages, though not on thioglycolate-elicited macrophages, capable of recognizing zymosan and *C. albicans* (*176*). Interestingly, the NIH3T3-SIGNR1 were poorly phagocytic, and this action was instead mediated by Dectin-1 (*176*). RAW264.7 (RAW) macrophages expressing SIGNR1 displayed enhanced TNFα production in response to zymosan and *C. albicans* in comparison with mock-transfected RAW cells (*176*, *177*). While TNFα production was primarily dependent on TLR2, it was also partially abrogated by blocking SIGNR1 with a specific mAb (*177*). Indeed, Takahara *et al.* confirmed physical association of SIGNR1 with the extracellular portion of TLR2 through CRD, potentiating TNFα production (*177*). Finally, SINGR1 participates in the induction of cellular oxidative burst in RAW-SIGNR1, which relied on Dectin-1 and Syk-mediated signaling, but not on TLR2 (*178*). As such, RAW-SIGNR1 cells presented significant candidacidal activity (*178*). Regarding downstream signaling events, antibody-mediated ligation of SIGNR1 on peritoneal macrophages triggered phosphorylation of several MAP kinases and IKK, and consequently IL-12 and TNFα production through NFκB activation (*179*).

Mannose Binding Lectin (MBL)

Mannose-binding lectin (MBL) is a constituent of the Group III C-type lectin subfamily: the collectins (*180*), which are a set of soluble oligomeric proteins that contain, in addition to the characteristic CRD, a collagenous moiety, a hydrophobic neck region, and a cysteine-rich N-terminus (*181*). While the basic functional unit of MBL is a homotrimer, MBL oligomerizes into higher order structures ranging from dimers to hexamers that recognize an array of carbohydrates, such as mannose, glucose, fucose, N-acetyl-mannosamine, and N-acetyl-glucosamine (*181*). This

versatile recognition, in turn, enables high avidity binding of MBL to microbial PAMPs present on bacteria, viruses, fungi, and protozoa parasites (*180*).

As the bouquet-like structure of the MBL oligomer is reminiscent of the classical complement pathway initiator protein C1q (*181*, *182*), it has been proposed that MBL is involved in opsonophagocytosis, thereby stimulating complement deposition (*183*) and potentiating the immune response. Indeed, several independent studies established that human MBL bound multiple clinically relevant microbial species *in vitro* by recognizing surface mannans in Ca^{2+}-dependent fashion, with a notable preference for yeasts of various species (*184-187*). Deposition of C3 and C4 on *C. parapsilosis, C. albicans,* or *C. neoformans*, and subsequent complement activation, was largely dependent on the presence of MBL in opsonizing sera (*186-188*), as was the efficacious uptake of yeasts by human neutrophils (*186*, *187*). In addition, exogenous MBL was shown to rescue inhibited phagocytic capacity of human neutrophils by blockade of Dectin-1 (*189*). Besides the evident role of MBL in *Candida* opsonophagocytosis, exposure of human monocytes to MBL-preincubated yeasts stimulated secretion of TNFα in a dose-dependent manner that could be abrogated by mannose supplementation (*190*). In contrast to the abovementioned studies, Kitz *et al.* observed that MBL hindered *C. albicans* phagocytosis by murine BMDM (*191*). Similarly, Ip *et al.* reported that MBL does not enhance opsonophagocytosis of *C. albicans* by human monocyte-derived dendritic cells (*188*). Rather, MBL promotes agglutination of hyphae, resulting in profound inhibition of growth.

The first genetic evidence that MBL participates in host defense against *C. albicans* stemmed from transgenic mice bearing the human *MBL* gene, a homologue of mouse *Mbl1* (aka *Mbl-A*), in which intravenous infection caused immediate reductions in serum MBP and complement activity (*192*). In knockout mice, however, only the combined deficiency of both forms of murine MBL (MBL-A/$C^{-/-}$) led to an increased susceptibility to both intraperitoneal and intravenous challenge (*193*), as MBL-A-deficient animals did not display altered survival or higher fungal burden following intraperitoneal infection (*194*). Held *et al.* postulated that an

opsonophagocytic defect in MBL-A/C$^{-/-}$ mice, characterized by the ablated recruitment of peritoneal cells, decreased phagocytosis, and limited clearance of fungal cells from the peritoneal cavity, accounted for the notable susceptibility to *C. albicans* infection (*193*). Analogously, parenteral administration of human MBL to BALB/c mice significantly improved their survival to hematogeneously disseminated candidiasis (*185*), while exposure to mannose promoted accelerated progression of *C. albicans* infection (*195*).

In humans, Pellis *et al.* demonstrated that MBL and C3, but not C1q, are present on clue cells of the vaginal cavity and act as sensing molecules for infectious agents that colonize the cervicovaginal mucosa (*196*). In line with these findings, several reports demonstrated a correlation between reduced levels of vaginal MBL and recurrent vulvovaginal candidiasis, which was strongly associated with a non-synonymous polymorphism in codon 54 of the *MBL* gene (*197*, *198*). More recently, the kinetics of circulating MBL levels during the course of invasive candidiasis (IC) were examined in a cohort of hospitalized patients with proven IC (*199*). While IC patients presented higher mean serum MBL concentrations compared to control subjects, a dramatic decline in MBL levels was observed during the two days before positive blood culture sampling, accompanied with a reciprocal peak in circulating mannose (*199*). Thus, these studies underscore the importance of MBL and the lectin complement pathway in innate host defense against *C. albicans* infection.

1.3.1.2 Toll-like receptors

Toll-like receptors (TLRs) are evolutionarily conserved homologues of the *Drosophila* toll protein (Toll), which has been shown to induce the antifungal innate immune response in adult *Drosophila* (*200*, *201*). The TLR family consists of 10 and 12 functional members in human and mouse, respectively (*202*). TLRs are type I transmembrane proteins that recognize PAMPs via the ectodomain, which contains leucine-rich repeats, and relay signals to downstream intracellular effectors through cytosolic Toll-IL-1 receptor (TIR) domains (*202*). TLRs that are expressed at the cell surface are involved in the recognition of microbial membrane components (TLR1,

TLR2, TLR4, TLR5, and TLR6), whereas those that detect nucleic acids (TLR3, TLR7, TLR8, and TLR9) are localized within endo-lysosomal compartments (*202*, *203*). Thus far, five TLRs (TLR2, TLR4, TLR6, TLR7, and TLR9) have been implicated in the recognition of *Candida* PAMPs (*202*).

The universal TLR downstream adaptor molecule, MyD88, was shown to be crucial for effective phagocytosis and candidiacidal activity of mouse macrophages and PMN (*204*, *205*). Moreover, absence of MyD88 virtually abolished secretion of TNFα, IL-12p70, and IFNγ by splenocytes in response to *C. albicans*, promoting Th2 polarization (*205*, *206*). MyD88-deficient mice were highly susceptible to invasive *C. albicans* infection, displaying high fungal burden in several tissues and severely abridged survival (*205*, *206*).

TLR2 and TLR4

Genetic and biochemical data established that TLR4 was the principal mediator of lipopolysaccharide (LPS) signaling (*207*, *208*), while TLR2 in cooperation with CD14 relayed signals from zymosan (a glucan) and Gram-positive bacteria, thereby inducing TNFα secretion (*209*). Similarly, Brown and colleagues confirmed that TLR2 was required for Dectin-1-mediated production of TNFα in response to zymosan and live *Candida* (*100*), while others observed that this interaction was necessary for generation of ROS and synergistic induction of TNFα and IL-12 (*102*, *116*). *C. albicans*-derived phospholipomannan is another TLR2 agonist that induces NF-κB nuclear translocation and triggers TNFα secretion in macrophages (*210*). Additionally, stimulation of human monocytes with *C. albicans* cell wall extracts or mannan induced TNFα production, which was inhibited with antagonistic antibodies against TLR4 and CD14, but not TLR2 (*211*). Rather than discerning a single most relevant PRR in immune sensing of *Candida*, Netea and colleagues provided evidence favoring a multilevel process in which the cooperation between the mannose receptor, TLR4, and Dectin-1/TLR2 complex dictates cytokine production (*115*).

The involvement of TLR2 and TLR4 in *C. albicans* recognition and host

antifungal defense has been controversial, with several groups reporting conflicting results. Following intravenous challenge with *C. albicans*, the TLR4-defective C3H/HeJ strain displayed increased renal fungal burden attributed to reduced KC and MIP-2 levels, impairing neutrophil recruitment (*212*). Aside from a chemotactic defect, TLR4-defective neutrophils were otherwise normal; conversely, TLR4-defective macrophages displayed aberrant functions, allowing dissemination and persistence of the pathogen to occur (*213*). Two additional independent studies assessed the survival of C3H/HeJ and $TLR4^{-/-}$ mice upon *C. albicans* infection and concluded that TLR4 is dispensable during invasive candidiasis (*205*, *214*). Moreover, Murciano *et al.* reported that neutrophil recruitment to the peritoneum is actually enhanced in C3H/HeJ mice. Antibodies directed against TLR2, but not TLR4, attenuated the production of TNFα, IL-1, and IL-8 by human PBMCs exposed to *C. albicans*, suggesting disparate requirements for both receptors (*212*). Paradoxically, the same group found that TLR2-deficient mice were more resistant to disseminated *C. albicans* infection than wild-type controls, showing increased survival and decreased tissue fungal load (*215*). Increased resistance in $TLR2^{-/-}$ KO mice was attributed to increased macrophage chemotaxis and enhanced candidacidal activity. While TNFα, IL-1β, and IL-6 production by macrophages was unchanged compared to controls, IL-10 release was severely impaired and accompanied by a decrease in the Treg population (*215*). In fact, Sutmuller *et al.* delineated a role for TLR2 in the expansion and proliferation of Tregs, which exacerbated the response to *C. albicans* infection via suppression of proinflammatory cytokines (*216*). In contrast, Villamón and colleagues reported that TLR2-deficient macrophages secreted little TNFα and MIP-2, resulting in reduced neutrophil recruitment and rapid mortality ensuing *C. albicans* infection (*217*). Neutrophils deficient in TLR2 exhibited a multitude of functional defects, including impaired MPO production and increased apoptosis (*218*). Several studies also illustrated a role for TLR2 in hematopoiesis in response to *C. albicans* both *in vitro* and *in vivo* (*219-221*). Actually, TLR2-dependent recognition of *Candida* yeasts geared differentiation of hematopoietic stem and progenitor cells (HSPCs) into macrophages and monocyte-derived DCs, which may serve to replenish the innate immune reservoir during *C. albicans* infection.

Despite a profound defect in mounting of Th1 responses following reinfection with *C. albicans*, TLR2$^{-/-}$ mice restored the TNFα secretion defect and developed vaccine-induced resistance (*222*). Lastly, in a gastric challenge with *C. albicans* hyphae, Bellocchio *et al.* described a skewed polarization in favor of IL-4-producing CD4^{+} T cells with a reciprocal reduction in IFNγ^{+}CD4^{+} T cells in TLR2-, TLR4-, TLR9-, IL1-RI-, and MyD88-deficient mice compared to wild-type controls (*205*).

In humans, genetic polymorphisms in TLR2 or TLR4 did not correlate with increased susceptibility to chronic mucocutaneous candidiasis or urogenital *C. albicans* infection (*223*, *224*). However, individuals bearing the TLR4 Asp299Gly and co-segregating Thr399Ile polymorphisms had an increased risk for developing *Candida* bloodstream infection, presumably by producing elevated IL-10 upon *Candida* stimulation (*225*).

TLR1 and TLR6

TLR1 or TLR6 act in concert with TLR2 to discriminate between the molecular patterns of triacyl and diacyl lipopeptide, respectively (*226*) and TLR2/TLR6 heterodimers are also able to recognize zymosan (*227*). In line with this, Jouault and colleagues demonstrated that phospholipomannan (PLM) purified from *C. albicans* induces translocation of the p65/RelA subunit of NF-κB and stimulates TNFα production in J774 macrophages (*210*). Consequently, deficiency in TLR6 led to a limited production of TNFα in peritoneal macrophages, while deletion of the TLR2 gene completely nullified the response (*210*). However, stimulation of *TLR1*$^{-/-}$ or *TLR6*$^{-/-}$ macrophages with *C. albicans* did not affect secretion of TNFα, IL-1α, IL-1β, or IL-6, but restimulation of splenocytes resulted in skewed T cell polarization with a reduction of IL-10 and a reciprocal increase in IFNγ in TLR6 knockout mice (*228*). Nevertheless, TLR1 and TLR6 were dispensable for host response to intravenous *C. albicans* challenge (*228*).

TLR7 and TLR9

Although signaling through endosomal TLRs TLR7 and TLR9, and ensuing induction of type I interferons (IFN-α/β), have been traditionally associated with antiviral responses (*229-231*), it has now been recognized that this axis is rather polyvalent. *C. albicans* DNA is recognized by TLR9 within endosomal compartments in DCs, and is dependent on the MyD88 adaptor protein for activation of NF-κB and cytokine production (*232*). *TLR9*$^{-/-}$ DCs produce little IL12p40 and IL12p70, but high amounts of IL-10 upon exposure with *C. albicans* DNA or *C. albicans* yeasts (*205*, *232*). Along the same line, Th2 T cell polarization predominated over Th1 in *TLR9*$^{-/-}$, with increased frequency of IL-4-producing $CD4^+$ T cells, and a reciprocal decrease in T cells producing IFNγ (*205*). Despite this disparate cytokine signaling, TLR9-defficiency had no discernable effect on phagocytosis and candidacidal activity of DCs (*205*), nor on tissue fungal burden and survival during *C. albicans* infection (*205*, *232*, *233*). Interestingly, immortalized macrophages from TLR9 KO mice displayed increased TNFα production and nitric oxide in response to *C. albicans* compared to WT mice, leading to increased microbicidal activity (*234*). More recently, it was shown that *C. albicans* or purified *C. albicans* RNA or DNA were able to induce type I IFN responses (IFNβ) in conventional DCs in part through TLR9 and TLR7 (*235*). Mice lacking the IFN-α/β receptor exhibited high fungal proliferation and increased mortality (*235*). Bourgeois *et al*, however, reported that stimulation of DCs with *C. glabrata* results in TLR7 but not TLR9 activation, and downstream activation of MyD88-IRF1 pathways (*236*). However, *IFNAR1*$^{-/-}$ mice were not susceptible to systemic *C. glabrata* infection (*236*). TLR7 was also partially required for IL-12p70 production, induced through the MyD88-IRF1 pathway (*237*). In disagreement with previous studies, TLR7- and TLR9-deficient mice were found to be highly susceptible to intravenous *C. albicans* infection (*237*).

1.3.1.3 NOD-like receptors and the inflammasome

In addition to TLRs and CLRs, mammals have evolved an auxiliary line of cytoplasmic PRRs, notably nucleotide-binding oligomerization domain-containing

(NOD)-like receptors (NLRs) that recognize a plethora of endogenous and exogenous agonists, as well as intracellular pathogens (reviewed in (*238*, *239*)). In response to these insults, NLRs activate caspase-1 through assembly of the inflammasome, a large multimeric complex that forms when each component is overexpressed in the cytosol (*238*, *239*). Ultimately, the inflammasome mediates caspase-1 clustering and triggers autoactivation, which is necessary for subsequent processing and secretion of proinflammatory cytokines, such as IL-1β and IL-18 (*240*).

The Nlrp3 inflammasome is composed of the Nlrp3 scaffold, the ASC (PYCARD) adaptor, and caspase-1, and plays an essential role in antifungal host defense. In fact, mice deficient in any of these components displayed higher fungal outgrowth and reduced survival compared to wild-type counterparts following intravenous (*112*, *241*, *242*) or oral challenge with *C. albicans* (*113*). Fungal β-glucans (*243*) or whole *C. albicans* yeasts (*112*, *113*, *242*) triggered caspase-1-dependent IL-1β secretion from human PBMCs, or mouse BMDM and DCs, albeit the fully hyphal form was less stimulatory (*113*, *242*). Interestingly, Joly and colleagues employed non-dimorphic *C. albicans* mutant strains or *C. glabrata* to demonstrate that morphologic switching was required to activate the Nlrp3 inflammasome (*242*). Consistently, secretion of IL-1β by *C. albicans*-stimulated BMDM and DCs derived from $Nlrp3^{-/-}$, $ASC^{-/-}$, or $caspase\text{-}1^{-/-}$ mice, was severely impaired (*112*, *113*, *241-243*). While the known fungal PRRs TLR2 and Dectin-1 (*113*) signal through Syk and the CARD9 adaptor protein (*112*) to mediate IL-1β gene transcription, CARD9 is dispensable for inflammasome activation (*112*). Instead, inflammasome activation and subsequent production of bioactive IL-1β by curdlan (*243*) or the fungus (*112*) involved reactive oxygen species production and potassium efflux. Aberrant inflammasome-mediated production of IL-1β has grave repercussions on the downstream induction of Th1 signature cytokines IL-17 and IFNγ (*241*, *244*), which are important for host defense against disseminated candidiasis. Kumar *et al.* reported that Nlrp3-deficient mice displayed normal Th1 and Th17 cell differentiation when curdlan was administered, whereas B cell activation and antibody production was impaired in these mice (*243*).

Lastly, NLR family member Nlrp10, but not Nlrp6, Nlrp12, and Nlrc4, was required for control of disseminated *C. albicans* infection *in vivo* (*245*). The effect of Nlrp10 deficiency on the extent of fungal burden and renal damage was most evident at later times during infection (*245*). Analogously to $Nlrp3^{-/-}$, $Nlrp10^{-/-}$ mice displayed a profound defect in Th1 and Th17 cell differentiation.

1.3.1.4 Other receptors

The aforementioned inventory of PRRs involved in recognition of *C. albicans* is certainly not exhaustive, as novel research continuously identifies additional players involved. For example, macrophage Galectin-3 has been shown to discriminate between pathogenic and nonpathogenic fungi by specifically recognizing β-1,2-linked oligomannosides on *C. albicans* surface (*246-248*) resulting in candidacidal activity (*247*). While Galectin-3 is dispensable for the recognition and endocytosis of yeasts, its partnership with TLR2 is essential for optimal downstream TNFα production (*248*). In addition, Esteban *et al.* reported that association of Galectin-3 and Dectin-1 triggered an appropriate TNFα response (*117*). Finally, Galectin-3 signaling played an important protective role against disseminated candidiasis (*249*), while it only modestly affected the gastrointestinal infection model (*250*).

Furthermore, although not an independent fungal receptor *per se*, the accessory FcγR was shown to interact with Dectin-2 to induce intracellular signals upon *C. albicans* hyphae recognition, as described earlier (*128*, *129*). Interestingly, Romani *et al*. found that entry through FcγR route suppressed mannose-receptor-dependent activity and resulted in the production of anti-inflammatory cytokines IL-4 and IL-10 by DCs, and ensuing pathology (*251*).

Finally, an shRNA screen in mouse macrophages uncovered two evolutionarily conserved members of the scavenger receptor family, SCARF1 and CD36, that participate in the recognition of *C. albicans* and *C. neoformans* (*252*). Using mouse macrophages, it was further established that CD36 binds *C. albicans* in a β -glucan-dependent manner, and that CD36 deficiency markedly abrogates

transcription of several proinflammatory cytokines and chemokines, notably IL-1β, TNFα, IL12p40, MIP-2, MIP-1α, MIP-1β, and RANTES, while IFNγ was not affected (*252*). The mechanisms underlying these observations remain to be resolved.

1.3.2 Complement pathway

The complement system is one of the evolutionarily oldest pillars of immunity, estimated to have emerged at least 600-700 million years ago (*253*). The term "complement" was coined over a century ago to describe a heat labile system that complements the action of immunotoxic serum (*254*). Traditionally, it was merely perceived as a supportive first line of defense against microbial intruders, rapidly detecting and eliminating pathogens. In recent years, the emerging roles of complement in a plethora of immunological and inflammatory processes led to the appreciation that this serum protein cascade operates as a central regulator of innate and adaptive immunity (reviewed in (*254-256*)).

1.3.2.1 Complement cascade

The complement system (Figure 3) consists of a set of soluble proteins that are present as inactive precursors in the plasma and are activated in a cascading manner via three distinct but intersecting activation pathways: the classical, lectin, and alternative pathway.

The classical pathway is often considered antibody-dependent as the C1 multimeric complex (consisting of a hexameric C1q, and two copies of C1r and C1s proteases; $C1qr_2s_2$ (*257*)) recognizes surface-bound immune complexes composed of IgG and IgM. However, the versatile pattern recognition molecule (PRM) C1q also binds to an array of non-immunoglobulin ligands, either directly on microbial and apoptotic cells, or via endogenous PRMs such as pentraxins (reviewed in (*258*)). In turn, this binding elicits consecutive activation of C1r and C1s, ultimately resulting in

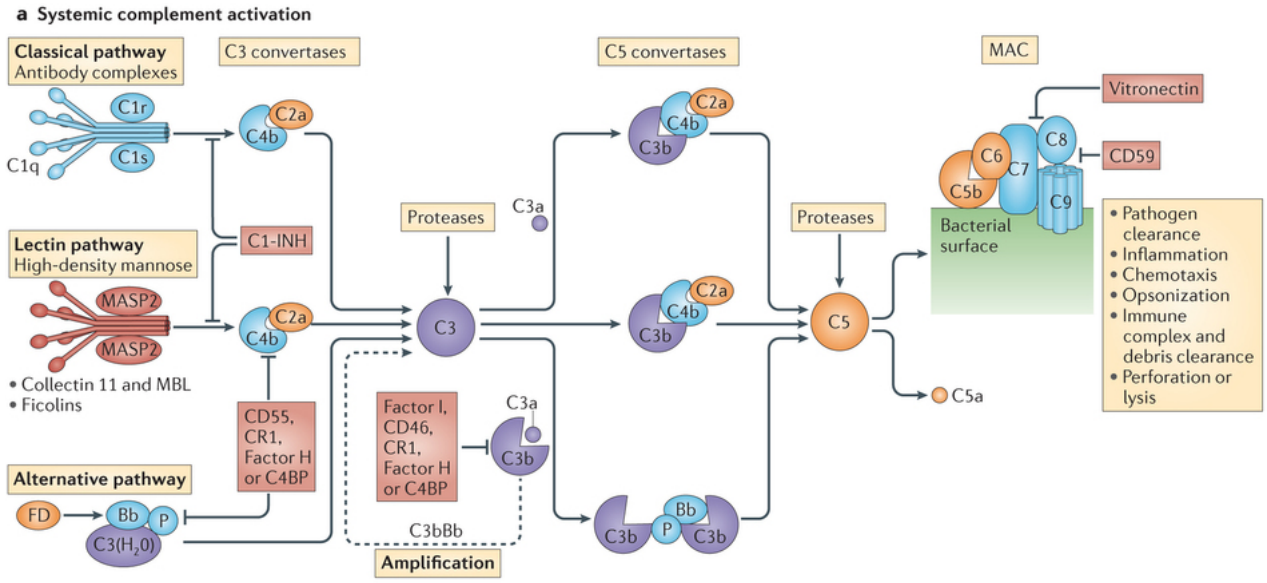

Figure 3. The complement cascade

Overview of the classical, lectin, and alternative pathways of complement cascade. Complement regulators are enclosed in red boxes. Please see the corresponding section for a detailed description. Figure reproduced, with permission, from *(256)*.

C1s-mediated cleavage of C4 and C2 substrates into the surface bound C3 convertase C4bC2a (also referred to as C4bC2b, depending on the nomenclature of the proteolytic C2 fragment) (*259*, *260*).

The lectin pathway is initiated through recognition of carbohydrate patterns on the invading microbe by collectins MBL (*261*) and collectin-11 (*262*), as well as the ficolin protein family members ficolin-1 (*263*), ficolin-2 (*264*), and ficolin-3 (*265*) (reviewed in (*266*)). These PRMs are assembled with the proenzyme form of MBL-associated serine proteases (MASPs) that share structural similarity with C1r and C1s (*267*). The present consensus is that MASP-2 cleaves both C2 and C4 to generate the same classical pathway C3 convertase C4bC2a, whereas MASP-1 probably amplifies the convertase formation through C2 cleavage (*268*, *269*).

The alternative pathway begins with the formation of an initial fluid-phase C3 convertase ($C3_{H2O}Bb$) that is constantly generated at a low rate (tick-over) in blood (*270*, *271*), acting as a sentinel keeping complement vigilant. A fraction of circulating C3 is spontaneously hydrolyzed to $C3_{H2O}$, thereby exposing high affinity binding sites for the protease factor B (fB) (*271*). Subsequent cleavage of fB into Bb and Ba by factor D (fD) yields the active C3 convertase $C3_{H2O}Bb$, which further perpetuates the pathway by generating the nascent C3b component. Analogously to C4b, the opsonin C3b is deposited on the cell surface targeting pathogens for phagocytosis, and/or recruiting fB, albeit with a lower affinity than $C3_{H2O}$ (*271*). This complex recruits fD, which cleaves fB into Bb and Ba to form a highly active enzymatic complex, C3bBb, which markedly amplifies the cycle of C3 cleavage and convertase assembly (*271*, *272*). Additionally, the alternative pathway may be triggered through a PRM-based mechanism, which entails recognition of pathogen- and danger-associated molecular patterns (PAMPs and DAMPs, respectively) on foreign and apoptotic cells by properdin (*273*). Once bound, properdin provides a platform for fluid-phase C3b binding and *de novo* convertase assembly (*273*), although it may also associate with and stabilize the already established C3bBb complex (C2bBbP) (*274*). Interestingly, Harboe and colleagues demonstrated through blockade of fD that the alternative pathway accounts for 80-90% of total complement activation, even when

triggered by the classical pathway (*275*).

The formation of C3 convertases C4bC2a or C3bBb represents the converging point of all complement activation pathways, ultimately generating the opsonin C3b and the anaphylatoxin C3a. Accumulation of deposited C3b gradually leads to the appendage of C3b molecules to C3 convertases (C4b2a3b or C3bBb3b), thereby altering substrate specificity from C3 to C5 (*276*). These C5 convertases cleave its substrate into the potent anaphylatoxin C5a and fragment C5b. The latter fragment associates with terminal components C6, C7, C8, which induce the insertion of several tubular units of C9 into the cell membrane to form a lytic pore, collectively referred to as the membrane attack complex (MAC or terminal complement complex (TCC)) (*277*). Besides MAC-mediated lysis, sublytic amounts of MAC or partial complexes direct a range of cellular signaling events, depending on the cell type and environmental context (*278*). Additionally, C3 and C5 activation can occur via convertase-independent auxiliary routes mediated by several proteases, such as those appertaining to the co-agglutination system, and the cathepsin and granzyme families (reviewed in (*256*)).

1.3.2.2 Role of complement in candidiasis

Earlier *in vitro* studies employing murine (*279*, *280*) or human peripheral blood leukocytes (*55*, *281-284*) delineated a central role for complement activation in phagocytosis and fungicidal activity against *C. albicans*. Efficient oxidative response of neutrophils exposed to *Candida* also relied on the integral complement system, notably via opsonization by heat labile components such as C3b (*285*, *286*).

As previously mentioned, the classical pathway is triggered by naturally occurring antibodies against highly immunogenic polysaccharide mannan, the major cell wall component of *Candida* (*287*, *288*). Uniform deposition of C3b through mannan-specific antibodies via the classical pathway occurred within the first minute of yeast exposure (*287*, *289*). A blockade of the classical pathway by absorption of serum antibodies or by calcium chelation introduced a lag in initial binding kinetics, and altered the pattern of C3b deposition to discrete alternative pathway initiation

sites (*287-289*). Recently, it was established that complement factors C3b/C3d were more readily deposited onto β-1,6-glucan moieties, although it remains unclear which activation pathway mediates this binding (*290*). Accordingly, human antibodies directed against mannan promoted phagocytosis and killing of *C. albicans* by mouse peritoneal macrophages, and conferred protection in a model of lethal intravenous infection (*291*). On the other hand, deficiency of the classical pathway in C1qa$^{-/-}$ mice had little impact on the survival rate and fungal growth in target tissues (*193*). In contrast, Peltz and colleagues reported a combinatorial genetic interaction involving *C5* and *C1r/s* alleles that accurately predict survival after *C. albicans* infection (*292*). They postulated that interaction between C1 components with different haplotypes might reduce the formation or stability of the C1 complex, thereby decreasing C1q binding to *Candida* and constituting a rate-limiting step for classical pathway activation.

The soluble pattern recognition receptor MBL binds to mannose residues on the *Candida* surface and activates the lectin pathway (*185*, *293*). Intravenous injection of *C. albicans* in mice caused a rapid decline in serum MBL, concomitant with increased C3 concentration and complement activity (*192*). Indeed, MBL deposition on fungal surface occurred almost instantaneously, sequentially promoting opsonization by C4 and C3 derivatives (*187*, *188*). Similarly, collectin-11 (CL-11) also induced binding of C4b, C3b, and TCC on *C. albicans* in a dose-dependent manner, while rCL-11 restored complement activation of CL-11-depleted sera (*262*). Although MBL facilitated opsonophagocytosis of *C. albicans* by human neutrophils (*186*, *187*), Ip and Lau did not observe this phenotype with human monocyte-derived DCs (*188*). Recently, Ma *et al.* provided evidence that MBL-pentraxin heterocomplexes can trigger cross-activation of complement, leading to enhanced C3 and C4 deposition as well as uptake of *C. albicans* by neutrophils (*294*). Moreover, exogenous MBL rescued anti-Dectin-1-blocked yeast phagocytosis by neutrophils, independently of complement activation (*189*). The increased mortality of MBL-A/C$^{-/-}$ mice (*193*) and improved survival rates of MBL-treated animals (*185*) during intravenous *C. albicans* challenge underline the role of the lectin pathway in host defense against disseminated candidiasis.

The fundamental role of C5 on survival and/or enhanced fungal clearance following *C. albicans* intravenous challenge was demonstrated using animals devoid of C5, such as CF-1 mice (*295*), B10.D2-*Hc*^{0} (*296*), inbred mouse strains A/J and DBA/2J (*9*, *10*, *297*), and BcA17 RCS (*298*). Indeed, genetic linkage analysis carried out in informative F2 animals derived from the resistant C57BL/6J and susceptible A/J strains verified the contribution of the C5 locus, explaining the majority of phenotypic variance observed for survival, fungal burden in all target tissues, and circulating TNFα levels (*7*). C5-deficiency in A/J and BcA17 mice was associated with defective granulocyte recruitment, high fungal burden in all tissues, and an unabated amplification of a cytokine response to invasive *C. albicans* infection, exemplified by high levels of proinflammatory TNFα, IL-6, MCP-1, MCP-5, and eotaxin (*298*). Additionally, A/J and BcA17 mice developed severe cardiomyopathy as a result of *C. albicans*-induced cytokine storm and pathological tissue damage that could be remedied by treatment with C5-sufficient serum (*299*). In the footpad model of local *C. albicans* infection, C5-deficient DBA/2 mice displayed higher level of colonization, and a reduced inflammatory infiltrate ascribed to a defective chemotactic response compared their complement sufficient DBA/1J counterparts (*300*). Passive transfer of C5-sufficient serum into susceptible DBA/2 mice markedly reduced the magnitude of renal and brain fungal burden (*301*).

Using sera from C5-deficient kindred, Rosenfeld and colleagues delineated its critical impact in the generation of neutrophil chemotactic activity, as opposed to a nonobligatory or minimal role in opsonophagocytosis of *S. cerevisiae* and *C. albicans* (*302*). While slight C5 activity was sufficient to promote normal phagocytosis and killing of *S. aureus*, serum entirely deplete of this complement component lacked bactericidal activity against *S. typhi* (*302*). More recent studies carried out with C5-deficient serum revealed that expression of tissue factor, cell adhesion molecules, and oxidative burst depended on C5a, while granule enzyme release relied on C3 (*303*). Interestingly, C5 induced release of IL-1β and IL-8, while IL-1ra was inhibited (*303*). While Lappegard *et al*. claimed that phagocytosis and killing of *E. coli* were reduced under C5-deficient conditions, Cheng and colleagues reported no inadequacies in candidacidal activity (*304*). Blocking of C5a or C5aR decreased *C. albicans*-induced

production of IL-6 and IL-1β and the effect could be phenocopied using C5-deficient serum (*304*). Taken together, these findings reveal a central role of C5a in proinflammatory cytokine production upon contact with *C. albicans.*

Furthermore, mice deficient in C3 (*8*) or both factor B and C2 (Bf/C2$^{-/-}$) (*193*), as well as guinea pigs treated with cobra venom factor (CVF) or deficient in C4 (*305*), were found to be highly susceptible to *C. albicans* infection as they are unable to transduce complement activation. Tsoni and colleagues affirmed that the absence of C3 impaired fungal clearance, but did not affect the inflammatory response in an intraperitoneal infection model (*8*). The inability to activate the complement cascade led Bf/C2$^{-/-}$ mice to rapidly succumb to *C. albicans* infection possibly through inadequate granulocyte mobilization (*193*).

A case report describing complete deficiency of factor I (CFI) and lowered factor H levels (CFH), concomitant with decreased serum C3 concentration and curtailed hemolytic activity, revealed an aberrant chemotactic and opsonophagocytic activity of the patient's serum (*306*). Indeed, CFH family proteins were found to mediate adhesion of human neutrophils to *C. albicans*, thereby enhancing the generation of ROS and potentiating the release of lactoferrin, which in turn augmented fungal killing (*307*).

Direct yeast lysis via formation of the MAC is considered unlikely because of the thickness and complexity of the fungal cell wall (*289*). Nevertheless, the reduced neutrophil phagocytic efficiency in the absence of C6 and C7 unveiled a modest but discernable role for the terminal complement factors in immune defense against *C. albicans* (*308*). Moreover, formation of the MAC on the fungal surface modulated neutrophil functions, triggering a rapid and sustained release of C6 and C7, which markedly subsided when *C. albicans* was opsonized with serum deficient in or depleted of these complement factors (*309*).

Evidently, *Candida* activates all three pathways of the complement system, with a preponderant role of the alternative and lectin pathways over the classical activation in antifungal defense, and a bona fide requirement for C5 in host defense

against invasive *C. albicans* infection.

1.3.3 Innate immunity effectors

The innate immune system, which encompases the complement system and additional cellular effectors (Figure 4), constitutes a highly efficacious first line of defense against invading pathogens. In response to invasive *C. albicans* infection, the competency of innate immunity will dictate disease outcome.

1.3.3.1 Neutrophils

Neutrophils are the most notorious players in antifungal immunity. Their contribution to host defense has been appreciated for more than half a century, based on the observation that neutrophil-depleting cytotoxic chemotherapy for treatment of acute leukemia coincided with the rise of fatalities caused by bacterial and fungal infections in these patients (*310*). Subsequent studies using neutrophils derived from patients with inherent phagocyte disorders, such as MPO deficiency and CGD, enabled Lehrer and others to delineate some of the key mechanisms involved in host defense to *Candida* infections (*55*, *57*, *58*, *311*). Neutrophils readily interact with, phagocytose, and kill *C. albicans*. Phagocytic efficiency is heavily dependent on heat-labile complement opsonins as well as antibodies, which spur the classical and alternative pathway of complement activation, respectively (*55*, *187*, *283*, *284*, *312*, *313*). As depicted in Figures 3 and 4, neutrophils recognize β-1,6-glucan moieties on *C. albicans* (*290*) and initiate phagocytosis largely through a concerted action of Dectin-1 and C3R (also known as Mac-1) (*120*, *314*). Human neutrophils avidly ingested opsonized *Candida* with an average of 2 blastospores per neutrophil, although up to 10 yeasts in a given cell have been observed (*284*, *315*). Approximately 30 percent of ingested yeasts are killed, irrespective of the number of phagocytosed blastospores, while persisting yeasts germinate and escape by rupturing

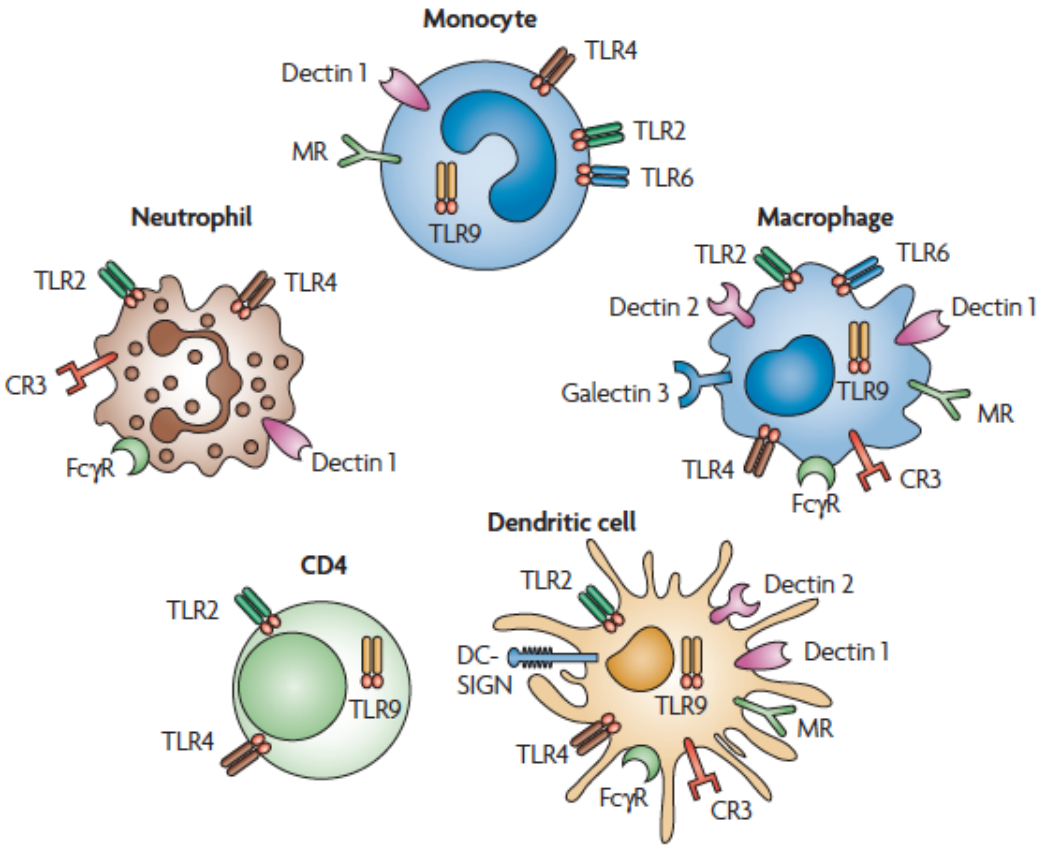

Figure 4. Major cellular effectors in response to *C. albicans* infection

Equipped with an array of PRRs, the innate immune effectors constitute the first line of defense against invading pathogens. *C. albicans* is phagocytosed and killed mainly by neutrophils and monocytes, while macorphages and DCs present antigen to naïve CD4 lymphocytes that will ultimately polarize into an appropriate effector subset. The figure is reproduced, with permission, from *(493)*.

the cell wall (*25*, *55*, *284*). Neutrophils possess a battery of both oxidative and non-oxidative killing mechanisms (reviewed in (*316*)). In earlier studies, Lehrer and colleagues correlated MPO and NADPH oxidase activity with neutrophil candidacidal potential, as genetic deficiencies in these components manifested in aberrant killing of *C. albicans* (*55*, *57*, *58*). As illustrated in Figure 5, while NADPH oxidase provides electrons for the generation of superoxide anions within the phagosome, MPO consumes H_2O_2 to oxidize chloride to hypochlorous acid, a potent microbicidal agent (*316*, *317*). In the absence of MPO, neutrophils might resort to the far less effective superoxide and H_2O_2, resulting in a considerable delay in killing (*56*, *57*). Aratani *et al.* reiterated the critical impact of MPO, as MPO-deficient mice were deemed susceptible to pulmonary and intraperitoneal *C. albicans* challenge, albeit moderately compared to X-CGD mice ($gp91^{phox}$ knockout) (*59*, *60*). In addition, live imaging of disseminated candidiasis in zebrafish in the setting of $p47^{phox}$ deficiency enabled Brothers *et al.* to demonstrate that NADPH oxidase was required for restraint of *C. albicans* filamentation *in vivo* (*318*). Nonetheless, the ability of MPO-deficient and CGD neutrophils to kill certain *Candida* species provided evidence for a secondary non-oxidative killing mechanism involving antimicrobial proteins (*68*, *311*, *319*, *320*).

Neutrophils possess a compendium of antimicrobial proteins contained within cytoplasmic granules (reviewed in (*321*)). Upon phagocytosis of opsonized zymosan and hyphae, actin polymerization is increased concomitant with degranulation and release of β-glucuronidase and lactoferrin (*322*). Murthy and colleagues reported that purified preparations of lactoferrin, myeloperoxidase, lysozyme, HNP-1, cathepsin G, and elastase did not exert candidacidal effect; instead, the candidastatic property of the cytosol was associated with the calprotectin complex (*323*). Mice deficient in calprotectin were susceptible to both intranasal and invasive *C. albicans* infection (*324*). Moreover, Lehrer *et al.* demonstrated that purified human defensins, HNP-1 and HNP-2, killed *C. albicans in vitro* (*325*). Neutrophils from a transgenic mouse strain ($Def^{+/+}$) that expresses approximately 10% of HNP-1 and HNP-2 human content exhibited significantly improved *C. albicans* killing compared to wild-type mice (*25*). In addition, lactoferrin peptide supplementation induced increased

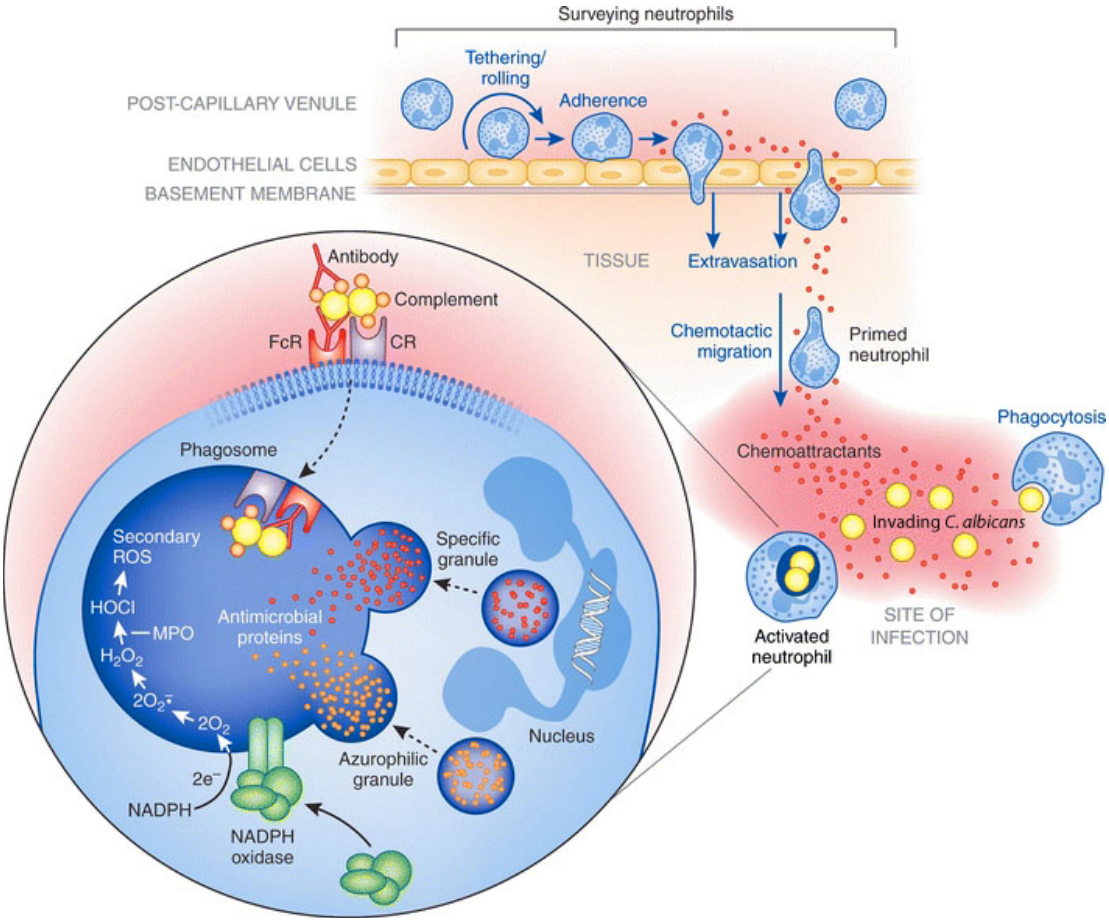

Figure 5. Neutrophil recruitment to the site of infection and their effector functions

Prompt recruitment of neutrophils to the site of infection entails several sequential steps, which prime the neutrophil. Activated neutrophils contain an arsenal of antimicrobial effector functions to confront invading *C. albicans*, such as ROS production, antimicrobial proteins, and NETs (not shown). Adapted, with permission, from *(317)*.

phagocytosis, ROS production, and *C. albicans* killing by neutrophils, improving the survival of mice challenged with *C. albicans* intraperitoneally (*326*). While IL-8 stimulated the release of azurophilic enzymes (*327*), LPS induced release of lactoferrin (*328*), both of which inhibited *Candida* growth.

It has been recognized for decades that neutrophil death and dissolution may represent an alternative host defense mechanism against invasive *C. albicans* infection (*329*). Brinkman and colleagues recently defined a novel aspect of neutrophil death, whereby PMA- or IL-8-activated neutrophils release extracellular fibers (neutrophil extracellular traps; NETs) that contain chromatin and granular proteins (*324*, *330*). It is postulated that NETs form to ensnare invading microbes, prevent them from spreading, and provide a rich antimicrobial milieu to degrade virulence factors and kill pathogens. Besides bacteria, NETs also captured and killed *C. albicans*, whereas incubation with DNAse abolished NET formation and extracellular killing (*331*). The killing aptitude of NETs was recently challenged, as entrapped bacteria and yeasts are released and recovered in cell medium when NETs are dismantled with DNAse (*332*). Nonetheless, Urban *et al.* demonstrated that granular extracts, rather than histones, exerted candidacidal activity (*331*). In particular, calprotectin (S100A8/A9) is a major antifungal component associated with NETs, limiting *C. albicans* growth in a Zn^{2+}- and Mn^{2+}-dependent manner (*324*). Abrogation of calprotectin by means of antagonistic antibodies or genetic deficiency limited the candidacidal capacity of NETs, leading to increased susceptibility of calprotectin-deficient mice to invasive *C. albicans* infection (*324*). Formation of NETs in CGD patients is restored by addition of exogenous hydrogen peroxide, implying an important role for the NADPH oxidase (Nox) (*333*). Accordingly, $gp91^{-/-}$ mice deficient in the Nox complex are thus unable to form NETs (*334*). Similarly, neutrophils from MPO-deficient individuals failed to form NETs, indicating that MPO is required for NET production (*54*). Taken together, the inability to form NETs may undermine the antifungal host defense in these patients.

There is a growing body of evidence suggesting that neutrophils are not only capable of secreting cytokines themselves, but can also transiently interact with and

modulate the behavior of other cellular effectors. Neutrophils exposed to *C. albicans* released TNFα, which in turn prolonged their survival, as did exogenous TNFα (*335*, *336*). In response to LPS, neutrophils produced TNFα, IL-1β, and IL-6 (*328*), whereas stimulation of murine neutrophils with curdlan induced release of IL-10 (*111*). Dependent on contact via ligation of CD18, *C. albicans*-loaded neutrophils delivered activation signals to DCs that elicited IFNγ and IL-2 production by T cells (*337*). Interestingly, *in vitro* data suggest that NK cells assume a phagocytic role in the absence of neutrophils (*338*). In a co-culture system, however, neutrophils showed enhanced activation and counteracted the proinflammatory response of NK cells (*338*). Similarly, neutrophils dampened production of the proinflammatory cytokines IL-1β and TNF-α by human PBMCs in response to *C. albicans* and LPS via protease-mediated degradation (*339*).

Moreover, human or murine neutrophils can be stimulated with TNFα (*340*, *341*), IFNγ (*340*, *342*, *343*), IL-15 (*344*), or IL-33 (*345*) to further enhance phagocytosis, prime the respiratory burst, or augment *C. albicans* killing. IL-15 (*344*) and IL-2 (*346*) enhanced both transcriptional and translational expression of the chemokine IL-8 in neutrophils, which was further amplified in the presence of *C. albicans* (*344*). Moreover, administration of IFNγ to mice limited fungal outgrowth in tissues, and potentiated neutrophil killing of *C. albicans ex vivo* (*347*). IL-33 treatment conferred protection to invasive *C. albicans* challenge, augmenting neutrophil mediated antifungal functions and thereby survival (*345*). LPS or zymosan pretreatment also enhanced neutrophil candidacidal activity, whereas LTA completely abolished *Candida* killing (*205*, *328*). Conversely, the anti-inflammatory cytokine IL-10 suppressed *C. albicans* phagocytosis and hyphal damage by human neutrophils (*348*).

In humans, and in mouse models, efficient granulopoiesis, timely recruitment to the site of infection, and robust effector functions are required for protection during *C. albicans* infection (Figure 5). The induction of neutropenia in mice, either by ablative cyclophosphamide treatment (*349*) or via depletion with Gr-1 mAb (*350*, *351*), rendered mice highly susceptible to systemic *C. albicans* challenge. Neutrophil

depletion also impaired resistance to reinfection in immunized mice (*352*). On the other hand, administration of an activated neutrophil-like cell line, HL-60, markedly improved survival and enhanced fungal clearance in *C. albicans*-infected neutropenic mice (*353*). Granulocyte colony stimulating factor (G-CSF) is the major cytokine governing the steady-state production of neutrophils *in vivo*, with further contributions from GM-CSF and IL-6 (reviewed in (*354*)). While G-CSF is commonly prescribed to correct neutropenia that accompanies immunosuppressive therapy (*355*), several studies examined its effect on neutrophil functional activity in the context of opportunistic infections. Notably, G-CSF-stimulated neutrophils exhibited increased ROS production (*342*, *356*, *357*), with (*343*, *357*, *358*) or without (*342*, *356*, *359*) an enhanced effect on phagocytosis or *Candida* killing. Concordantly, G-CSF administration improved survival of neutropenic mice following systemic *C. albicans* infection (*360-362*). Similarly, GM-CSF potentiated candidacidal activities of human neutrophils (*357*, *363*).

Interestingly, although G-CSF$^{-/-}$, G-CSF$^{-/-}$/GM-CSF$^{-/-}$, and G-CSF$^{-/-}$/IL-6$^{-/-}$ mice are neutropenic at steady-state, they all mounted peripheral neutrophilia in response to systemic *C. albicans* challenge, reflecting the complex, redundant regulation of granulopoiesis (*364*). Nonetheless, these mice displayed elevated renal fungal burden, underscoring the importance of an adequate supply of neutrophils during infection, even in the context of functional competency (*364*, *365*). Using FACS and immunohistochemistry, Lionakis and colleagues recently delineated the temporal and spatial dynamics of cellular immune response in various organs of C57BL/6J mice infected systemically with *C. albicans* (*366*). Neutrophils constituted the principal leukocyte subset recruited to the spleen, liver, and kidney, albeit significantly less neutrophils were encountered in the kidney during the initial 24h after infection onset, which might account for the untamed fungal growth and enhanced *Candida* filamentation in this organ (*366*). Indeed, mice deficient in TNF$\alpha^{-/-}$/LT$^{-/-}$ (*367*), IL-8Rh$^{-/-}$ (CXCR2) (*368*), IL-17AR$^{-/-}$ (*369*), and TLR4$^{C3H/HeJ}$ (*212*) were more susceptible to systemic *C. albicans* challenge due to impaired recruitment of neutrophils to the site of infection. In TNF$\alpha^{-/-}$/LT$^{-/-}$ and IL-8Rh$^{-/-}$ mice, reduced neutrophil recruitment was additionally compounded with impaired neutrophil

phagocytosis (*367*) and ROS generation (*368*), respectively. Alternatively, MRL/lpr mice showed increased resistance to *C. albicans* infection compared to their wild type counterparts, possibly due to enhanced neutrophil recruitment rather than functional alterations (*370*). Similarly, platelet-activating factor (PAF) rendered mice more resistant to candidiasis by markedly increasing neutrophil recruitment to kidneys (*371*). Neutrophil emigration is a multi-step process (reviewed in (*372*)), which can be impeded by insufficient chemotactic stimuli and/or loss of adhesion molecules. The human chemokine CXCL2 (also known as IL-8) and the mouse analogues CXCL1 (also known as KC), CXCL2, and CXCL5 signal through the CXCR2 receptor and constitute potent tandems for neutrophil activation and adhesion to the endothelium (*372*). In fact, exposure of human neutrophils to recombinant IL-8 stimulated chemotaxis, which was counteracted by antagonistic antibody treatment (*346*). Consequently, mice deficient in CXCR2 were more susceptible to *C. albicans* infection (*368*), as were mice deficient in the cell adhesion molecule ICAM-1 (*373*). However, persistent neutrophil infiltration at later time points, driven by Ccr1, resulted in severe immunopathology, decreased kidney function, and accelerated mortality (*374*). The role of type I interferons in systemic *C. albicans* infection remains controversial. Using Ifnar1$^{-/-}$ mice, Majer and colleagues reported that IFN-I signaling results in overt recruitment of inflammatory monocytes and neutrophils that drive hyper-inflammation and lethal kidney pathology (*375*). In contrast, del Fresno *et al*. claimed that type I interferons were crucial for host defense, as Ifnar1$^{-/-}$ mice exhibited increased mortality and elevated fungal burden, attributed partly to aberrant chemokine production and poor neutrophil recruitment (*376*).

Novel genes implicated in neutrophil innate antifungal immunity include calcineurin B (*CnB*) (*111*), Jun dimerization protein 2 (*Jdp2*) (*377*), lipocalin 24p3 (*24p3*) (*378*), and Jagunal homolog 1 (*Jagn1*) (*379*). Conditional deletion of *CnB* in neutrophils display increased fungal burden and compromised survival (*111*), while susceptibility of Jdp2$^{-/-}$ mice was attributed to defects in neutrophil differentiation and function (*377*). Deficiency of the neutrophil secondary granule protein, 24p3, compromised neutrophil chemotaxis and extravasation to sites of infection (*378*). Consequently, 24p3$^{-/-}$ mice displayed elevated fungal outgrowth and increased

mortality upon systemic *C. albicans* infection (*378*). *Jagn1* deletion under the *Vav1 iCre* driver impaired neutrophil migration and formation of cytotoxic granules, resulting in increased fungal outgrowth and reduced survival (*379*). Altogether, intact neutrophil function is key to the establishment of a competent innate antifungal immune response, ultimately protecting mice from fungal outgrowth, organ pathology and mortality.

1.3.3.2 Monocytes/macrophages

While neutrophils take center stage in host defense against systemic candidiasis, the contribution of monocytes/macrophages during infection has been less credited. Early *in vitro* studies with human peripheral blood monocytes produced contentious results, either supporting an increased (*380*), reduced (*55*, *68*) or comparable (*282*) candidacidal activity to that of neutrophils, owing to methodological variations. Nonetheless, Nelson and colleagues quantified ROS generated in response to bacteria, fungi, or zymosan, corroborating the aptness of human monocytes to produce superoxide, albeit to a lesser extent than neutrophils (*381*). As monocytes differentiate into macrophages, the loss of MPO is concomitant with the inability to generate a strong oxidant such as hypochlorous acid, thereby accounting for diminished ROS production and limited candidacidal potential of macrophages (*382*, *383*). The notion of MPO-independent superoxide generation by NADPH oxidase was pioneered by Lehrer and colleagues on the premise that monocytes from a patient with MPO deficiency could kill *C. parapsilosis*, but those from CGD-afflicted individuals could not (*68*). This idea was further supported by Decker et al., who reported that addition of catalase to Kupffer cells hardly influenced generation of ROS in response to *C. albicans* (*384*), while Diamond and colleagues observed non-oxidative damage to hyphae (*385*). Alternatively, a combination of NO together with MPO-independent superoxide (O^{2-}) gives rise to the formation of another potent oxidant, peroxinitrine ($ONOO^{-}$) (*386*). It is believed that enhanced resistance of mice to systemic candidiasis initially attributed to macrophage-derived NO production (*387*), is actually mediated by peroxinitrite (*388*).

Moreover, several studies have shown that the fungicidal capacity of monocytes/macrophages can be potentiated by priming with IFNγ (*154*, *389-391*), TNFα (*341*), IL-15 (*392*), and CSFs (*52*, *152*, *393*, *394*). Conversely, IL-4 suppressed uptake of blastospores by human mononuclear phagocytes, generation of ROS, and hence candidacidal activity (*395*). Similar observations were reported with IL-10, with the exception of an unusual increase in phagocytosis (*396*). In agreement with these studies, Cenci and colleagues reported that IL-4 and/or IL-10 abrogated NO production, and consequently candidacidal potential, by IFNγ-activated murine peritoneal or splenic macrophages (*397*).

Although monocytes/macrophages may not be as competent in killing as neutrophils, they produce an array of chemokines and cytokines, such as IL-8 (*327*, *398*), TNFα (*340*, *398*, *399*), IL-1β (*398*), thereby potentiating neutrophil phagocytic and fungicidal activity (*400*).

Mice in which macrophages were selectively ablated using clodronate displayed increased mortality and augmented fungal outgrowth in target organs, demonstrating a protective role of macrophages during disseminated *C. albicans* challenge (*401*). In contrast, monocytopenia induced by etoposide did not exacerbate infection parameters; rather, granulocytes were ascribed a dominant role during the course of disseminated infection (*402*). Both studies may not accurately portray the complex heterogeneity of monocyte/macrophage subsets present in various anatomical sites, as Decker and colleagues illustrated subset-specific capacity and mechanism engaged to inhibit *C. albicans* growth (*384*). A more recent report assessed the expansion and/or infiltration of various leukocytes into tissues in response to *C. albicans* infection, underscoring highly idiosyncratic immune responses for each organ tested (*366*). A pivotal study by Geissmann *et al.* unveiled two existing functional monocyte populations in mice and humans, notably the inflammatory and patrolling monocytes (*403*). Inflammatory monocytes are designated as $CCR2^{+}Ly6C^{hi}$ and $CD14^{++}CD16^{-}$ in mouse and human, respectively; whereas murine $CCR2^{-}Ly6C^{lo}$ (resident/patrolling) monocytes are analogous to human $CD14^{+}CD16^{+}$ monocytes (*404*). Human inflammatory monocytes exhibited a

robust proinflammatory cytokine production and candidacidal activity *in vitro* compared to their patrolling counterparts, inducing a protective Th17 response upon *Candida* recognition (*167*). Consonantly, studies in $Ccr2^{-/-}$ and Ccr2 DTR depleter mice revealed that inflammatory monocytes rapidly infiltrated infected kidneys, exerting a protective effect by limiting fungal growth in the kidneys and brain, thus promoting survival (*405*). However, overt infiltration and activation of inflammatory monocytes and neutrophils into kidneys, mediated by type I interferons, was shown to promote hyper-inflammation and lethal kidney pathology (*375*). Furthermore, Cx3cr1 deficiency in mice abates resident macrophage accumulation in the kidney, rendering mice more susceptible to systemic candidiasis compared to $Ccr2^{-/-}$ knock out animals (*406*).

In humans, the role of monocytes in antifungal immunity is less well established. Deficiencies in *GATA2* (*407*, *408*) or *IRF8* (*409*) cause inherent monocytopenia, predisposing patients to nontuberculous mycobacterial infections, although invasive infections with *Aspergillus* and *Cryptococcus*, as well as oral candidiasis have been reported in some patients. It remains debatable whether the preservation of tissue-resident macrophages in these patients is directly responsible for protection against invasive candidiasis. However, in two independent patient cohorts, the dysfunctional *CX3CR1-M280* allele constituted a risk factor for development of candidemia and disseminated candidiasis (*406*), implying a role for resident macrophages in human antifungal defense.

1.3.3.3 Dendritic cells (DC)

Dendritic cells (DCs) are highly efficacious professional antigen-presenting cells that sense and patrol the body for intruding pathogens, initiating a host response and tailoring pathogen-specific adaptive immune responses (*410-412*). Although host resistance against *C. albicans* infections is mediated predominantly by neutrophils and monocytes/macrophages, *C. albicans* is phagocytosed, killed and processed for antigen presentation by mouse and human DCs (*413*, *414*). As described earlier, DCs express a myriad of PRRs, including TLRs, CLRs, Fc receptors, scavanger receptors,

and complement receptors, and are therefore capable of recognizing different carbohydrate moieties on *C. albicans* surface (Figure 2 and 4). Work by d'Ostiani and colleagues revealed that DCs can discriminate between the yeast and hyphal morphologies of *C. albicans* (*413*). In fact, murine splenic DCs produce IL-12 and prompt protective Th1 protective immunity when activated with the yeast form, while the hyphal form triggers a detrimental Th2 response concomitant with the signature cytokine IL-4 (*413*). On the other hand, Romagnoli and colleagues report that human DCs exposed to either morphotype undergo a full maturation process and produce Th1-inducible cytokines, such as IL12p70 and IFNγ, albeit germ-tube forms trigger enhanced IL-10 production (*415*). While they are potent antigen-presenters, DCs are actually poor in both intracellular killing and damaging of *C. albicans* hyphae compared to monocytes and macrophages (*416*). Since *C. albicans* is primarily internalized through the mannose receptor on DCs, the Dectin-1-dependent NADPH oxidase activation is bypassed and ROS production not induced, unless stimulated by an alternative route, such as PMA and/or IFNγ (*105*). A role of DCs in the context of human invasive fungal disease has not yet been firmly established. However, CMC patients with or without autoimmune polyendocrinopathy candidiasis ectodermal dystrophy (APECED), exhibit an altered monocyte-derived DC maturation and function in response to *C. albicans* (*417*, *418*). It is therefore reasonable to assume that the intricate interplay of particular *Candida*-recognizing receptors expressed by distinct DC species and/or subsets against each fungal form dictates the ultimate nature of DC contribution during host response to *C. albicans* infection.

1.3.3.4 Natural killer (NK) cells

There is a notable paucity of literature examining the role of NK cells during invasive *C. albicans* infection. Initial experiments carried out in the *beige* mutant mouse suggested that impaired NK function underlies susceptibility to invasive candidiasis (*419*, *420*), while Balish *et al.* reported that mice with combined T-cell and NK cell deficiency (Tgepsilon26) are resistant to systemic *C. albicans* challenge (*421*). In contrast, reports by Gaforio and Ortega demonstrated that enhancing NK cell activity *in vivo* by administering tilorone increases the phagocytic capacity of

splenic macrophages and prolongs survival of treated mice compared to controls following invasive *C. albicans* infection (*422*, *423*). Consequently, NK cell depletion suppressed the phagocytic activity of splenic macrophages against *C. albicans* (*422*, *424*). Moreover, a direct candidacidal effect was observed in murine NK cells (*425*), whereas human counterparts displayed little to none antifungal activity despite interacting with *C. albicans* (*426*, *427*). Finally, *in vitro* and *in vivo* studies have shown that NK cells constitute an important source of IFNγ and TNFα (*399*, *428*, *429*), thereby potentiating candidacidal activity of macrophages and neutrophils (*154*, *340*, *341*, *430*). Most recently, Voigt *et al*. built on a previous study by Djeu *et al.* (*430*) and demonstrated that activation of neutrophils is enhanced in the presence of NK cells; in the absence of neutrophils, NK cells assume the role of phagocytes, leading to cellular degranulation, *Candida* killing, and secretion of pro-inflammatory factors (*338*). In summary, NK cells appear to amend the role of professional phagocytes during invasive candidiasis, but additional studies are necessary to fully dissect their cooperative role with neutrophils in this disease in vivo.

1.3.4 Adaptive immunity effectors

In stark contrast to the *sine qua non* requirement of innate immunity and phagocyte effector cells in host defense against systemic candidiasis, adaptive immunity and lymphocytes are dispensable.

1.3.4.1 T lymphocytes

Studies in congenitally athymic (nude) mice (*431-435*), an analogous model where T lymphocyte depletion was achieved by thymectomy, irradiation, and bone marrow reconstitution (TBX) (*436*), in severe combined immunodeficiency (SCID) mice which lack both T and B lymphocyte populations (*350*, *435*, *437*, *438*), and in Tgepsilon26 mice having combined defects in natural killer (NK) and T cells (*421*) have yielded insight into the role of T cells during candidiasis. All reports unanimously demonstrated that T lymphocytes were not relevant for protection against a primary challenge with *C. albicans*; in most instances, deficiency of T cells

even conferred hyperresistance (*431-434*, *436-438*), suggesting that T cells may inhibit clearance and contribute to the overall pathology of acute systemic candidiasis. Moreover, antibody-mediated depletion of phagocytic cells or impairment of their function in SCID mice resulted in heightened susceptibility compared to control SCID animals (*350*), further supporting the role of innate immunity above that of lymphocytes in antifungal host defense. Similarly, *Rag2*$^{-/-}$ mice lacking adaptive immunity were as resistant as wildtype animals to invasive *C. albicans* infection, unless immunosupression was induced by cyclosporine A (*111*). Interestingly, SCID mice raised in conventional facilities present an enhanced capacity to clear *C. albicans* from kidneys than their gnotobiotic counterparts (*438*), indicating that intestinal bacterial flora may potentiate the candidacidal activity of the innate immune system.

As the aforementioned models lack T cells altogether, several groups have investigated the contribution of individual T cell subsets in antifungal host defense by antibody depletion (*439-441*) or in β2-microglobulin knockout (β2m$^{-/-}$) mice lacking CD8α/β T cells (*442*), and T-cell receptor α- and δ-chain knockout mice deficient in αβ- or γδ-T cells, respectively (*443*). While Coker *et al.* claim that CD4^{+} depletion significantly increased survival following *C. albicans* systemic challenge (*439*), Romani and colleagues report that CD4^{+} T cells participate in resistance to primary challenge, albeit with an attenuated vaccine strain of *C. albicans* (*440*); depletion of CD8^{+} T cells had no impact on the survival of mice in either study. Similarly, CD4^{+} T cells, and to a lower extent CD8^{+} T cells, were shown to reduce the severity of tissue damage (*441*). The dispensable role of CD8^{+} T cells was also exemplified in β2m$^{-/-}$ mice that were as resistant to systemic candidiasis as immunocompetent controls (*442*). Finally, neither the αβ- or γδ-T cells appear to be required for murine resistance to acute systemic candidiasis; in fact, lower renal fungal burden observed in these mice suggests that T cells may contribute to ensuing immunopathology (*443*). The major role of T cells in protection against systemic candidiasis appears to be in the induction of persistent systemic anticandidal immunity, as TBX (*436*) and CD4^{+}-depleted mice (*440*) do not develop resistance to re-infection.

1.3.4.2 B lymphocytes

Conclusions regarding B cell participation during invasive candidiasis can be inferred from studies in SCID mice, which lack both T and B lymphocytes (*350*, *437*, *438*) and are resistant to *C. albicans* infection. Alternatively, B cell contribution was also examined in the CBA/N strain that carries an X-linked immune defect (XID), characterized by a variety of deficiencies in the humoral immune response (*444*). Compared with B cell competent CBA/J counterparts, no difference in response to intravenous challenge with *C. albicans* was perceived, alluding to a non-essential effect of B cells. Along the same line, mice depleted of B cells with anti-μ treatment (*445*), or genetically-engineered μMT mice (*446*) were capable of efficiently restricting fungal growth as were the control mice, but μMT mice were unable to survive the re-infection with *C. albicans*. Additionally, B cell deficient mice bearing a homozygous deletion of the *igh* locus and SCID mice succumbed as equally as immunocompetent controls to a high infectious inoculum with a filamentous form of *C. albicans* strain (*435*). More recently, it was established that CD37-deficiency on B cells was directly responsible for elevated IgA production, which conveyed protection against systemic candidiasis (*447*). Thus, similarly to T cells, B cells are summoned at later timepoints during invasive candidiasis and participate in the formation of an adaptive response.

1.3.5 T helper responses

Although T lymphocytes are *per se* expendable for initiation of host antifungal immunity during primary systemic infection with *C. albicans*, the cytokine production by T helper (Th) cells can influence infection outcome. As described earlier, the array of PRRs capable of recognizing particular carbohydrate moieties on *C. albicans* and activating distinct intracellular signaling pathways confers tremendous plasticity to innate immune cells, particularly DCs and monocytes/macrophages, that contribute to shaping T cell responses during infection. The profile of cytokines secreted by cellular effectors on the first line of defense will drive naïve T cells to differentiate towards a specific Th lineage.

Resistance to systemic *C. albicans* infection is associated with a Th1 profile, typified by cytokines such as IFNγ, IL-12, and IL-18. Numerous early studies have established that IFNγ activates neutrophils (*340*, *342*, *343*, *448-451*) or monocytes/macrophages (*154*, *389*, *451-453*) of either mouse or human origin, causing increased production of reactive oxygen radicals, and consequently potentiating their candidacidal activity. Consonantly, impaired survival and increased fungal burden in target organs of IFNγ-deficient mice following systemic *C. albicans* challenge further validated the protective effect of IFNγ *in vivo* (*454*, *455*). Accordingly, IFNγ treatment substantially ameliorated survival of WT mice inoculated with lethal *C. albicans* dosage (*453*). On the other hand, Romani and colleagues reported that although neither IFNγ neutralization nor the absence of IFNγ receptor significantly altered the outcome of primary infection, combined depletion of IFNγ and $CD4^+$ cells resulted in rapidly death despite infection with an attenuated yeast (*440*, *456*). Experiments investigating the role of IL-12 during systemic infection underscore the intricate balance of Th1 cytokines during infection progression. IL-12 is mainly produced by APCs and primes naïve T cells for IFNγ production, which in turn establishes a positive feedback loop through enhanced phagocytic cell activation and onset of inflammation (reviewed in (*457*)). While endogenous IL-12 was not required during primary systemic candidiasis (*458*), exogenous IL-12 administration exacerbated disease severity, allegedly by eliciting IFNγ overproduction (*459*). Mencacci *et al*. demonstrated that the IL-12p40 subunit was required for protection against reinfection, whereas antagonistic therapy with IL-12-depleting antibodies conferred protection to the same extent as abrogation of IL-10 (*460*). However, *C. albicans*-pulsed DCs from IL-12p40$^{-/-}$ mice primed lymphocytes toward a Th2 cytokine profile, failing to confer resistance to infection *in vivo* (*413*). IL-18 was identified as a novel cytokine that synergized with IL-12 to induce IFNγ production by T and NK cells, and perpetuate Th1 development (*461*, *462*). Antibody-mediated neutralization of endogenous IL-18 in murine splenocytes strikingly curtailed production of IL-12-induced IFNγ (*463*). Similarly, neutralization of endogenous IL-18 during disseminated candidiasis exacerbated infection parameters (*464*), while therapeutic administration of recombinant murine IL-18

decreased mortality and yeast outgrowth in the kidneys (*465*). Congruent with these observations, IL-18$^{-/-}$ mice succumbed more rapidly to disseminated *C. albicans* infection than IL-12$^{-/-}$ and WT controls (*458*). Although peritoneal macrophages from both IL-18$^{-/-}$ and IL-12$^{-/-}$ exhibited a decreased proinflammatory cytokine response upon contact with heat-killed *C. albicans*, significant reduction of MIP-2 was observed solely in IL-18$^{-/-}$, concomitant with aberrant monocyte recruitment to the peritoneum, and increased renal fungal burden (*458*). Moreover, this group showed that both endogenous IL-18 and IL-12 are involved in the production of IFNγ in human whole blood stimulated with *C. albicans* (*466*). Indeed, patients diagnosed with HIES exhibited an impaired IL-12/IL-18/IFNγ axis (*467*).

In contrast, the Th2 cytokine response, characterized by the presence of anti-inflammatory cytokines such as IL-4 and IL-10, associates with an adverse outcome to systemic *C. albicans*. Antibody-mediated neutralization of IL-4 in *C. albicans*-infected mice promoted production of IFNγ and IL-2 by CD4^{+} T cells, thereby improving control of fungal replication in target organs and prolonged survival (*468*). Comparably, IL-10 depletion or IL-10-deficiency limited fungal outgrowth during systemic candidiasis infection (*434*). Conversely, supplementation therapy with IL-4 or IL-10 in *Candida*-infected mice inhibited IL-12 production, led to a progressive Th2 dominance, and ultimately exacerbated the disease (*469*). *In vitro* studies with human or mouse mononuclear phagocytes demonstrated that a skewing towards Th2 differentiation by IL-4 and IL-10 downregulates phagocyte candidacidal activity by attenuating ROS and NO generation (*395*, *397*, *470*, *471*). In fact, IL-10 neutralization in DBA/2J macrophages partially rescued the aberrant NO phenotype and improved candidacidal activity (*472*). Some reports suggest that efficient fungicidal capacity of neutrophils, rather than NO-mediated immunity, accounted for the observed hyperresistance of IL-10$^{-/-}$ mice to *C. albicans* infection (*473*), while IL-10 suppressed phagocytic and antihyphal activities of human neutrophils in a dose-dependent manner (*348*). In addition, Naundorf and colleagues demonstrated that IL-10 can directly hinder TCR-induced IFNγ production in human memory T cells, without contribution of APCs (*474*). A prevalent IFNγ response conferred protection to IL-4$^{-/-}$ mice during the onset of systemic infection with *C. albicans*; interestingly,

IL-4 itself is a requirement for efficient control of *C. albicans* during the late stage of infection (*475*). Likewise, IL-10 was required for the generation of Tregs, which modulated inflammation and restored resistance to reinfection (*476*).

More recently, the Th1/Th2 paradigm in host response to *C. albicans* has been reappraised to include the newly discovered third subset of IL-17-producing effector T helper cells, coined Th17 (*477*, reviewed in *478*). Mice deficient in IL-17A (*127*) and the IL-17A receptor (*369*) exhibit substantially reduced survival following systemic *C. albicans* challenge. Consistent with the role of IL-17 in granulopoiesis (*479*, *480*), mobilization and the influx of neutrophils into the kidneys were severely impaired in IL-17AR$^{-/-}$ mice, leading to unrestrained fungal outgrowth and increased susceptibility (*369*). During the initial stage of systemic candidiasis in mice, IL-17-producing γδ T cells recruit neutrophils to the lung to contain the infection, which is compromised in IL-17A$^{-/-}$ and Cδ mice (lacking γδ T cell population) (*481*). As demonstrated by *in vitro* studies in human mononuclear cells, *Candida*-mediated induction of IL-17 depends on the mannose receptor and monocytes (*166*), with particular emphasis on the inflammatory CD14^{++}CD16^{-} subset (*167*). While full appreciation of Th17 immunity in host response to systemic *C. albicans* infection compels additional investigation, the requirement of an intact Th17 response is most notable in mucosal antifungal host defense. In the mouse model of oropharyngeal candidiasis, several groups reported that Th17 differentiation and signaling are required for resistance (*482-484*). In humans, the genetic etiology of chronic mucocutaneous candidiasis was recently correlated with inborn errors in various genes of the IL-17 circuit (Table 2) (*6*, reviewed in *30*, *31*, *123*, *485-491*).

In the light of recent immunological advances, the prior notion of protective inflammatory and detrimental anti-inflammatory responses against *C. albicans* may represent a rather gross oversimplification of the intricate relationship between anatomical location, various cellular effectors, and cadence of cytokine production.

1.4 Animal models of invasive candidiasis

Substantial strides have been made in the field of fungal pathogenesis over the past decade owing to the modeling of invasive candidiasis in animals. While *in vitro* cell-based models have yielded valuable insight into immune and epithelial cell interactions with *C. albicans* (*492*, *493*), animal models offer an integrative view of disease initiation and progression, allow testing of antifungal agents, and permit development and evaluation of novel diagnostic tools.

A number of invertebrate minihosts (reviewed in (*494*, *495*)), such as the fruit fly *Drosophila melanogaster* (*496-504*), the greater wax moth *Galleria melonella* (*505-512*), and the roundworm *Caenorhabditis elegans* (*252*, *513-517*), have been amenable to study aspects of *Candida* disseminated infection. The attractiveness of these models lies in the evasion of logistical, economical, and ethical obstacles otherwise encountered with large-scale forward genetic screening in mammalian models (*494*, *495*). Despite the realization that several components of the innate immune system are evolutionarily conserved across phylogeny, invertebrate models are not directly comparable to mammals (*518*). Hence, small mammals, including rabbits, rats, and especially mice, display relative anatomic and immunological similarities to humans and represent the gold standard for pathogenesis studies.

1.4.1 Mouse models of systemic *Candida* infection

Ideally, an animal model of fungal pathogenesis is considered pertinent if it closely portrays human disease with respect to colonization and invasion at the specific portal of entry, and induction of comparable immune defense pathways. Mouse models have been instrumental in understanding host responses during the onset and progression of systemic *Candida* infection. Human invasive candidiasis can be recapitulated and studied using two main mouse models of disseminated *Candida* infection: the intravenous infection model (*519-521*) and the gastrointestinal colonization and dissemination model (*522*, *523*).

To mimic infection development after fungal cells originating from the gastrointestinal tract or medical intravascular devices breach the blood barrier and enter the bloodstream, mice are injected with *C. albicans* blastospores via the lateral tail-vein. The choice of inocula and strains of *C. albicans* used to study susceptibility in the mouse can be tailored to the specific experiment or hypothesis. Generally, the median lethal dose (LD_{50}) for most *C. albicans* isolates tested in immunocompetent mice ranges between 10^4 and 10^6 yeasts (*19*), though overall lethality during infection can be modulated by both the fungal strain and inoculum growth conditions (*524*). Detailed examination of the course of *C. albicans* infection following intravenous challenge in mice revealed that fungal cells are rapidly eliminated from circulation, followed by a sequential rise in renal and brain fungal burdens (*521*). Conversely, liver, lung, and heart exhibit highest burdens immediately following challenge that gradually decline over time, while spleen colonization remains low and relatively constant throughout the infection (*521*, *525*). Macroscopically, the kidney is studded with white abscesses, composed of focal clusters of *Candida* yeasts, hyphae, and pseudohyphae, as well as polymorphonuclear and/or monocytic cellular infiltrates (*19*, *526*). Whereas histopathological evaluation of tissue damage in the kidney and in the brain may reflect the interplay between *Candida* and the host cellular immune response, accurate determination and quantification of infiltrating leukocyte subsets in various organs, at any given time following infection can now be achieved using flow cytometry (*366*). Nonetheless, tissue fungal burden remains a reliable quantitative measure of infection that reflects the candidacidal or candidastatic efficiency of the host response (*527*), while mortality indicates the overall susceptibility to infection. Ultimately, mice succumb to infection by developing progressive sepsis concomitant with acute pyelonephritis and cardiomyopathy (*299*, *528*, *529*), which closely resembles severe clinical cases of disseminated candidiasis.

Alternatively, the gastrointestinal colonization and dissemination models require sustained colonization of the mouse gastrointestinal tract with *C. albicans* and facilitation of dissemination, either in infant mice (*522*, *530*-*532*) or antibiotic-treated and/or immunocompromised adult animals (*533*-*536*). In the infant mouse model, systemic spread of yeasts occurs 30 minutes following oral-intragastric inoculation of

five to six day-old mice, and persistent colonization is detected in the stomach, small intestine, and large intestine throughout a period of 20-30 days (*522*, *530*, *531*). Subsequent administration of an immunosuppressive regimen consisting of cortisone acetate and cyclophosphamide significantly increases fungal burden in the gastrointestinal tract, as well as in visceral organs (*522*, *532*). Otherwise, immunosuppressed or gut flora-depleted adult mice are infected with *C. albicans* in the drinking water or by gavage (*533*-*536*). The presence of the fungus is highest in the stomach, caecum, and small intestine, and contrary to the infant mouse model, colonization is maintained by continuous antibiotic therapy in some instances (*534*, *535*). Subsequent treatment with immunosuppressive or mucosal-irritating agents leads to the formation of intraepithelial abscesses in the gastric mucosa and particularly in the region of cardial-atrium fold (*34*, *537*), resulting in *Candida* extravasation from the confined environment into the bloodstream, and dissemination to the liver, kidneys, and spleen (*533*, *534*, *536*). Although this model may most accurately reflect the onset and progression of candidiasis in humans, the considerable variability in animals that go on to develop disseminated candidiasis commands development of a reliable, and more reproducible model (*495*).

1.4.2 Differential susceptibility of inbred strains

The creation of some of the most widely used inbred mouse strains can be ascribed to mouse fanciers of the late 19th and early 20th centuries, who bred mice for their peculiar phenotypes (*538*). The diverse repertoire of genetic backgrounds offers an appealing approach toward identifying host genetic factors involved in disease onset, control of pathogen replication and subsequent eradication, type of inflammatory immune response mounted, and survival. Not surprisingly, inbred strains of mice vary considerably in their susceptibility to *C. albicans*, as assessed by two most commonly used phenotypes, fungal load and mortality (*9*, *212*, *296*, *297*, *529*, *539*-*541*) (reviewed in (*542*)). Although experimental settings may differ, strains such as BALB/c and C57BL/6J were consistently found to be highly resistant, displaying low fungal burden in target organs, mild tissue damage, and increased mean survival time. Conversely, A/J and DBA/2J are highly susceptible to infection,

exhibiting overwhelming fungal proliferation and succumbing to infection within 24-48 hours of initial inoculation. The participation of the complement system in innate resistance to systemic candidiasis was apparent from earlier studies in inbred strains (*10*, *297*, *301*), where A/J and other susceptible strains carry a defective *C5* allele. Tuite *et al.* provided concrete genetic evidence for the critical role of C5 in differential susceptibility to *C. albicans* in susceptible A/J and resistant C57BL/6J progenitors, through linkage analysis and strain distribution pattern using informative F2 mice and AcB/BcA recombinant congenic strains, respectively (*7*). C5 was found to control tissue fungal burden, survival time, and serum levels of the inflammatory cytokine TNFα during infection (*7*). Interestingly, roughly 40% of inbred mouse strains carry a naturally occurring 2-bp deletion in the exon 6 of the *Hc/C5* gene, resulting in a premature stop codon and a complete absence of the C5 protein in the serum (*543*, *544*). While the exact role of C5 during *C. albicans* infection remains elusive, C5-deficient A/J mice display reduced infiltration of immune cells in the kidneys, concomitantly with exuberant levels of circulating proinflammatory cytokines TNFα, IL-6, MCP-1, MCP-5 and eotaxin (*298*, *299*), resulting in multiple organ failure including cardiomyopathy (*299*). Although C5 is the major determinant of susceptibility in inbred mouse strains and accounts for 50-70% of observed phenotypic variance depending on the phenotype, the presence of strains displaying moderate susceptibility to *C. albicans*, such as C3H/HeJ (*297*, *545*), allows for the dissection of additional components of host antifungal defense. In fact, C3H/HeJ mice bear a point mutation in the *Tlr4* gene which renders them hyporesponsive to LPS signaling compared to the C3H/HeN counterparts (*207*), which permitted Netea *et al.* to examine the involvement of TLR4 in susceptibility to disseminated candidiasis (*212*). These findings outline the complex genetic etiology of candidiasis, which can be dissected and investigated in suitable inbred mouse strains and subsequently derived informative intercrosses.

1.4.3 Phenotyping of recombinant congenic strains (RCS)

The AcB/BcA recombinant congenic strain (RCS) set was generated to dissect the complex genetic basis underlying the differential response of A/J and B6 parental

strains to various diseases and traits of clinical relevance in humans (*546*, *547*). The breeding scheme used to generate 17 AcB and 19 BcA strains involves systematic inbreeding from a double backcross (N3) between A/J and B6 strains (*546*, *547*). The resulting individual strains harbor 12.5% of genome donated from either A/J (in BcA strain) or B6 (in AcB strains), fixed as a set of discrete congenic segments onto 87.5% of the reciprocal parental background (*547*). The AcB/BcA strains have been bred to homozygosity for over 20 generations and genotyped across all chromosomes to delineate the position of congenic segments (*547*). Phenotyping of this strain set enabled the identification of discordant strains, which may carry informative congenic segments that confer the unique resistance or susceptibility to the studied phenotype. Further association analysis using the strain distribution pattern (SDP) or linkage analysis in an informative F2 cross derived from the discordant RCS can be carried out to map the genetic locus underlying the examined phenotype (*546*, *547*). The AcB/BcA platform has been successfully used by our laboratory and others to decipher genes implicated in host response to *Legionella pneumophila* (*548*), *Plasmodium chabaudi* (*549*), *Salmonella typhimurium* (*550*), influenza (*551*), carcinogen-induced colorectal cancer (*552*), radiation-induced lung response (*553*), and airway hyperresponsiveness (*554*).

The systematic survey of AcB/BcA mice for response to *C. albicans* infection laid the foundation for the work outlined in this thesis. Using this RCS panel, Tuite *et al.* investigated the possible involvement of additional genetic modifiers, alone or in combination with the major determinant C5 (*7*). Two discordant strains whose C5 status did not correlate with ensuing outcome to *C. albicans* challenge were identified: BcA67 showed an intermediate level of susceptibility despite harboring functional *C5* alleles, while the C5-deficient BcA72 females displayed resistance comparable to B6 controls (*7*). These observations support the premise that genetic control of susceptibility to *C. albicans* infection is complex and involves the participation of multiple gene effects.

1.4.4 Identification of the *Carg* loci

Attempts toward identifying gene effects controlling susceptibility to systemic candidiasis have been scarce, and solely two loci controlling severity of tissue damage have been proposed. Ashman and colleagues have opted to segregate the response to intravenous *C. albicans* infection in inbred strains according to the severity of histopathologic tissue damage, rather than mortality or colony counts (*555*, *556*). BALB/c mice were thus deemed resistant, whereas CBA/CaH were considered susceptible. The segregation pattern of brain lesions in [BALB/c x CBA/CaH]F2 progeny followed the Mendelian pattern for a single gene effect, whose effect was intrinsic to cells derived from the bone marrow (*556*). Employing the same qualitative strategy, tissue damage in the kidney and brain was examined in a set of 15 AKXL recombinant inbred (RI) strains derived from the AKR strain which displays moderate tissue damage and C57/L that exhibits mild lesion severity (*11*, *557*). The strain distribution pattern coincided with a locus on chromosome 14, given the appellation *Candida albicans resistance gene 1* (*Carg1*) (*11*). While *Carg1* is hypothesized to control the overall response to tissue damage, the presence of more severe tissue damage surpassing the susceptible parental line AKR suggested the presence of another locus modulating specifically the extent of kidney damage upon fungal infection (*12*, *557*). Designated *Carg2*, this locus is yet unmapped and postulated to have relatively minor effects in overall susceptibility to *C. albicans* (*12*). Besides the putative role of bone marrow derived cells in overall *Carg1*-modulated tissue susceptibility to *C. albicans* infection, the positional cloning of genetic modifiers underlying *Carg1* and *Carg2*, along with their mechanistic implication in response to infection awaits further elucidation.

PREFACE TO CHAPTER 2

As described in Chapter 1, the complement system, and particularly its fifth component C5, plays an imperative role in host response to systemic *C. albicans* infection in mice. Previous work by Ashman and colleagues, however, revealed that presence of the null allele at *C5* was not a sufficient determinant for the development of severe histopathological lesions in the AKXL set of recombinant inbred (RI) strains following intravenous *C. albicans* challenge. The extent of tissue damage sustained in the brain and the kidney was attributed to two independent loci given the appellation *Carg1* and *Carg2*, with the former located on chromosome 14 and the latter unmapped. Similarly, the imperfect genotype/phenotype correlation observed in a panel of AcB/BcA recombinant congenic strains suggests that response to infection is rather complex and entails the participation of additional genetic modifiers. Although many studies have documented the differential response to *C. albicans* infection among inbred strains, few have attempted to elucidate genetic factors underlying these differences.

Chapter 2 describes the systematic approach that we undertook toward identifying novel host genetic modifiers controlling response to disseminated *C. albicans* infection, independently of C5. We attain this by surveying a cohort of 23 inbred mouse strains, whereby AKR/J is found to be uniquely resistant to *C. albicans* infection despite bearing a null *C5* allele, and conversely, the C5-sufficient SM/J deemed susceptible. Combining genome-wide association in inbred strains with genetic linkage analysis in an F2 cross derived from resistant AKR/J and susceptible A/J strains, fixed for *C5* null alleles, uncovers multiple putative associations and validates loci on chromosomes 8 (*Carg3*) and 11 (*Carg4*) as regulating fungal replication in the host.

Chapter 2:

Genetic control of susceptibility to infection with *Candida albicans* in mice

2.1 ABSTRACT

Candida albicans is an opportunistic pathogen that causes acute disseminated infections in immunocompromised hosts, representing an important cause of morbidity and mortality in these patients. To study the genetic control of susceptibility to disseminated *C. albicans* in mice, we phenotyped a group of 23 phylogenetically distant inbred strains for susceptibility to infection as measured by extent of fungal replication in the kidney 48 hours following infection. Susceptibility was strongly associated with the loss-of-function mutant complement component 5 (*C5*/*Hc*) allele, which is known to be inherited by approximately 40% of inbred strains. Our survey identified 2 discordant strains, AKR/J (C5-deficient, resistant) and SM/J (C5-sufficient, susceptible), suggesting that additional genetic effects may control response to systemic candidiasis in these strains. Haplotype association mapping in the 23 strains using high density SNP maps revealed several putative loci regulating the extent of *C. albicans* replication, amongst which the most significant were C5 (P value=2.43×10^{-11}) and a novel effect on distal chromosome 11 (P value=7.63×10^{-9}). Compared to other C5-deficient strains, infected AKR/J strain displays a reduced fungal burden in the brain, heart and kidney, and increased survival, concomitant with uniquely high levels of serum IFNγ. C5-independent genetic effects were further investigated by linkage analysis in an [A/JxAKR/J]F2 cross (n=158) where the mutant *Hc* allele is fixed. These studies identified a chromosome 11 locus (*Carg4*, *Candida albicans* resistance gene 4; LOD=4.59), and a chromosome 8 locus (*Carg3*; LOD=3.95), both initially detected by haplotype association mapping. Alleles at both loci were inherited in a co-dominant manner. Our results verify the important effect of C5-deficiency in inbred mouse strains, and further identify two novel loci, *Carg3* and *Carg4*, which regulate resistance to *C. albicans* infection in a C5-independent manner.

2.2 INTRODUCTION

Candida albicans is an opportunistic fungal pathogen that exists commensally in the gastrointestinal and genitourinary tracts of healthy individuals (*558*), but that causes severe disseminated and often lethal infections in immunocompromised patients, such as those suffering from HIV infection or undergoing cancer chemotherapy (*559*). In the United States alone, *Candida* species constitute the fourth most common causative agent of nosocomial bloodstream infections, and are associated with significant attributable mortality in both adults and children (47% vs. 29%) (*35*, *560*, *561*). Despite the rising trend of infections with non-*albicans Candida* species, *Candida albicans* remains the most common isolate recovered from bloodstream infections worldwide, with the frequency of occurrence ranging from 37% to 70% (*2*). Genetic effects have long been suspected to play a role in the initial susceptibility and subsequent development of severe *C. albicans* infection in humans (*562*) and in animal models of experimental infections (*9*, *297*). Genetic predisposition to disseminated candidiasis in non-immunocompromised humans has not yet been associated to any particular gene, although individuals presenting impaired phagocyte function are more susceptible to *Candida* infections (*563*), as observed in myeloperoxidase (MPO) deficiency. In addition, deleterious mutations in multiple direct or downstream immune effectors, notably CLEC7A (*123*), STAT3 (*564*), and CARD9 (*6*), have been found in human cohorts with high prevalence of chronic mucocutaneous candidiasis (CMC) and have been recapitulated and studied in mice.

In mouse models of infection, response to *C. albicans* is under a complex genetic control that affects onset of infection, type and severity of disease developed and associated pathologies (oropharyngeal, mucosal, or systemic forms), and extent of immune response elicited (*527*). Inbred mouse strains vary widely in their degree of innate susceptibility to systemic candidiasis, being either highly susceptible (A/J, DBA/2) or highly resistant (BALB/c, C57BL/6J). Studies in inbred strains (*10*, *301*), together with genetic linkage and association studies in informative backcross and F2 mice, and experiments in AcB/BcA recombinant congenic strains (*7*) derived from

susceptible A/J and resistant C57BL/6J progenitors, have identified a critical role for the complement component 5 (C5) in differential susceptibility of these two inbred mouse strains. A/J and other susceptible strains carry a defective *C5* allele, which causes susceptibility to infection with *C. albicans*, as well as *Cryptococcus neoformans* (*565*, *566*). Phenotypically, resistant C5-sufficient C57BL/6J mice die late in infection due to high kidney fungal loads, and associated strong neutrophil-driven inflammatory response at that site, while C5-deficient A/J mice succumb within 24 hrs of infection with little kidney damage, but displaying an allergic-like response associated with high levels of circulating TNFα, IL-6, MCP-1, MCP-5 and eotaxin (*298*, *299*), resulting in multiple organ failure including cardiomyopathy (*299*). The complement pathway represents the first line of defense of the innate immune system and plays a major role in eliciting an inflammatory response to the site of infection (*254*, *542*, *567*). The complement system can be activated by several pathways triggered by microbial products, which ultimately result in the activation of C3 convertase, cleavage of C5, release of chemotactic factors (C3a and C5a), and generation of the membrane attack complex (MAC) (*567*). The importance of complement cascade is further demonstrated in $C3^{-/-}$ animals which show impaired fungal clearance and higher mortality than wild type controls when infected with *C. albicans* or *C. glabrata* (*8*).

Studies in inbred strains and in AcB/BcA recombinant congenic strains have suggested that the deleterious effect of the *C5* allele on fungal load and survival time of *C. albicans* infected mice may be further modulated by genetic background effects (*7*, *9*, *10*). In addition, the genetic analysis of histopathological responses in target organs following systemic *C. albicans* infection has pointed to C5-unrelated genetic loci, temporarily given the appellation *Carg1* and *Carg2* (*11*, *12*). Although the genes underlying these effects remain unknown, these studies have clearly pointed at additional complexity in the genetic control of host response to *C. albicans* infection. With the aim of identifying such additional gene effects, we have herein phenotyped a total of 23 phylogenetically distant inbred strains of mice for susceptibility to *C. albicans*. These studies have identified two strains (AKR/J and SM/J) that show discordant genotype/phenotype relationships with respect to C5 status and

susceptibility to infection. Haplotype association mapping in the 23 inbred strains using high density SNP maps, together with genetic linkage analyses in informative crosses derived from discordant strains, have uncovered two C5-independent genetic effects and loci controlling fungal replication in the host, and mapping to chromosomes 8 (*Carg3*), and 11 (*Carg4*).

2.3 MATERIALS AND METHODS

Mice

Inbred strains 129S1/SvlmJ, A/J, AKR/J, BALB/cByJ, BPL/1J, BTBRT+tf/J, BUB/BnJ, C3H/HeJ, C57BL/6J, C57BLKS/J, CAST/EiJ, CBA/J, DBA/2J, DDY/JclSidSeyFrkJ, FVB/J, KK/HlJ, MRL/MpJ, MSM/Ms, NOD/ShiLtJ, NZW/LacJ, PWD/PhJ, SM/J, and SJL/J were obtained as pathogen-free mice at 8-12 weeks of age from the Jackson Laboratory (Bar Harbor, ME) as part of a collaboration with the Mouse Phenome Database project. Survey data will be deposited in MPD (www.phenome.jax.org) and made publically available. [A/JxAKR/J] F2 progeny were bred by systematic brother-sister mating of [A/JxAKR/J] F1 mice. All housing and experimental procedures were conducted under the guidelines of the Canadian Council of Animal Care and were approved by the Biotechnology Research Institute (BRI) Animal Care Committee (Protocol number: 08-SEP-I-017) and the Animal Care Committee of McGill University (Protocol number: 5618).

Infection with Candida albicans

C. albicans strain *SC5314* was grown overnight in YPD medium (1% yeast extract, 2% Bacto Peptone and 2% dextrose) at 30^{o}C. Blastospores were harvested by centrifugation, washed twice in phosphate-buffered saline (PBS), counted using a hemacytometer and resuspended in PBS at the required density. For experimental infections, mice were inoculated via the tail vain with 200 μl of a suspension containing $5x10^4$ *C. albicans* blastospores in PBS. In dose-response experiments, additional doses were tested: $5x10^4$, $1x10^5$, $3x10^5$, and $6x10^5$ *C. albicans*. Forty-eight hours following infection (unless otherwise indicated), target organs were removed aseptically and homogenized in 5 ml of PBS. The homogenate was then serially diluted and plated on YPD-agar plates containing 34 μg/ml of chloramphenicol. The plates were incubated at 30^{o}C for 24-48 hours and the colony-forming units (CFU) counted and expressed as $\log_{10}$CFU per organ. The maximum sensitivity for this assay was 100 CFU, and the animals displaying titers below the detection limit were

assigned an arbitrary value of 100 CFU. For the survival study, mice were injected intravenously with 200 µl of a suspension containing 3 x 10^5 *C. albicans* blastospores in PBS. Mice were closely monitored for clinical signs such as lethargy, hunched back, and ruffled fur. Mice exhibiting extreme lethargy were deemed moribund and were euthanized.

Cytokine detection

Mice were anesthetized and exsanguinated by cardiac puncture. Serum was isolated by collection of blood, followed by centrifugation and storage at -80^{o}C until used to measure cytokine levels. To determine the levels of cytokines in the circulation, 12.5 µl of serum was analyzed using the BD™ CBA Flex sets according to the manufacturer's instructions. Fluorescence levels were recorded using the BD™ LSRII flow cytometry system (Becton-Dickinson Biosciences, CA, USA) using BD FACSDiva acquisition software and the data analysis was carried out using the FCAP Array software.

Evaluation of kidney function

At 24 h or 48 h, mice were exsanguinated by cardiac puncture under anesthesia, and blood was collected in microtubes with separation gel (Sarstedt, Montreal, Canada). Serum was isolated by centrifugation and stored at –20°C until used for blood urea nitrogen (BUN) determination. A commercially available kit that allows quantitative urease/Berthelot determination was used to measure BUN levels (Sigma).

Histology

Whole kidneys were fixed in 10% neutral buffered formalin, dehydrated in ethanol/xylene and embedded in paraffin, as described previously (*568*). Histological sections were cut longitudinally at 5 µm on a microtome and fixed onto glass slides. Sections were deparaffinized, then stained with periodic acid Schiff's reagent (PAS) to detect *C. albicans* elements and counterstained with hematoxylin to visualize

immune cells infiltration. Stained sections were examined under a light microscope at 100X and 400X magnification and photographed.

Genotyping

As described previously (*547*), genomic DNA was isolated from tail clips of individual F2 mice collected at the time of sacrifice. A total of 158 [A/JxAKR/J]F2 mice were genotyped at the McGill University and Genome Quebec Innovation Centre (Montreal, QC, Canada) using Sequenome iPlex Gold technology and a custom panel that contained 225 informative SNPs distributed across the genome. Additional microsatellite markers were obtained from the Mouse Genome Informatics Database (www.informatics.jax.org) and used for gap filling and fine mapping by a standard PCR-based method employing (α-^{32}P) dATP labeling and separation on denaturing 6% polyacrylamide gels.

Linkage analysis

QTL mapping was performed using Haley-Knott multiple regression analysis (*569*) or EM maximum likelihood algorithm (*570*). A two-dimensional scan was performed using the two-QTL model and empirical genome-wide significance was calculated by permutation testing (1000 tests). All linkage analysis was performed using R/qtl (*571*).

EMMA scan

The detailed algorithm underlying the efficient mixed-model for association mapping have been previously published (*572*). The EMMA algorithm is based on the mixed-model association where a kinship matrix accounting for genetic relatedness between inbred mouse strains is estimated and then fitted to the vector of the phenotype, thereby reducing false positive rates. Prior to the analysis, a minor allele frequency cutoff (MAF<0.05) was applied. In order to identify the most highly associated loci, the Bonferroni multiple testing correction (*573*) was computed. EMMA is publically available as an R package implementation.

Statistical analysis

An unpaired, two-tailed Student's t-test was used to establish significance of differences in mean CFU per organ, BUN levels, and cytokine concentrations between different mouse strains. Survival of AKR/J mice was analyzed by a Log-rank test and survival fractions were compared using the χ^2 statistic. These data were analyzed using GraphPad Prism 4.0 statistical software. P-values < 0.05 were considered significant.

2.4 RESULTS

Response to C. albicans infection in inbred mouse strains. To identify novel C5-independent genetic effects regulating the proliferation of *C. albicans* organisms in target organs during disseminated infection, we surveyed 23 strains from the panel of 36 commonly used inbred mouse strains represented in the Jackson Mouse Phenome Database. These strains have been selected to be genetically diverse, on the basis of their phylogenetically distinct breeding background, and thus likely to be representative of the natural allelic pool. The mice were challenged intravenously with a low dose of *C. albicans* SC5314 and the fungal replication was assessed in the kidney 48 h following infection. We observed wide differences in the extent of *C. albicans* colonization and replication in kidneys of these inbred strains (Figure 1), ranging from very low levels ($\log_{10}$CFU=2.3±0.5) such as in the BPL/1J strain, to approximately 10 000-fold greater number of fungi in the highly susceptible A/J ($\log_{10}$CFU=6.0±0.1), along with a number of strains showing a wide range of intermediate phenotypes. To determine the impact of the C5 locus and its mutant *Hc* allele on the response to *C. albicans* infection in these strains, we established the C5 genotype of the 23 strains (Table 1). We also segregated strains into a susceptible group ($\log_{10}$CFU > 5.1) consisting of 7 strains and a resistant group ($\log_{10}$CFU < 4.2) consisting of 16 strains. Using this arbitrary segregation, we noted a very strong effect and near perfect correlation of C5 allelic status and extent of replication of *C. albicans* in kidney with two notable exceptions (Table 1). Despite being C5-sufficient and producing serum C5a during infection (data not shown), SM/J mice display a significantly higher mean fungal load ($\log_{10}$CFU=5.2±0.4) when compared to the reference B6 strain ($\log_{10}$CFU=4.1±0.5) or other C5-sufficient strains. AKR/J mice are C5-deficient (*543*), yet they showed mean $\log_{10}$CFU counts at 3.9±0.4 similar to that seen in the resistant B6 strain, and clearly distinct from that seen in the C5-deficient strains group ($\log_{10}$CFU > 5.1).

Although these results confirm the critical impact of the *C5* mutant allele on the response of inbred strains to disseminated *C. albicans* infection, the wide

Table 1. Phenotypic response of inbred mouse strains to *C. albicans* infection, with respect to the C5 status.

Inbred strain	Hc allele[a]	Number of mice (females)	Log kidney CFU (mean ± s.d.)	Phenotype[b]
A/J	0	9	6.0 ± 0.1	S
KK/HlJ	0	10	5.9 ± 0.2	S
BTBR T+ tf/J	0	10	5.7 ± 0.3	S
FVB/NJ	0	10	5.5 ± 0.8	S
DBA/2J	0	10	5.3 ± 0.5	S
SM/J	1	7	5.2 ± 0.4	S
NOD/ ShiLtJ	0	10	5.1 ± 0.7	S
C3H/HeJ	1	10	4.2 ± 0.5	R
C57BL/6J	1	8	4.1 ± 0.5	R
AKR/J	0	10	3.9 ± 0.4	R
CBA/J	1	8	3.8 ± 0.3	R
BALB/cByJ	1	7	3.5 ± 0.6	R
SJL/J	1	8	3.5 ± 0.3	R
NZW/LacJ	1	10	3.4 ± 0.6	R
DDY/JclSidSeyFrkJ	1	8	3.4 ± 0.8	R
C57BLKS/J	1	8	3.4 ± 0.3	R
BUB/BnJ	1	8	3.3 ± 1.0	R
MRL/MpJ	1	8	3.0 ± 0.8	R
129S1/SvImJ	1	10	2.9 ± 0.5	R
PWD/PhJ	1	9	2.9 ± 0.6	R
MSM/Ms	1	8	2.9 ± 0.6	R
CAST/EiJ	1	10	2.6 ± 0.6	R
BPL/1J	1	8	2.3 ± 0.5	R

Inbred mouse strains are classified by the extent of the kidney fungal burden and susceptibility (S) or resistance (R). AKR/J and SM/J mouse strains, shaded in gray, were found to be discordant. All strains were gentoyped to confirm their *C5* allele.

[a]0-C5 deficient; 1-C5 sufficient.
[b]R-resistant; S-susceptible.

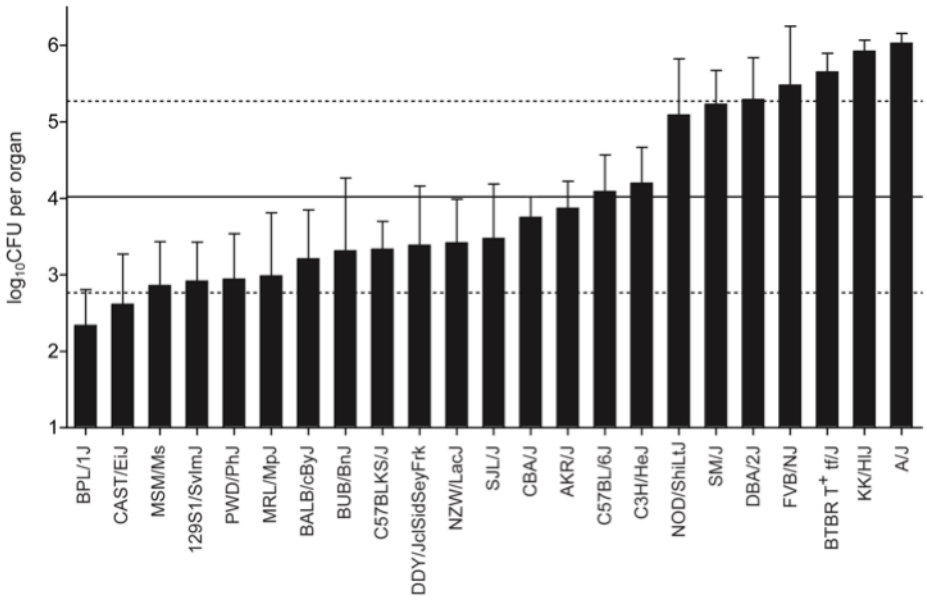

Figure 1. Kidney fungal burden, a measure of susceptibility to *C. albicans* infection, in 23 inbred mouse strains.

23 out of 36 commonly used inbred strains from the Jackson Mouse Phenome Database were phenotyped for susceptibility to *C. albicans*. 7-10 female mice per strain were infected intravenously with $5x10^4$ *C. albicans* blastospores and the kidney fungal load was measured 48 h post-infection. Bars represent strain mean ± SD. Horizontal lines represent mean (solid line) across all 23 strains ± SD (dashed lines).

variation of CFU counts observed within mouse strains bearing wild type *C5* alleles and the presence of two clearly discordant strains (AKR/J, SM/J), together strongly suggested the presence of C5-independent genetic effects in the cohort of 23 strains tested.

Chromosomes 2 and 11 are highly associated with response to C. albicans infection in inbred mouse strains. To explore the genetic basis for inter-strain differences in response to *C. albicans*, we used the strain distribution pattern (kidney CFU counts), and high density SNP datasets available for the 23 strains (Mouse HapMap SNP data) to perform whole genome association mapping. We utilized a statistical method EMMA (*572*) that corrects for population structure and genetic relatedness between inbred strains by estimating a kinship matrix. EMMA analysis identified multiple significant loci (Figure 2A, P value < $1x10^{-5}$) on chromosomes 1, 2, 4, 6, 7, 8, 11, 12, and 15 (Table S1). The Bonferroni correction (*573*) was used to provide a very conservative threshold (α=0.01, P value = $7.99x10^{-8}$) which identified SNPs on chromosomes 2 and 11 as the most highly associated with CFU counts. As expected, the top 3 significant SNPs (P value= $2.43x10^{-11}$, $3.04x10^{-10}$, $4.65x10^{-9}$) are situated between 33.74 and 33.96 Mb on chromosome 2, and correspond to the *C5* gene located less than 1 Mb away. Repeating the EMMA analysis after removing phenotypically discordant AKR/J and SM/J strains, increases the significance of the Chr. 2 (C5) locus dramatically (P value=$6.60x10^{-19}$, Figure S1). Examination of the haplotype structure of chromosome 2 near the peaks of highest association (Figure 2B) shows segregation of the A/J-type allele (30.26-34.88 Mb) in all susceptible strains, except for SM/J. Conversely, the AKR/J strain carries the A/J haplotype block, but is resistant. The structure of the Chr. 2 haplotype block is more difficult to follow in wild-derived strains MSM/Ms (*M. m. molossinus*), PWD/PhJ (*M. m. musculus*), and the CAST/EiJ (*Mus castaneus*). The next most significant association (P value=$7.63x10^{-9}$) was detected on the distal portion of chromosome 11 (98.87 Mb). Haplotype analysis of the corresponding Chr. 11 shows a haplotype block less conserved in inbred strains than the Chr. 2 haplotype, including multiple possible recombination events within the haplotype map (Figure 2C). Nevertheless, a small haplotype block (97.84-99.44 Mb) is preserved where most of the resistant strains,

Figure 2. Genome-wide association mapping using EMMA.

Using the R package implementation of EMMA, genome-wide association mapping was conducted across 23 inbred mouse strains. We obtained genotype data consisting of 132 000 SNPs from the Mouse HapMap project and rejected SNPs with MAF < 0.05, which yielded a final set of 125 113 SNPs. These were then correlated with the kidney fungal burden as the phenotypic data and consequently, the analysis yielded $-\log_{10}$ transformed P values indicating association significance for each SNP genome-wide (A). Standardized threshold was set at P value 1.0×10^{-5} (solid line) and the Bonferroni multiple testing correction threshold was calculated to be 7.99×10^{-8} (dashed line). The most significant hits on chromosomes 2 and 11 are depicted (B and C) along with respective haplotype maps of susceptible (S) and resistant (R) strains at those locations. The conserved haplotype blocks are indicated with brackets, along with the *Hc* position (B) and the arrow showing the most conserved area (C). Asterisk denotes discordant strains with respect to the C5 genotype. Haplotype map colour coding: light gray (NA), gray (A/J like), and white (B6 like).

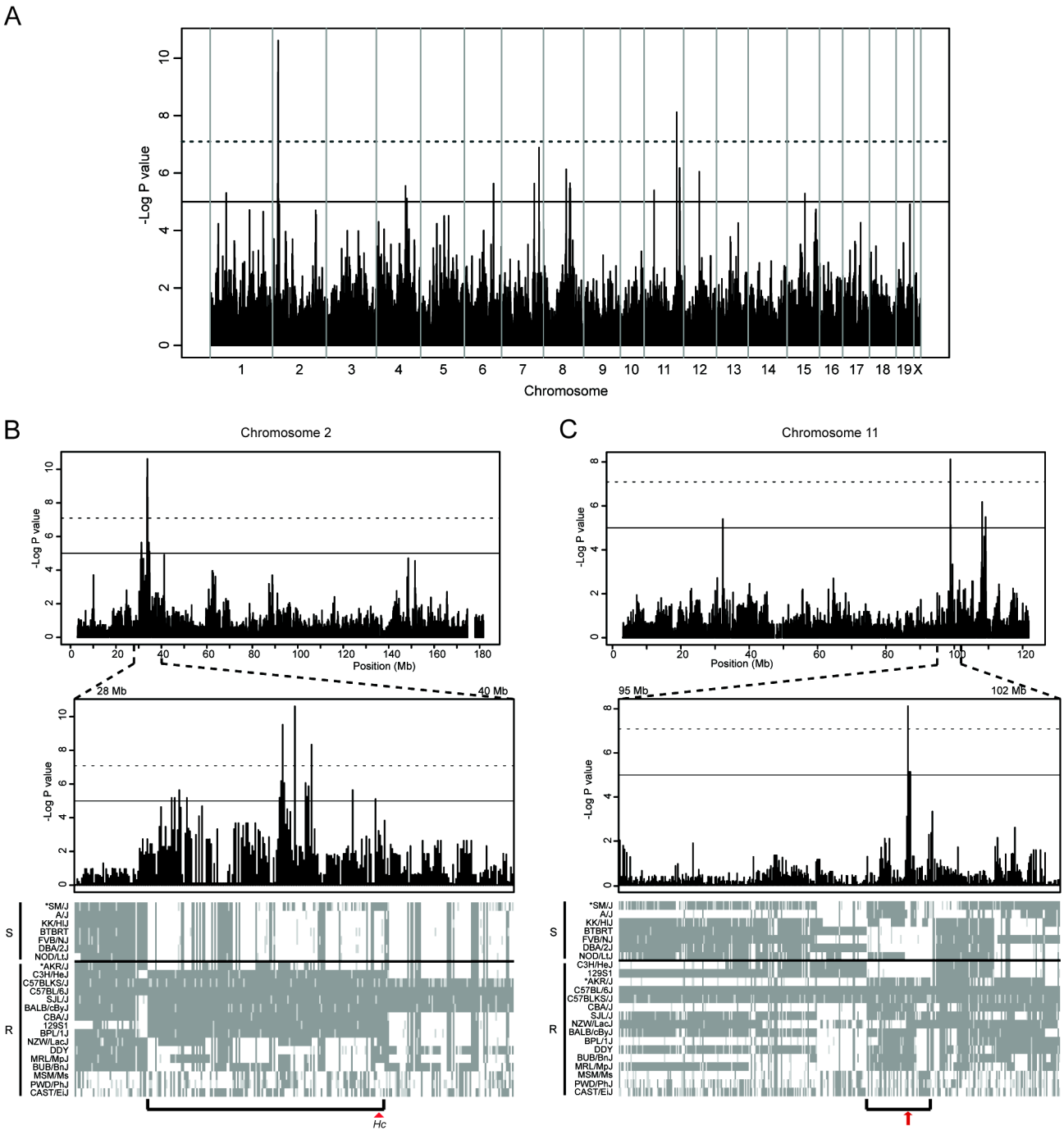
A
-Log P value
Chromosome
1 2 3 4 5 6 7 8 9 10 11 12 13 14 15 16 17 18 19X
B
Chromosome 2
Position (Mb)
28 Mb
40 Mb
S
R
*SM/J
A/J
KK/HlJ
BTBRT
FVB/NJ
DBA/2J
NOD/LtJ
*AKR/J
C3H/HeJ
C57BLKS/J
C57BL/6J
SJL/J
BALB/cByJ
CBA/J
129S1
BPL/1J
NZW/LacJ
DDY
MRL/MpJ
BUB/BnJ
MSM/Ms
PWD/PhJ
CAST/EiJ
Hc
C
Chromosome 11
95 Mb
102 Mb

including the AKR/J strain, carry B6 alleles. These results imply that although C5 plays a crucial role in response to *C. albicans* infection, several additional loci, including the locus on chromosome 11, can modulate response to infection in inbred strains.

Phenotypic expression of resistance to C. albicans infection in AKR/J mice. The differential susceptibility of A/J and AKR/J mouse strains to *C. albicans* infection occurs despite relatively close phylogeny and genetic relatedness of the two strains as assessed by the fraction of concordant alleles based on 8.27 million SNPs distributed across the genome (*574*). Frazer *et al.* (*574*) have reported this fraction to be 0.899 between A/J and AKR/J strains. To explore further the phenotypic expression of AKR/J-associated resistance, C57BL/6J, A/J and AKR/J mice were challenged intravenously with $5x10^4$ *C. albicans* blastospores, and fungal replication was assessed 48 h post-infection in brain, heart and kidney. Compared to A/J susceptible controls, AKR/J mice showed a significantly lower fungal load in brain (log_{10}CFU: 4.1±0.3 vs. 2.2±0.4; Figure 3B) and kidney (log_{10}CFU: 6.3±0.3 vs. 4.4±0.4; Figure 3C). Histological analysis of kidney sections (Figure 3D) showed massive proliferation of the *C. albicans* hyphae and moderate recruitment of cellular infiltrates in A/J mice. Kidney sections from B6 and AKR/J mice also showed cellular infiltrates and presence of pseudohyphal fungal elements, but to a much lesser extent than observed in A/J. Although the heart fungal burden was significantly reduced in AKR/J mice compared to A/J mice (log_{10}CFU: 3.2±0.4 vs. 4.3±0.7; Figure 3A), it was nevertheless significantly higher than that of B6 (log_{10}CFU: 2.1±0.1). We have previously established that C5-deficiency is associated in A/J mice with a striking cardiac phenotype, prior to and during *C. albicans* infection (*299*). Therefore, it is possible that the intermediate level of *C. albicans* replication may be linked to such a heart-specific effect of C5-deficiency present in AKR/J. Together, these results strongly suggest that AKR/J mice are able to contain *C. albicans* replication in all organs, despite C5-deficiency.

We further challenged AKR/J and A/J mice with several infectious doses of *C. albicans*, ($5x10^4$, $1x10^5$, $3x10^5$, and $6x10^5$ blastospores) and monitored in these

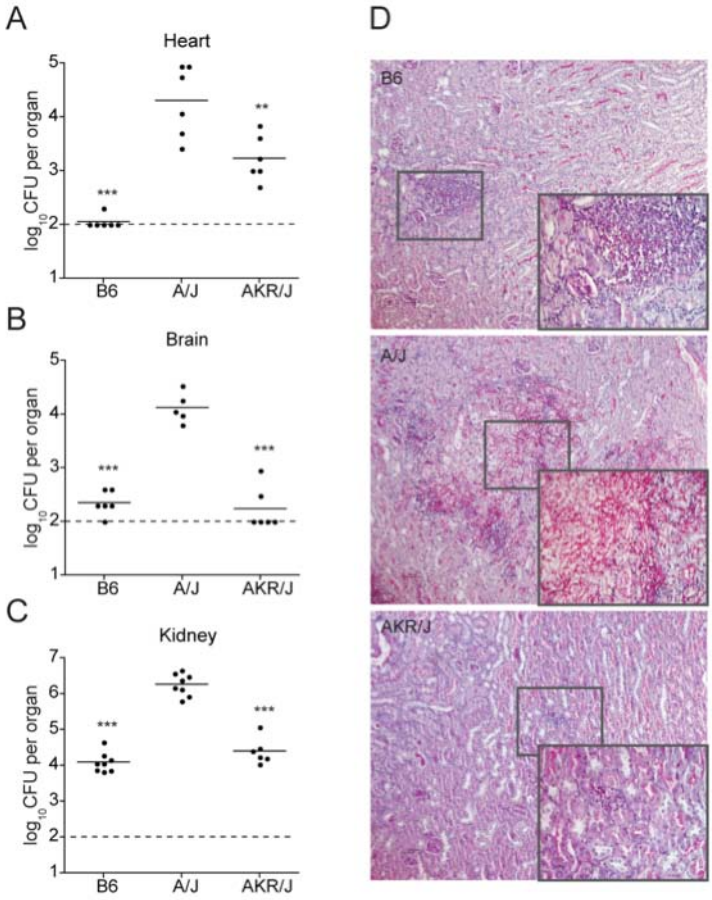

Figure 3. Phenotypic responses of discordant AKR/J mouse strain upon *C. albicans* infection.

In 6 mice per strain, the heart (A), brain (B), and kidney (C) fungal load was measured 48 h after a low dose ($5x10^4$, i.v.) infection with *C. albicans*. In all organs, fungal load was significantly lower in AKR/J mice compared to A/J (**P<0.01, ***P<0.0001). Periodic acid-Schiff staining was performed on kidney sections (D) showing the extent of fungal burden and granulocyte infiltration. Magnification 100X and 400X (insert).

animals: a) organ CFUs, b) kidney function as measured by BUN (blood urea nitrogen), and c) survival (Figure 4). With respect to fungal load, the inter-strain difference between AKR/J (resistant) and A/J (susceptible) is clearly visible and is dose-dependent; it is most visible at lower doses and fades at the high infectious dose. Moreover, these observations are paralleled by measurements of kidney function: BUN levels were always lower in the AKR/J strain (retained kidney function), and this for all infectious doses tested. Finally, we challenged A/J, AKR/J, and B6 mice with a high dose of *C. albicans* ($3x10^5$, i.v.) as done previously and monitored survival daily. All A/J mice succumbed after 24 hours (highly susceptible), whereas the median survival time (MST) for AKR/J mice was 3 days (significant by a Log-rank test; $p<0.0001$), while MST for resistant B6 mice was 4 days.

Pro-inflammatory cytokines IL-6, TNF-α, and MCP-1 are found at high concentrations in circulating blood and kidney of C5-deficient mice (exemplified by A/J) at 24 and 48 h following *C. albicans* infection (*298*, *575*), and elevated KC levels in kidney correlate with subsequent damage to this organ (*575*). We compared serum cytokine profiles of A/J, AKR/J and C57BL/6J prior to and 48 h following *C. albicans* infection using the BD™ CBA Flex system (Figure 5). As expected, we observed high serum levels of pro-inflammatory cytokines IL-6, TNF- α, MCP-1, and KC as well as the Th2-specific cytokine IL-10 in infected A/J mice (*472*, *473*). On the other hand, and similar to B6 animals, AKR/J mice had undetectable levels of IL-10 even 48 h post-infection and no statistically significant increase in concentrations of IL-6, TNF-α, MCP-1 or KC. Interestingly, we observed a strong induction and elevated serum levels of IFNγ in infected AKR/J mice, which were significantly higher than those measured in infected C57BL/6J (resistant) and A/J (susceptible) controls. Studies in IFNγ mutant mice have previously demonstrated a protective effect of this Th1 cytokine against disseminated candidiasis (*455*), suggesting that the elevated levels of this cytokine during infection may have a protective effect in C5-deficient AKR/J mice.

Genetic analysis of the C. albicans resistance trait of AKR/J mice. The inheritance and complexity of the C5-independent genetic control to *C. albicans*

Figure 4. Differential susceptibility of A/J and AKR/J mice to *C. albicans* infection.

6 mice per strain were challenged with the indicated dose of *C. albicans* and sacrificed at either 24 h or 48 h time point to determine the kidney fungal burden (A) and serum BUN levels (B). The fungal load was significantly lower in AKR/J mice compared to A/J, and was associated with lower BUN levels (*P<0.05, ***P≤0.0001, n.d. not done due to premature death of A/J mice). Bars represent group mean ± SD. For the survival study, 8 mice per strain were infected intravenously with a high dose ($3x10^5$) of *C. albicans* and monitored daily for clinical signs of morbidity (C). Survival curves were compared by a Log-rank test and the median survival of AKR/J (3 d) was found to be significantly different from A/J (1 d) (P<0.0001).

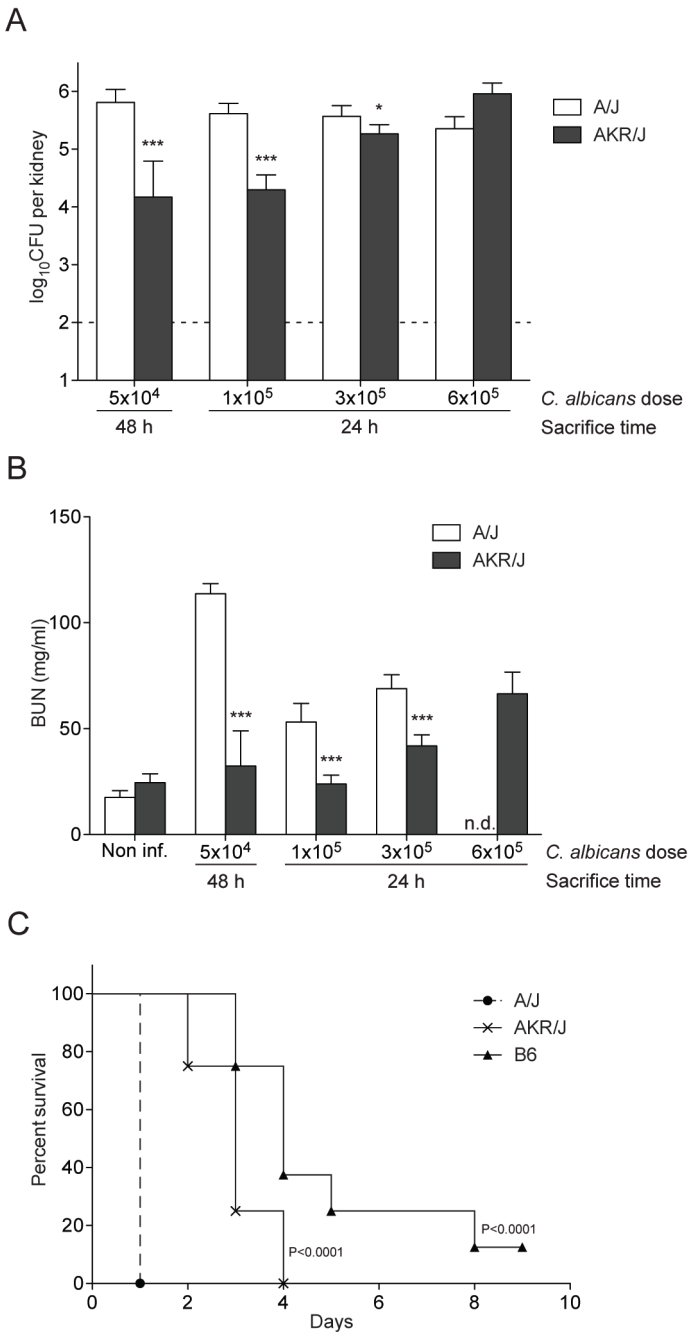
A
log10CFU per kidney
A/J
AKR/J
***
***
*
5x10^4
1x10^5
3x10^5
6x10^5
C. albicans dose
48 h
24 h
Sacrifice time
B
BUN (mg/ml)
A/J
AKR/J
***
***
***
n.d.
Non inf.
5x10^4
1x10^5
3x10^5
6x10^5
C. albicans dose
48 h
24 h
Sacrifice time
C
Percent survival
A/J
AKR/J
B6
P<0.0001
P<0.0001
Days

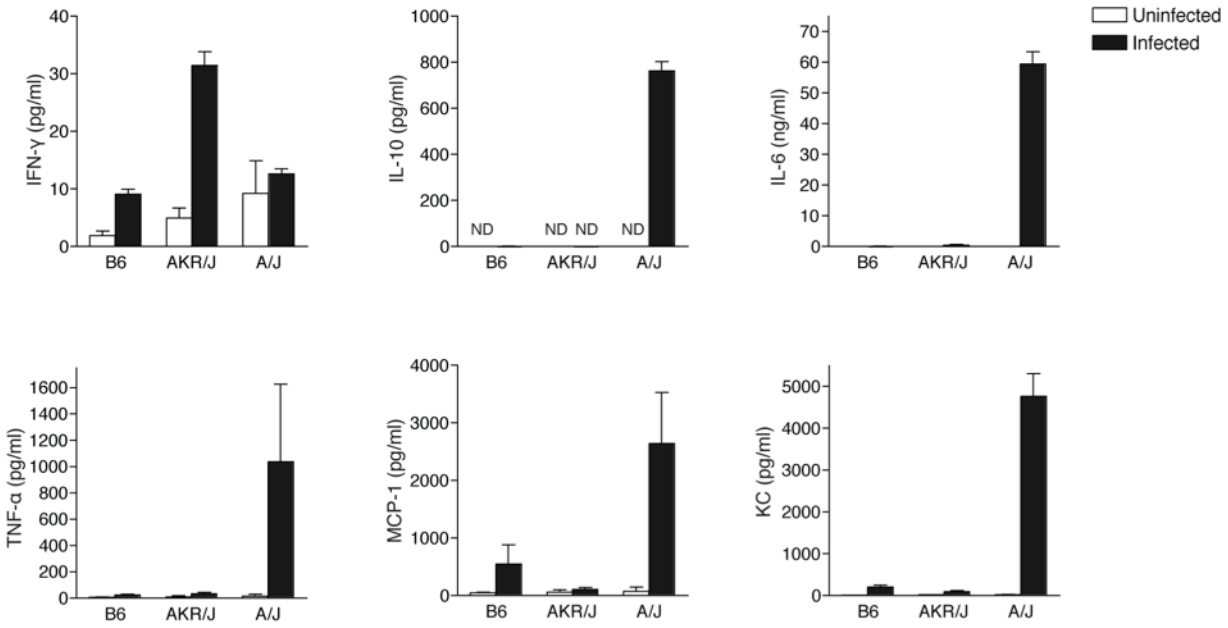

Figure 5. Inflammatory cytokine levels in the AKR/J mouse strain.

Serum cytokine levels in 3-6 mice of each strain were measured prior to infection and at the 48 h time point, as described in Materials and methods. Cytokine response of AKR/J mice resembled closely that of B6 strain and was significantly different from A/J mice. The standard deviation is indicated for each group. For all cytokines, infected AKR/J shows a statistically significant difference from infected A/J mice.

resistance of AKR/J mice was investigated by phenotyping mice from an informative F2 cross generated between resistant AKR/J and susceptible A/J progenitors, and in which all mice are fixed for C5 deficiency. [A/JxAKR/J]F1 hybrids showed an intermediate level of susceptibility with respect to kidney fungal load (Figure 6A) compared to the parental controls, suggesting that resistance to *C. albicans* in AKR/J mice is inherited in a co-dominant fashion. A total of 158 [A/JxAKR/J]F2 animals were infected intravenously with $5x10^4$ *C. albicans* blastospores in four separate infections (Figure 6A). The kidney fungal burden was determined and used as a quantitative phenotypic measure of susceptibility in linkage analyses. The results of four infections were combined and regressed in an experiment- and sex-dependent manner, where the mean was set at 0. The distribution frequency (Figure 6B) and the $\log_{10}$CFU counts of [A/JxAKR/J]F2 mice (Figure 6A) show a normal distribution, with an approximate 1:1 ratio of resistant to susceptible mice confirming a co-dominant pattern of inheritance. Informative F2 mice were genotyped with a custom panel of 257 polymorphic informative markers (SNPs and microsatellites) distributed across the genome. Whole-genome multiple regression linkage analysis in R/qtl was performed for males (N=96) and females (N=72), or both genders together (Figure 6C). This analysis identified a highly significant linkage associated with fungal burden in the kidney on chromosome 11 (LOD=4.59, P<0.01) and chromosome 8 (LOD=3.95, P<0.05) (Figure 7A and 7B). These loci contributing resistance to *C. albicans* in the AKR/J strain were given a temporary identification *Carg3* (*Candida albicans* resistance gene 3) for chromosome 8 QTL and *Carg4*, for chromosome 11 QTL. The Bayesian 95% credible intervals were determined to be 53.6-96.9 Mb for *Carg3* and 70.7-103.8 Mb for *Carg4*, whereas the peak LOD scores were identified at 75 Mb (peak SNP: rs3722665) and 98.8 Mb (peak SNP: rs3661058), respectively. Both *Carg3* and *Carg4* loci were present amongst the initial SNP associations uncovered by EMMA analysis (Figure 2A and Table S1) and were found to be significant (P value < $1x10^{-5}$), however, only *Carg4* passed the stringent Bonferroni correction. These results confirm results of the haplotype mapping studied in the 23 inbred strains, with respect to the effect of the *Carg4* locus on response to disseminated *C. albicans* infection. They also suggest that the *Carg4* locus strongly

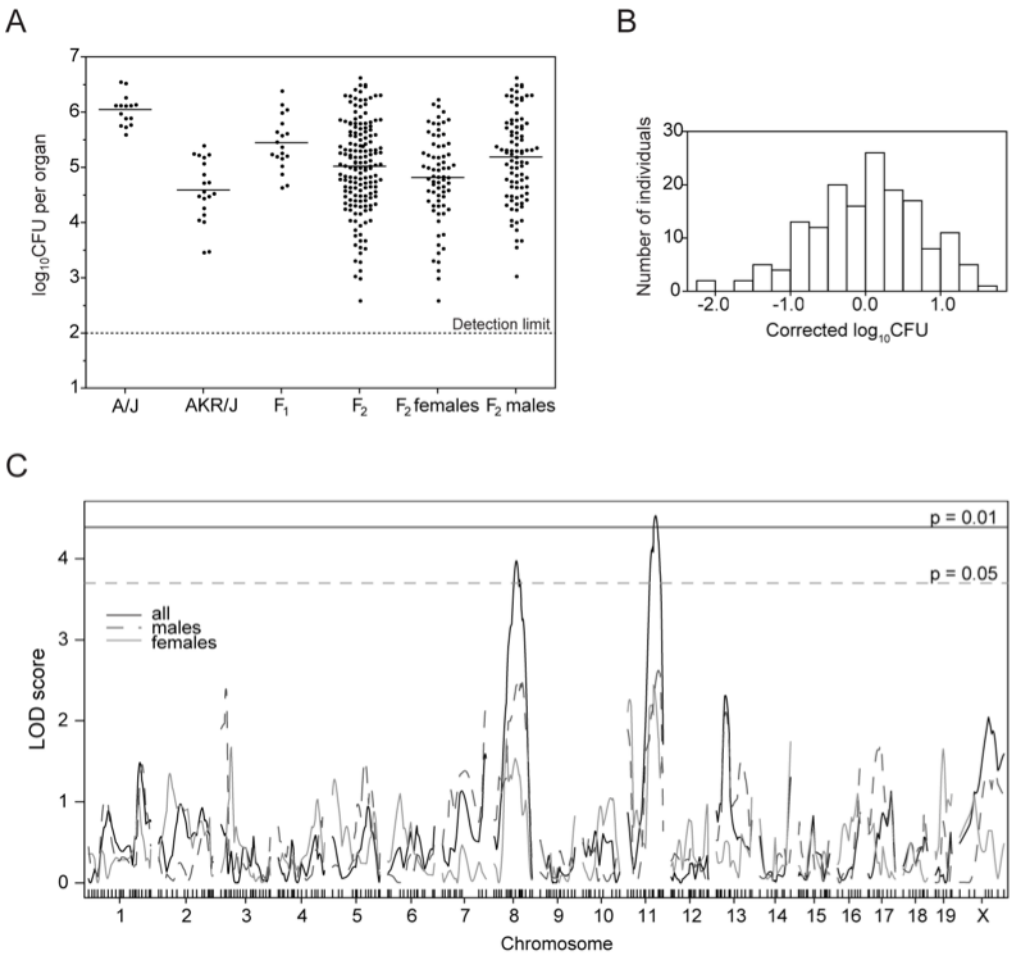

Figure 6. Linkage analysis in the informative [A/JxAKR/J]F2 population.

[A/JxAKR/J]F2 mice (n=158) were infected with *C. albicans* ($5x10^4$, i.v.) and kidneys were harvested 48 h post infection. CFU were determined as previously mentioned and results from four separate infections are plotted along with A/J, AKR/J, and [A/JxAKR/J]F1 controls (A). Each dot represents a single mouse. Distribution of kidney fungal load is shown in the entire [A/JxAKR/J]F2 population (B), after regression of log_{10}CFU to an experiment and gender-specific mean (set at 0). Mice were genotyped at 257 SNPs and markers across the entire genome and interval mapping was carried out using the R/qtl software package. Whole genome LOD score traces are shown for genetic effects controlling kidney fungal burden in [A/JxAKR/J]F2 mice (C), identifying linkage to chromosome 8 (LOD=3.95) and chromosome 11(LOD=4.59), designated *Carg3* and *Carg4*, respectively. Results for males and females are shown separately (dashed and dotted lines) and together (solid line), with marker positions on the x-axis. Permutation testing (1000 tests) identified genome-wide thresholds at P=0.01 and 0.05.

contributes to the noted resistance of AKR/J mice, acting independently of the C5 locus, for which susceptibility alleles are fixed in the analyzed AKR/JxA/J cross.

To examine whether these loci acted in an additive or epistatic manner, we performed a two-dimensional Haley-Knott multiple regression analysis using R/qtl. This analysis revealed that the joint effect of *Carg3* and *Carg4* increased the LOD score to 11.5, suggesting an additive effect which explains 28% of phenotypic variance observed. This additive effect is clearly illustrated when the extremities of the F2 distribution are segregated according to the more significant *Carg4* locus (Figure 7C) and exhibit a predominance of the AKR/J and A/J alleles in the resistant and susceptible F2 mice, respectively. Indeed, mice carrying the A/J allele at both *Carg3* and *Carg4* loci display a significantly higher kidney fungal load than mice carrying AKR/J alleles at both loci ($P<0.0008$, t-test). Although a few select resistant F2 animals carry the A/J allele at one locus, they consistently bear a non-A/J allele (AKR/J or heterozygous) at the other locus. The opposite is also true for susceptible F2 mice which inherited the AKR/J allele at either *Carg3* or *Carg4*. Finally, to illustrate the overlap achieved by EMMA and linkage analysis, association scores for chromosome 11 and 8 are depicted along with respective LOD score traces (Figure 7D and 7E). These results point to *Carg3* and *Carg4* as a novel two-locus system regulating C5-independent resistance to *C. albicans* infection in AKR/J mice.

Figure 7. Additive effect of the *Carg3* and *Carg4* loci on kidney fungal burden in [A/JxAKR/J]F2 mice.

Detailed LOD score traces are shown for chromosome 11 (*Carg4*) (A) and chromosome 8 (*Carg4*) (B) loci for males, females, and both sexes combined. The shaded area designates the Bayesian 95% confidence interval for each locus and the genome-wide thresholds are indicated at P=0.01 and P=0.05. The additive effect of *Carg3* and *Carg4* loci is demonstrated by segregating the alleles of susceptible and resistant mice found at extremities (± 1 standard deviation from the mean) of the distribution (C). Haplotype map colour coding: light gray (AKR/J), gray (A/J), and white (heterozygous). Each line represents a single mouse. Genome-wide association mapping results are depicted along with LOD score traces for chromosomes 11 (D) and 8 (E). The 10 Mb blocks examined for candidate genes are indicated for both loci.

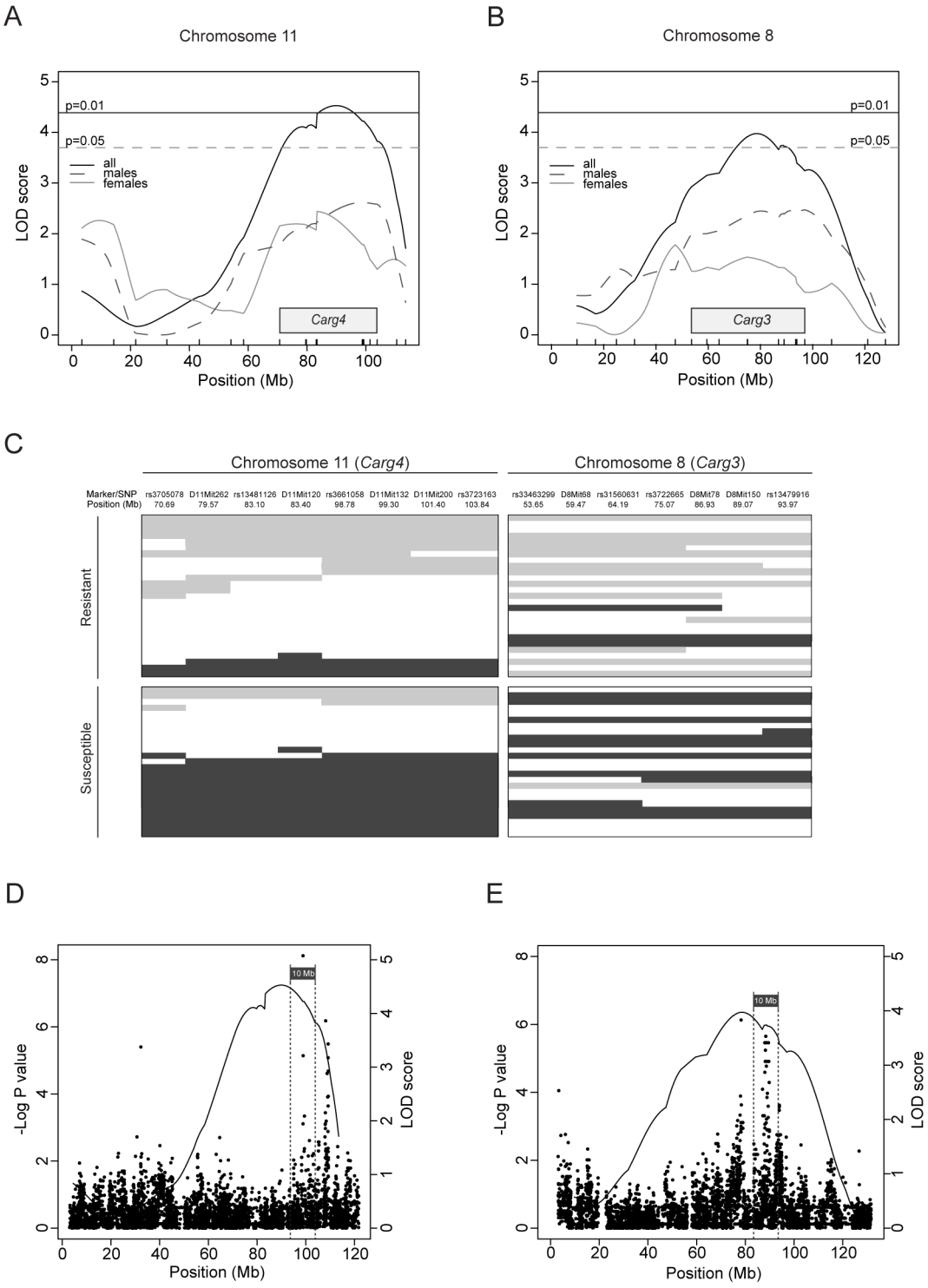
A
Chromosome 11
LOD score
p=0.01
p=0.05
all
males
females
Carg4
Position (Mb)
B
Chromosome 8
LOD score
p=0.01
p=0.05
all
males
females
Carg3
Position (Mb)
C
Chromosome 11 (Carg4)
Chromosome 8 (Carg3)
Marker/SNP rs3705078 D11Mit262 rs13481126 D11Mit120 rs3661058 D11Mit132 D11Mit200 rs3723163 rs33463299 D8Mit68 rs31560631 rs3722665 D8Mit78 D8Mit150 rs13479916
Position (Mb) 70.69 79.57 83.10 83.40 98.78 99.30 101.40 103.84 53.65 59.47 64.19 75.07 86.93 89.07 93.97
Resistant
Susceptible
D
-Log P value
LOD score
10 Mb
Position (Mb)
E
-Log P value
LOD score
10 Mb
Position (Mb)

2.5 DISCUSSION

We have used a representative panel of 23 phylogenetically distant inbred mouse strains to study the genetic control of susceptibility to acute and disseminated *C. albicans* infection. At the time of starting this survey, the critical impact of the mutant *C5* deficiency allele, fixed in certain inbred strains, on susceptibility to infection has been firmly established (*7*). Additional genetic effects, in the form of the unmapped *Carg1* and *Carg2* loci, had suggested that additional genetic effects may further modulate response of inbred strains to this infection (*11*, *12*, *557*). Our inbred strains survey produce two key findings. Firstly, it readily identified two strains that show discordant genotype/phenotype relationships with respect to C5 status and susceptibility to infection (Figure 1 and Table 1), namely AKR/J which carries the mutant *C5* allele but is resistant to infection, and SM/J which is susceptible despite a wild type allele at *C5*. Secondly, haplotype association mapping in the 23 inbred strains using kidney fungal load as a quantitative measure of susceptibility uncovered several candidate loci (in addition to C5 on Chr. 2) controlling fungal replication in the host. Subsequent genome scan in informative F2 mice generated between susceptible A/J and resistant AKR/J (fixed for mutant *C5* alleles) progenitors identified two highly significant linkages on chromosomes 8 (Carg3, LOD score=3.95, P value<0.05) and 11 (*Carg4*, LOD score=4.59, P value<0.01), as regulating permissiveness to *C. albicans* in these mice. *Carg3* and *Carg4* are novel loci that regulate susceptibility to *C. albicans* in a C5-independent fashion.

Genome-wide haplotype association in inbred strains of mice has proven to be a useful experimental strategy to detect loci that regulate complex traits (*576*, *577*). The limitations of this type of analysis reside in the relatively small number of inbred strains that were surveyed (*572*, *578*), which limits the power of association study using single marker mapping (SMM) strategy (*579*). SMM assigns a bi-allelic genotype to individual SNPs, and can therefore incorrectly model SNPs that possess three or even four predominant genotypes in inbred strains. This limits both the power of detecting relevant genetic effects, and the accuracy with which the

corresponding loci and associated haplotype can be delineated. Also, loci that do not explain a substantial percentage of phenotypic variance (*572*) may go unnoticed. Therefore, the results of our analysis probably represent an underestimate of the number of genetic effects regulating susceptibility to *C. albicans* in inbred strains. A noteworthy advantage of the EMMA algorithm is the avoidance of inflation of false positives due to a kinship matrix that corrects for genetic relatedness amongst inbred strains (*572*). Su *et al.* (*578*) and other groups (*580*) have acclaimed the strength of combining genome-wide association mapping and linkage analysis in an F2 cross to identify QTLs underlying complex traits and avoid false-positive loci. We created an informative [A/JxAKR/J]F2 cross in order to corroborate the loci identified by EMMA analysis, but in the context of C5 deficiency. Linkage mapping in the [A/JxAKR/J]F2 progeny identified a novel gene effect located on chromosome 8 and termed *Carg3* (LOD=3.95) and confirmed the chromosome 11 locus (*Carg4*, LOD=4.59) (Figure 6). In fact, the peak associated SNPs on chromosomes 8 and 11 are located directly below the significant LOD score traces and overlap with *Carg3* and *Carg4*, respectively (Figure 7C, 7D) strongly suggesting that the same loci were detected by both approaches.

Recently, it was demonstrated that elevated levels of IL-6, MIP-1β, and mostly KC in kidney extracts of *C. albicans* infected mice correlate with kidney damage (*575*). This is exemplified by the susceptible A/J strain (Figure 5), which displays an acute and possibly pathological inflammatory response upon systemic *C. albicans.* The phenotypic response to infection in C5-deficient AKR/J mice with respect to serum cytokine profiles is clearly distinct from that of C5-deficient A/J mice, but rather resembles that of resistant and C5-sufficient C57BL/6J strain, with one notable exception. Indeed, infected AKR/J mice show strikingly elevated levels of serum IFNγ compared to either resistant C57BL/6J or susceptible A/J. Although we cannot yet establish that elevated serum IFNγ seen in AKR/J are solely or partly responsible for resistance in this strain, a protective role for this cytokine in *C. albicans* infection has been established. Indeed, mice deficient for IFNγ (*455*) or IFNγ receptor (*456*) show increased susceptibility to *C. albicans*, and passive administration of IFNγ (*347*) causes a reduction in tissue fungal burden in normal

mice. In addition, *in vitro* studies have also shown that IFNγ potentiates phagocytosis and killing of *C. albicans* by neutrophils (*340*) and macrophages (*154*). Moreover, IFNγ is used as a prophylactic treatment of infection in patients with chronic granulomatous disease (CGD), a genetically inherited disease characterized by an increased susceptibility to fungal infections (*581*). Therefore, we hypothesized that elevated levels of this cytokine during infection may have a protective effect in C5-deficient AKR/J mice by directly potentiating the fungicidal effect of immune cells and/or stimulating host genes implicated in antifungal defense and which underlie *Carg3* and *Carg4* loci.

Signaling by IFNγ activates the JAK-STAT pathway, which leads to the binding of phosphorylated STAT1 to IFNγ activation site (GAS) elements and also interferon-stimulated response elements (ISREs) (*582*, *583*). Robertson *et al.* recently used chromatin immunoprecipitation and DNA sequencing to map all functional STAT1 binding sites (and associated genes) which are induced by IFNγ treatment of human HeLa S3 cells (*584*). We therefore investigated the *Carg3* and *Carg4* for the presence of positional candidates that may be bound by STAT1 in response to IFNγ. The minimal genetic interval inferred by linkage analysis at *Carg3* extends over 40 Mb, while that at *Carg4* is 30 Mb. As both regions are extremely gene rich, we restricted the size of the genomic candidate regions by combining linkage analysis and the haplotype association mapping results. Therefore, we prioritized for analysis blocks of 10Mb centered around the SNPs showing the highest scores in the haplotype association studies for both loci (Figure 7D). This analysis identified a total of 59 (*Carg3*) and 147 such genes (*Carg4*) (Tables S2 and S3). We also superimposed on this dataset, those genes whose mRNA expression has been shown by transcript profiling to be modulated at 2h, 4h, or 6h following exposure to IFNγ (*585*). An intersection of genes containing high STAT1 binding ChIP-Seq peaks (identified by combination of chromatin immunoprecipitation and DNA sequencing; ChIP/seq) and genes whose mRNAs were significantly modulated by IFNγ, yielded a list of 4 and 11 genes. We consider these genes as priority candidate genes for the *Carg3* and *Carg4* effects.

Four genes in the *Carg3* interval fulfill both criteria: *Adcy7*, *Dnaja2*, *Gab1* and *Inpp4b*. *Adcy7* is of particular interest for the following reasons. *Adcy7* codes for an isoform of adenylate cyclase that is expressed at high levels and regulates the intracellular levels of cyclic adenosine monophosphate (cAMP) in macrophages, T cells and B cells (*586*, *587*). cAMP is as a potent immunosuppressor in antigen-presenting cells and T lymphocytes acting as an intracellular signal to dampen synthesis of pro-inflammatory cytokines in these cells (*588-590*). For example, cAMP acts as a second messenger for the anti-inflammatory action of prostaglandin E2 (PGE2) in macrophages, which ultimately leads to reduced phagocytosis, decreased production of reactive oxygen species, attenuation of TNFα, MIP-1α, LTB4 secretion, and increased IL-10 production by these cells. *Adcy7* expression is abundant in macrophages, stimulated by IFNγ, and associated with STAT-1 binding to the *Adcy7* gene promoter (Table S2). Tissue-specific ablation of *Adcy7* in the hematopoietic system causes a defect in cAMP production, and is associated with increased production of TNFα by macrophages following exposure to LPS *ex vivo*, and hyper-sensitivity to LPS-induced endotoxin shock *in vivo* (*586*). Therefore, it is tempting to speculate that high levels of circulating IFNγ in AKR/J mice may stimulate expression of *Adcy7* in immune cells, with concomitant effects on intracellular cAMP levels and intensity of inflammatory response in these mice. The noted absence of infiltrating inflammatory cells in the kidneys of *C. albicans* infected AKR/J mice (Figure 3D) is consistent with a dampened inflammatory response associated with elevated adenylate cyclase activity and cAMP levels (*591*). Additional experimentation will be required to formally test this proposal.

Amongst the list of 11 *Carg4* positional candidates whose expression is regulated by IFNγ and which display IFNγ regulated STAT1 recruitment to their promoters (Table S3), we note the presence of *Ifi35*. Ifi35 belongs to the family of interferon-inducible proteins, a group of proteins whose expression is rapidly induced by both type I and type II interferons, and that have been associated with different pathologies including systemic lupus erythematosus (*592*), cancer (*593*), and antiviral host defense (*594*). IFI35 is a leucine zipper-containing transcriptional regulator which is normally found in the cytoplasm of cells, and is translocated to the nucleus

following exposure to IFNγ (*595*). In the nucleus, IFI35 heterodimerizes with other proteins (Nmi, CKIP-1) (*596*), including the transcription factor B-ATF (*52*). The physical interaction between B-ATF (basic leucine zipper transcription factor, ATF-like) and IFI35 suggests a role for IFI35 in cytokine signaling, and early polarization of the T helper response (*52*). B-ATF is a member of the AP-1 family of transcription factors expressed primarily in hematopoietic cells (*52*, *597*). B-ATF binds to the promoter of the *Il17* gene and plays a critical role in Th17 differentiation of helper T cells (*597*). Indeed, *Batf*$^{-/-}$ deficient mice display normal Th1, and Th2 response but are deficient in Th17 differentiation, and are resistant to experimental autoimmune encephalitis (*597*). Il17 and Th17 differentiation of T cells is essential for protection against fungal pathogens, and Il17$^{-/-}$ mice are hyper-susceptible to infection with *C. albicans* (*127*). In addition, alterations in Th17 response have been associated with susceptibility to candidiasis in human clinical cases (*6*, *488*, *598*). Therefore, Ifi35 may play a role in anti-fungal defenses by modulating Th17 response, a hypothesis that can be tested experimentally.

In conclusion, we have combined genome-wide association mapping and linkage analysis to identify and validate two novel loci that modulate response to systemic *C. albicans* infection in mice. These two loci exert their effect in a complement C5-independent fashion. The identification of the genes involved should provide valuable insight into host defenses against acute candidiasis.

2.6 ACKNOWLEDGMENTS

We would like to thank Dr. Molly Bogue, Director of the Mouse Phenome Project at The Jackson Laboratory, for providing mice for this collaboration.

2.7 SUPPLEMENTARY MATERIAL

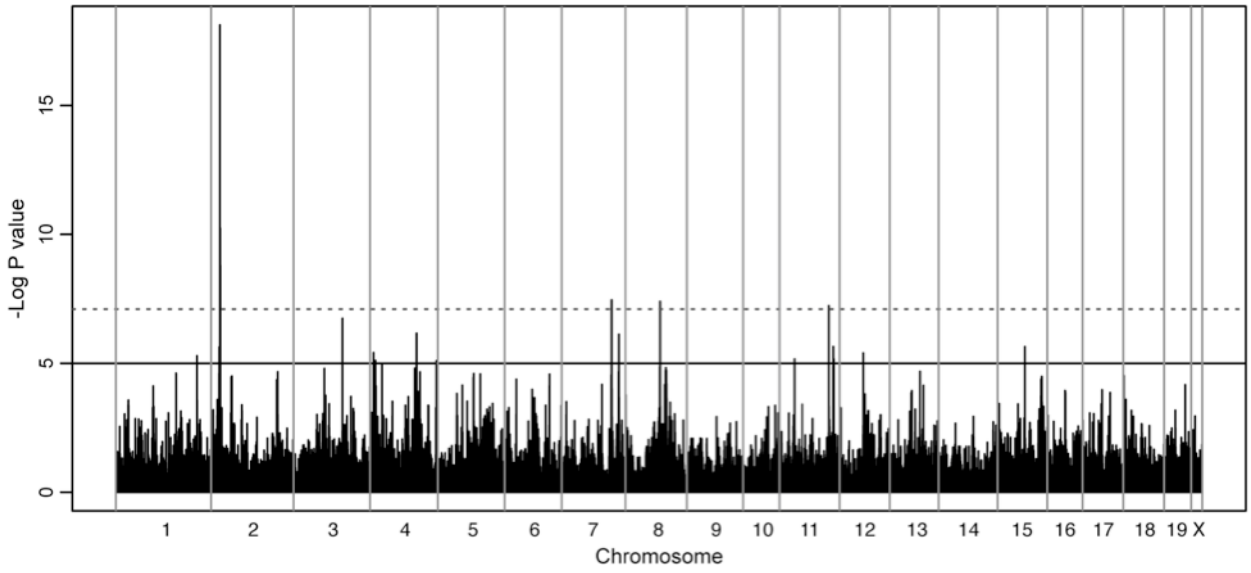

Figure S1. Genome-wide association mapping without discordant AKR/J and SM/J strains.

EMMA analysis was conducted as described earlier (see Materials and Methods, and Figure 2) while omitting the AKR/J and SM/J discordant strains. $-Log_{10}P$ values are depicted and represent genome wide significance of association for each SNP. Standardized threshold was set at P value $1.0x10^{-5}$ (solid line) and the Bonferroni multiple testing correction threshold was calculated to be $7.87x10^{-8}$ (dashed line).

Table S1. *In silico* identified loci controlling response to *C. albicans* infection in inbred mouse strains.

Chromosome	Position (Mb)	P value	-Log_{10} P value
1	61.10	4.96E-06	5.30
2	31.14	6.66E-06	5.18
	31.19	6.66E-06	5.18
	31.22	2.30E-06	5.64
	31.29	6.66E-06	5.18
	33.74	6.51E-06	5.19
	33.74	6.70E-07	6.17
	33.74	3.04E-10	9.52
	33.76	8.71E-07	6.06
	33.82	2.43E-11	10.61
	33.90	8.71E-07	6.06
	33.92	5.74E-06	5.24
	33.95	1.36E-06	5.87
	33.96	4.65E-09	8.33
	34.45	2.28E-06	5.64
	34.75	7.78E-06	5.11
4	106.21	2.81E-06	5.55
	111.05	7.69E-06	5.11
	111.17	7.69E-06	5.11
	111.20	7.69E-06	5.11
	111.24	7.69E-06	5.11
	136.62	1.17E-07	6.93
6	120.43	2.32E-06	5.63
7	122.15	2.33E-06	5.63
	133.22	1.31E-07	6.88

8	78.25	7.43E-07	6.13
	87.98	3.43E-06	5.46
	88.00	3.43E-06	5.46
	88.00	3.43E-06	5.46
	88.02	3.43E-06	5.46
	88.24	5.77E-06	5.24
	88.38	3.43E-06	5.46
	88.39	2.26E-06	5.65
	88.63	3.43E-06	5.46
	89.49	3.43E-06	5.46
11	32.27	4.01E-06	5.40
	98.87	7.63E-09	8.12
	98.91	7.17E-06	5.14
	98.91	7.17E-06	5.14
	108.16	6.66E-07	6.18
	109.16	3.25E-06	5.49
	109.17	3.25E-06	5.49
	109.17	8.39E-06	5.08
12	50.93	9.02E-07	6.04
15	54.18	5.19E-06	5.28

SNPs that have passed the Bonferroni cutoff (α=0.01, P value = 7.99×10^{-8}) are shaded in gray.

Table S2. Candidate genes in the *Carg3* region.

Gene symbol	Gene name	ChIP-Seq Peak height ≥ 20	Gene expression Orange=Up, Green=Down
2310036O22Rik	RIKEN cDNA 2310036O22 gene		N/A
4921524J17Rik	RIKEN cDNA 4921524J17 gene		N/A
Abcc12	ATP-binding cassette, sub-family C (CFTR/MRP), member 12		
Adcy7	adenylate cyclase 7	✓	
Asf1b	ASF1 anti-silencing function 1 homolog B (S. cerevisiae)	✓	
Best2	bestrophin 2	✓	
Cacna1a	calcium channel, voltage-dependent, P/Q type, alpha 1A subunit	✓	
Calr	calreticulin		
Ccdc130	coiled-coil domain containing 130		
Cd97	CD97 antigen		N/A
Chd9	chromodomain helicase DNA binding protein 9		
Dand5	DAN domain family, member 5		
Dcaf15	DDB1 and CUL4 associated factor 15		N/A
Dhps	deoxyhypusine synthase		
Dnaja2	DnaJ (Hsp40) homolog, subfamily A, member 2	✓	
Dnajb1	DnaJ (Hsp40) homolog, subfamily B, member 1	✓	
Elmod2	ELMO domain containing 2		
Farsa	phenylalanyl-tRNA synthetase, alpha subunit		N/A
Gab1	growth factor receptor bound protein 2-associated protein 1	✓	
Gadd45gip1	growth arrest and DNA-damage-inducible, gamma interacting protein 1	✓	
Gcdh	glutaryl-Coenzyme A dehydrogenase		
Gipc1	GIPC PDZ domain containing family, member 1	✓	
Gm16994	predicted gene, 16994		N/A
Gpt2	glutamic pyruvate transaminase (alanine aminotransferase) 2	✓	
Hook2	hook homolog 2 (Drosophila)	✓	
Ier2	immediate early response 2		
Il15	interleukin 15	✓	
Inpp4b	inositol polyphosphate-4-phosphatase, type II	✓	
Itfg1	integrin alpha FG-GAP repeat containing 1	✓	
Junb	Jun-B oncogene	✓	
Lonp2	lon peptidase 2, peroxisomal		
Mir1199	microRNA 1199		N/A
Mir181c	microRNA 181c		N/A
Mir181d	microRNA 181d		N/A
Mir23a	microRNA 23a	✓	N/A
Mir24-2	microRNA 24-2	✓	N/A
Mir27a	microRNA 27a	✓	N/A
N4bp1	NEDD4 binding protein 1		
Nacc1	nucleus accumbens associated 1, BEN and BTB (POZ) domain containing		
Nanos3	nanos homolog 3 (Drosophila)		
Ndufb7	NADH dehydrogenase (ubiquinone) 1 beta subcomplex, 7		
Nfix	nuclear factor I/X		
Papd5	PAP associated domain containing 5		
Phkb	phosphorylase kinase beta		
Pkn1	protein kinase N1		
Prdx2	peroxiredoxin 2		
Prkaca	protein kinase, cAMP dependent, catalytic, alpha		
Rnaseh2a	ribonuclease H2, large subunit		
Rnf150	ring finger protein 150		
Rtbdn	retbindin		
Samd1	sterile alpha motif domain containing 1	✓	
Scoc	short coiled-coil protein		
Siah1a	seven in absentia 1A	✓	N/A
Tbc1d9	TBC1 domain family, member 9		
Tecr	trans-2,3-enoyl-CoA reductase		N/A
Tmem188	transmembrane protein 188	✓	
Trmt1	TRM1 tRNA methyltransferase 1 homolog (S. cerevisiae)		
Vps35	vacuolar protein sorting 35		
Zfp330	zinc finger protein 330	✓	N/A

A total of 59 genes containing IFNγ-inducible STAT1 binding sites and their overall mRNA expression (>2X) upon IFNγ stimulation in Hela cells are represented. Genes considered for further prioritization had a high (>20) ChIP-Seq peak height and a significant (>2X) gene expression. N/A designation in the gene expression column was given for genes that were not represented on the microarray.

Table S3. Candidate genes in the *Carg4* region.

Gene symbol	Gene name	ChIP-Seq Peak height ≥ 20	Gene expression Orange=Up, Green=Down
1110035M17Rik	RIKEN cDNA 1110035M17 gene		N/A
1700028N14Rik	RIKEN cDNA 1700028N14 gene		N/A
1810046J19Rik	RIKEN cDNA 1810046J19 gene		N/A
Aarsd1	alanyl-tRNA synthetase domain containing 1		
Abcc3	ATP-binding cassette, sub-family C (CFTR/MRP), member 3	✓	
Acly	ATP citrate lyase		
Acsf2	acyl-CoA synthetase family member 2		
Ankrd40	ankyrin repeat domain 40	✓	
Arhgap23	Rho GTPase activating protein 23		
Arl4d	ADP-ribosylation factor-like 4D		
Asb16	ankyrin repeat and SOCS box-containing 16	✓	
Atp6v0a1	ATPase, H+ transporting, lysosomal V0 subunit A1	✓	
Atxn7l3	ataxin 7-like 3		
BC030867	cDNA sequence BC030867	✓	N/A
Becn1	beclin 1, autophagy related	✓	
Brca1	breast cancer 1		
Cacna1g	calcium channel, voltage-dependent, T type, alpha 1G subunit		
Cacnb1	calcium channel, voltage-dependent, beta 1 subunit		
Calcoco2	calcium binding and coiled-coil domain 2		
Ccdc103	coiled-coil domain containing 103		
Ccdc43	coiled-coil domain containing 43	✓	
Ccr10	chemokine (C-C motif) receptor 10		
Ccr7	chemokine (C-C motif) receptor 7	✓	
Cd300lg	CD300 antigen like family member G		
Cdc6	cell division cycle 6 homolog (S. cerevisiae)	✓	
Cdk12	cyclin-dependent kinase 12		N/A
Cnp	2',3'-cyclic nucleotide 3' phosphodiesterase		
Coasy	Coenzyme A synthase	✓	
Col1a1	collagen, type I, alpha 1		
Cwc25	CWC25 spliceosome-associated protein homolog (S. cerevisiae)		N/A
Dcakd	dephospho-CoA kinase domain containing		
Dhx8	DEAH (Asp-Glu-Ala-His) box polypeptide 8	✓	
Dlx4	distal-less homeobox 4		
Dnajc7	DnaJ (Hsp40) homolog, subfamily C, member 7		
E130012A19Rik	RIKEN cDNA E130012A19 gene		N/A
Eftud2	elongation factor Tu GTP binding domain containing 2		
Eif1	eukaryotic translation initiation factor 1		
Epn3	epsin 3		
Fam117a	family with sequence similarity 117, memberA	✓	
Fmnl1	formin-like 1		
Fmnl1	formin-like 1		
G6pc3	glucose 6 phosphatase, catalytic, 3		
Gfap	glial fibrillary acidic protein		
Ghdc	GH3 domain containing		
Gjd3	gap junction protein, delta 3		
Gosr2	golgi SNAP receptor complex member 2	✓	
Gpatch8	G patch domain containing 8		
Grb7	growth factor receptor bound protein 7		
Grn	granulin		
Hap1	huntingtin-associated protein 1	✓	
Hdac5	histone deacetylase 5		
Hexim1	hexamethylene bis-acetamide inducible 1		
Hexim2	hexamthylene bis-acetamide inducible 2	✓	
Hsd17b1	hydroxysteroid (17-beta) dehydrogenase 1		
Ifi35	interferon-induced protein 35	✓	
Igf2bp1	insulin-like growth factor 2 mRNA binding protein 1	✓	
Igfbp4	insulin-like growth factor binding protein 4		
Ikzf3	IKAROS family zinc finger 3	✓	
Itga3	integrin alpha 3	✓	
Jup	junction plakoglobin		
Kif18b	kinesin family member 18B		
Krt10	keratin 10		
Krt15	keratin 15		
Krt16	keratin 16	✓	
Krt17	keratin 17	✓	
Krt24	keratin 24	✓	
Krt32	keratin 32		
Krt42	keratin 42		N/A
Lasp1	LIM and SH3 protein 1	✓	N/A
Lrrc46	leucine rich repeat containing 46		
Lrrc59	leucine rich repeat containing 59		

Lsm12	LSM12 homolog (S. cerevisiae)		
Luc7l3	LUC7-like 3 (S. cerevisiae)	✓	N/A
Lyzl6	lysozyme-like 6		
Map3k14	mitogen-activated protein kinase kinase kinase 14		
Med1	mediator complex subunit 1		
Mllt6	myeloid/lymphoid or mixed-lineage leukemia (trithorax homolog, Drosophila)	✓	
Mpp3	membrane protein, palmitoylated 3 (MAGUK p55 subfamily member 3)	✓	
Mrpl10	mitochondrial ribosomal protein L10		
Mrpl45	mitochondrial ribosomal protein L45	✓	
Msl1	male-specific lethal 1 homolog (Drosophila)		
Myst2	MYST histone acetyltransferase 2	✓	
Naglu	alpha-N-acetylglucosaminidase (Sanfilippo disease IIIB)	✓	
Nags	N-acetylglutamate synthase	✓	
Nbr1	neighbor of Brca1 gene 1		
Nbr1	neighbor of Brca1 gene 1		
Nfe2l1	nuclear factor, erythroid derived 2,-like 1		
Ngfr	nerve growth factor receptor (TNFR superfamily, member 16)		
Nkiras2	NFKB inhibitor interacting Ras-like protein 2		
Nme1	non-metastatic cells 1, protein (NM23A) expressed in	✓	
Nme2	non-metastatic cells 2, protein (NM23B) expressed in		N/A
Nmt1	N-myristoyltransferase 1	✓	
Nr1d1	nuclear receptor subfamily 1, group D, member 1	✓	
Nxph3	neurexophilin 3		
Osbpl7	oxysterol binding protein-like 7		
Pcgf2	polycomb group ring finger 2	✓	
Pgap3	post-GPI attachment to proteins 3		N/A
Plcd3	phospholipase C, delta 3		
Plekhh3	pleckstrin homology domain containing, family H (with MyTH4 domain) member 3		
Plxdc1	plexin domain containing 1	✓	
Pnpo	pyridoxine 5'-phosphate oxidase		
Ppp1r9b	protein phosphatase 1, regulatory subunit 9B	✓	
Ppy	pancreatic polypeptide		
Psmb3	proteasome (prosome, macropain) subunit, beta type 3	✓	
Psmd3	proteasome (prosome, macropain) 26S subunit, non-ATPase, 3	✓	
Ptrf	polymerase I and transcript release factor	✓	
Rab5c	RAB5C, member RAS oncogene family	✓	
Rapgefl1	Rap guanine nucleotide exchange factor (GEF)-like 1		
Rara	retinoic acid receptor, alpha	✓	
Rdm1	RAD52 motif 1		
Rpl19	ribosomal protein L19	✓	
Rpl27	ribosomal protein L27	✓	
Rsad1	radical S-adenosyl methionine domain containing 1		
Rundc1	RUN domain containing 1	✓	
Samd14	sterile alpha motif domain containing 14		
Sgca	sarcoglycan, alpha (dystrophin-associated glycoprotein)		
Sh3d20	SH3 domain containing 20		
Skap1	src family associated phosphoprotein 1		
Slc35b1	solute carrier family 35, member B1		
Slc4a1	solute carrier family 4 (anion exchanger), member 1		N/A
Snf8	SNF8, ESCRT-II complex subunit, homolog (S. cerevisiae)		
Snx11	sorting nexin 11		
Sost	sclerostin		
Spop	speckle-type POZ protein		
Srcin1	SRC kinase signaling inhibitor 1	✓	N/A
Stac2	SH3 and cysteine rich domain 2		
Stard3	START domain containing 3	✓	
Stat3	signal transducer and activator of transcription 3	✓	
Stat5a	signal transducer and activator of transcription 5A	✓	
Stat5b	signal transducer and activator of transcription 5B	✓	
Thra	thyroid hormone receptor alpha		
Tmub2	transmembrane and ubiquitin-like domain containing 2	✓	
Tns4	tensin 4	✓	
Tob1	transducer of ErbB-2.1	✓	
Top2a	topoisomerase (DNA) II alpha		
Ttc25	tetratricopeptide repeat domain 25		
Ttll6	tubulin tyrosine ligase-like family, member 6		
Tubg1	tubulin, gamma 1		
Tubg2	tubulin, gamma 2	✓	
Ube2z	ubiquitin-conjugating enzyme E2Z (putative)		
Ubtf	upstream binding transcription factor, RNA polymerase I	✓	
Vps25	vacuolar protein sorting 25 (yeast)		
Wfikkn2	WAP, follistatin/kazal, immunoglobulin, kunitz and netrin domain containing 2		
Wipf2	WAS/WASL interacting protein family, member 2		

Wnt3	wingless-related MMTV integration site 3	✓	
Xylt2	xylosyltransferase II		
Zfp652	zinc finger protein 652		N/A

A total of 147 genes containing IFNγ-inducible STAT1 binding sites and their overall mRNA expression (>2X) upon IFNγ stimulation in Hela cells are represented. Genes considered for further prioritization had both high (>20) ChIP-Seq peak height and a significant (>2X) gene expression. N/A designation in the gene expression column was given for genes that were not represented on the microarray.

PREFACE TO CHAPTER 3

As described in Chapter 2, we sought to uncover novel C5-independent host genetic factors modulating response to disseminated *C. albicans* infection by surveying a cohort of 23 phylogenetically diverse inbred mouse strains. Although our results reiterated the critical impact of C5, we identified two inbred strains whose phenotype is in discordance with the *C5* allelic status, notably AKR/J (C5-deficient, resistant) and SM/J (C5-suficient, susceptible). Genome-wide association in inbred strains has revealed multiple putative loci associated with renal fungal burden, amongst which loci on chromosomes 8 (*Carg3*) and 11 (*Carg4*) were corroborated by linkage analysis in an informative F2 cross derived from susceptible A/J and resistant AKR/J, in the context of C5-deficiency.

In the following chapter, we delineate a genetic locus on distal chromosome 15 (*Carg5*) that confers susceptibility in the SM/J strain, despite the presence of functional C5. Subsequent detailed immunophenotyping and functional analyses of the innate immune compartment, namely neutrophils and monocytes, reveal a pleiotropic myeloid defect in SM/J that accounts for heightened susceptibility to *C. albicans* challenge. We also utilize a novel genomic approach to catalog and prioritize positional candidates underlying the *Carg5* locus.

Chapter 3:

Genetic control of susceptibility to *Candida albicans* in SM/J mice

3.1 ABSTRACT

In the immunocompromised host, invasive infection with the fungal pathogen *Candida albicans* is associated with high morbidity and mortality. Sporadic cases in otherwise normal individuals are rare, and are thought to be associated with genetic predisposition. Using a mouse model of systemic infection with *C. albicans*, we identified the SM/J mouse strain as unusually susceptible to infection. Genetic linkage studies in informative [C57BL/6JxSM/J]F2 mice identified a major locus on distal chromosome 15, given the appellation *Carg5*, that regulates *C. albicans* replication in SM/J mice. Cellular and molecular immunophenotyping experiments, as well as functional studies in purified cell populations from SM/J and C57BL/6J, and in [C57BL/6JxSM/J]F2 mice fixed for homozygous or heterozygous *Carg5* alleles, indicate that *Carg5*-regulated susceptibility in SM/J is associated with a complex defect in the myeloid compartment of these mice. SM/J neutrophils express lower levels of Ly6G, and importantly, they show significantly reduced production of reactive oxygen species in response to stimulation with fMLF and PMA. Likewise, $CD11b^{+}Ly6G^{-}Ly6C^{hi}$ inflammatory monocytes were present at lower levels in the blood of infected SM/J, recruited less efficiently at the site of infection, and displayed blunted oxidative burst. Studies in F2 mice establish strong correlations between *Carg5* alleles, Ly6G expression, production of serum CCL2 (MCP-1), and susceptibility to *C. albicans*. Genomic DNA sequencing of chromatin immunoprecipitated for myeloid pro-inflammatory transcription factors IRF1, IRF8, STAT1 and NFkB, as well as RNA sequencing, were used to develop a "myeloid inflammatory score" and systematically analyze and prioritize potential candidate genes in the *Carg5* interval.

3.2 INTRODUCTION

Candida albicans is a commensal microbe which resides in the gastrointestinal and genitourinary tracts of healthy individuals (*558*). Breaching of the host barrier or immunological defenses results in *C. albicans* infections, which may range from superficial and benign to disseminated infections with significant morbidity and mortality. Notably, *Candida* species constitute the fourth most common cause of nosocomial bloodstream infections (*39*), with *C. albicans* accounting for over half of all *Candida* infections, and for ~37% of the associated mortality. In the non-immunocompromised host, cases of chronic mucocutaneous candidiasis are sporadic, but multiplex families with dominant (*31*, *490*, *564*) and recessive (*6*, *31*, *599*) inheritance have been described. The study of these rare familial cases has identified genes that play critical roles in host response to *Candida*, including recognition of fungal antigens, as well as Th1 and Th17 polarized immune responses. In parallel, invasive dermatophytic disease has been reported in individuals deficient in CARD9 (*6*, *600*), and more recently, in IL12Rβ1 (*80*).

Besides CARD9 deficiency (*6*), the genetic component of susceptibility to systemic *C. albicans* infection in humans is still unknown. Parallel genetic studies in inbred and mutant mouse strains have identified the complement system as playing a critical and determining role in early innate defenses against blood borne *Candida* (*7*, *8*). Both arms of the complement system (classical, and lectin pathway) are engaged in this response. Activation of the classical pathway relies on C1q-dependent recognition of fungal antigens alone or in association with host cells, or complexed with immunoglobulins (*255*). Alternatively, *Candida* surface carbohydrate structures such as mannoproteins interact with the mannan-binding lectin (MBL) thereby triggering the lectin pathway, and associated activation of C2 and C4 (*255*). Both pathways converge at the formation of a C3 convertase, which produces the potent chemotactic factors C3a and C5a. Their release causes recruitment of inflammatory cells such as neutrophils and inflammatory monocytes to the site of infection. On the other hand, cleavage of C5 into C5a (activator) and C5b initiates the formation of the membrane attack complex (MAC), a macromolecular lytic complex composed of

C5b and other complement subunits (*255*). Studies in mice deficient in factor B, MBL, C1q, C2, C3, and C5 have validated the role of both arms of the complement pathway in defenses against *C. albicans* infection (*8*, *193*, *279*, *297*, *298*).

In humans, and in mouse models, efficient production of inflammatory leukocytes (neutrophils, inflammatory monocytes) and timely recruitment of these cells to the site of infection is required for protection during *C. albicans* infection. Indeed, increased vulnerability to invasive fungal infection is observed in clinical neutropenia (*2*, *601*), and in mutant mice deficient in the cell adhesion molecule ICAM-1 (*373*), and in the neutrophil chemokine receptor CXCR2 (*368*). NADPH oxidase (PHOX) dependent production of reactive oxygen species (ROS) by neutrophils is essential for fungicidal activity, and deficiency in PHOX components in patients suffering from chronic granulomatous disease (CGD) causes recurrent and severe infections with bacterial and fungal pathogens (*54*, *69*). The early egress of monocytes to the site of infection, and the ultimate contribution of these inflammatory monocytes to anti-fungal defenses is poorly understood. In humans, monocytopenia caused by deficiency in *GATA2* (*407*, *408*) and *IRF8* (*409*) predisposes to mycobacterial infections (following BCG vaccination), although invasive infections with fungal pathogens such as *Aspergillus* and *Cryptococcus*, as well as oral candidiasis, have been reported in some of these patients. During systemic infection with *C. albicans* in mice, $Ly6C^{hi}$ inflammatory monocytes rapidly infiltrate infected kidneys, potentiating innate antifungal immunity to reduce fungal burden (*366*). In line with these results, monocytopenic mice exhibit exacerbated infection parameters (*405*).

We have previously shown that roughly half of the inbred laboratory mouse strains carry a naturally occurring 2-bp deletion in the *C5* gene (*Hc* allele) that causes C5 deficiency (*543*), which renders the affected strains susceptible to acute infection with *C. albicans* (*7*, *298*, *602*). In addition to the major effect of the C5 status on fungal replication in target organs (kidney, brain) and overall survival from *C. albicans* infection (*7*), early studies in AcB/BcA recombinant congenic mouse strains suggested that additional, C5-unrelated, genetic loci could also contribute to host

response to *C. albicans* infection (*7*, *9*, *10*). Other studies by Ashman *et al*. suggested that severity of infection evaluated by type and extent of histopathological damage in target organs is regulated by other loci (*Carg1*, *Carg2*), whose map location and identity have remained unknown (*11*, *12*). We recently surveyed a representative cohort of 23 phylogenetically distant inbred mouse strains for susceptibility to disseminated *C. albicans* infection using kidney fungal load as the phenotypic measure (*602*). These studies confirmed the critical role of the *C5* locus in susceptibility to infection, and identified two discordant strains, AKR/J (C5-deficient, resistant) and SM/J (C5-sufficient, susceptible)(*602*). Additional haplotype and linkage mapping studies identified two loci *Carg3* (Chr 8) and *Carg4* (Chr 11) as regulating resistance to *C. albicans* infection in the context of C5 deficiency (*602*).

Here, we have studied the genetic basis and phenotypic expression of C5-independent susceptibility to *C. albicans* infection in the SM/J strain. We show that a locus on Chr 15, that we designate *Carg5*, regulates susceptibility expressed as increased fungal replication in the kidney. Detailed cellular immunophenotyping and molecular studies strongly suggest that *Carg5*-regulated susceptibility to *C. albicans* infection in SM/J is caused by a pleiotropic myeloid defect, characterized by an altered number and function of neutrophils and inflammatory monocytes, including altered expression of Ly6G, and aberrant production of reactive oxygen radicals in both cell types. Studies in [C57BL/6JxSM/J]F2 mice fixed for different allelic combinations at *Carg5* further establish a strong correlation between neutrophil Ly6G expression, production of serum CCL2, and susceptibility to *C. albicans* (fungal load).

3.3 MATERIALS AND METHODS

Mice

A/J, C57BL/6J, and SM/J inbred strains were obtained from the Jackson Laboratories (Bar Harbor, ME) as pathogen-free 8- to 12-week-old mice. [C57BL/6JxSM/J] F2 progeny were bred by systematic brother-sister mating of [C57BL/6JxSM/J] F1 mice. Animal housing and experimental procedures were conducted under the guidelines of the Canadian Council of Animal Care and were approved by the Animal Care Committee of McGill University.

Infection with Candida albicans

C. albicans strain *SC5314* was grown overnight in YPD medium (1% yeast extract, 2% Bacto Peptone and 2% dextrose) at 30^{o}C with shaking. Blastospores were harvested by centrifugation, washed twice in phosphate-buffered saline (PBS), counted using a hemacytometer and resuspended in PBS at the required density. For experimental infections, mice were inoculated via the tail vein with 200 μl of a suspension containing 5x10^{4} *C. albicans* blastospores in PBS. 48h following infection, target organs were harvested, homogenized in PBS, serially diluted, and plated on YPD-agar Petri dishes containing 34 μg/ml of chloramphenicol. The plates were incubated at 30^{o}C for 24-48 hours, the colony-forming units (CFU) counted, and expressed as $\log_{10}$CFU per organ.

Genotyping and linkage mapping

As described previously (*547*), genomic DNA was isolated from tail clips of individual F2 mice collected at the time of sacrifice. A total of 150 [C57BL/6JxSM/J]F2 male mice were genotyped at the McGill University and Genome Quebec Innovation Centre (Montreal, QC, Canada) using Sequenome iPlex Gold technology and a custom panel that contained 126 informative SNPs distributed evenly across the genome. Nine additional microsatellite markers annotated in the Mouse Genome Informatics Database (www.informatics.jax.org) were used for gap filling and fine mapping (*602*). An additional cohort of 204 female and 40 male

[C57BL/6JxSM/J]F2 were subsequently genotyped for markers underlying loci of interest near the *Carg5* locus. Linkage analysis was performed using Haley-Knott multiple regression analysis assuming a normal model, a nonparametric analysis, or a 2-part model (*569*, *603*) with the qtl implementation of the R software (*571*). Empirical genome-wide significance was calculated by permutation testing (1000 tests).

Histology

Whole kidneys were decapsulated, fixed in 4% paraformaldehyde, dehydrated in ethanol/xylene, and embedded in paraffin, as described previously (*568*). Histological 5 μm sections were cut longitudinally with a microtome and fixed onto glass slides. Sections were deparaffinized, then stained with periodic acid Schiff's reagent (PAS) (Sigma-Aldrich, Oakville, ON) to detect *C. albicans* elements, and counterstained with hematoxylin (Sigma-Aldrich). Stained sections were examined under a light microscope using 10X and 40X objectives and photographed.

Single-cell suspension and flow cytometry

C57BL/6J and SM/J male mice were sacrificed 48h following *C. albicans* infection along with non-infected controls, then exsanguinated, perfused with PBS containing 2 mM EDTA, and their organs harvested. In brief, approximately 100 to 125 μl of anti-coagulated peripheral blood was lysed with ACK lysis buffer, centrifuged, and the resulting leukocyte pellet was washed and suspended in FACS buffer (PBS, 2% FBS, 2 mM EDTA). Whole blood was collected from a subset of [C57BL/6JxSM/J]F2 animals 48h post-infection and leukocytes prepared as described. Spleens were finely minced and single-cell suspensions obtained through triturating. Red blood cells (RBCs) were eliminated by incubation with ACK lysis buffer. The resulting leukocyte pellet was washed, filtered through a 40 μm cell strainer and suspended in FACS buffer. Femoral bone marrow was flushed with RPMI supplemented with 0.5% FBS, followed by RBC lysis. The pellet was washed, filtered through a 40 μm cell strainer and suspended in FACS buffer. Infiltrating kidney leukocytes were enriched by Percoll gradient centrifugation, as previously

described (*374*). Briefly, decapsulated kidneys were finely minced and digested at 37°C in RPMI containing liberase TL and grade II DNAse I for 30 minutes. Digested tissue was washed and the remaining red cells were briefly lysed with ACK lysis buffer. The cells were then passed through a 40 μm filter, washed, and separated over a discontinuous 40/70% Percoll gradient. The leukocytes at the interphase were isolated, washed, and suspended in FACS buffer.

Cells were first stained with the Zombie Aqua viability dye (Biolegend, San Diego, CA), then surface stained for 30 minutes in the dark at 4°C with the following antibodies: APC-eFluor780 anti-CD45 (30-F11), PE-Cy7 anti-CD11b (M1/70), PE anti-Ly6C (HK1.4), and BV421 anti-Ly6G (1A8, Biolegend). Acquisition was performed using an eight-color FACS Canto II flow cytometer (BD Biosciences), and data analyzed using FlowJo software (Tree Star). Cell aggregates were gated out based on the forward scatter (FSC)-height versus FSC-area plot, and the live cell gate established based on the exclusion of viability dye. Leukocytes were gated as $CD45^+$ cells; neutrophils were further identified as $CD11b^+Ly6G^+$, while $CD11b^+Ly6G^-Ly6C^{hi}$ denoted inflammatory monocytes. The gating strategy is also illustrated in Figure S2. Data were expressed as the percentage of total $CD45^+$ cells. All antibodies are from eBioscience, unless otherwise stated.

Preparation of neutrophils and macrophages from bone marrow

Bone marrow neutrophils (BMN) were isolated by Percoll density gradient centrifugation as previously described (*604*). Briefly, bone marrow from 8- to 16-week-old male mice was flushed from tibiae and femurs with HBSS-Prep (Ca^{2+}-/Mg^{2+}-free HBSS (Wisent), supplemented with 0.5% FBS, 20 mM HEPES). RBCs were lysed by hypotonic lysis and bone marrow cells resuspended in HBSS-Prep, filtered through a 70 μm cell strainer, gently layered over a 62.5% Percoll layer and centrifuged at 1000g for 30 minutes. Mature neutrophils were harvested from the bottom layer of the gradient and the purity was evaluated by flow cytometry; standard preparations yielded neutrophils of >85% purity, determined by characteristic forward and side scatter, and high expression of Gr-1 or Ly6G. In some experiments, cytospin preparations were made and stained with Diff-Quick to visualize neutrophil

morphology. Bone marrow-derived macrophages (BMDM) were isolated from femurs of 8- to 16-week-old male mice and were cultured in DMEM (Thermo Scientific) containing 10% heat-inactivated FBS, 20% L-cell-conditioned medium (LCCM) as a source of M-CSF, 100 U/ml penicillin, and 100 μg/ml streptomycin in bacteriological grade dishes at 37°C in a humidified atmosphere containing 5% CO_2. Seven days later, cells were harvested by gentle washing of the monolayer with PBS Citrate.

Reactive oxygen species (ROS) production

ROS production was measured in neutrophils and BMDM by luminol-enhanced chemiluminescence as previously described (*54*, *103*) with slight modifications. Briefly, 10^5 neutrophils were resuspended in HBSS containing 100 μM luminol in a 96-well luminometer plate (Costar). Following 10 minutes incubation at 37°C, neutrophils were activated with 3 μM fMLF (Sigma-Aldrich) or 100 nM PMA (Sigma-Aldrich) delivered by the injector port of EnSpire multiplate reader, and luminescence measured every 10s for 45 minutes. BMDM were plated at $2x10^5$/well in a 96-well luminometer plate and primed with IFNγ (50 U/ml) for 18 hours. BMDM were gently washed and incubated with HBSS supplemented with 100 μM luminol for 10 minutes at 37°C. ROS production was induced with 200 nM PMA and acquired as above.

BMDM phagocytosis assay and immunofluorescence

BMDM ($2x10^5$) were seeded onto glass coverslips in a 24-well plate and allowed to incubate overnight. The cells were gently washed and an appropriate suspension of opsonized CAI4-GFP *Candida* yeast cells in culture media was added at a multiplicity of infection (MOI) of 10, and brought in contact with BMDM by brief centrifugation. After 30 minutes of coincubation at 37°C and 5% CO_2, cells were gently washed twice with PBS to remove nonphagocytosed *Candida*. Cells were fixed with 4% paraformaldehyde (Mecalab) for 20 minutes at room temperature and after being blocked with 5% BSA in PBS, the cells were incubated with rabbit anti-*Candida* antibody (Accurate Chemical & Scientific Corp.). Finally, the coverslips

were incubated with the Cy3-conjugated anti-rabbit secondary antibody, followed by DAPI staining (Molecular Probes) and mounting of coverslips on glass slides. Phagocytosis was analyzed using a 63X immersion oil objective and images were acquired with a Zeiss LSM5 Pascal laser scanning confocal microscope. The percentage of phagocytosis was determined by counting the number of macrophages containing at least one *Candida* cell, and divided by the total number of macrophages, using ImageJ. The percentage of phagocytosis was calculated from a total of 12 images from two independent experiments.

BMDM killing assay

$2x10^5$ BMDM were seeded in 96-well plates and allowed to create a monolayer at 37°C. The cells were gently washed and an appropriate suspension of opsonized SC5314 blastospores in culture media was added to achieve an MOI of 10, followed by a brief centrifugation. After 30 minutes of coincubation at 37°C, non-phagocytosed *Candida* were removed by gentle washing with PBS, and killing was allowed to proceed during an additional 2 h. At the end of incubation, BMDM were lysed with distilled water, and the wells gently rinsed with PBS. Liberated yeast cells were loaded with 5 μM FUN1 yeast viability dye (Molecular Probes) for 30 minutes at 30°C and the red (viable yeast) fluorescence acquired on the EnSpire multiplate reader. The percentage of live *Candida* was calculated by dividing the fluorescence of the sample incubated for 2 h by its corresponding phagocytosis control.

CCL2 determination

Whole blood was collected from *C. albicans* infected [C57BL/6JxSM/J]F2 animals 48h post infection. Serum was separated by centrifugation and circulating CCL2 levels were determined with a commercial ELISA kit, according to the manufacturer's instructions (R&D Systems).

Statistical analysis

All data were analyzed using GraphPad Prism 6.0 statistical software. An unpaired, two-tailed Student's t-test was used to establish significance of differences

and these were deemed significant when $p<0.05$.

Computation of the Myeloid Inflammatory Score (MIS)

Chromatin immunoprecipitation sequencing (ChIP-seq) and RNA sequencing (RNA-seq) from myeloid cells (C57BL/6 bone marrow-derived macrophages) prior to and following IFNγ stimulation were performed to identify and quantify binding of the pro-inflammatory transcription factors IRF1, IRF8 (Langlais *et al*., unpublished), STAT1 (*605*), and NFκB (p65) (*606*), in the context of IFNγ stimulation. This analysis was conducted for the 231 genes located under the *Carg5* minimal confidence interval. We computed a "ChIP-seq score" for each gene and that summarizes gene-to-DNA-binding association of the core inflammatory transcription factors IRF8, IRF1, STAT1 and NFκB (p65). This score was weighed with 2/3 coming from peak proximity to gene transcriptional start site (TSS) using a 20kb window, and 1/3 from peak height relative to the median of peak heights for each transcription factor.

$$\text{ChIP-seq score: } S_{tf,g} = \sum_{i=1}^{n} \frac{\left(1-\left(\frac{di}{w}\right)\right)+(Pi * 50\%)}{1.5}$$

$$\text{where } P_i = \frac{hi}{2H} \text{ ; IF } P_i > 1 \text{ THEN } P_i = 1$$

where *tf* = transcription factor; *g* = gene; *w* = genomic window size (20 kbp); *d* = distance of peak from TSS; *n* = number of peaks in the window; *h* = peak height; *H* = median of peak height. Genes showing detectable mRNA expression (from RNA-seq data; FPKM ≥ 20) were attributed an "Expression score" of 1. These expressed genes were also given a "Responsive score" of 1 if they were significantly regulated by a 3h IFNγ treatment (Fold change ≥ |2| and p Value ≤ 0.05). The ChIP-seq score and RNA-seq scores were added to attribute each gene a "Myeloid Inflammation Score". This MIS was used as an indicator of a possible participation of the gene in inflammatory processes.

3.4 RESULTS

Genetic analysis of susceptibility of SM/J mice to C. albicans. C5 sufficient C57BL/6J (B6) and SM/J mice were challenged intravenously with $5x10^4$ *C. albicans* blastospores and the fungal growth was determined in the kidney by enumeration of CFUs 48 h later (Figure 1A). Compared to resistant C57BL/6J controls, SM/J displayed significantly higher fungal load, particularly in female mice (Figure 1A, left panel; log_{10}CFU: 4.8±0.1 vs. 2.9±0.2) although this difference was still visible and significant in male mice (Figure 1A, right panel; log_{10}CFU: 5.0±0.1 vs. 4.4±0.1). Susceptibility of the SM/J strain was not limited to the kidney, but was also evident in secondary target organs, such as the brain (Figure S1A; log_{10}CFU: 2.8±0.2 vs. 2.2±0.1, p=0.0056) and the heart (Figure S1B; log_{10}CFU: 2.6±0.3 vs. 2.0±0.1, p=0.0341). Histological analysis of infected kidney sections (Figure 1B) showed extensive fungal invasion, and numerous infection foci in SM/J, despite noticeable recruitment of leukocytes. Kidney sections from C57BL/6J mice were characterized by an attenuated presence of fungal elements that consisted mostly of pseudohyphal morphology. These results indicate that although C5-sufficient, SM/J mice are unable to control *C. albicans* replication in target organs.

Inheritance and genetic control of C5-independent susceptibility to *C. albicans* in SM/J was investigated in informative F1 and F2 crosses generated between resistant C57BL/6J and susceptible SM/J, in which all mice bear wild type *C5* alleles. A total of 190 male and 204 female [C57BL/6JxSM/J]F2 animals, along with F1 hybrids, were infected with *C. albicans* and kidney fungal load was used as the phenotypic measure of susceptibility (Figure 2A). [C57BL/6JxSM/J]F1 were as resistant to the infection as C57BL/6J controls (Figure 2A), indicating that susceptibility to *C. albicans* in SM/J is inherited in a recessive manner, while the distribution of CFU in the [C57BL/6JxSM/J]F2 population extending between and beyond the extremes of parental values suggested a complex genetic control. Although CFU counts in the male F2 population appeared to follow a Gaussian distribution, D'Agostino and Pearson omnibus normality test revealed that fungal distribution (Log_{10}CFU) in neither male nor female F2 animals passed the normality

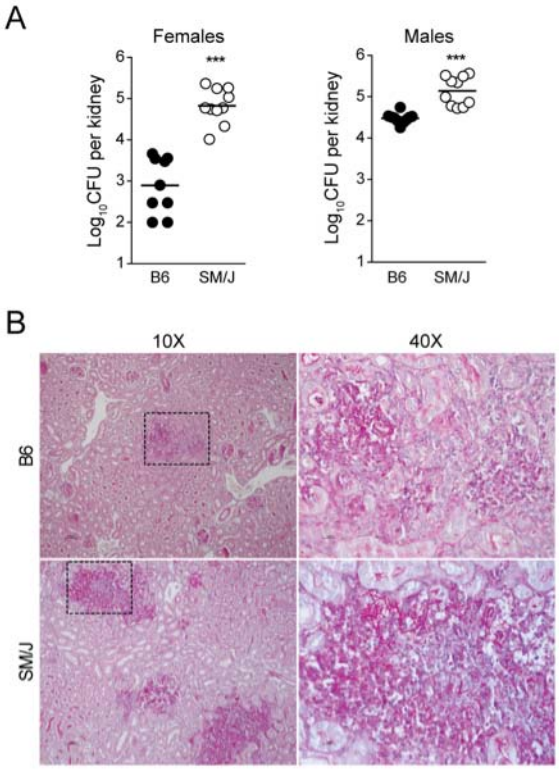

Figure 1. SM/J mice display increased fungal burden following *C. albicans* infection.

(A) C57BL/6J (B6) and SM/J mice (n=9-10) were infected with $5x10^4$ *C. albicans* blastospores and CFUs were enumerated 48 hours later in the kidney and segregated according to gender. (B) Histological analysis (PAS staining) shows increased fungal infiltration and growth in SM/J male mice, where hyphae and tissue damage are more prominent compared to the resistant C57BL/6J (B6) strain. Dashed rectangles identify the area of magnification (40X).

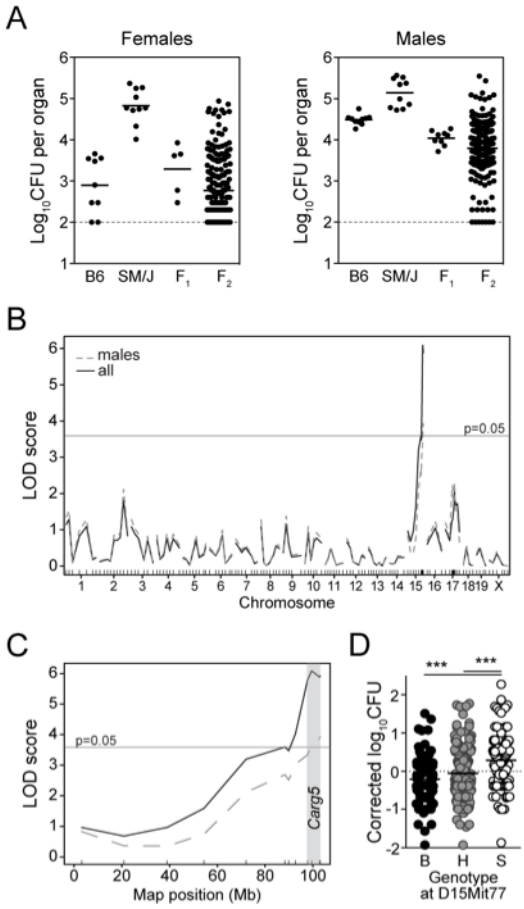

Figure 2. A novel locus on distal chromosome 15, *Carg5*, confers susceptibility to *C. albicans* infection in the SM/J strain.

A total of 190 male and 204 female [C57BL/6JxSM/J]F2 animals, along with [C57BL/6JxSM/J]F1 controls, were infected intravenously with $5x10^4$ *C. albicans* blastospores and sacrificed 48 hours later. **(A)** Fungal load was assessed in the kidney and segregated according to gender. Fungal burden from C57BL/6J (B6) and SM/J parental controls from Figure 1 is included for comparative purposes. Whole genome scan was carried out in 150 [C57BL/6JxSM/J]F2 male progeny using 134 informative markers, and using kidney fungal load (regressed to gender-specific mean) as the phenotypic trait. **(B)** Genome-wide LOD score traces identify a significant linkage peak on chromosome 15 (LOD=3.93). Addition of 204 female and 40 male [C57BL/6JxSM/J]F2 mice genotyped for 8 markers underlying this locus augmented the significance of the chromosome 15 QTL (B, solid line, LOD=6.09). The horizontal line designating genome-wide threshold for the entire F2 population (LOD=3.59, p=0.05) was calculated by performing 1000 permutations. **(C)** Minimal Bayesian interval for *Carg5* is located between 97.8 and 103.1 Mb. **(D)** Effect of allele combination (B, homozygote C57BL/6J; S, homozygote SM/J; H, heterozygote) at marker *D15Mit77* on kidney fungal loads (regressed to gender-specific mean).

test ($p=0.0016$ and $p<0.0001$, respectively). The $Log_{10}CFU$ were thus regressed to an experiment-specific, as well as gender-specific mean, yielding the "corrected $Log_{10}CFU$" approaching normal distribution and amenable for linkage analysis. The [C57BL/6JxSM/J]F2 male population was genotyped for 134 informative SNPs and microsatellite markers dispersed evenly across the entire genome. Linkage analysis in R/qtl was performed by Haley-Knott regression using corrected $Log_{10}CFU$ (Figure 2B), or a non-parametric method using crude $Log_{10}CFU$ (data not shown). Either analysis identified a highly significant locus on distal chromosome 15 (Figure 2B, dashed line; LOD=3.93) that regulates fungal load in the kidney, and that was given the temporary designation *Carg5* (*Candida albicans resistance gene 5*). Studies in additional F2 progeny (204 female, 40 male) validated the effect of *Carg5* (peak LOD=6.09; Figure 2B, solid line), and delineated a minimal Bayesian interval (95% confidence limit) situated between 97.8 and 103.1 Mb (Figure 2C). It was estimated that *Carg5* explains 11.3% of the phenotypic variance suggesting additional genetic regulators of the host response to *C. albicans* infection in the two parental strains. A pairwise scan, however, failed to detect any significant interacting or additive loci. Segregation analysis indicated that homozygosity for SM/J alleles at the peak marker *D15Mit77* is associated with higher kidney fungal load, while homozygosity or heterozygosity for C57BL/6J alleles resulted in reduced fungal load (Figure 2D, $p<0.0001$). These results identify *Carg5* as a novel locus that regulates *C. albicans* proliferation in the SM/J mouse strain in a C5-independent manner, with susceptibility alleles being inherited in a recessive fashion.

Neutrophil recruitment and function in SM/J. Early engagement of the myeloid compartment, including mobilization of neutrophils to the site of infection, is required for protection against *C. albicans* (*352*, *369*). Hence, flow cytometry was used to monitor blood and bone marrow (BM) populations of $CD11b^+Ly6G^+$ neutrophils 48 hours after infection with *C. albicans*, using the gating strategy described in Figure S2. Compared to resistant C57BL/6J controls, SM/J mice displayed lower numbers of granulocytes (expressed as fraction of $CD45^+$ cells) in BM at steady state and following *C. albicans* challenge (Figure S3A, right panel; $p=0.0022$ and $p<0.0001$, respectively). Nevertheless, infection induced a strong

recruitment of $CD11b^{+}Ly6G^{+}$ neutrophils in the blood and spleen of both strains (Figure S3A). Interestingly, flow cytometry analysis indicated that blood and BM neutrophils from SM/J expressed lower levels of Ly6G compared to their C57BL/6J counterparts (Figure 3A). Indeed, quantification of Ly6G fluorescence indicates a ~50% reduction in mean fluorescence intensity (MFI) of SM/J neutrophils compared to C57BL/6J in blood and BM (Figure 3B, $p<0.0001$); this difference in MFI was noted both at steady state and following infection (data not shown).

We next investigated the relationship between Ly6G expression level (MFI) on SM/J and C57BL/6J neutrophils and *Carg5*-regulated susceptibility to *C. albicans in vivo*. For this, a cohort of [C57BL/6JxSM/J]F2 mice was infected with *C. albicans*, and 48 h later blood was collected for cellular immunophenotyping, and kidney harvested for fungal load determination. We assessed the effect of homozygosity for SM/J (S) or C57BL/6J (B) alleles or heterozygosity (H) at *Carg5* on blood cellular immunophenotypes (Ly6G MFI calculated for individual mice) and on fungal replication, exploring possible correlations between the two. No effect of *Carg5* alleles was detected for the level of blood neutrophils in infected F2 mice (Figure 3C). However, there was a significant effect of *Carg5* alleles on neutrophil Ly6G MFI, with $Carg5^{S}$ homozygotes showing significantly less expression than $Carg5^{B6}$ homozygotes or heterozygotes (Figure 3D, $p=0.0008$ and $p=0.0001$, respectively). In addition, linear regression analysis of Ly6G MFI vs. kidney fungal load in individual F2 mice identified a modest but significant correlation between the two phenotypes (Figure 3E, $R^2=0.1482$, $p=0.0075$). The distribution of susceptible vs. resistant genotypes (Figure 3E) may also be indicative of a threshold effect. That is, the dot cloud of F2 animals that possess lower levels of Ly6G (MFI<1) clusters around higher fungal counts ($\geq \text{Log}_{10}4.25$), and conversely, F2 mice exhibiting higher levels of Ly6G (MFI>1) generally display lower fungal burden ($>\text{Log}_{10}4.25$). However, this hypothesis could not be validated by Fisher's exact test ($p=0.2443$). These results show that *Carg5* modulates both Ly6G expression on neutrophils, and fungal replication in the kidney, suggesting a possible role of Ly6G in neutrophil antifungal effector function.

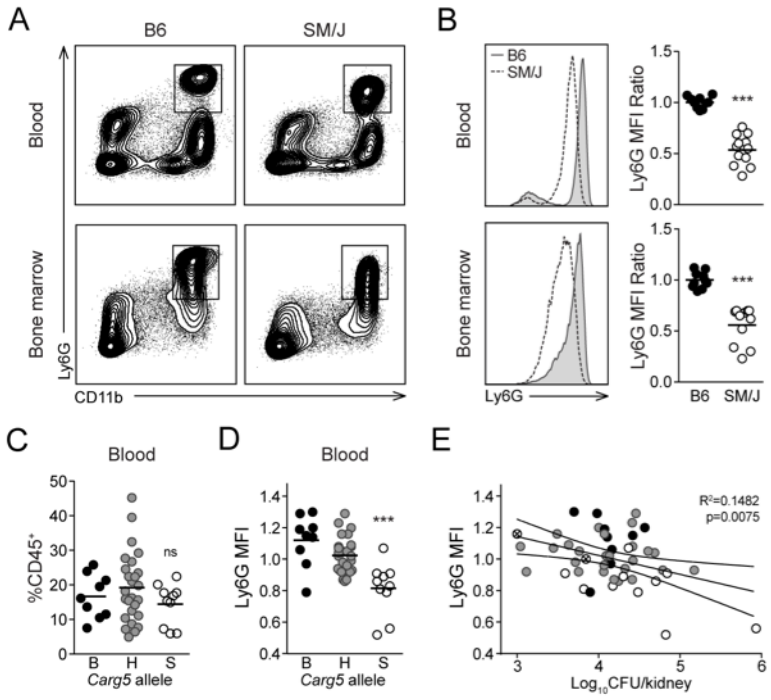

Figure 3. *Carg5* regulation of Ly6G expression on neutrophils of SM/J mice.

Single cell suspensions from blood and bone marrow of C57BL/6J and SM/J male mice 48h following *C. albicans* infection; stained for CD45, CD11b, Ly6G, and analyzed by flow cytometry**. (A)** Representative contour plots showing neutrophils (boxed), defined as $CD11b^{+}Ly6G^{+}$, are provided for both C57BL/6J (B6) and SM/J strains. **(B)** Gating on neutrophils, Ly6G intensity profiles were constructed for C57BL/6J (B6, grey) and SM/J (dashed line). The Ly6G mean fluorescence intensity (MFI) of SM/J cells quantified relative to the C57BL/6J strain and illustrates a reduced expression of the Ly6G antigen in the SM/J strain (***, $p<0.001$). **(C)** In [C57BL/6JxSM/J]F2 mice of both genders, *Carg5* alleles (marker *D15Mit77*) have no impact on the number of circulating $Ly6G^{+}$ cells in blood, but they have a strong effect on Ly6G MFI ($p=0.0008$; panel **D**). **(E)** In these F2 progeny, linear regression analysis identifies a significant correlation between Ly6G MFI and kidney fungal load ($R^2=0.1482$, $p=0.0075$); the 95% confidence interval is identified. *Carg5* alleles are abbreviated as follows: S=SM/J, white circles; H=Heterozygote, grey circles; B=C57BL/6J, black circles.

Ly6G is a small GPI-linked protein specifically expressed on the surface of neutrophils (*607*, *608*). Although its functional role in these cells is still debated, its expression is regulated during maturation, with the highest expression detected in the most mature cells that bear segmented nuclei and have lost colony-forming potential (*609*). Examination of neutrophil cytospins from SM/J and C57BL/6J (Figure 4A) did not detect major morphological anomalies, suggesting that reduced expression of Ly6G is not associated with an obvious block in maturation of these cells. In addition to the alleged role for Ly6G in granulocyte maturation, Wang *et al*. reported that transient antibody ligation of Ly6G attenuates neutrophil migration to sites of inflammation (*610*). We did not, however, detect differences in the proportions of neutrophils recruited (% of $CD45^+$ cells) to *C. albicans*-infected kidneys from SM/J vs. C57BL/6J mice (Figure S3B). Hence, we examined functional aspects of neutrophils isolated from SM/J and C57BL/6J. The importance of reactive oxygen species (ROS) production by neutrophils is evidenced by increased susceptibility to fungal infections in individuals diagnosed with chronic granulomatous disease (CGD), which is caused by reduced or absent generation of ROS (*69*, *71*). Neutrophils were purified from bone marrow of SM/J and C57BL/6J mice and production of ROS in response to stimulation with fMLF (Figure 4B) or PMA (Figure 4C) was assessed by chemiluminescence. SM/J neutrophils showed a maximal ROS burst in response to fMLF that was lower than that of C57BL/6J neutrophils ($8.499x10^3$ RLU vs $1.337x10^4$ RLU). Similarly, reduced total ROS (area under the curve) in SM/J neutrophils was also noted after stimulation with PMA ($3.878x10^6$ RLU vs $8.384x10^6$ RLU). In both instances, the initial burst kinetics were identical, but the peak amount of ROS produced was significantly reduced in SM/J. These results demonstrate reduced ROS production by neutrophils from *C. albicans*-susceptible SM/J compared to their *C. albicans*-resistant C57BL/6J counterpart.

Inflammatory monocyte recruitment and function in SM/J. $CD11b^+Ly6G^-Ly6C^{hi}$ inflammatory monocytes are essential for protection against systemic candidiasis (*405*). This population was investigated in naïve and *C. albicans*-infected SM/J and C57BL/6J mice (Figure 5A). While no significant inter-strain difference in the levels of inflammatory monocytes could be discerned at steady state (Figure 5A),

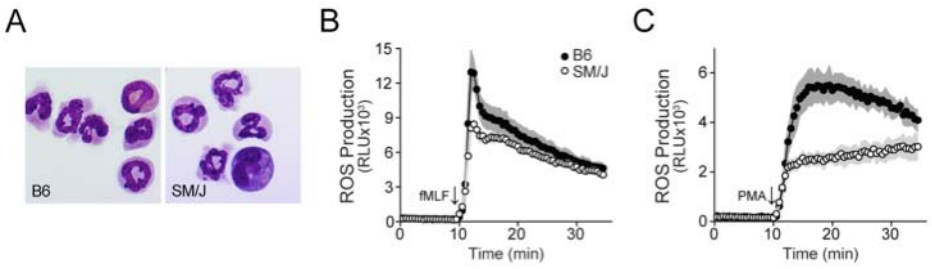

Figure 4. SM/J neutrophils display diminished production of reactive oxygen species (ROS).

(A) Cystospin images of neutrophils from male SM/J and C57BL/6J (B6) show similar morphology (segmented nuclei). Production of reactive oxygen radicals measured by luminescence and following stimulation with 3μM fMLF **(B)** or 100 nM PMA **(C)** by SM/J (white circles) and C57BL/6J (B6) neutrophils (black circles). Grey hatching identifies confidence limit calculated from quadruplicate technical replicates and 2-3 mice per strain; the results are representative of two independent experiments.

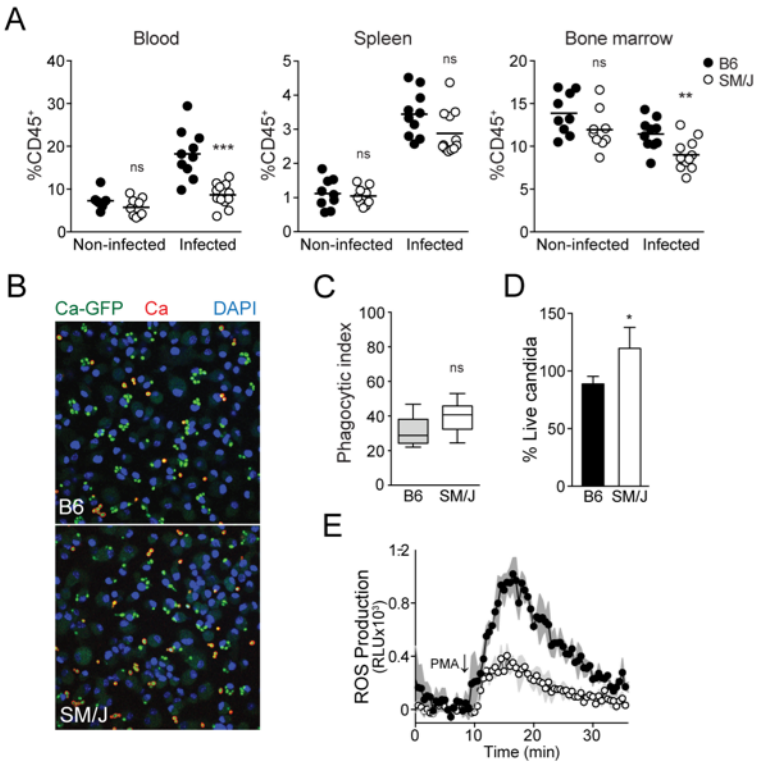

Figure 5. Mononuclear phagocyte numbers and function in response to *C. albicans* infection in SM/J.

(A) Forty eight hours following *C. abicans* infection, single cell suspensions were prepared from blood, spleen and bone marrow, stained for CD45, CD11b, Ly6C and Ly6G, and analyzed by flow cytometry. Proportions of inflammatory monocytes, defined as $CD11b^{+}Ly6G^{-}Ly6C^{hi}$, are shown. SM/J mice display a reduced reservoir of inflammatory monocytes in the bone marrow ($p=0.0044$) and in blood ($p<0.0001$). **(B)** Phagocytosis of GFP-CAI4 yeast cells by bone marrow derived macrophages from male SM/J and C57BL/6J (B6) mice; green yeast cells are intracellular, while orange/red yeast cells are extracellular (see Materials and Methods). **(C)** Phagocytic index was calculated from the number of macrophages having internalized at least one yeast cell. **(D)** Intracellular viability and growth of yeast cells was determined by FUN1 stain after 2h of incubation at an MOI of 10, and shows significant *C. albicans* fungal growth in SM/J macrophages ($p=0.0233$). **(E)** Generation of ROS upon PMA stimulation was significantly decreased in SM/J macrophages (white circles) compared with C57BL/6J (black circles).

48h post *C. albicans* challenge, their numbers were severely reduced in blood (Figure 5A, left panel; p<0.0001) and BM (Figure 5A, right panel; p=0.0044) of SM/J mice compared to C57BL/6J, with a similar trend in the spleen (albeit not reaching statistical significance; Figure 5A, middle panel; p=0.0606). Upon exposure to microbial products or pro-inflammatory factors, $Ly6C^{hi}$ monocytes can migrate to tissues and differentiate into professional phagocytes (*611*). Hence, inter-strain differences in functional properties of BMDM from SM/J and C57BL/6J macrophages were investigated. Phagocytosis of *C. albicans* was measured using a GFP-expressing *C. albicans* CAI4 strain (Figure 5B and 5C), and an anti-*C. albicans* antibody which allows discrimination of intracellular and extracellular yeast cells and permits calculation of a phagocytic index (fraction of macrophages with at least one internalized yeast cell). SM/J and C57BL/6J macrophages phagocytosed *C. albicans* with similar avidity (Figure 5C). However, C57BL/6J macrophages displayed a modest, but significantly enhanced fungicidal activity compared to their SM/J counterpart (measured as yeast metabolic activity 2 h following incubation) (Figure 5D, p=0.0233). As such, the capacity of IFNγ-primed macrophages to produce ROS in response to PMA was investigated (Figure 5E). Strikingly, peak and total (area under the curve) ROS production by SM/J macrophages was significantly reduced by a factor of ~3 fold compared to C57BL/6J, suggesting that SM/J macrophages have diminished anti-microbial function. Together, these results point to a myeloid defect in SM/J mice, expressed as inadequate mobilization of inflammatory monocytes and weakened anti-microbial defenses (oxidative burst) of macrophages.

Carg5-regulated serum Ccl2 levels predict renal fungal burden in C. albicans infected mice. During systemic *C. albicans* infection, rapid recruitment of $CD11b^{+}Ly6G^{-}Ly6C^{hi}$ inflammatory monocytes to the kidney occurs within 48 h, and is required for protection in this organ (*366*, *405*). Flow cytometry analysis of renal infiltrating leukocytes in SM/J and C57BL/6J mice demonstrated reduced accumulation of inflammatory monocytes in SM/J compared to C57BL/6J (Figure 6A, p=0.0008). Since CCL2 (MCP-1) is a critical pro-inflammatory myeloid chemokine that is required for inflammatory monocyte egress from bone marrow and into affected tissues (*612*), we investigated a possible effect of *Carg5* alleles on

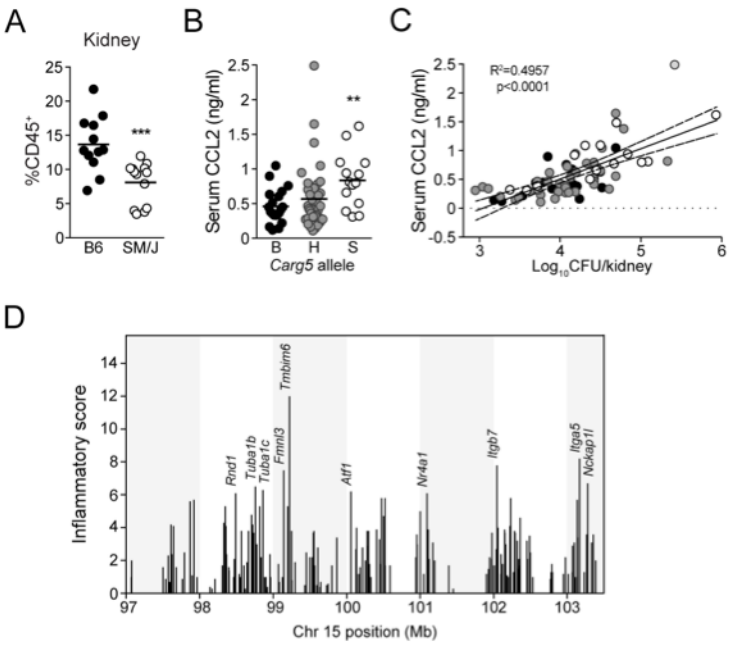

Figure 6. *Carg5* regulation of serum CCL2 levels and correlation with kidney fungal load.

(A) Two days post infection, kidney infiltrating leukocytes were analyzed by flow cytometry, showing reduced recruitment of inflammatory monocytes in SM/J (p=0.0008). **(B)** In [C57BL/6JxSM/J]F2 progeny of both genders, *Carg5* alleles (peak marker D15Mit77; p=0.0018) have a strong influence on CCL2 serum levels. **(C)** Linear regression analysis illustrates a highly significant positive correlation between serum CCL2 levels and renal fungal burden (R^2=0.4957, p<0.0001) in the F2 progeny. *Carg5* alleles are abbreviated as follows: S=SM/J, white circles; H=Heterozygote, grey circles; B=C57BL/6J, black circles. **(D)** 231 genes mapping to the minimal *Carg5* genetic interval were given a myeloid inflammatory score computed based on the integration of ChIP-Seq and RNA-Seq data, as described in Materials and Methods. The 10 highest scoring genes are identified.

CCL2 serum levels (measured 48 h post-infection) in a subset of [C57BL/6JxSM/J]F2 mice (Figure 6B). Interestingly, F2 animals bearing the SM/J allele at *Carg5* showed higher levels of serum CCL2 than those homozygous or heterozygous for C57BL/6J alleles (Figure 6B, p=0.0018). This suggests that reduced or delayed leukocyte recruitment into infected kidneys occurs in the context of robust CCL2 serum production in SM/J mice. Furthermore, we observed a highly significant positive correlation (Figure 6C, R^2=0.4957, p<0.0001) between serum CCL2 levels and kidney fungal load, with higher levels of CCL2 being associated with higher fungal load in [C57BL/6JxSM/J]F2 mice segregating *Carg5* alleles. Nevertheless, we cannot exclude the possibility that heightened circulating CCL2 levels occur as a consequence of higher CFU in susceptible [C57BL/6JxSM/J]F2 mice.

Candidate gene analysis of the Carg5 interval. Lastly, we scrutinized the *Carg5* interval for the presence of candidate genes that could play a role in host defenses to infection in general, and in myeloid cell function in particular. The *Carg5* minimal physical interval (97-103.4 Mb) is very gene-rich and contains over 200 genes, including clusters of keratin and olfactory receptor gene families. Considering the noted effect of *Carg5* alleles on the function of the myeloid compartment, we inspected the interval for "myeloid" genes involved in early inflammatory response that could be prioritized as morbid candidates for the *Carg5* effect on antifungal defenses. For this, we computed a "myeloid inflammatory score" for each gene in the *Carg5* interval (Table S1, Figure 6E).

Using chromatin immunoprecipitation and DNA sequencing (ChIP-seq), we identified and quantified the intensity of binding peaks for the myeloid transcription factors Irf1, Irf8, Stat1 and NFkB (p65) in the vicinity of all the genes in the interval, and detected following treatment of macrophages with IFNγ (IRF8, IRF1, STAT1) or LPS (NFkB p65). The number of peaks, the peak height and proximity of the peaks to the transcription start site were used to give each gene a ChIP-seq score. RNA-seq was used to establish baseline and IFNγ-responsive mRNA expression in myeloid cells, and used to produce an expression score for each gene. The ChIP-seq score and expression scores were tabulated to produce a Myeloid Inflammatory Score for each

gene in the interval (Figure 6D and Table S1). This analysis allowed us to generate a list of the ten most significant positional candidates (Figure 6D). These include *Rnd1*, *Tuba1b/Tuba1c*, *Fmnl3*, *Tmbim6*, *Atf1*, *Nr4a1*, *Itgb7*, *Itga5*, and *Nckap1l*.

3.5 DISCUSSION

We have used genetic analysis in the mouse model of systemic infection with *Candida albicans* to understand the early host defense mechanisms that are required for protection against pathogenic fungi. Earlier studies in inbred mouse strains have documented the critical role of the C5 complement component, whose deficiency in the form of a naturally occurring 2-bp mutation (*543*) causes strong susceptibility to *C. albicans* infection (fungal proliferation, overall survival) (*7*, *9*, *297*, *298*, *301*). In addition, we and others have mapped *Carg* (*Candida albicans resistance genes*) loci, namely *Carg1* through *Carg4*, that additionally regulate susceptibility to *C. albicans* infection in a C5-independent fashion (*11*, *12*, *602*). Here, we characterized the genetic component and the mechanistic basis of unique susceptibility to *C. albicans* in the "phenodeviant" SM/J strain that is C5-sufficient and expected to be resistant to infection. Susceptibility in SM/J is expressed as increased fungal replication in target organs (Figure 1 and S1), with a noticeable gender bias, where male mice showed increased susceptibility compared to females (*613-615*). Subsequent linkage mapping in [C57BL/6JxSM/J]F2 progeny mapped a novel locus on distal chromosome 15 that we term *Carg5* (cumulative peak LOD 6.09; Figure 2), and whose alleles regulate fungal replication in the kidney. The *Carg5* locus was not detected in our previous haplotype association (EMMA analysis) studies in 23 inbred mouse strains (*602*), implying that the *Carg5* effect is unique to the SM/J strain.

Comparative immunophenotyping of the innate immune compartment, and anti-microbial functional analysis of immune cells from SM/J and C57BL/6J mice and from [C57BL/6JxSM/J]F2 demonstrate that *Carg5* alleles have a pleiotropic effect on several aspects of myeloid cell function. Neutrophils play a key role in defenses against fungal infections (*2*, *352*). Compared to their C57BL/6J counterpart, SM/J mice show lower proportions of neutrophils in the bone marrow, and mature neutrophils produced in SM/J show a lower level of surface expression of the Ly6G antigen (Figure 3A-B). Studies in [C57BL/6JxSM/J]F2 mice demonstrate that *Carg5* alleles are associated with expression of Ly6G (Figure 3D), and establish a correlation between the level of Ly6G expression and replication of *C. albicans* in

kidneys, with the major effect contributed by homozygosity for SM/J alleles in these mice (Figure 3E). Hence, it is tempting to speculate that *Carg5* alleles have an impact on functional maturation of $Ly6G^+$ neutrophils in SM/J mice. Interestingly, the effect of *Carg5* on neutrophil Ly6G expression does not appear to affect recruitment of these cells to different sites of infection in SM/J mice (Figure S3). Rather, we found that SM/J neutrophils produced less ROS upon stimulation with fMLF or PMA (Figure 4B-C), both with respect to peak and total production. Decreased ROS production by neutrophils is expected to provide a permissive environment for fungal survival and replication in infected organs. Indeed, patients suffering from chronic granulomatous disease (CGD) caused by mutations in components of the ROS generating NADPH enzyme complex are susceptible to fungal infections (*69*, *71*). Moreover, Ly6G directly associates with β2-integrins (*610*); therefore, it is possible that reduced Ly6G expression on SM/J neutrophils leads to decreased interaction with CD11a/CD18 (LFA-1), further contributing to diminished ROS generation (*616*).

Finally, neutrophils release granule proteins, including LL-37, azurocidin, and cathepsin G (*617*, *618*), that are important for further recruitment of ROS-producing inflammatory ($Ly6C^{hi}$) monocytes (*619*) to the site of infectious or inflammatory insults. In mice, two monocyte subsets can be distinguished by chemokine receptors and adhesion molecule expression. Inflammatory monocytes express $Ly6C^{hi}CCR2^+$ and represent counterparts to human $CD14^+CD16^-$, whereas mouse $Ly6C^{lo}CX_3CR1^+$ resident monocytes correlate with human non-classical $CD14^+CD16^+$ monocytes (*403*, *404*). In mice, both subsets play important roles in the host defense against systemic fungal infection (*405*, *406*), with inflammatory monocytes conferring protective antifungal activity during the first 48 hours following infection (*405*). The protective role of inflammatory monocytes and their derivatives is further demonstrated in the pulmonary infection with *Cryptococcus neoformans* (*620*) and *Aspergillus fumigatus* (*621*), where $CCR2^{-/-}$ and diphteria toxin-treated CCR2-DTR mice, respectively, exhibit increased fungal growth and/or decreased survival. We show that the myeloid defect in the SM/J strain is also expressed as an altered number and function of inflammatory monocytes, including reduced or delayed recruitment

of these cells to the site of infection, and diminished production of ROS in BMDM from these mice (Figure 5 and 6). CCL2 is the main ligand for the CCR2 receptor involved in inflammatory monocyte mobilization and recruitment (*612*, *622*). In [C57BL/6JxSM/J]F2 mice, we observed a strong effect of *Carg5* alleles on the level of serum CCL2, and we detected a strong correlation between CCL2 serum levels and kidney fungal replication, with higher CCL2 levels (in $Carg5^{s}$ mice) associated with higher fungal loads (Figure 6C). Similarly, the hyper-susceptible A/J strain exhibits elevated levels of CCL2 following infection with *C. albicans* (*298*, *299*), prompting us to postulate that the effect of *Carg5* on CCL2 serum levels, albeit highly correlated with fungal load, may be secondary and adaptive to a primary myeloid defect. Whether SM/J mice possess impaired emergency myelopoiesis remains to be ascertained and will entail challenging this strain with other pathogens. Thus far, SM/J mice have been deemed susceptible to blood-stage malaria caused by *Plasmodium chabaudi* (*623*), and are considered a non-healer strain when the ear pinnae is wounded (*624*). The wound-healing trait is controlled by multiple loci, including a locus *Heal4* mapping to distal chromosome 15 and overlapping with *Carg5*. Taken together, our findings strongly suggest that susceptibility of SM/J mice to *C. albicans* infection is associated with a weakened myeloid compartment in this strain, affecting both neutrophils and inflammatory monocytes, with the mapped *Carg5* locus contributing significantly to several aspects of this myeloid phenotype.

Since *Carg5* affects the myeloid compartment of SM/J mice, we scrutinized the minimal confidence interval (97-103.8 Mb) for putative positional candidates underlying these effects. Initial recognition of *Candida* yeast and filamentous forms occurs through pathogen-associated molecular patterns (PAMPs) and corresponding pattern recognition receptors, such as C-type lectin receptors (CLRs) and Toll-like receptors (TLRs), whose synergistic interaction can result in augmented downstream immune activation via NFkB (*100*, *102*). Additionally, the protective role for the IFNγ axis in *C. albicans* infection has been demonstrated by increased susceptibility of mice deficient for IFNγ (*455*) or IFNγ receptor (*456*). Signaling by IFNγ activates the JAK-STAT pathway and results in binding of interferon regulatory factors, IRF1 and IRF8, as well as STAT1 to IFNγ activation site (GAS) elements and interferon-

stimulated response elements (ISREs), thereby orchestrating and controlling many facets of innate and adaptive immune responses (*625*). We therefore used data from chromatin immunoprecipitation sequencing for IFNγ-responsive IRF8, IRF1 and STAT1, and LPS-responsive NFkB (p65) DNA-binding, together with RNA-seq expression profiling prior to, and following IFNγ treatment, to compute a "Myeloid Inflammatory Score" for each gene in the *Carg5* interval.

Amongst the ten most significant positional candidates (Figure 6E and Table S1), *Tmbim6*, which encodes the anti-apoptotic BAX inhibitor-1 (BI-1), ranked first. BI-1 was identified in a functional screen in yeast searching for suppressors of BAX-induced apoptosis (*626*). BI-1 was shown to negatively regulate ER stress-associated reactive oxygen species in a dose-dependent manner, thereby protecting cells from apoptosis (*627*, *628*). Cells from mice deficient in BI-1 exhibit hypersensitivity to apoptosis induced by ER stress (*629*); conversely, BAX-deficient neutrophils demonstrated delayed apoptosis (*630*). Therefore, it is tempting to speculate that SM/J neutrophils express higher levels of BI-1 than C57BL/6J, which results in lower ER stress-induced ROS production and decreased apoptosis. In turn, neutrophil apoptosis during infection is essential to convey "eat-me" signals that attract inflammatory monocytes to the site of inflammation (*631*). BI-1 also plays a role in actin polymerization and cell adhesion (*632*), mechanisms tightly regulated during leukocyte egress and extravasation (*633*). The second most significant gene product, ITGA5 (α5) is the alpha subunit of the fibronectin receptor (α5β1) expressed on various immune cells, mediating binding to fibronectin and extravasation toward infectious stimulus (*634-636*). Blockade of α5β1 resulted in attenuated zymosan-induced recruitment of neutrophils and monocytes to the peritoneum, by reducing cell adhesion and transmigration (*637*). In addition, activation of α5β1 in human PMNs suppressed β -glucan-mediated superoxide production, which could be reverted by blocking α5β1 (*638*). We observed that SM/J BMDM displayed reduced migration in the wound-healing assay compared to C57BL/6J BMDM (data not shown), suggesting increased adhesion or decreased polarization, which can further be translated *in vivo* as diminished monocyte recruitment and/or shunted superoxide production during *C. albicans* infection. Another integrin, ITGB7 (β7), was shown to

mediate homing of lymphocytes to the gut via binding to the mucosal addressin MAdCAM-1 (*639-641*). β7 is expressed in the monocyte-macrophage cell line (THP-1) and its RNA is up-regulated upon stimulation with PMA and to some extent, by IFNγ (*642*). β7-deficient mice β7-deficient mice show no major defect in biogenesis of lymphocytes or myelocytes (*643*). On the other hand, *in vitro* studies showed that the β7 cytoplasmic domain mediates reduced cell migration, fibronectin matrix assembly and focal adhesion formation (*644*). This is particularly pertinent during the establishment of *C. albicans* infection, where efficient and prompt recruitment of innate immune effectors to the site of injury is essential for protection. Interestingly, other *Carg5* genes implicated in actin cytoskeleton or cell adhesion obtained high Myeloid Inflammatory Scores, notably *Fmnl3, Nckap1l*, *Tuba1b*/*Tuba1c,* and *Rnd1*, suggesting that regulation of adhesion, reactive oxygen species production, and apoptosis are closely regulated events in myeloid cells by the same set of transcriptional regulators.

In conclusion, we have identified a novel C5-independent locus, *Carg5*, regulating not only *C. albicans* proliferation in the susceptible SM/J strain, but also expression of Ly6G, and affecting levels of circulating CCL2. The implication of candidate genes, particularly *Tmbim6* and *Itga5,* in susceptibility to fungal infection needs to be validated and is currently being investigated.

3.6 ACKNOWLEDGMENTS

The authors are indebted to Patricia D'Arcy for technical help with animal studies. We would also like to thank Dr. Malcolm Whiteway for kindly providing the CAI4-GFP strain, and to Dr. Donald Sheppard and Dr. Martine Raymond for helpful experimental suggestions.

3.7 SUPPLEMENTARY MATERIAL

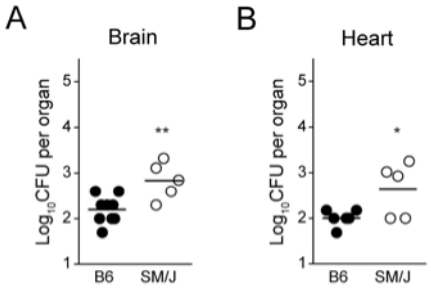

Figure S1. *C. albicans* replication in brain and heart of C57BL/6J and SM/J mouse strains.

Mice (n=5-9) were infected with $5x10^4$ *C. albicans* blastospores and CFUs were determined 48h later in the brain (A) and heart (B).

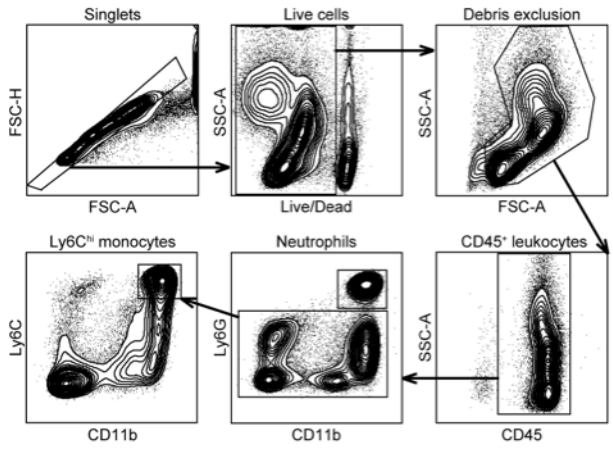

Figure S2. Gating strategy for flow cytometric analysis of neutrophils and inflammatory monocytes.

Single cell suspensions were prepared from blood, spleen, and bone marrow of *C. albicans* infected mice, and were analyzed using the following gating strategy. An initial gate to isolate single cells was established based on the FSC-H and FSC-A. Dead cells were then excluded using the viability dye Zombie Aqua and debris gated out by characteristic SSC-A and FSC-A. The leukocyte population was selected according to the $CD45^+$ staining. Neutrophils were identified as $CD11b^+Ly6G^+$, and further gating on the $Ly6G^-$ population identified inflammatory monocytes as $CD11b^+Ly6G^-Ly6C^{hi}$.

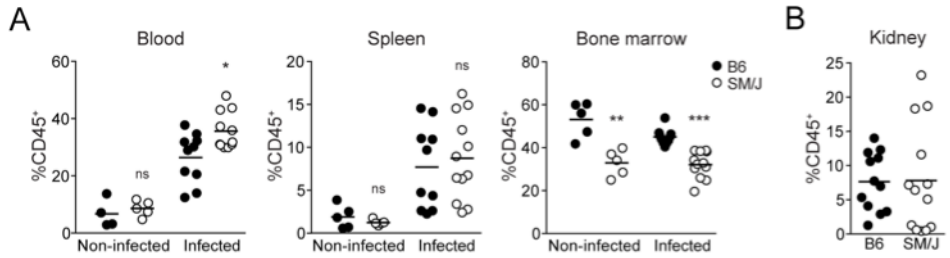

Figure S3. Neutrophil populations in response to *C. albicans* infection.

Blood, spleen and bone marrow were collected from naïve or *C. albicans*-infected (48h) B6 and SM/J mice, single cell suspensions were stained for CD45, CD11b, Ly6C and Ly6G, and analyzed by flow cytometry. (A) Proportions of neutrophils, defined as $CD11b^{+}Ly6G^{+}$, are reported for blood, spleen, and bone marrow. SM/J mice show reduced numbers of neutrophils in bone marrow compared to B6 (non-infected, $p=0.0022$; infected, $p<0.0001$), while infection induces neutrophil recruitment to spleen and blood in both mouse strains ($p<0.0119$). (B) Flow cytometric analysis of kidney infiltrating neutrophils 48h post infection is similar in SM/J and B6 mice.

Table S1. Candidate gene prioritization using functional genomic data.

MOUSE ANNOTATION						FINAL SCORE		IRF8		IRF1		Stat1		p65 (NFkB)		BMDM RNA-seq					
Ensembl Gene ID	Symbol	Chr	Gene Start (bp)	Gene End (bp)	Strand	Total	Rank	Peaks	Score	Peaks	Score	Peaks	Score	Peaks	Score	Ctl (mean FPKM)	IFNg 3h (mean FPKM)	Fold change	Adj pValue	Expr. Score	Resp. score
ENSMUSG00000048218	Amigo2	chr15	97074505	97077718	-	1.0	152			1	0.96					5	8	1.61	1	0	0
ENSMUSG00000044250	Fam113b	chr15	97077538	97216120	+	2.0	92			1	0.95					600	444	0.74	0.47	1	0
ENSMUSG00000022466	Rpap3	chr15	97505536	97536253	-	1.6	119					1	0.58			741	759	1.02	1	1	0
ENSMUSG00000022468	Endou	chr15	97541450	97561836	-	0.9	156					1	0.86							0	0
ENSMUSG00000022469	Rapgef3	chr15	97575384	97598403	-	2.3	79					3	1.01	1	0.31	37	21	0.54	1	1	0
ENSMUSG00000086601	Gm16257	chr15	97590839	97597392	+	0.7	160					1	0.73							0	0
ENSMUSG00000087397	Gm16256	chr15	97596980	97599144	+	0.7	161					2	0.72							0	0
ENSMUSG00000081534	Slc48a1	chr15	97614786	97623123	+	4.2	25			1	0.75	2	1.63	1	0.86	16273	12801	0.79	0.51	1	0
ENSMUSG00000022475	Hdac7	chr15	97623095	97674933		2.4	75			1	0.22	2	0.87	1	0.35	674	551	0.82	0.81	1	0
ENSMUSG00000090780	Gm17532	chr15	97645855	97647131	+	4.1	28			1	0.54	5	2.93	1	0.68					0	0
ENSMUSG00000022479	Vdr	chr15	97684856	97741061	-	1.6	114			1	0.35	1	0.26			52	90	1.73	0.84	1	0
ENSMUSG00000089233	7SK	chr15	97765716	97766026	+	0.9	155			1	0.49	1	0.39							0	0
ENSMUSG00000052369	Tmem106c	chr15	97794710	97800705	+	2.5	72					1	0.78	1	0.74	1081	1133	1.05	1	1	0
ENSMUSG00000022483	Col2a1	chr15	97806033	97835155	-	0.0	174													0	0
ENSMUSG00000033075	Senp1	chr15	97871660	97923836	-	5.6	16	1	0.63	1	0.87	3	2.19	1	0.92	1972	2388	1.21	0.68	1	0
ENSMUSG00000088325	SNORA17	chr15	97900183	97900311	+	1.1	139	1	0.10	1	0.34	2	0.66							0	0
ENSMUSG00000033065	Pfkm	chr15	97923020	97962878	+	5.7	14	1	0.66	1	0.90	3	2.23	1	0.92	932	901	0.97	1	1	0
ENSMUSG00000048175	Asb8	chr15	97965068	97996056	-	1.0	144									1437	2265	1.58	0.019	1	0
ENSMUSG00000029875	AI836003	chr15	97998237	98000565	+	0.0	175													0	0
ENSMUSG00000075427	Olfr288	chr15	98016444	98051408	-	0.0	176													0	0
ENSMUSG00000090129	Olfr287	chr15	98037402	98051487	-	0.0	177													0	0
ENSMUSG00000059460	Olfr286	chr15	98057106	98058074	-	0.0	178													0	0
ENSMUSG00000048077	H1fnt	chr15	98086413	98087738	-	0.0	179													0	0
ENSMUSG00000022987	Zfp641	chr15	98116019	98126561	-	0.0	180													0	0
ENSMUSG00000062037	Olfr285	chr15	98143020	98143979	-	0.4	169			1	0.39									0	0
ENSMUSG00000051793	Olfr284	chr15	98170453	98171370	-	0.3	171			1	0.31									0	0
ENSMUSG00000056184	Olfr283	chr15	98208527	98209628	-	0.9	157	1	0.42			1	0.44							0	0
ENSMUSG00000063780	Olfr282	chr15	98267901	98268828	+	0.0	181													0	0
ENSMUSG00000032987	Olfr281	chr15	98286743	98287822	+	0.0	182													0	0
ENSMUSG00000022991	Lalba	chr15	98310831	98313114	-	1.7	108					2	1.71							0	0
ENSMUSG00000054036	Olfr279	chr15	98327905	98328837	+	4.3	24	2	0.60	2	0.56	6	2.83	1	0.31					0	0
ENSMUSG00000022992	2310037I24Rik	chr15	98349243	98364669	-	3.2	56					2	1.43	1	0.73	629	374	0.60	0.06	1	0
ENSMUSG00000065336	Snora34	chr15	98350147	98350284	-	5.3	18	2	1.08	2	1.04	5	2.56	1	0.60					0	0
ENSMUSG00000065939	Snora2b	chr15	98356777	98356913	-	4.1	27	2	0.64	2	0.60	5	2.05	2	0.86					0	0
ENSMUSG00000011960	Ccnt1	chr15	98369120	98401354	-	2.4	76			1	0.66	1	0.78			3657	3231	0.88	0.85	1	0
ENSMUSG00000091050	9330020H09Rik	chr15	98397755	98400014	+	1.6	115			1	0.74	1	0.87							0	0
ENSMUSG00000022993	4930415O20Rik	chr15	98401452	98420010	+	1.4	122			1	0.65	1	0.78							0	0
ENSMUSG00000022994	Adcy6	chr15	98420425	98438064	-	0.0	183									9	12	1.35	1	0	0
ENSMUSG00000003352	Cacnb3	chr15	98462651	98474961	+	1.0	145									46	40	0.87	1	1	0
ENSMUSG00000003360	Ddx23	chr15	98475565	98493320	-	2.1	86							2	1.15	6308	7016	1.11	0.93	1	0
ENSMUSG00000054855	Rnd1	chr15	98493852	98507892	-	6.1	9					2	1.23	5	2.85	242	542	2.25	0.00069	1	1
ENSMUSG00000003354	Ccdc65	chr15	98538625	98553757	+	1.2	132					1	0.81	1	0.36					0	0
ENSMUSG00000003355	Fkbp11	chr15	98554804	98558629	-	1.0	146									99	93	0.94	1	1	0
ENSMUSG00000051853	Arf3	chr15	98568052	98593645	-	3.8	39					2	1.64	2	1.13	13881	21156	1.52	0.026	1	0
ENSMUSG00000022996	Wnt10b	chr15	98602184	98608581	-	1.7	111					2	0.64	2	1.03	8	8	0.94	1	0	0
ENSMUSG00000022997	Wnt1	chr15	98620288	98624268	+	0.3	170							1	0.32					0	0
ENSMUSG00000059213	Ddn	chr15	98634213	98638356	-	0.0	184									3	5	1.29	1	0	0
ENSMUSG00000085373	B130046B21Rik	chr15	98637463	98646508	+	0.0	185													0	0
ENSMUSG00000067713	Prkag1	chr15	98643229	98661939	-	1.9	96					1	0.89			3760	3384	0.90	0.96	1	0
ENSMUSG00000048154	Mll2	chr15	98662100	98701614	-	3.8	41	1	0.46	2	1.43	1	0.87			5321	4816	0.91	1	1	0
ENSMUSG00000023755	Rhebl1	chr15	98708209	98711835	-	4.8	21	1	0.80	3	2.08	2	0.96			196	164	0.84	0.96	1	0
ENSMUSG00000023000	Dhh	chr15	98723462	98728971	-	4.2	26	1	0.24	2	1.28	1	0.65			2	28	18.69	0.021	1	1
ENSMUSG00000022999	Lmbr1l	chr15	98734352	98748662	-	3.7	44			2	1.04	4	1.41	1	0.23	429	450	1.05	1	1	0
ENSMUSG00000023004	Tuba1b	chr15	98761856	98764996	-	6.5	6			2	1.68	4	3.09	1	0.74	14266	14735	1.03	1	1	0
ENSMUSG00000072235	Tuba1a	chr15	98780272	98783982	-	3.0	61			2	1.10	3	0.80	1	0.11	3267	3861	1.18	0.94	1	0
ENSMUSG00000087446	4930578M01Rik	chr15	98816396	98819712	+	5.3	17			1	0.99	5	2.82	2	1.48					0	0
ENSMUSG00000064081	Gm8973	chr15	98836487	98836801	+	2.2	81					4	1.85	1	0.39					0	0
ENSMUSG00000043091	Tuba1c	chr15	98860322	98868536	+	6.3	7					6	4.33	2	0.98	9364	7760	0.83	0.62	1	0
ENSMUSG00000023484	Prph	chr15	98885605	98889409	+	1.0	141					1	0.60	1	0.44	9	6	0.71	1	0	0
ENSMUSG00000032783	Troap	chr15	98905006	98913783	+	1.0	147									1123	717	0.64	0.07	1	0
ENSMUSG00000001076	C1ql4	chr15	98915117	98918248	-	0.2	173							1	0.22					0	0
ENSMUSG00000038009	Dnajc22	chr15	98923601	98935168	+	0.4	168							1	0.40					0	0
ENSMUSG00000051934	Spats2	chr15	98957009	99043637	+	2.4	74							2	1.45	712	400	0.56	0.35	1	0
ENSMUSG00000088377	SNORA40	chr15	98963498	98963603	-	1.0	142							2	1.01					0	0
ENSMUSG00000087991	7SK	chr15	99005281	99005368	-	0.0	186													0	0
ENSMUSG00000037579	Kcnh3	chr15	99055292	99073248	+	0.0	187									2	3	1.52	1	0	0
ENSMUSG00000037570	Mcrs1	chr15	99073249	99082392	-	1.8	99					1	0.82			509	560	1.10	0.97	1	0
ENSMUSG00000093139	AC161198.1	chr15	99085313	99085445	-	0.7	159					1	0.73							0	0
ENSMUSG00000078907	Fam186b	chr15	99101449	99117611	-	0.0	188													0	0
ENSMUSG00000023007	Prpf40b	chr15	99125518	99147449	+	1.0	148									367	266	0.72	0.45	1	0
ENSMUSG00000023008	Fmnl3	chr15	99147656	99200913	-	7.5	4	2	0.82	1	0.18	6	3.55	4	1.96	7134	8066	1.13	1	1	0
ENSMUSG00000064723	U6	chr15	99198460	99198566	-	5.3	19	1	0.73	1	0.10	5	2.91	3	1.53					0	0
ENSMUSG00000023010	Tmbim6	chr15	99223313	99240480	+	12.0	1	1	0.62	2	1.59	8	6.06	4	2.69	23469	37833	1.61	0.0054	1	0

MOUSE ANNOTATION						FINAL SCORE		IRF8		IRF1		Stat1		p65 (NFkB)		BMDM RNA-seq					
Ensembl Gene ID	Symbol	Chr	Gene Start (bp)	Gene End (bp)	Strand	Total	Rank	Peaks	Score	Peaks	Score	Peaks	Score	Peaks	Score	Ctl (mean FPKM)	IFNg 3h (mean FPKM)	Fold change	Adj pValue	Expr. Score	Resp. score
ENSMUSG00000023009	Nckap5l	chr15	99252466	99288179	-	3.8	40					4	2.23	1	0.52	714	1393	1.95	0.91	1	0
ENSMUSG00000089968	4921518J05Rik	chr15	99258132	99265744	+	0.8	158					2	0.77							0	0
ENSMUSG00000037525	Bcdin3d	chr15	99300515	99305161	-	1.9	95					2	0.93			191	168	0.88	1	1	0
ENSMUSG00000023011	Faim2	chr15	99327436	99358448	-	0.0	189													0	0
ENSMUSG00000023013	Aqp2	chr15	99409487	99414976	+	0.0	190													0	0
ENSMUSG00000044217	Aqp5	chr15	99421280	99425260	+	0.0	191													0	0
ENSMUSG00000043144	Aqp6	chr15	99431831	99435908	+	0.5	166	1	0.26			1	0.24							0	0
ENSMUSG00000023015	Racgap1	chr15	99450927	99482087	-	2.5	71					3	1.19	1	0.35	6963	6754	0.97	1	1	0
ENSMUSG00000092859	AC139317.1	chr15	99452555	99452641	-	1.9	97	1	0.73			2	1.12							0	0
ENSMUSG00000023017	Accn2	chr15	99501149	99531561	+	2.2	83					1	0.59	1	0.58	58	39	0.66	0.82	1	0
ENSMUSG00000091604	Gm17349	chr15	99532607	99532900	-	1.2	136					2	1.16			3	3	1.38	1	0	0
ENSMUSG00000023018	Smarcd1	chr15	99532718	99544426	+	2.2	85					2	1.16			1215	1162	0.96	1	1	0
ENSMUSG00000092065	Gm17241	chr15	99536940	99537278	-	1.7	103					5	1.75			5	7	1.39	1	0	0
ENSMUSG00000089671	Gm16537	chr15	99545974	99554905	-	2.8	65					4	2.84							0	0
ENSMUSG00000023019	Gpd1	chr15	99547946	99555436	+	3.7	46					5	2.65			28	18	0.65	0.97	1	0
ENSMUSG00000023020	2310016M24Rik	chr15	99556049	99558567	+	3.8	35					4	2.84			928	959	1.03	1	1	0
ENSMUSG00000023021	Lass5	chr15	99566023	99602946	-	1.7	105					1	0.74			5417	4922	0.91	0.93	1	0
ENSMUSG00000090406	Gm17058	chr15	99596422	99612763	+	0.5	164					1	0.52							0	0
ENSMUSG00000023022	Lima1	chr15	99608901	99705859	-	2.8	66					1	0.76			3252	1505	0.46	0.0032	1	1
ENSMUSG00000065643	U6	chr15	99633451	99633557	-	0.0	192													0	0
ENSMUSG00000092014	Gm4468	chr15	99640720	99641013	-	0.4	167					1	0.41							0	0
ENSMUSG00000090500	Gm17057	chr15	99649451	99665001	+	0.7	162					1	0.69							0	0
ENSMUSG00000037438	Gm9763	chr15	99728718	99728987	-	0.5	165					1	0.51							0	0
ENSMUSG00000045350	1700030F18Rik	chr15	99748779	99797378	-	0.6	163					1	0.63							0	0
ENSMUSG00000077443	U12	chr15	99767738	99767872	-	0.0	193													0	0
ENSMUSG00000023025	Larp4	chr15	99800505	99846782	+	1.7	106					1	0.73			4737	3421	0.72	0.16	1	0
ENSMUSG00000023026	Dip2b	chr15	99869095	100049904	+	3.4	52					2	1.24	2	1.17	3125	2329	0.75	0.28	1	0
ENSMUSG00000023027	Atf1	chr15	100058250	100091675	+	6.2	8	1	0.79	1	0.84	6	3.57			2401	2469	1.03	1	1	0
ENSMUSG00000045631	Tmprss12	chr15	100111257	100123484	+	0.0	194													0	0
ENSMUSG00000067657	Gm5474	chr15	100127542	100128062	+	2.7	68	1	0.38	1	0.48	2	0.87			64	54	0.86	1	1	0
ENSMUSG00000054619	Mettl7a1	chr15	100135248	100144782	+	4.0	30	1	0.63	1	0.74	3	1.65			934	649	0.69	0.9	1	0
ENSMUSG00000058057	Gm10035	chr15	100165360	100170772	+	1.2	131			1	0.31	2	0.87							0	0
ENSMUSG00000056487	AB099516	chr15	100183631	100214866	+	1.6	116			1	0.72	1	0.88			5	1	0.10	0.85	0	0
ENSMUSG00000056487	AB099516	chr15	100183631	100214866	+	1.6	117			1	0.72	1	0.88			5	1	0.10	0.85	0	0
ENSMUSG00000056487	AB099516	chr15	100183631	100214866	+	1.6	118			1	0.72	1	0.88			5	1	0.10	0.85	0	0
ENSMUSG00000023030	Slc11a2	chr15	100218329	100255503	-	2.8	67					1	0.88	1	0.88	4993	9622	1.93	7.2E-05	1	0
ENSMUSG00000087444	Gm5475	chr15	100252578	100258581	+	2.0	93					1	0.98	1	0.97	4	3	0.83	1	0	0
ENSMUSG00000084688	n-R5s43	chr15	100280115	100280224	+	3.8	38			1	0.34	6	3.44							0	0
ENSMUSG00000092050	5330439K02Rik	chr15	100290171	100299122	-	2.9	64			1	0.52	5	2.36							0	0
ENSMUSG00000037353	Letmd1	chr15	100299465	100309683	+	3.8	36			1	0.51	5	2.33			1884	1732	0.92	1	1	0
ENSMUSG00000044636	Csrnp2	chr15	100310001	100325670	-	1.8	102			1	0.47	1	0.29			346	210	0.61	0.15	1	0
ENSMUSG00000009733	Tcfcp2	chr15	100333230	100382439	-	1.0	149									378	290	0.77	0.74	1	0
ENSMUSG00000009739	Pou6f1	chr15	100405750	100430415	-	3.9	33			1	0.89	3	1.27	1	0.76	712	732	1.03	1	1	0
ENSMUSG00000090611	C330013E15Rik	chr15	100444571	100445541	-	2.4	78			1	0.38	3	1.70	1	0.27					0	0
ENSMUSG00000000346	Dazap2	chr15	100446069	100451184	+	3.3	53			1	0.37	3	1.68	1	0.25	14622	16246	1.11	0.88	1	0
ENSMUSG00000053559	Smagp	chr15	100451773	100467296	-	1.8	100					1	0.76			327	644	1.97	0.0045	1	0
ENSMUSG00000075411	Bin2	chr15	100475214	100499933	-	5.8	11	1	0.66			6	3.55	1	0.64	2872	2217	0.77	0.33	1	0
ENSMUSG00000023031	Cela1	chr15	100504856	100518351	-	4.7	22	1	0.35			5	3.32			111	51	0.45	0.14	1	0
ENSMUSG00000037280	Galnt6	chr15	100522244	100559807	-	5.8	13	1	0.72	1	0.71	4	2.51	1	0.83	6874	5228	0.76	0.36	1	0
ENSMUSG00000090062	1810009N23Rik	chr15	100526211	100535327	+	1.7	104					4	1.74							0	0
ENSMUSG00000023032	Slc4a8	chr15	100592178	100654399	+	1.7	113					2	0.66			28	65	2.32	0.2	1	0
ENSMUSG00000090536	Scn8a	chr15	100763860	100771229	+	0.0	195													0	0
ENSMUSG00000023033	Scn8a	chr15	100785829	100876360	+	0.0	196													0	0
ENSMUSG00000047034	Ankrd33	chr15	100946186	100950453	+	2.2	82			1	0.67	2	1.52							0	0
ENSMUSG00000000530	Acvrl1	chr15	100958953	100975767	+	3.6	47	1	0.23	2	0.67	5	1.74			1166	1573	1.35	0.96	1	0
ENSMUSG00000087690	Gm16031	chr15	100960347	100962023	-	3.0	60	1	0.34	2	0.87	5	1.84							0	0
ENSMUSG00000000532	Acvr1b	chr15	101004556	101043032	+	5.0	20					5	2.49	3	1.55	1889	2145	1.14	0.93	1	0
ENSMUSG00000087511	A330009N23Rik	chr15	101051627	101054552	-	0.0	197													0	0
ENSMUSG00000000531	Grasp	chr15	101054638	101063186	+	1.2	133					1	0.17			32	18	0.56	0.8	1	0
ENSMUSG00000023034	Nr4a1	chr15	101097277	101105223	+	6.1	10			2	0.94	5	1.96	3	2.16	298	171	0.57	0.095	1	0
ENSMUSG00000037204	9430023L20Rik	chr15	101114732	101121365	+	3.9	34			1	0.89	2	1.73	1	0.27	1158	951	0.82	0.75	1	0
ENSMUSG00000075408	6030408B16Rik	chr15	101123643	101127046	+	2.1	88			1	0.59	3	1.54							0	0
ENSMUSG00000037185	Krt80	chr15	101177875	101200556	-	3.1	58			1	0.67	1	0.83	1	0.62	96	68	0.71	0.84	1	0
ENSMUSG00000088459	Mir1941	chr15	101199783	101199865	+	2.0	91			1	0.64	1	0.81	1	0.59					0	0
ENSMUSG00000023039	Krt7	chr15	101241474	101260744	+	0.0	198													0	0
ENSMUSG00000047641	Krt83	chr15	101261921	101269235	-	0.0	199													0	0
ENSMUSG00000063971	1700011A15Rik	chr15	101278176	101284340	+	0.0	200													0	0
ENSMUSG00000067615	Krt81	chr15	101289492	101294196	-	0.0	201													0	0
ENSMUSG00000067614	Krt86	chr15	101303909	101310414	+	0.0	202													0	0
ENSMUSG00000067613	5430421N21Rik	chr15	101315562	101321943	-	0.0	203													0	0
ENSMUSG00000044294	Krt84	chr15	101355457	101363251	-	0.0	204													0	0
ENSMUSG00000049548	Krt82	chr15	101371660	101381098	-	0.0	205													0	0
ENSMUSG00000048699	4732456N10Rik	chr15	101382787	101393381	-	0.0	206													0	0

MOUSE ANNOTATION						FINAL SCORE		IRF8		IRF1		Stat1		p65 (NFkB)		BMDM RNA-seq					
Ensembl Gene ID	Symbol	Chr	Gene Start (bp)	Gene End (bp)	Strand	Total	Rank	Peaks	Score	Peaks	Score	Peaks	Score	Peaks	Score	Ctl (mean FPKM)	IFNg 3h (mean FPKM)	Fold change	Adj pValue	Expr. Score	Resp. score
ENSMUSG00000022986	Krt75	chr15	101393776	101404335	-	**1.7**	**112**					2	1.13	1	0.54					0	0
ENSMUSG00000064232	Gm5414	chr15	101454459	101458619	-	**0.3**	**172**							1	0.27					0	0
ENSMUSG00000023041	Krt6b	chr15	101506465	101510720	-	**0.0**	**207**													0	0
ENSMUSG00000058354	Krt6a	chr15	101520363	101524738	-	**0.0**	**208**													0	0
ENSMUSG00000061527	Krt5	chr15	101537501	101543322	-	**0.0**	**209**													0	0
ENSMUSG00000051879	Krt71	chr15	101564381	101573540	-	**0.0**	**210**													0	0
ENSMUSG00000067596	Krt74	chr15	101584690	101593935	-	**0.0**	**211**													0	0
ENSMUSG00000056605	Krt72-ps	chr15	101606603	101616889	-	**0.0**	**212**													0	0
ENSMUSG00000063661	Krt73	chr15	101623739	101632774	-	**0.0**	**213**													0	0
ENSMUSG00000064201	Krt2	chr15	101641120	101648600	-	**0.0**	**214**													0	0
ENSMUSG00000046834	Krt1	chr15	101675859	101681217	-	**0.0**	**215**													0	0
ENSMUSG00000067594	Krt77	chr15	101689163	101700136	-	**0.0**	**216**													0	0
ENSMUSG00000075402	Krt76	chr15	101714782	101723351	-	**0.0**	**217**													0	0
ENSMUSG00000059668	Krt4	chr15	101748967	101755166	-	**0.0**	**218**													0	0
ENSMUSG00000061397	Krt79	chr15	101759763	101770755	-	**0.0**	**219**													0	0
ENSMUSG00000050463	Krt78	chr15	101776435	101784718	-	**0.0**	**220**													0	0
ENSMUSG00000049382	Krt8	chr15	101827142	101834773	-	**0.0**	**221**													0	0
ENSMUSG00000023043	Krt18	chr15	101858647	101862457	+	**0.0**	**222**									3	5	1.60	1	0	0
ENSMUSG00000058655	Eif4b	chr15	101904204	101927603	+	**1.2**	**130**					1	0.18			15996	12365	0.77	0.29	1	0
ENSMUSG00000037003	Tenc1	chr15	101930909	101946832	+	**1.5**	**121**					1	0.47			112	61	0.54	0.28	1	0
ENSMUSG00000036966	Spryd3	chr15	101946776	101966665	-	**2.2**	**80**			1	0.41	1	0.51	1	0.33	2591	2555	0.99	1	1	0
ENSMUSG00000023046	Igfbp6	chr15	101974793	101979942	+	**2.1**	**89**			1	0.68	1	0.78	1	0.60	10	11	1.15	1	0	0
ENSMUSG00000023045	Soat2	chr15	101980957	101993905	+	**3.7**	**45**			1	0.88	1	0.99	1	0.80	96	164	1.71	0.28	1	0
ENSMUSG00000023044	Csad	chr15	102007429	102019474	-	**1.7**	**107**					2	0.72			197	184	0.93	1	1	0
ENSMUSG00000046897	Zfp740	chr15	102034079	102046037	+	**2.7**	**69**					2	1.66			2372	1782	0.75	0.27	1	0
ENSMUSG00000001281	Itgb7	chr15	102046426	102062366	-	**7.8**	**3**			2	1.28	7	4.47	2	1.06	5444	5674	1.04	1	1	0
ENSMUSG00000001288	Rarg	chr15	102065369	102087948	-	**4.0**	**31**	1	0.19	1	0.30	3	1.31	2	1.18	1061	645	0.61	0.11	1	0
ENSMUSG00000053724	Gm9918	chr15	102100994	102104552	+	**1.2**	**135**	1	0.63			1	0.54							0	0
ENSMUSG00000045665	Mfsd5	chr15	102109887	102112175	+	**2.4**	**77**	1	0.57			1	0.83			3867	3364	0.87	0.91	1	0
ENSMUSG00000058290	Espl1	chr15	102126724	102154787	+	**1.8**	**98**					2	0.58	1	0.27	4487	3058	0.68	0.067	1	0
ENSMUSG00000001289	Pfdn5	chr15	102156547	102162304	+	**3.9**	**32**			1	0.77	3	1.87	1	0.30	2150	2243	1.04	1	1	0
ENSMUSG00000001285	Myg1	chr15	102162140	102168570	+	**3.7**	**42**			2	0.72	3	1.90	1	0.12	1306	1195	0.92	1	1	0
ENSMUSG00000036678	Aaas	chr15	102168678	102181190	-	**3.0**	**62**			1	0.77	2	1.21			2163	2178	1.01	1	1	0
ENSMUSG00000060284	Sp7	chr15	102187040	102197285	-	**1.1**	**137**			1	0.23	2	0.90			3	3	1.10	1	0	0
ENSMUSG00000088286	U6	chr15	102204311	102204414	+	**1.0**	**140**					2	0.87	1	0.18					0	0
ENSMUSG00000090274	Gm17671	chr15	102227862	102227948	-	**4.1**	**29**					6	3.38	1	0.71					0	0
ENSMUSG00000001280	Sp1	chr15	102236574	102266835	+	**5.8**	**12**					6	4.37	1	0.42	5625	5335	0.95	0.99	1	0
ENSMUSG00000023047	Amhr2	chr15	102275798	102285061	+	**1.3**	**123**					3	1.33			3	6	2.20	1	0	0
ENSMUSG00000090630	Gm17403	chr15	102285957	102314153	-	**0.9**	**153**			1	0.37	1	0.54							0	0
ENSMUSG00000089168	U6	chr15	102286994	102287092	+	**2.6**	**70**			1	0.35	4	2.23							0	0
ENSMUSG00000023048	Prr13	chr15	102289459	102293237	+	**3.8**	**37**			1	0.44	4	2.39			5986	10954	1.83	0.0064	1	0
ENSMUSG00000056851	Pcbp2	chr15	102301063	102330490	+	**3.7**	**43**			1	0.81	3	1.87			9929	10861	1.09	0.96	1	0
ENSMUSG00000023050	Map3k12	chr15	102328080	102347495	-	**3.2**	**55**					1	0.68	1	0.53	820	393	0.48	0.0035	1	1
ENSMUSG00000071586	Gm10337	chr15	102334153	102334317	+	**1.5**	**120**					1	0.87	1	0.65					0	0
ENSMUSG00000023051	Tarbp2	chr15	102348623	102354107	+	**2.1**	**87**					1	0.65	1	0.49	861	788	0.92	1	1	0
ENSMUSG00000023052	Npff	chr15	102354274	102355052	-	**1.7**	**110**					1	0.43	1	0.27	29	29	1.03	1	1	0
ENSMUSG00000071584	Atf7	chr15	102359067	102359456	-	**1.0**	**150**									171	167	0.98	1	1	0
ENSMUSG00000052414	Atf7	chr15	102364008	102455881	-	**4.6**	**23**			2	1.48	3	2.11			963	902	0.94	1	1	0
ENSMUSG00000065111	U6	chr15	102458210	102458316	-	**3.2**	**54**			2	1.35	3	1.89							0	0
ENSMUSG00000036305	Gm15430	chr15	102465410	102465767	+	**2.1**	**90**			2	0.88	3	1.18							0	0
ENSMUSG00000062683	Atp5g2	chr15	102493299	102501478	-	**3.5**	**50**			1	0.74	1	0.99	1	0.77	50	43	0.85	1	1	0
ENSMUSG00000076009	Mir688	chr15	102502223	102502297	-	**2.5**	**73**			1	0.72	1	0.97	1	0.80					0	0
ENSMUSG00000023055	Calcoco1	chr15	102537210	102552609	-	**1.0**	**151**									983	922	0.94	1	1	0
ENSMUSG00000091182	Gm17649	chr15	102751146	102751251	-	**0.0**	**223**													0	0
ENSMUSG00000001655	Hoxc13	chr15	102751534	102759245	+	**0.0**	**224**													0	0
ENSMUSG00000050328	Hoxc12	chr15	102767188	102769040	+	**0.0**	**225**													0	0
ENSMUSG00000086903	Gm16258	chr15	102774493	102778851	-	**0.9**	**154**	1	0.45	1	0.46									0	0
ENSMUSG00000001656	Hoxc11	chr15	102784858	102788139	+	**1.3**	**127**	1	0.65	1	0.66									0	0
ENSMUSG00000022484	Hoxc10	chr15	102797227	102802324	+	**1.8**	**101**	1	0.87	1	0.88									0	0
ENSMUSG00000092585	RP24-459N19.4	chr15	102797874	102846107	+	**1.7**	**109**	1	0.85	1	0.86									0	0
ENSMUSG00000092194	AC124345.1	chr15	102803772	102803881	+	**1.3**	**125**	1	0.65	1	0.66									0	0
ENSMUSG00000065488	Mir196a-2	chr15	102803772	102803881	+	**1.3**	**126**	1	0.65	1	0.66									0	0
ENSMUSG00000036139	Hoxc9	chr15	102806870	102815530	+	**1.1**	**138**	1	0.55	1	0.56									0	0
ENSMUSG00000001657	Hoxc8	chr15	102821053	102824698	+	**0.0**	**226**													0	0
ENSMUSG00000001661	Hoxc6	chr15	102828688	102842312	+	**0.0**	**227**													0	0
ENSMUSG00000022485	Hoxc5	chr15	102844246	102847860	+	**0.0**	**228**													0	0
ENSMUSG00000092424	AC124345.2	chr15	102845341	102845432	+	**0.0**	**229**													0	0
ENSMUSG00000076010	Mir615	chr15	102845341	102845432	+	**0.0**	**230**													0	0
ENSMUSG00000075394	Hoxc4	chr15	102849367	102867274	+	**0.0**	**231**													0	0
ENSMUSG00000086435	D930007P13Rik	chr15	102953501	102977259	-	**1.2**	**134**					2	1.16							0	0
ENSMUSG00000036061	Smug1	chr15	102983738	102988383	-	**2.2**	**84**					2	1.16			579	505	0.87	0.9	1	0
ENSMUSG00000009575	Cbx5	chr15	103021975	103070247	-	**1.2**	**129**					1	0.23			9786	6932	0.71	0.11	1	0
ENSMUSG00000046434	Hnrnpa1	chr15	103070945	103074445	+	**1.3**	**128**					1	0.26			758	734	0.97	1	1	0

MOUSE ANNOTATION						FINAL SCORE		IRF8		IRF1		Stat1		p65 (NFkB)		BMDM RNA-seq					
Ensembl Gene ID	Symbol	Chr	Gene Start (bp)	Gene End (bp)	Strand	Total	Rank	Peaks	Score	Peaks	Score	Peaks	Score	Peaks	Score	Ctl (mean FPKM)	IFNg 3h (mean FPKM)	Fold change	Adj pValue	Expr. Score	Resp. score
ENSMUSG00000058794	Nfe2	chr15	103078643	103088834	-	2.9	63			1	0.89	2	1.03			263	105	0.40	0.29	1	0
ENSMUSG00000060992	Copz1	chr15	103103342	103130293	+	3.1	57			1	0.55	3	1.59			7320	8700	1.19	0.59	1	0
ENSMUSG00000065560	Mir148b	chr15	103115556	103115652	+	1.0	143					2	1.01							0	0
ENSMUSG00000063234	Gpr84	chr15	103138667	103140869	-	5.7	15					3	2.35	3	2.33	5907	5712	0.97	1	1	0
ENSMUSG00000000552	Zfp385a	chr15	103144319	103170517	-	3.4	51	2	1.40			3	1.03			3363	2580	0.77	0.39	1	0
ENSMUSG00000000555	Itga5	chr15	103174720	103197194	-	8.2	2	1	0.66	1	0.62	6	3.28	4	2.67	22835	28477	1.25	1	1	0
ENSMUSG00000022487	Gtsf1	chr15	103232836	103260901	-	1.3	124	1	0.70			1	0.63			8	7	0.91	1	0	0
ENSMUSG00000053508	BC048502	chr15	103269396	103278890	-	3.6	49			1	0.57	6	2.66	1	0.34					0	0
ENSMUSG00000022488	Nckap1l	chr15	103284256	103329240	+	6.7	5			1	0.75	7	4.13	2	0.78	47450	53284	1.12	1	1	0
ENSMUSG00000022489	Pde1b	chr15	103333465	103360483	+	3.1	59			1	0.90	3	1.17			2409	3941	1.64	0.45	1	0
ENSMUSG00000022490	Ppp1r1a	chr15	103360710	103368423	-	3.6	48					3	1.73	2	0.91	21	21	1.01	1	1	0
ENSMUSG00000022491	Glycam1	chr15	103393193	103395509	-	2.0	94					2	0.94	2	1.01					0	0

The *Carg5* locus regulates susceptibility to *C. albicans* infection in B6 vs. SM/J, and has a major effect on myeloid cell function. The *Carg5* minimum genetic interval contains 231 annotated genes (Ensembl known genes NCBIm37). Using a combination of functional genomic data generated in myeloid cells in response to inflammatory triggers, we calculated a "Myeloid Inflammatory Score" in order to rank candidate causal genes by their possible implication in inflammatory processes. Specifically we used high throughput sequencing of chromatin immunoprecipitation for IFNγ-responsive IRF8, IRF1 and STAT1, and LPS-responsive NFkB (p65) DNA-binding, together with RNA-seq expression profiling performed prior to and after IFNγ treatment. For each gene, the presence and extent of binding (peak height) for IRF1, IRF8, STAT1 and NFkB (p65) is shown (ChIP-seq) as well as the presence and extent IFNγ regulated expression in myeloid cells (RNA-Seq). Both datasets were combined to calculate a "Myeloid Inflammatory Score" (see Materials and Methods for description of calculations).

PREFACE TO CHAPTER 4

In Chapters 2 and 3, we aimed to uncover novel C5-independent host genetic factors modulating response to disseminated *C. albicans* infection in a murine model. We employed a combinatorial forward genetic approach, where we conducted a GWAS to uncover putative associations in a set of inbred strains and subsequently validated these by linkage analysis in informative F2 crosses. These studies led to the discovery of several loci, namely *Carg3* (Chr 8), *Carg4* (Chr 11), and *Carg5* (Chr15). In Chapter 3, we extended our approach to encompass immunophenotyping of the innate immune compartment, enabling us to ascribe susceptibility to *C. albicans* to a pleiotropic myeloid defect.

In Chapter 4, we explore the genetic basis of differential permissiveness of A/J and B6 mouse strains to the cestode *T. crassiceps*. Using an analogous forward genetic strategy described in Chapter 2, we phenotype the AcB/BcA RCS panel to detect putative loci controlling parasite replication, which are then validated by linkage analysis in F2 progeny derived from resistant AcB55 and susceptible DBA/2J mice. This first genetic study demonstrates that C5 underlies the major locus on chromosome 2 (*Tccr1*), which confers restrictiveness to *T. crassiceps* cysticercosis.

Chapter 4:

Identification of loci controlling restriction of parasite growth in experimental *Taenia crassiceps* cysticercosis

4.1 ABSTRACT

Human neurocysticercosis (NC) caused by *Taenia solium* is a parasitic disease of the central nervous system that is endemic in many developing countries. In this study, a genetic approach using the murine intraperitoneal cysticercosis caused by the related cestode *Taenia crassiceps* was employed to identify host factors that regulate the establishment and proliferation of the parasite. A/J mice are permissive to *T. crassiceps* infection while C57BL/6J mice (B6) are comparatively restrictive, with a 10-fold difference in numbers of peritoneal cysticerci recovered 30 days after infection. The genetic basis of this inter-strain difference was explored using 34 AcB/BcA recombinant congenic strains, derived from A/J and B6 progenitors, that were phenotyped for *T. crassiceps* replication. In agreement with their genetic background, most AcB strains (A/J-derived) were found to be permissive to infection while most BcA strains (B6-derived) were restrictive with the exception of a few discordant strains, together suggesting a possible simple genetic control. Initial haplotype association mapping using >1200 informative SNPs pointed to linkages on chromosomes 2 (proximal) and 6 as controlling parasite replication in the AcB/BcA panel. Additional linkage analysis by genome scan in informative [AcB55xDBA/2]F1 and F2 mice (derived from the discordant AcB55 strain), confirmed the effect of chromosome 2 on parasite replication, and further delineated a major locus (LOD=4.76, $p<0.01$; peak marker *D2Mit295,* 29.7Mb) that we designate *Tccr1* (*T. crassiceps cysticercosis restrictive* locus *1*). Resistance alleles at *Tccr1* are derived from AcB55 and are inherited in a dominant fashion. Scrutiny of the minimal genetic interval reveals overlap of *Tccr1* with other host resistance loci mapped to this region, most notably the defective *Hc/C5* allele which segregates both in the AcB/BcA set and in the AcB55xDBA/2 cross. These results strongly suggest that the complement component 5 (C5) plays a critical role in early protective inflammatory response to infection with *T. crassiceps*.

4.2 INTRODUCTION

Taenia solium seriously affects human health in many countries of Latin America, Asia and Africa (*645*). The life cycle of *T. solium* includes a larval phase (cysticercus), which develops in both pigs and humans from ingested eggs contaminating the environment. When humans ingest improperly cooked pork meat infected with live cysticerci, the cysticerci develop to the stage of an adult intestinal tapeworm, which produces millions of eggs that are then shed to the environment in human faeces (*646*). In rural communities where the disease is endemic, unsanitary conditions and presence of free-roaming pigs result in up to 9 % of the human open population of these areas to be infected. Despite this high infection rate, only a small fraction of carriers become symptomatic and develop NC, suggesting intrinsic differences in host susceptibility to infection and pathogenesis of the disease (*647*). Indeed, several reports have pointed at possible genetic effects in response to cysticercosis in human and pigs. In humans, multi-case families were identified in areas of highly endemic disease, favoring the idea of the participation of multiple genes in NC causality (*647*). In a case-control study, resistance to NC was found associated to HLA (*648*). Also, a three to five fold difference in parasite load was detected in a genetically heterogeneous pig cohort experimentally challenged with *T. solium* eggs (*649*).

Taenia crassiceps is a tapeworm of wild and domestic animals, which does not cause clinical disease in non-immunocompromised humans (*650*). *T. crassiceps* has been used as an experimental model for cysticercosis due to its ability to proliferate by budding (*651*) and colonize the peritoneal cavity of the murine host (*651*), where its replication can be measured over time by enumeration of recovered metacestodes. Although the *T. crassiceps* ORF strain is unable to develop into adult tapeworms (*652*), its property to rapidly multiply in the peritoneal cavity of infected mice has been extensively used to explore the relevance of biological factors in host-parasite interactions (*653*), and to identify protective antigens of interest for vaccine development (*653*, *654*). The mechanisms involved in the protective immunity against *T. crassiceps* cysticercosis have been extensively studied, but are not fully

understood. Studies in inbred mouse strains (growth permissive H2d-bearing BALB/c; growth restrictive H2b-bearing C57BL/6J) initially pointed at the importance of the major histocompatibility locus (MHC) and MHC-linked genes in regulating intraperitoneal growth of the parasite (*655*). This was confirmed by additional studies of H2 congenic BALB/c substrains, where BALB/cJ mice express the Qa2 protein and are significantly more resistant than the BALB/cAnN mice (*656*, *657*). This differential susceptibility may be explained in part by activation of antigen presenting cells, and production of pro-inflammatory cytokine and modulatory chemokines both early and late during *T. crassiceps* infection (*658*). Furthermore, phenotyping of different inbred strains has suggested that an additional, non-MHC linked genetic component may contribute to regulation of *T. crassiceps* replication (*659*). Finally, clear differences between the parasite load of male and female have been noted in inbred mouse strains (*660*). Females show higher numbers of cysticerci compared to males due to a significant effect of sex hormones on response to infection (*661*, *662*).

With the aim of further characterizing the host genetic factors that affect host response to *T. crassiceps* cysticercosis, the differential susceptibility of A/J (permissive) and C57BL/6J (restrictive) mouse strains was studied. For this, a set of 34 reciprocal AcB/BcA recombinant congenic strains (RCS) derived by systematic inbreeding from a double backcross (N3) between A/J and C57BL/6J parents (*547*) was phenotyped for response to *T. crassiceps* infection. In the breeding scheme used to derive the AcB/BcA strains set, each of the strains harbors 12.5% of its genome from either A/J or B6, fixed as a set of discrete congenic segments onto 87.5% of the reciprocal parental background. The vast range of permissiveness to *T. crassiceps* growth in 34 RCS, as measured by the parasite load 30 days post-infection, along with haplotype association mapping suggested that response to *T. crassiceps* cestode is under complex genetic control, with identifiable contributions of chromosomes 2 and 6. Subsequent genetic linkage analysis in informative crosses validated the chromosome 2 locus, and established the regional position of the regulating locus.

4.3 MATERIALS AND METHODS

Mice

The AcB/BcA set of recombinant congenic strains (RCS) were derived from a double backcross (N3) between A/J and C57BL/6J parents at McGill University and were provided by Emerillon Therapeutics. The breeding, genetic characteristics and genotype of RCS have been described earlier (*547*). Inbred strains A/J, B6, and DBA/2 were obtained as pathogen-free mice at 7-8 weeks of age from the Jackson Laboratory (Bar Harbor, ME) and maintained as breeding colonies at UNAM. [AcB55xDBA/2] F2 progeny were bred by systematic brother-sister mating of [AcB55xDBA/2] F1 mice.

Ethics statement

The study protocol (register number 021) was approved by the ethics committee of the Instituto de Investigaciones Biomédicas, Universidad Nacional Autónoma de México (UNAM). All housing and experimental procedures were performed according to the principles set forth in the Guide for the Care and Use of Laboratory Animals, Institute of Laboratory Animal Resources, National Council, Washington, D.C. 1996.

Infection with Taenia crassiceps

The fast growing ORF strain of *T. crassiceps*, originally isolated by R. S. Freeman (*651*), was maintained by serial intraperitoneal (i. p.) passage in female BALB/cAnN mice, as previously described (*657*). All experimental mice were inoculated intraperitoneally with 10 small (< 2 mm) non-budding *T. crassiceps* larvae, re-suspended in sterile isotonic saline. Thirty days following infection, parasites were harvested from the peritoneal cavity and counted using a stereoscopic microscope (*663*) to determine the parasite burden. Organs inside the abdominal cavity were removed and carefully inspected for any remaining *T. crassiceps* larvae.

Genotyping

Genomic DNA was isolated from tail clips of individual F2 mice collected at the time of sacrifice, as previously described (*547*). A total of 185 female [AcB55xDBA/2]F2 mice were genotyped at the Centre for Applied Genomics (The Hospital for Sick Children, Toronto, Canada) using the Illumina Mouse Low Density Linkage panel containing 377 SNPs distributed across the genome, out of which 161 were polymorphic between AcB55 and DBA/2 strains. Additional microsatellite markers were obtained from the Mouse Genome Informatics Database (www.informatics.jax.org) and used for gap filling and fine mapping by a standard PCR-based method employing (α-^{32}P) dATP labeling and separation on denaturing 6% polyacrylamide gels. C5 status in the F2 mice was confirmed by RFLP analysis, as previously described (*7*). Briefly, C5 fragment was amplified by PCR and digested with *Bsg* I, which recognizes a novel restriction site introduced by the 2-bp deletion in exon 6 of the *Hc* gene (*7*, *543*). The fragments were resolved on 2% agarose gel; the expected size for wild-type C5 was 446 bp, while the sizes for the samples containing the deletion were 318 and 126 bp.

Linkage and association mapping

QTL mapping was performed using Haley-Knott multiple regression analysis (*569*) and the two-dimensional scan was performed using the two-QTL model. Empirical genome-wide significance was calculated by permutation testing (1000 tests). All linkage analysis was performed using R/qtl (*571*). The detailed algorithm underlying the efficient mixed-model for association mapping has been previously published (*572*). The EMMA algorithm is based on the mixed-model association where a kinship matrix accounting for genetic relatedness between inbred mouse strains is estimated and then fitted to the vector of the phenotype, thereby reducing false positive rates. EMMA is publically available as an R package implementation.

Statistical analysis

An unpaired, two-tailed Student's t-test was used to establish significance of differences in mean parasite burden between mouse *Tccr1* and *C5* genotypes. These

data were analyzed using GraphPad Prism 4.0 statistical software. P-values < 0.05 were considered significant.

4.4 RESULTS

Response to T. crassiceps infection in recombinant congenic strains. A/J and C57BL/6J (B6) mice show differential permissiveness to cysticercosis (*660*), following the intra-peritoneal inoculation of 10 small (<2 mm diameter) non-budding T. crassiceps larvae (Figure 1). In A/J mice, there is rapid parasite reproduction in the peritoneal cavity, which is detectable by visual and histological examination of the mice (Figure 1A, 1B), and by quantification of parasite load (Figure 1C, magnification in 1D). Enumeration of the parasites recovered 30 days following infection (Figure 2) indicates a 10-fold difference in parasite replication between A/J (200-250) and C57BL/6J (15-30). To study the genetic control of differential replication of T. crassiceps in restrictive B6 and permissive A/J strains, we phenotyped a set of 34 AcB/BcA recombinant congenic strains (*547*). The breeding scheme used to generate the reciprocal AcB/BcA strains set results in individual strains harboring 12.5% of its genome donated from either A/J (in BcA strains) or B6 (in AcB strains), fixed as a set of discrete congenic segments onto 87.5% of the reciprocal parental background (*547*). The AcB/BcA strain set has previously been used to characterize different genetic traits that control phenotypic differences between B6 versus A/J, including mapping of major monogenic trait (*547*), and dissection of complex genetic traits into several simple genetic effects (*664*, *665*). Between 5-10 animals from each strain were infected with T. crassiceps and the total parasite burden was determined 30 days later (Figure 2A and 2B). We segregated AcB/BcA strains according to the predominant genetic background (left and right panels in Figure 2), and further grouped them into permissive or restrictive categories based on the overall mean parasitic load, whereby strains harboring an average of >66 parasites were deemed permissive while those showing <66 were termed restrictive (determined as two standard deviations from the parasite load of restrictive B6 parental group). According to this arbitrary segregation, the majority of BcA strains were parasite growth restrictive, with the notable exception of strains BcA73, 70, 72 and 83 that showed parasite loads similar to those detected in the A/J controls (Figure 2B). Conversely, AcB strains were found to be generally permissive for parasite growth, with the notable exception of strains AcB55 and AcB60 that displayed an

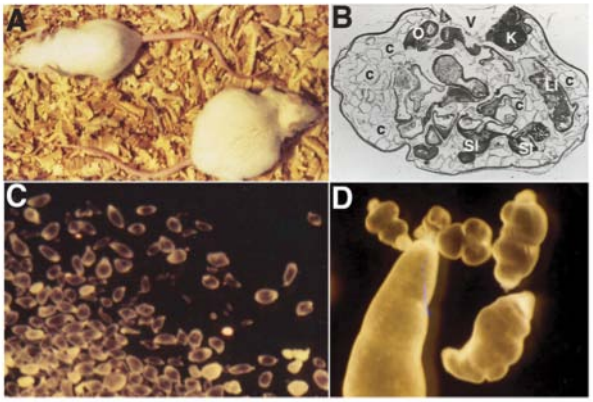

Figure 1. ***Taenia crassiceps*** **intraperitoneal murine cysticercosis.**

Aspect of the distended abdomen of a cysticercotic permissive mouse 30 days after intraperitoneal *T. crassiceps* infection compared to a non-infected littermate (A). Hematoxilin and eosin staining was performed on a cross-sectional slice of the abdomen of a cysticercotic mouse (B). Abdominal organs can be distinguished (O=ovary, K=kidney, SI=small intestine, LI=large intestine, V=vertebral column space), whereas cysticerci (denoted by c) appear as thin dark septa limiting the empty spaces. (C) Aspect of cysticerci recovered from the peritoneal cavity of an infected permissive mouse 30 days post-infection, with and without attached buds (D). Photographs kindly provided by Dr. Carlos Larralde.

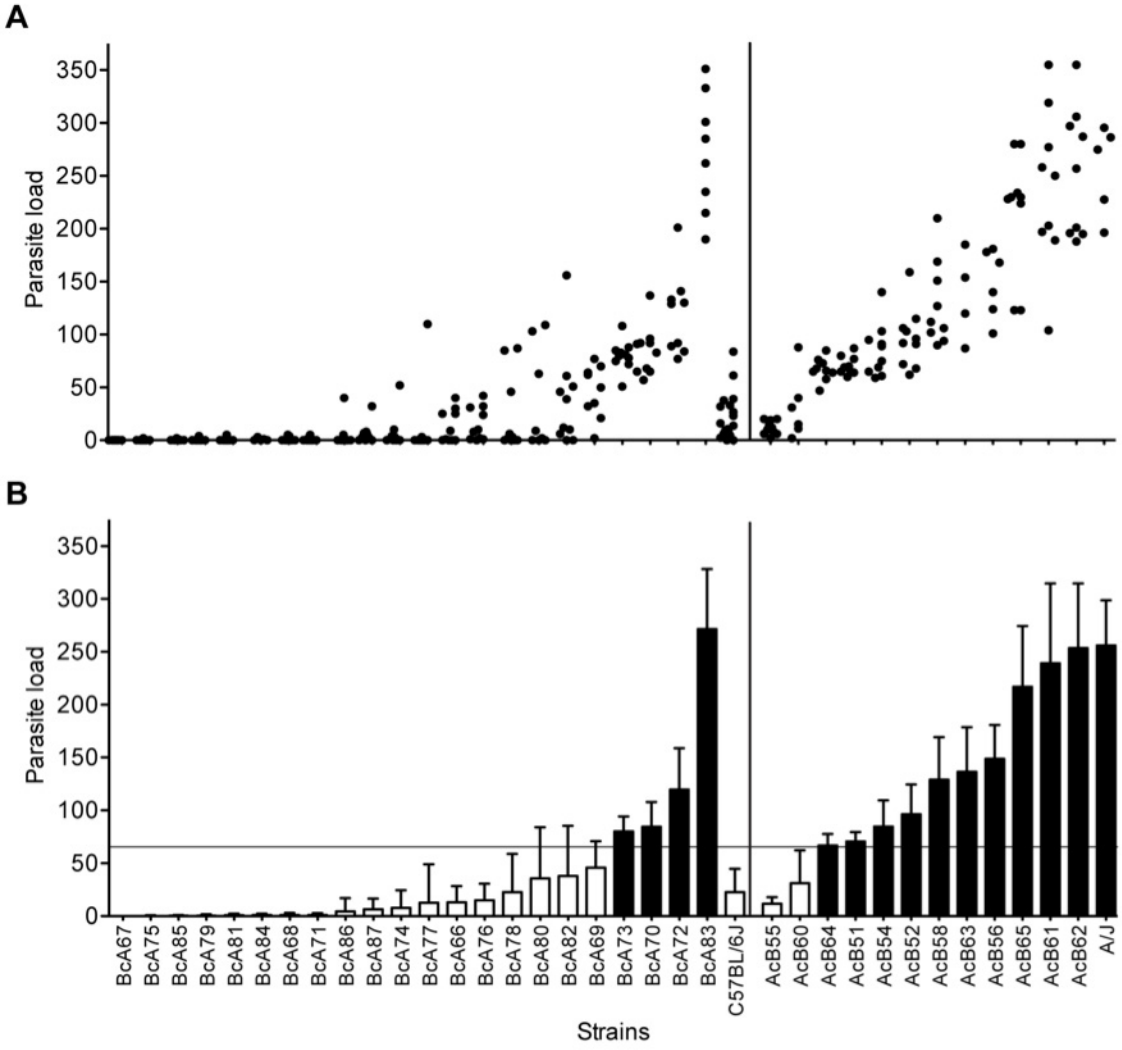

Figure 2. Response of AcB/BcA strains to *T. crassiceps* infection.

Parasite load recovered from female A/J, C57BL/6J (B6) and 34 recombinant congenic AcB/BcA mice 30 days after infection. 4-10 mice per strain were intraperitoneally infected with 10 non-budding *T. crassiceps* larvae. The average number of parasites is shown (B) along with raw data (A) where each dot represents a single mouse. Bars represent strain mean ± SD. Horizontal line corresponds to two standard deviations from the mean parasite load of resistant B6 strain, which was used to stratify strains into susceptible (black bars), or resistant (white bars) categories.

average of 12 and 31 cysticerci, respectively. The presence of such discordant strains in both sets of RCS suggests the possibility that the restrictiveness/permissiveness trait is under simple genetic control, and that transfer of a single congenic fragments onto the opposite strain background strongly influences the phenotype of the recipient strain. Such a situation would be similar to the segregation of the *Ccs3* (colorectal cancer) (*552*), *Ity* (susceptibility to *Salmonella*) (*666*) and *Lgn1* loci (susceptibility to *Legionella*) (*547*) we previously reported in these strains.

Chromosomes 2 and 6 are associated with response to T. crassiceps infection in AcB/BcA strains. To explore the nature and complexity of the genetic control of parasite replication in the AcB/BcA strains set, we performed haplotype association mapping using parasite load as the primary phenotype and 1200 informative polymorphic genetic markers. We applied a statistical model EMMA (*572*) that corrects for genetic relatedness and population structure of the RCS by computing a kinship matrix in a manner analogous to an inbred mouse strain analysis, as we previously described (*602*). Using this approach, we detected suggestive association of chromosome 2 (proximal region) and chromosome 6 alleles with *T. crassiceps* permissiveness (Figure 3). In the case of chromosome 6, both proximal (weaker) and distal (stronger) portions of the chromosome showed association. Also, for both chromosomes 2 and 6, A/J alleles are associated with permissiveness while B6 alleles are associated with restrictiveness, as expected. Additional strength for these associations is provided by some of the phenodeviant strains; for example, for the proximal part of chromosome 2 (~35Mb), susceptible BcA70, 72, and 73 harbor A/J haplotypes, while resistant AcB55 and AcB60 harbor B6-derived haplotypes (Figure S1). Likewise, for distal chromosome 6, BcA72, 73 and 83 have A/J alleles, while AcB55 and 60 have B6 alleles (Figure S1). Nevertheless, the imperfect correlation for both chromosomes requires validation in secondary crosses. It also suggests presence of additional genetic effects controlling *T. crassiceps* permissiveness in the strain set.

Linkage analysis in [AcB55xDBA/2]F2 cross validates association of chromosome 2 locus with response to T. crassiceps. The genetic control of host response to *T. crassiceps* was further investigated in strain AcB55. This strain

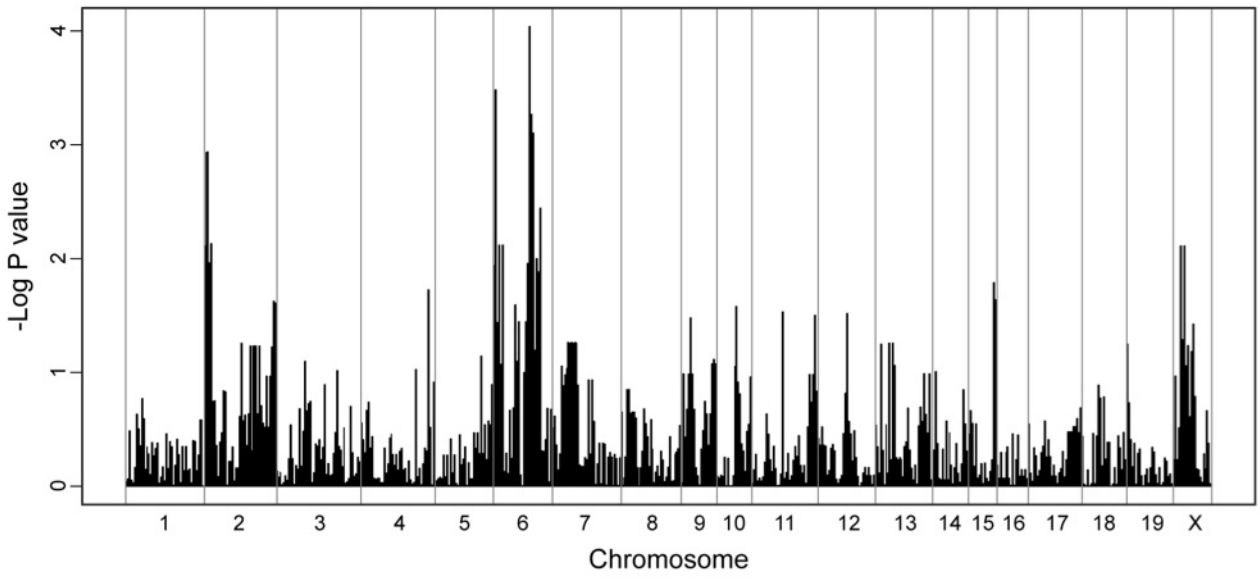

Figure 3. Genome-wide association mapping in 34 AcB/BcA strains using EMMA.

Using the R package implementation of EMMA, genome-wide association mapping was conducted across 34 RCS as well as the original parental A/J and B6 inbred strains. The genotyping data consisted of ~1200 SNPs and informative dinucleotide repeats and was correlated with the parasite load, yielding $-\log_{10}$ transformed P values indicating genome-wide association significance for each SNP. Each line represents a single SNP or marker.

consistently showed the lowest parasite burden in the AcB set (Figure 2, mean parasite load = 11.7), despite ~87.5% of its background being inherited from the highly susceptible A/J parent (mean parasite load = 256). Therefore, we hypothesized that AcB55 is likely to carry B6-derived chromosomal segments responsible for restrictiveness in both AcB55 and B6. To map such segments, AcB55 was crossed to the permissive strain DBA/2 (Figure 4A, mean parasite load = 108) to produce an [AcB55xDBA/2] F2 population in which individual animals would be informative for the entire genome in linkage analyses. [AcB55xDBA/2] F1 hybrids and 379 [AcB55xDBA/2] F2 animals were infected intraperitoneally with 10 non-budding *T. crassiceps* larvae in three separate infections, and parasite burden was measured 30 days later (Figure 4A). Due to the previously reported gender-associated differential permissiveness to *T. crassiceps*, where higher concentrations of estrogen and estradiol are concomitant with increased parasite burdens (*661*, *662*) typically occurring in female mice, we segregated males and females in the analysis (Figure 4A). Both male and female [AcB55xDBA/2] F1 hybrids were fully resistant with parasite load similar to the AcB55 controls (Figure 4A), suggesting that resistance to *T. crassiceps* is inherited in a dominant fashion. The parasite load of [AcB55xDBA/2] F2 mice followed a continuous distribution between highly permissive and highly restrictive animals, with a clustering of F2 animals in the resistant range. This suggests both a complex genetic control of permissiveness to infection, with a dominant pattern of inheritance of restrictiveness more apparent in the female population (Figure 4A). Interestingly, we observed an identical pattern of inheritance of restrictiveness (dominant) in a distinct F2 population, where the AcB55 strain was crossed to the permissive A/J founder (Figure S2). However, due to limited genetic diversity in the [AcB55xA/J] F2 progeny (~12.5% due to B6 genomic segments), we conducted genetic linkage analysis by whole genome scanning in the [AcB55xDBA/2] F2 population. Because the frequency distribution of parasite load in F2 females was skewed, we applied a log2 correction to normalize the distribution, followed by regression to an experiment-specific mean (set at 0) (Figure 4B).

A total of 185 [AcB55xDBA/2] F2 female mice were genotyped with the Illumina Mouse Low Density Linkage Panel consisting of 161 informative

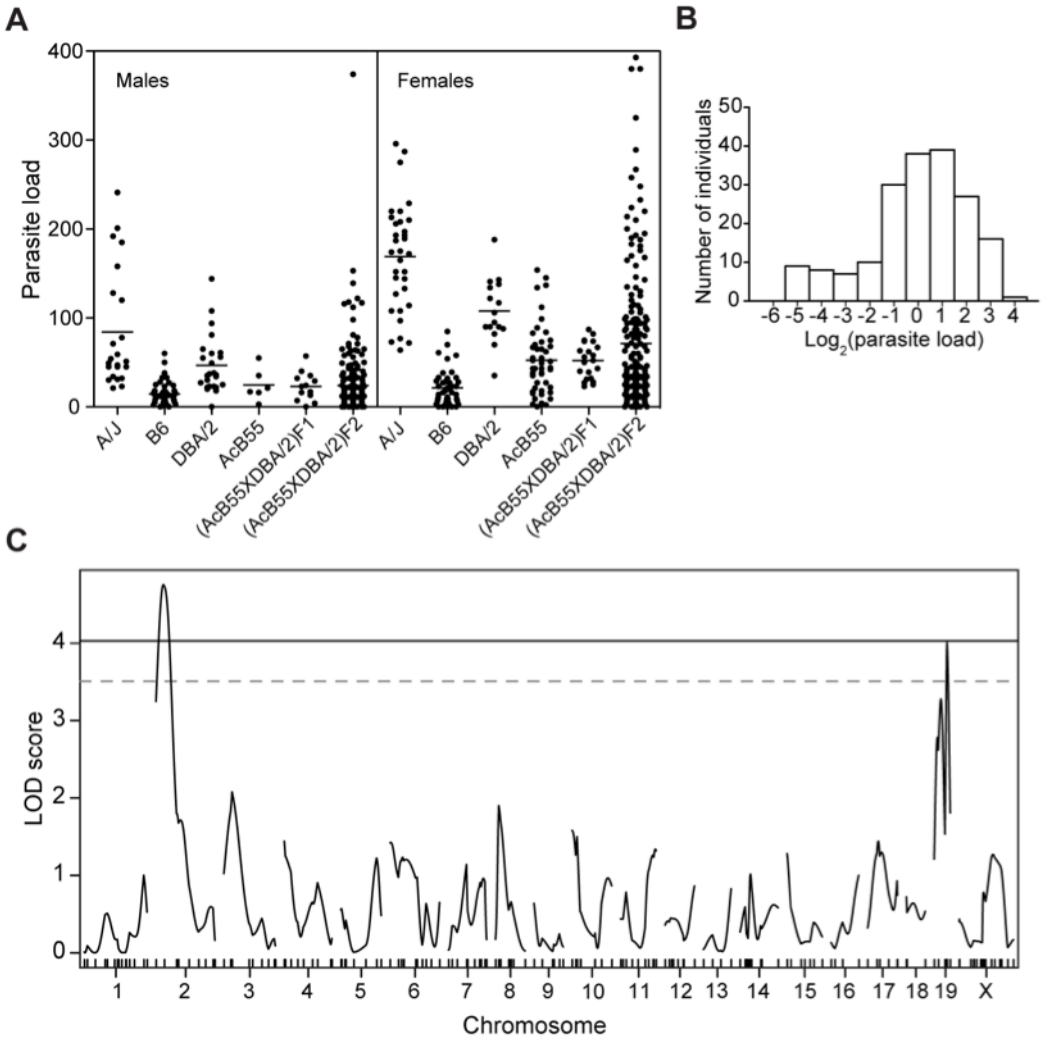

Figure 4. Linkage analysis in the informative [AcB55xDBA/2]F2 population.

[AcB55xDBA/2]F2 mice (n=379) were infected intraperitoneally with 10 non-budding *T. crassiceps* larvae and parasite number was determined 30 days post-infection. The results from three separate infections are plotted along with A/J, B6, DBA/2, and [AcB55xDBA/2]F1 controls (A). Each dot represents a single mouse. Distribution of parasite load is shown in the female [AcB55xDBA/2]F2 population (B), after regression of $\log_2$(parasite load) to an experiment-specific mean (set at 0). Mice were genotyped at 171 SNPs and dinucleotide repeats across the genome and interval mapping was carried out using the R/qtl software package. Whole genome LOD score trace is shown for genetic effects controlling parasite burden in female [AcB55xDBA/2]F2 mice (n=185) (C), identifying linkage to chromosome 2 (LOD=4.75) and chromosome 19 (LOD=4.0), designated *Tccr1* and *Tccr2*, respectively. Marker positions are indicated on the x-axis and genome-wide thresholds at P=0.01 and 0.05 were identified by permutation testing (1000 tests).

polymorphic markers with 10 additional microsatellite markers to complete genome coverage. Whole-genome multiple regression linkage analysis in R/qtl (Figure 4C) identified a highly significant locus associated with parasite burden on chromosome 2 (LOD=4.76, P<0.01) and an additional suggestive linkage on chromosome 19 (LOD= 4.03, P<0.05) (Figure 4C and S3). These loci contributing restrictiveness to *T. crassiceps* in the AcB55 strain were given a temporary appellation *Tccr1* (*Taenia crassiceps cysticercosis restrictiveness 1*) for chromosome 2 QTL and *Tccr2*, for chromosome 19 QTL. The Bayesian 95% credible intervals were determined to be 13.1-44.1 Mb for *Tccr1* (Figure 5A) and the entire chromosome 19 for *Tccr2* (Figure S3), whereas the peak LOD scores were identified at 29.7 Mb (peak marker: D2Mit295) and 46.7 Mb (peak SNP: rs13483650), respectively.

To examine the effect of the most significant *Tccr1* locus on parasite load, F2 mice were segregated according to genotype at the most significant chromosome 2 marker *D2Mit295* (Figure 5B). Mice carrying the DBA/2 alleles at *Tccr1* have significantly higher number of cysticerci (P=0.0009; Student's t-test) than those harboring one or two AcB55 alleles. This indicates that restrictiveness alleles at *Tccr1* are inherited in a strictly dominant fashion. We also examined the LOD score trace for chromosome 19 and the inheritance of parental alleles underlying *Tccr2* at the peak marker (rs13483650) (Figure S3). We observed two prominent peaks, suggesting that *Tccr2* may be due to multiple genetic effects contributing to lower parasite loads in the AcB55 strain. However, once we segregated the female F2 mice according to their genotype (Figure S3B), we observed that the *Tccr2* QTL is driven by heterozygosity, with homozygosity for neither the AcB55- nor the DBA/2-derived alleles having a significant effect on the parasite burden. To determine whether *Tccr1* and *Tccr2* acted in an additive or epistatic manner, a two-dimensional Haley-Knott multiple regression analysis was carried out, followed by simulation of an overall QTL model using R/qtl. This analysis revealed that, although *Tccr1* and *Tccr2* are non-interacting loci, their individual and joint contribution to the full QTL model raises the LOD score to 11.26 and explains 25% of observed phenotypic variance.

Interestingly, linkage analysis in the AcB55xDBA/2 cross was successful in

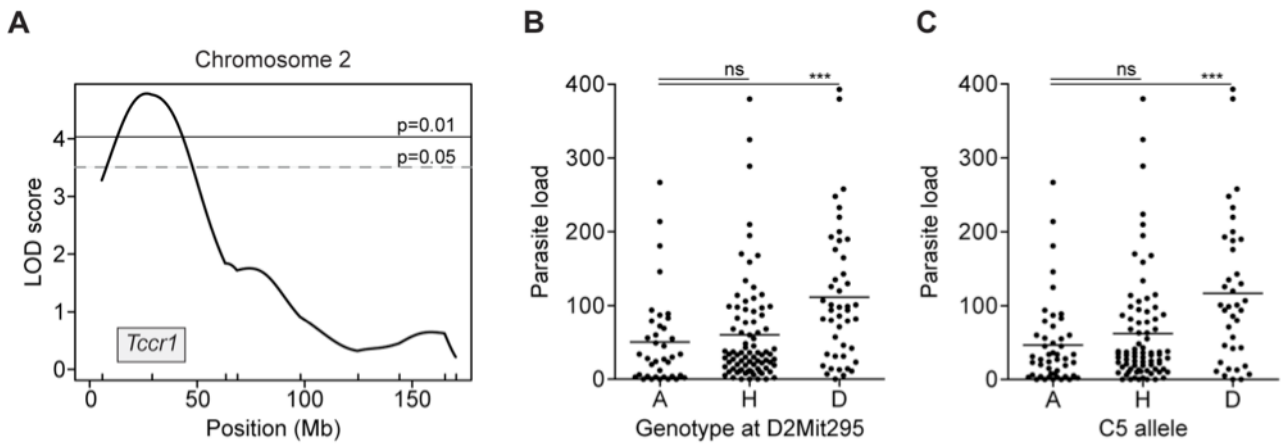

Figure 5. Effect of the *Tccr1* locus on parasite burden in [AcB55xDBA/2]F2 mice.

Detailed LOD score traces are shown for chromosome 2 (*Tccr1*) locus for [AcB55xDBA/2]F2 females (A). The shaded area designates the Bayesian 95% confidence interval and the genome-wide thresholds are indicated at P=0.01 and P=0.05. The effect of the AcB55 (A), DBA/2 (D) or heterozygous (H) allele on parasite load is depicted for *Tccr1* (B) at the D2Mit295 peak marker and for the underlying *C5* gene (C).

validating the chromosome 2 association initially detected by EMMA analysis in 34 RCS (Figure 3), but not the more significant chromosome 6 association. In fact, detailed examination of the region underlying chromosome 6 indicated that both AcB55 and DBA/2 strains harbor similar haplotype blocks at the proximal and distal regions of chromosome 6 (data not shown) and would therefore not segregate in the analyzed F2 cross. Together, haplotype association mapping in 34 RCS along with linkage analysis in an informative F2 cross strongly suggest that *T. crassiceps* replication in the murine host is controlled by multiple genetic factors, amongst which *Tccr1* strongly contributes to the noted resistance of AcB55 mice.

Hemolytic complement (Hc/C5) underlies Tccr1. Maximum linkage for *Tccr1* locus is coupled to the *D2Mit295* marker, which lies at 29.7 Mb and was previously associated to the gene coding for hemolytic complement (*Hc/C5*) (*7*) located approximately 5 Mb further downstream (34.8-34.9 Mb). Since *C5* was mapped in an F2 cross derived from A/J and B6 strains and its deficiency correlated to high susceptibility to the fungal pathogen *Candida albicans* in the majority of RCS (*7*), we examined the involvement of *C5* in the context of *T. crassiceps* infection. We genotyped the parental AcB55 and DBA/2 strains for the deficiency-causing 2-bp deletion in the *C5* gene and confirmed that DBA/2 is C5-deficient (*543*), while AcB55 is wild type for C5 and does not harbor the deletion (*7*). C5 status was also determined in 185 female [AcB55xDBA/2] F2 mice and the parasite replication permissiveness was associated with *C5*-deficiency (Figure 5C) in a recessive manner, where mice harboring at least one functional copy of the gene are fully resistant. In addition, classifying the set of 34 RCS according to permissiveness to infection and C5 status further corroborates the association of wild-type C5 alleles with increased protection against *T. crassiceps* (Table 1).

Taken together our results suggest a critical role for the complement component 5 in restricting proliferation of *T. crassiceps* in mice.

Table 1. Phenotypic response of RCS to *T. crassiceps* infection, with respect to the C5 status.

RCS	Hc allele[a]	Parasite load (mean ± s. d.)	Phenotype[b]
BcA83	0	271.5 ± 56.6	P
BcA73	0	80.1 ± 14.2	P
BcA72	0	119.6 ± 39.1	P
BcA70	0	84.6 ± 23.2	P
AcB65	0	216.9 ±57.5	P
AcB64	0	66.9 ± 10.8	P
AcB63*	1	136.5 ± 42.4	P
AcB62	0	253.6 ± 61.1	P
AcB61	0	239.1 ± 75.5	P
AcB58	0	129.0 ± 40.2	P
AcB56	0	148.7 ± 32.4	P
AcB54	0	84.7 ± 24.7	P
AcB52	0	96.4 ± 28.0	P
AcB51	0	70.8 ± 8.8	P
A/J	0	256.1 ± 42.5	P
BcA87	1	6.6 ± 10.0	R
BcA86	1	4.5 ± 12.6	R
BcA85	1	0.3 ± 0.7	R
BcA84	1	0.8 ± 1.3	R
BcA82	1	38.1 ± 47.2	R
BcA81	1	0.5 ± 1.6	R
BcA80	1	35.8 ± 48.3	R
BcA79	1	0.4 ± 1.3	R
BcA78	1	22.9 ± 36.1	R
BcA77	1	12.6 ± 36.6	R
BcA76*	0	15.1 ± 15.7	R
BcA75	1	0.2 ± 0.6	R
BcA74	1	7.8 ± 16.9	R
BcA71	1	1.0 ± 1.8	R
BcA69	1	45.9 ± 25.0	R
BcA68	1	1.0 ± 2.0	R
BcA67	1	0.0 ± 0.0	R
BcA66	1	13.0 ± 15.4	R
B6	1	22.8 ± 21.9	R
AcB60*	0	31.2 ± 31.1	R
AcB55	1	11.7 ± 6.4	R

[a]0-C5 deficient; 1-C5 sufficient.
[b]R-restrictive; P-permissive.
*Discordant strains.

34 RCS along with A/J and B6 controls are classified as permissive (P) or restrictive (R) to *T. crassiceps* infection. Discordant strains are denoted by *.

4.5 DISCUSSION

The panel of 34 reciprocal AcB/BcA RCS has been used to map major monogenic traits (*547*, *552*) or to facilitate identification of multiple loci involved in complex trait diseases (*664*, *665*). This approach is based on the premise that unique small congenic fragments derived from the donor strain are fixed and delineated for each strain, which may allow for detection of causative haplotype by the sole study of the strain distribution pattern in relation to the phenotype of interest (*547*). Here, we have phenotyped the set of 34 RCS to study the genetic control of susceptibility to *T. crassiceps* cysticercosis (Figure 2), where the majority of AcB strains were found to be permissive for parasite replication and conversely, most of the BcA strains were deemed restrictive, similarly to progenitor strains A/J and B6, respectively. The presence of phenodeviant strains allowed us to conduct haplotype association mapping and identify significant genomic regions associated with response to infection on chromosomes 2 and 6 (Figure 3). Subsequent genome scan in informative F2 mice generated between resistant AcB55 and susceptible DBA/2 progenitors (fixed for chromosome 6 locus) identified a highly significant linkage on chromosome 2 (*Tccr1*, LOD score=4.76, P value<0.01) as conferring resistance to AcB55 in a dominant fashion along with an additional heterozygous-driven effect observed on chromosome 19 (*Tccr2*, LOD score=4.03, P value=0.05) (Figure 4 and Figure 5).

Interestingly, the *Tccr1* locus was analogous to a previously identified susceptibility locus for the fungal pathogen *Candida albicans* attributable to the complement component 5 gene (*Hc/C5*) (*7*). The complement pathway represents the initial line of defense of the innate immune system and elicits an inflammatory response to the site of infection (*254*, *567*). Activation of the complement cascade is triggered by microbial products via several pathways, which ultimately results in the activation of C3 convertase, cleavage of C5, release of chemotactic factors (C3a and C5a), and generation of the membrane attack complex (MAC) (*567*). Similarly to *T. crassiceps* infection, inbred mouse strains display various degrees of susceptibility to *C. albicans*, where A/J is highly susceptible and B6 resistant (*7*). This differential

susceptibility was attributed to the major gene *C5*, where a single allele of the wild-type C5 confers complete resistance to infection (*7*). As previously described (*543*), C5-deficiency is caused by a 2-bp deletion in the exon 6, leading to a premature stop codon and a product that is not secreted in the serum (*544*). We have confirmed that AcB55 carries the B6 allele at C5 and is therefore C5-suficient and resistant to *T. crassiceps*, whereas DBA/2 is C5-deficient and susceptible. C5 status was also determined in 185 [AcB55xDBA/2]F2 progeny (Figure 5C), where resistance segregated with one or two copies of the wild-type C5 indicating that C5 exerts an early dominant protective effect upon *T. crassiceps* infection.

In the mouse model of *T. crassiceps* infection, although the extent of parasite replication depends on the orchestration of immune and hormonal responses, the parasite restriction is initiated by the early immunological response, which was shown to destroy the peritoneal larvae (*667*) and involve the complement system in innate resistance to *T. taeniaeformis* (*668*). Earlier studies demonstrated that C3 along with IgG is deposited on larval *T. taeniaeformis* (*668*, *669*) as early as 2 days post infection, but that it is not directly involved in lytic activity through formation of the MAC. Rather, the complement system indirectly triggers host cell recognition and/or activation (*668*), leading to parasite elimination. Inhibition of complement by cobra venom factor administration to the resistant BALB/cByJ mice prior to *T. taeniaformis* infection results in decreased parasite mortality, indicating that complement component deposition and activation is necessary in host defense against taenid infection (*668*). More precisely, the role of complement component 5 (C5) was established in the mouse model of hyatid disease, caused by the *Echinococcus granulosus* cestode. C5-deficiency in B10.D2 o/SnJ mice infected with *E. granulosus* was associated with poor eosinophil infiltration and increased growth of established cysts (*670*), indicating that C5-mediated mechanisms are detrimental for parasite growth.

The immunopathology of *T. crassiceps* cysticercosis in mice is that of an initial non-permissive Th1 type, which shifts to a parasite permissive Th2 type during chronic stage of infection and is accompanied by an increase in IL-4, IL-6 and IL-10

cytokines (*671-673*). This transition was also reported in individuals with *T. solium* neurocysticercosis (*674*) and more precisely, in the brain granulomas surrounding *T. solium* parasite (*675*). Although A/J mice succumb to *C. albicans* infection early after infection (48 h), they mount a similar Th2-like cytokine storm consisting of high levels of IL-6, IL-10 and TNFα (*298*, *575*), suggesting a common role for C5 in both pathologies. In addition, animals deficient for the Th1 hallmark cytokine IFNγ or upon its neutralization exhibit increased susceptibility to *C. albicans* (*455*) and *T. crassiceps* (*672*), respectively. Regarding the role of complement in parasite damage, it is known that cysticerci are able to inhibit both classical and alternative pathways of the complement cascade, through C1q inhibition by parasite's paramyosins (*676*), but the relevance of the complement component 5 (C5) in the restrictiveness to parasite growth remains to be elucidated, especially considering that C5 is cleaved in two different active forms: C5a, which is a potent anaphylatoxin and chemotactic protein, and C5b, which has a binding site for C6 and is the molecule responsible for promoting the MAC (membrane attack complex) assembling in cell membrane. To assess the importance of C5 and possible involvement of additional genetic effects in the A/J versus B6 differential susceptibility to *T. crassiceps*, we classified the RCS according to susceptibility and C5 status (Table 1). In the majority of RCS, C5 status was a strong predictor of response to *T. crassiceps* infection with C5 deficiency causing increased parasite replication permissiveness, even when present on the B6 background as seen in BcA73, BcA70, BcA72 and BcA83 strains. Conversely, the presence of wild-type alleles at C5 on an otherwise permissive A/J background, as seen in AcB55 strain, conferred restrictiveness to infection. We noted the presence of several discordant strains (Table 1, denoted by an asterisk), such as BcA76, AcB60 and AcB63. Although C5 explains 25% of phenotypic variance, discordant strains suggest that additional susceptibility and resistance genetic factors, distinct from the dominant C5 effect, modulate response to *T. crassiceps* infection. In fact, STAT4 and STAT6 transcription factors were recently involved in modulation of the immune response to *T. crassiceps* in mice. Permissiveness of BALB/c mice was abrogated in $STAT6^{-/-}$ mice of the same background, as they were able to efficiently mount a strong Th1 response and control the infection (*677*). Conversely, Th1 response

induced via STAT4-dependent signaling pathway is essential for development of immunity against cysticercosis (*678*). Also, macrophage activation and subsequent production of nitric oxide represent additional mechanisms essential for host resistance to *T. crassiceps* infection (*679*). Interestingly, we did not uncover any associations of the MHC with susceptibility in our AcB55xDBA/2 cross where DBA/2 mice carry parasite permissive H2-d (*655*). This further suggests that the differential permissiveness observed in BALB/c susbstrains and attributed to H2-d haplotype is in fact, BALB-background specific. Similarly, the *Tccr2* locus represents a novel effect that arose upon combination of the AcB55 and DBA/2 genetic backgrounds and further emphasizes the importance of genetic modifiers in *T. crassiceps* permissiveness. Finally, generation of additional informative crosses will be necessary to validate and study the effect contributed by the chromosome 6 underlying genetic effect(s) in *T. crassiceps* cysticercosis, independently of C5 or in conjunction.

In conclusion, we have combined haplotype association mapping in 34 recombinant congenic strains and linkage analysis to identify and validate a novel locus that modulates the outcome to *T. crassiceps* infection in mice. We have demonstrated that C5 underlies the *Tccr1* locus and uncovered an important role of the complement pathway in susceptibility to *T. crassiceps* cysticercosis.

4.6 ACKNOWLEDGMENTS

The authors thank Sean Wiltshire and Silvia Vidal for helpful discussions.

4.7 SUPPLEMENTARY MATERIAL

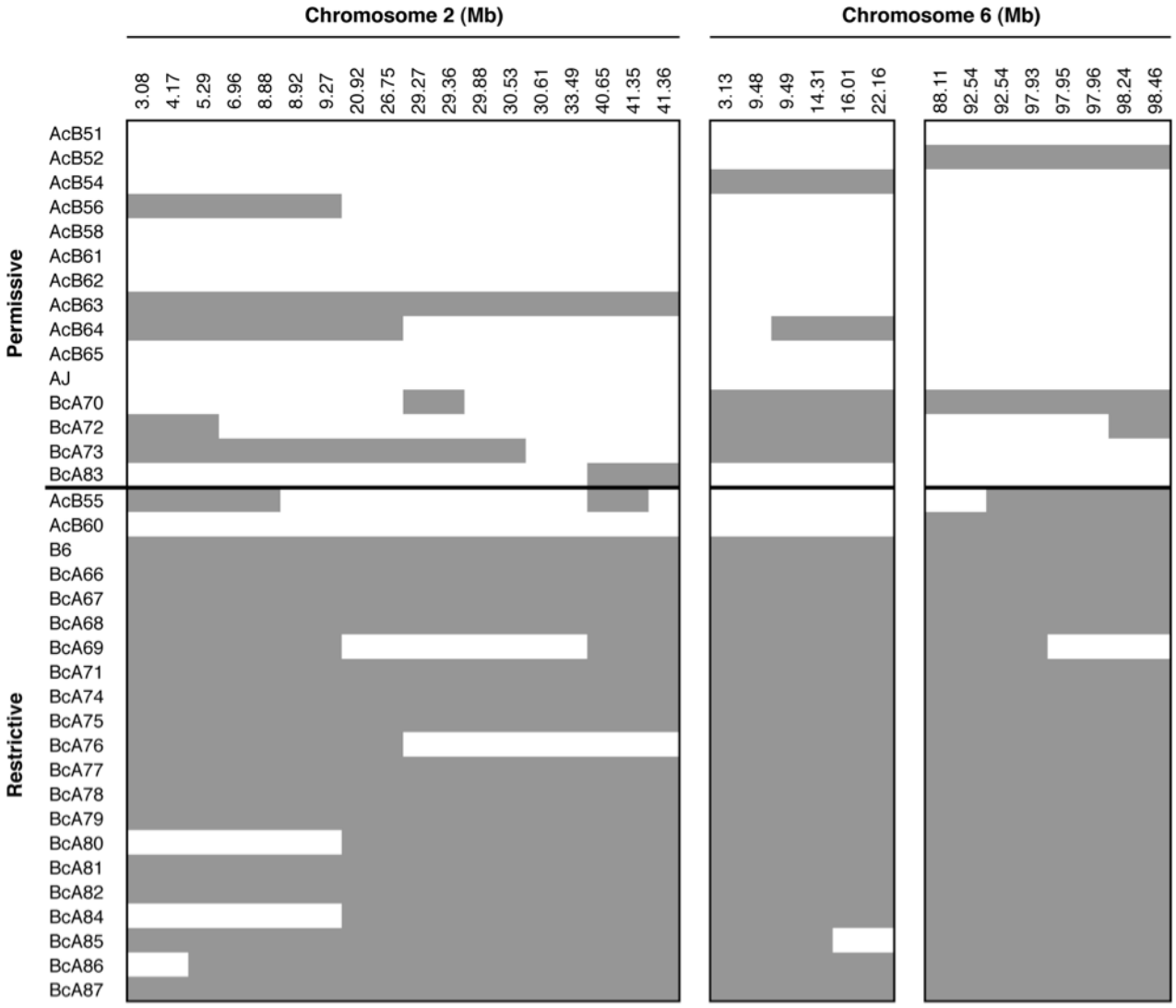

Figure S1. Haplotype maps underlying EMMA-identified chromosome 2 and chromosome 6 associations in RCS.

Haplotype maps of permissive and restrictive RCS are depicted for the most significant associations on proximal chromosome 2 along with proximal and distal regions of chromosome 6, illustrating segregation of B6 allele (gray) with restrictiveness and A/J (white) allele with permissiveness to *T. crassiceps*.

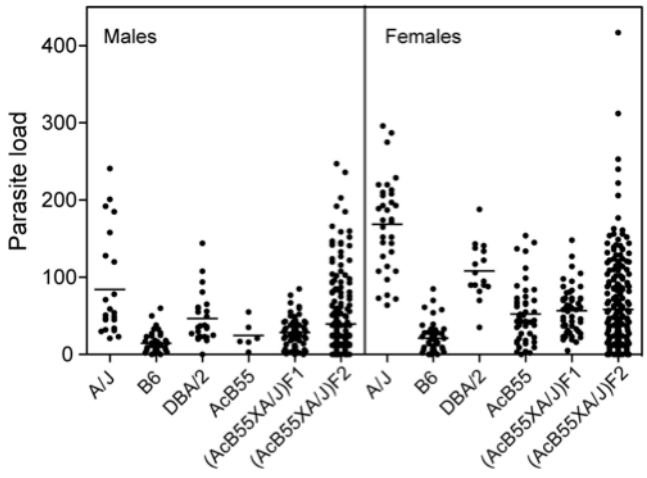

Figure S2. Parasite load in the [AcB55xA/J]F2 population.

[AcB55xA/J]F2 mice (n=427) were infected intraperitoneally with 10 non-budding *T. crassiceps* larvae and parasite number was determined 30 days post-infection. The results from three separate infections are plotted along with A/J, B6, DBA/2, and [AcB55xA/J]F1 controls.

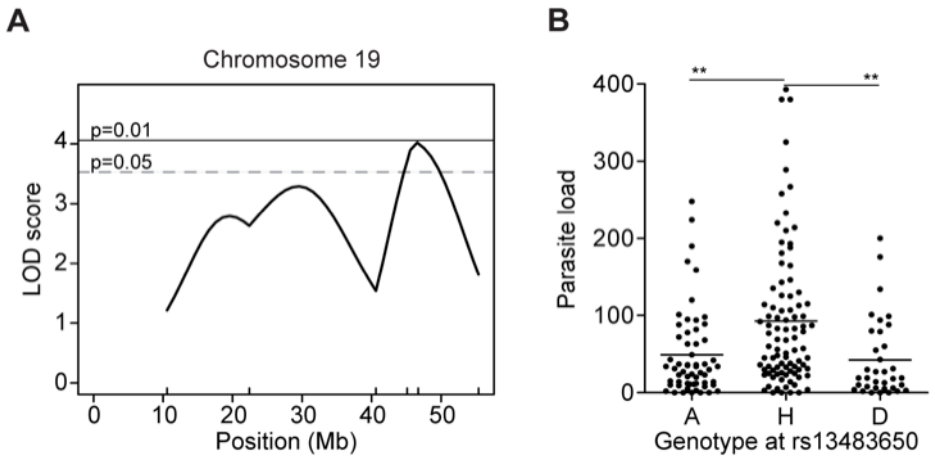

Figure S3. Effect of the *Tccr2* locus on parasite burden in [AcB55xDBA/2]F2 mice.

Detailed LOD score traces are shown for chromosome 19 (*Tccr2*) locus for [AcB55xDBA/2]F2 females (A). The genome-wide thresholds are indicated at P=0.01 and P=0.05. The heterozygous-driven permissiveness to *T. crassiceps* in F2 mice is illustrated for *Tccr2* by segregating the parasite load according to the AcB55 (A), DBA/2 (D) or heterozygous (H) alleles at the rs13483650 peak SNP (B).

Chapter 5:

Summary and future directions

5.1 Summary

Considerable efforts have been allotted to elucidate pathogenesis and the genetic component of some of the most detrimental global infectious diseases, such as malaria and tuberculosis. However, a number of other infectious and parasitic diseases remain neglected thus far. Such is the case with *C. albicans*, an opportunistic fungal commensal that causes important morbidity and mortality in immunocompromised individuals. While several genes involved in Th1 and Th17 axes have been linked to CMC (Chapter 1, Table 2; reviewed in (*42*)), the genetic component governing susceptibility to systemic candidiasis in humans remains largely undeciphered (*6*). To elucidate the genetic component underlying susceptibility to *C. albicans*, we employed an unbiased forward genetic approach as outlined in Chapters 2 and 3. Furthermore, the cestode *T. solium* is the causative agent of NC, a neglected tropical disease associated with important sequelae and the most frequent preventable cause of epilepsy in developing countries (*645*). While host genetic factors have been suspected to account for the heterogeneous development of disease in seropositive humans and pigs, complex etiology hinders their detection. In Chapter 4, we used the mouse model of intraperitoneal cysticercosis caused by the related cestode *T. crassiceps* to identify host genetic factors that regulate the establishment and proliferation of the parasite.

In Chapter 2, we explored the genetic basis for inter-strain differences in response to disseminated *C. albicans* infection by conducting a GWAS across a cohort of 23 phylogenetically distinct inbred mouse strains. In addition to the main effect of the C5 locus, we uncovered several novel putative loci that control *C. albicans* replication in the host, as inferred by the presence of discordant strains AKR/J and SM/J. C5-deficient AKR/J mice exhibited a unique resistance to infection, characterized by reduced fungal burden and increased survival, concomitant with high levels of circulating IFNγ. Linkage analysis in an informative F2 cross derived from susceptible A/J and resistant AKR/J revealed that resistance to *C. albicans* in the context of C5-deficiency is governed by loci on chromosomes 8 (*Carg3*) and 11 (*Carg4*), both *a priori* detected by GWAS. Finally, we scrutinized the

minimal genetic intervals for *Carg3* and *Carg4* for presence of positional candidates whose expression is regulated by STAT-1 in an IFNγ-dependent manner.

Furthermore, in Chapter 3, we followed up on the unusual susceptibility trait of SM/J mice, despite the presence of normally protective *C5* alleles. By performing genetic linkage analysis in [B6xSM/J]F2 animals, we demarcated distal chromosome 15 (*Carg5*) as liable for C5-independent susceptibility to disseminated *C. albicans* infection. Detailed cellular immunophenotyping of innate immune effectors revealed a pleiotropic myeloid defect in SM/J that accounts for heightened susceptibility. Notably, SM/J neutrophils displayed altered expression of Ly6G that segregated with $Carg5^{SM/J}$ alleles, concomitant with aberrant ROS. Moreover, elevated circulating CCL2 along with altered numbers and ablated function of inflammatory monocytes in SM/J mice pointed to a delayed and/or impaired response by inflammatory monocytes. Lastly, we described a novel genomic approach to catalog and prioritize positional candidates for any given locus that regulates inflammatory responses by myeloid cells.

Finally, in Chapter 4, we uncovered a novel role for C5 in the early protective inflammatory response to infection with the cestode *T. crassiceps*. Differential permissiveness to *T. crassiceps* cysticercosis in B6 and A/J mice was studied by performing haplotype association mapping in 34 AcB/BcA RCS, attributing the control of parasite replication to proximal chromosome 2. Subsequent linkage analysis in an F2 population derived from resistant AcB55 (on an otherwise susceptible background) and susceptible DBA/2 further validated this association, delineating *Tccr1* as the first *T. crassiceps* restrictive genetic locus. Surprisingly, *Tccr1* coincided with the *C5* allele, whose deficiency segregated with increased parasite load in both the AcB/BcA set and in the AcB55xDBA/2 cross.

In summary, although the work presented in this thesis dissected the genetic component of susceptibility to infection with pathogens appertaining to different kingdoms, we identified a common core requirement for C5 during the initial host immune response in addition to three novel C5-independent loci controlling fungal replication.

5.2 Limitations of the *C. albicans* mouse models

Thus far, mouse models of systemic *Candida* infection have substantially improved our understanding of the host-fungus interplay during systemic infection and presented a mainstay for testing antifungal agents and evaluating novel diagnostic tools. In order to extrapolate results obtained from preclinical mouse models to humans, it is prudent to acknowledge their potential limitations.

Until recently, it was believed that mice were not natural carriers of *C. albicans* and other human pathogenic *Candida* species (*680*). The advent of novel sequencing technologies has provided means to delineate microbial communities populating the murine gut, challenging the current paradigm (*681*, *682*). In fact, Iliev *et al.* demonstrated that the opportunistic pathogen *C. tropicalis* is one of the major constituents of the indigenous murine "mycobiome" (*682*). Whether a distinct fungal commensal signature modulates the response of each inbred mouse strain to systemic *C. albicans* infection remains to be determined. The involvement of intestinal bacterial (and/or fungal) flora is supported by the failure of gnotobiotic SCID mice to clear *C. albicans* from their kidneys following intravenous challenge compared to their counterparts raised in a conventional facility (*438*). Furthermore, non-filamentous *C. albicans* mutants, *C. glabrata*, or *C. krusei* are considered hypovirulent in the laboratory mouse (*683-685*), while the latter two cause lethal infections in severely immunocompromised patients (*686*, *687*). This raises two concerns regarding the aptness of the mouse as a model organism. The first is whether interactions occurring between the non-filamentous fungi and the human host are reproduced in the mouse model in view of such divergent outcomes. The second caveat is that *C. glabrata* and *C. krusei* may colonize a sicker cohort of individuals in the clinical setting, thereby impeding an accurate assessment of the impact of infection towards mortality in the presence of numerous confounding effects (*20*). Therefore, the use of mice may be inadequate to study virulence and dissect mechanisms of host defense against non-*albicans Candida* species.

Despite the high conservation between mouse and human genomes, there are notable physiological differences in immunity that warrant caution in interpretation of

results stemming from mouse disease models. This is precisely what Mestas and Hughes sought to accomplish in their review (*688*), whereby they compiled and described some of the most prominent immunological disparities. Of particular relevance to our systemic candidiasis model are those of the innate arm of immunity, such as the composition of peripheral blood leukocytes (*689*) and neutrophil antimicrobial agents (reviewed in (*316*, *321*)). Circulating leukocytes diverge greatly between mice and humans, with the former having a strong preponderance of lymphocytes (~75-90%) and the latter being neutrophil-rich (50-70%) (*688*, *689*). As invasive candidiasis in humans predominantly arises in the context of neutropenia or impaired neutrophil responses (*2*), it is tempting to speculate that neutrophil-biased shift in peripheral leukocytes bestows protection against invading fungal pathogens. Recently, Ermert and colleagues observed that murine neutrophils exhibit significantly reduced candidacidal activity compared to their human counterparts (*25*). The conversion to hyphal morphology, a key fungal virulence trait, and subsequent escape of *Candida* from human neutrophils are deterred by higher levels of MPO activity (*24*, *25*) and the presence of α-defensins (*25*, *325*, *690*). Indeed, neutrophils derived from knock-in *Def*$^{+/+}$ mice that express 10% of the normal human phagocyte HNP content exhibited 20-30% more enhanced killing of *C. albicans*, hence illustrating the contribution of α-defensins HNP-1 and HNP-2 in the containment of the fungus (*25*). The authors hypothesize that human neutrophils might have acquired such honed fitness as a result of coevolution with *C. albicans*, in order to maintain this opportunistic pathogen in a commensal state (*25*).

5.3 Functional characterization of *Carg3* and *Carg4*

Initially, we hypothesized that elevated levels of circulating IFNγ in infected AKR/J mice may be solely or partly responsible for resistance to *C. albicans* infection in this strain (*602*). We therefore inspected the corresponding 10 Mb regions surrounding peak markers on *Carg3* and *Carg4* for genes whose expression is regulated by STAT1 in an IFNγ-dependent manner. *Ifi35* (beneath *Carg4*) constituted a particularly interesting candidate, as it reportedly heterodimerized with B-ATF and likely prevented transcription of target genes, such as *Il17* (*52*, *597*). IL-17-producing

Th17 T cells are essential for protection against invasive (*127*, *369*) and oropharyngeal candidiasis (*482*, *484*) in the mouse, while CMC in humans arises in the setting of impaired IL-17 immunity (*31*, *488*, *598*). Therefore, we postulated that Ifi35 might play a role in antifungal defenses by modulating Th17 responses. Coincidentally, our laboratory identified an N-ethyl-N-nitrosourea (ENU)-induced mutation in *Ifi35* during a chemical mutagenesis screen for novel genes that confer protection against experimental cerebral malaria (ECM) caused by the parasite *Plasmodium berghei* ANKA (PbA). Interestingly, C5/C5a was implicated in the pathogenesis of ECM by amplifying PbA-induced inflammation and exacerbating disease, with resistance correlating with C5-deficiency (*691*). This inverse correlation between ECM and invasive candidiasis prompted us to investigate the response to invasive *C. albicans* infection in this pedigree. In fact, Ifi35 mutants displayed comparable fungal burden to that of B6 controls in all target organs (Figure A1), implying that *Ifi35* does not underlie *Carg4*. Nonetheless, any subtle contributions of genetic modifiers may be masked by the robust effect of C5 and thus go undetected in our experimental setup.

As both AKR/J and A/J mice succumb very rapidly to *C. albicans* infection, this implied that the innate immune compartment is the major denominator of host resistance in this model. Since we noted a dose-dependent increase in renal fungal burden in AKR/J mice (Chapter 2, Figure 4) and neutrophils are the predominant cellular effectors involved in antifungal immunity, we hypothesized that resistance observed in this strain stems from either a sole or combinatorial effect of enhanced granulopoiesis and/or a more potent functional competency. To this end, we undertook a kinetic study examining the capacity of A/J and AKR/J mice to restrict fungal outgrowth in the kidney (Figure A2A). Compared to their A/J counterparts, AKR/J mice contain the infection more effectively, as evidenced by the reduced fungal burden even at 6h post infection. Flow cytometric analysis of the granulocyte compartment at these time points revealed that AKR/J mice show higher neutrophil egress to the bloodstream and spleen, especially at 24h (Figure A2B and A2C). Peculiarly, AKR/J mice dispose of a larger granulocytic pool in the bone marrow at steady state, along with altered granulopoiesis and/or mobilization following

infection (Figure A2D). Interestingly, the *Carg4* locus harbors the granulocyte-colony stimulating factor gene (*csf3*), and common variants in this region are associated with white blood cell (WBC) and neutrophil counts in humans (*692-695*). As outlined earlier, G-CSF administration improved survival and restricted renal fungal outgrowth in neutropenic mice following systemic *C. albicans* infection (*360-362*). To establish whether stimulating granulopoiesis can restore resistance to *C. albicans* in A/J mice, augmentation of neutrophil counts through adoptive neutrophil transfer or treatment with recombinant G-CSF can be performed. Additionally, the peritoneal *C. albicans* infection model could yield insight into the ability and efficacy of A/J and AKR/J neutrophils to extravasate to the site of infection, as we have detected striking differences in circulating levels of the chemotactic factor KC during systemic infection (Chapter 2, Figure 5). Furthermore, a kinetic analysis of infiltrating leukocytes into the kidney may pinpoint the relative contribution of specific innate immune cell population(s) to the resistance phenotype mediated by *Carg3* and *Carg4*. To further inspect whether AKR/J mice display altered neutrophil functions, we examined ROS production upon stimulation with PMA, fMLF, and TNFα (Figure A2E). Although no difference was observed with PMA and fMLF, AKR/J neutrophils were more responsive to TNFα treatment. The effect of TNFα on neutrophils is dichotomous and dose-dependent, with lower concentrations promoting neutrophil survival, while higher concentrations induce neutrophil apoptosis (*696*, *697*). Once recruited to the site of infection where they contribute to pathogen eradication, neutrophil apoptosis launches signals for inflammation resolution and subsequent return of tissue homeostasis (reviewed in (*698-700*)). Recently, Geering and colleagues described a novel TNFα-triggered apoptosis pathway in neutrophils, where phosphoinositide 3-kinase (PI3K)-mediated ROS production represents the key event in limiting cell survival and triggering programmed cell death (*701*). Because A/J mice exhibit a hyperinflammatory state concomitant with prominent tissue damage following *C. albicans* infection (*298*, *602*), as well as curtailed TNFα-induced ROS production compared to AKR/J mice (Figure A2E), it is plausible that AKR/J neutrophils undergo apoptosis more readily than their A/J counterparts. Elevated ROS generation in TNFα-stimulated AKR/J neutrophils might, in addition

to clearing *Candida*, attenuate inflammation by a) inhibiting further neutrophil recruitment, b) preventing the release of histotoxic contents from dying cells, or c) ensuring appropriate disposal of phagocytosed cargo. Assessment of phagocytic and killing capacities of neutrophils may further delineate the precise cellular mechanism of resistance observed in the AKR/J strain.

Together with neutrophils, monocytes and macrophages collaborate and orchestrate the onset, progression, and resolution of inflammation (reviewed in (*702*)). In mice, both inflammatory and resident subsets of monocytes play important roles in host defense against systemic infection (*405*, *406*), with the former conferring an essential antifungal role in the first 48 hours following challenge (*405*). In Chapter 3, we also show that reduced or delayed recruitment of these cells to the kidney, along with diminished ROS production in BMDM, governs susceptibility in the SM/J strain (*703*). Spatiotemporal examination of inflammatory monocyte proportions in A/J and AKR/J (Figure A3) revealed modest perturbations. Notably, AKR/J mice exhibited a rise in monocyte numbers in the spleen (Figure A3B) at 6h and 24h, while A/J mice failed to recruit monocytes altogether throughout the course of the infection. In fact, Swirski *et al.* recently identified spleen as a monocyte reservoir in mice, allowing rapid deployment in case of emergency (*704*). Moreover, egress from the bone marrow is comparable until 24h, where AKR/J mice appear to cease monocyte egress and/or stimulate monopoiesis compared with A/J (Figure A3C). Thus far, our experimental framework does not preclude a role for monocyte infiltration in the kidney nor any functional disparity in the differential response of both investigated strains to disseminated *C. albicans* infection. Anticipating a potential role for these phagocytes in our disease model, particularly since AKR/J mice exhibit high IFNγ in serum, we applied the methodology utilized in Chapter 3 and computed a myeloid inflammatory score for each gene under entire *Carg3* and *Carg4* intervals (Figure A4A and A4B, respectively). Although we did perform a similar exercise *a priori* to nominate candidate genes in these intervals, the current improved analysis relies on a) data arising from primary BMDM rather than immortalized HeLa cells, b) ChIP-seq for IRF8, IRF1, STAT1, and NFkB (p65) DNA-binding, compared to solely STAT1, c) RNA-seq for expression profiling following IFNγ treatment, compared to

microarray-based methodology, and d) a newly devised formula integrating the number, height, and proximity to gene transcriptional start sites of ChIP-seq peaks for each transcription factor, mRNA expression, and IFNγ-responsiveness, for a total "Myeloid Inflammatory Score" (*703*).

Within the *Carg3* genetic interval, *prdx2* and *il15* rank amongst the ten most significant positional candidates. Peroxiredoxins are thiol-based peroxidases with dual functionality as both cytoprotective antioxidants and regulators of H_2O_2-mediated signal transduction (*705*). Prdx1 (*706*) and Prdx2 (*707*) were shown to reduce intracellular ROS in response to oxidants and growth factors, respectively, while overexpression of Prdx2 inhibited TNFα- or H_2O_2-induced NFkB activation (*707*). Recently, Sobotta and colleagues demonstrated that Prdx2 acts as an ultrasensitive H_2O_2 receptor, catalyzing transient oxidization and oligomeric assembly of STAT3, which is compromised in transcriptional activity (*708*). In the context of LPS-stimulation, macrophages release glutathionylated Prdx2, which in turn acts as a danger signal and triggers TNFα production in macrophages (*709*). With respect to the resistance trait in AKR/J mice, increased Prdx2 levels could potentially dampen cellular ROS, attenuate STAT3-dependent inflammatory responses and favor resolution of inflammation. The pleiotropic cytokine IL-15 was identified on the basis of functional similarity to IL-2 in its ability to promote T cell and NK cell proliferation (*710*, *711*). As aforementioned, IL-15 is a potent stimulator of the respiratory burst and antifungal activities of neutrophils (*344*) and monocytes (*392*). Aside from directly inhibiting *C. albicans* growth (*338*, *425*), *in vitro* and *in vivo* studies have shown that NK cells represent an important source of IFNγ and TNFα (*399*, *428*, *429*), further potentiating candidacidal functions of phagocytic cells. Therefore, it is tempting to speculate that high IFNγ levels in circulation of AKR/J mice lead to enhanced transcriptional activation and translation of *il15*, thereby promoting fungal clearance through NK cells, neutrophils, or monocytes.

Other likely positional candidates underlying *Carg4* include chemokines CCL2 and CCL7, which constitute the predominant CCR2 ligands involved in mobilization of inflammatory monocytes from the bone marrow (*612*, *622*, *712*).

Also, both CCL2 and CCL7 are required for an optimal innate immune defense against *Listeria monocytogenes* (*713*), while early induction of CCL7, but not CCL2, contributes to optimal immunity against *C. neoformans* (*714*). Peculiarly, infected AKR/J mice did not upregulate CCL2 compared to both B6 and A/J controls (Chapter 2, Figure 5), albeit earlier timepoints prior to 48h were not examined. While faster recruitment of inflammatory monocytes to sites of infection may aid fungal clearance, inadequate CCL2 production by endothelial cells and macrophages in the context of C5 deficiency may in fact limit unrestricted hyperinflammation in AKR/J mice.

Collectively, these data support the notion that AKR/J mice exhibit a highly efficacious and controlled inflammatory response that leads to rapid fungal clearance while constraining tissue damage.

5.4 The role of C5 in *T. crassiceps* infection

The work outlined in Chapter 4 revealed that C5 and the complement pathway play a decisive role in the onset of a protective inflammatory response to infection with the cestode *T. crassiceps* (*715*). To ascertain that C5 was the causal gene underlying the *Tccr1* locus, we assessed parasite load in C5-sufficient and C5-deficient B10.D2 congenic mice (B10.D2-Hc^1 and B10.D2-Hc^0, respectively) following *T. crassiceps* infection (Figure A5). Indeed, C5 deficiency provided a permissive environment for unrestricted parasite replication, resulting in threefold higher parasite numbers than in C5-sufficient counterparts. The common requirement for C5 in both *C. albicans* and *T. crassiceps* infections argues for analogous innate immune pathways controlling host resistance to these eukaryotic pathogens. Earlier studies showed that opsonization by C3 and IgG, rather than MAC-mediated lysis of the larvae, are essential for subsequent immune cell infiltration and parasite containment (*668*, *669*). Kinetic examination of immunological changes in subcutaneous *T. crassiceps* cysticercosis in resistant B6 mice revealed granuloma formation at the site of inoculation, composed of neutrophils and macrophages (*716*). The signature Th1 cytokine IFNγ mediates parasite restriction throughout the course of infection (*672*), possibly by enhancing antiparasitic phagocyte functions. Although

this hypothesis remains to be experimentally validated, concordant mechanisms have been reported during invasive candidiasis.

Emerging evidence suggests that γδ-T cells are key players during cysticercosis, with opposing roles that are contingent on the anatomical site of infection. Intracranial infection with the *T. solium*-related cestode *Mesocestoides corti* in susceptible BALB/c mice revealed a predominant accumulation of pathologic γδ-T cells in the CNS (*717*). It is now recognized that γδ-T cells are the major initial IL-17 producers in acute infection ((*480*), reviewed in (*718*)). Accordingly, γδ-T cell-deficient mice exhibited reduced neurological symptoms, immunopathology, and low levels of mixed Th1/Th2 cytokines (*719*). In the peritoneal *T. crassiceps* cysticercosis model, splenocytes from resistant STAT6$^{-/-}$ animals exhibit a proinflammatory Th1/Th17 profile in ex vivo stimulation compared to susceptible controls (*679*), suggesting involvement of γδ-T cells in parasite restriction. Interestingly, recent findings underscore a complex role for C5 in the regulation of adaptive immune responses. Notably, deficiency in C5aR signaling abolished Th17 cell differentiation and expansion in several experimental models of autoimmunity (*720*, *721*). Along this line, mice deficient in both C3aR and C5aR show impaired T cell activation, decreased viability (*722*), and compromised Th1 or Th17 differentiation (*721*). Strainic and colleagues recently reported that in the absence of anaphylatoxin-mediated signaling, CD4^{+} cells perpetuate TGF-β1 signaling leading to Foxp3^{+} expression and iTreg formation (*723*). Hence, we can presume that in the context of *T. crassiceps* cysticercosis, C5 deficiency has a pronounced pleiotropic effect impeding on opsonization, curtailing innate immune responses, and promoting an anti-inflammatory iTreg induction.

5.4 Final conclusions

Forward genetic analysis represents an unbiased approach toward dissecting complex traits and uncovering novel host genetic modifiers linked to a given phenotypic observation. Since the 90s, nearly 5000 quantitative trait loci (QTLs) have been uncovered for an assortment of phenotypes, while only a fraction of these have

been characterized at the molecular level. This sluggish rate of discovery commands the use of complementary approaches to refine gene-rich regions and prioritize putative candidate genes. For instance, the advent of flow cytometry provides a means for detailed immunophenotyping in virtually any organ, providing a spatiotemporal stance of the intricate host-pathogen interactions occurring in the context of infection. Once the relevant cellular subset is pinpointed, novel genomic approaches such as ChIP-seq and RNA-seq along with publically available datasets can be harnessed to compute a rank/score of relevance for each gene underlying a QTL. As demonstrated in this thesis, the Myeloid Inflammatory Score proved to be an elegant mode of classifying genes for further functional analysis. This methodology allowed us to uncover several genetic modifiers controlling resistance or susceptibility to *C. albicans* independently of C5, a chief component of complement activation. Identification of a common requirement for C5 in the diametrically divergent cestode *T. crassiceps* allowed us to extrapolate and merge findings, with the greater aim of bettering our understanding of both pathologies.

ORIGINAL CONTRIBUTIONS TO KNOWLEDGE

1. Genome-wide association mapping (GWAS) in 23 inbred mouse strains uncovered novel associations controlling fungal replication in the host on chromosomes 1, 4, 6, 7, 8, 11, 12, and 15.

2. Resistance to *C. albicans* in the C5-deficient AKR/J strain is regulated by a two-locus system on chromosomes 8 (*Carg3*) and 11 (*Carg4*), previously identified by GWAS.

3. Increased susceptibility to *C. albicans* in C5-sufficient SM/J mice is linked to a locus on distal chromosome 15 (*Carg5*) that correlates with a pleiotropic myeloid defect in these mice.

4. *Hc/C5* underlies the *Tccr1* locus and is responsible for the differential permissiveness to *T. crassiceps* cysticercosis in B6 and A/J mice, uncovering an important role of the complement pathway in susceptibility to cestode infection.

REFERENCES

1. M. Morrell, V. J. Fraser, M. H. Kollef, Delaying the Empiric Treatment of Candida Bloodstream Infection until Positive Blood Culture Results Are Obtained: a Potential Risk Factor for Hospital Mortality. *Antimicrobial Agents and Chemotherapy* **49**, 3640–3645 (2005).

2. M. A. Pfaller, D. J. Diekema, Epidemiology of invasive candidiasis: a persistent public health problem. *Clin. Microbiol. Rev.* **20**, 133–163 (2007).

3. P. Eggimann, J. Garbino, D. Pittet, Epidemiology of Candida species infections in critically ill non-immunosuppressed patients. *Lancet Infect Dis* **3**, 685–702 (2003).

4. P. Muñoz, A. Burillo, E. Bouza, Criteria used when initiating antifungal therapy against Candida spp. in the intensive care unit. *Int. J. Antimicrob. Agents* **15**, 83–90 (2000).

5. N. Yapar, Epidemiology and risk factors for invasive candidiasis. *Ther Clin Risk Manag* **10**, 95–105 (2014).

6. E. O. Glocker *et al.*, A homozygous CARD9 mutation in a family with susceptibility to fungal infections. *N. Engl. J. Med.* **361**, 1727–1735 (2009).

7. A. Tuite, M. Elias, S. Picard, A. Mullick, P. Gros, Genetic control of susceptibility to Candida albicans in susceptible A/J and resistant C57BL/6J mice. *Genes Immun* **6**, 672–682 (2005).

8. S. V. Tsoni *et al.*, Complement C3 plays an essential role in the control of opportunistic fungal infections. *Infect. Immun.* **77**, 3679–3685 (2009).

9. R. B. Ashman, E. M. Bolitho, J. M. Papadimitriou, Patterns of resistance to Candida albicans in inbred mouse strains. *Immunol Cell Biol* **71 (Pt 3)**, 221–225 (1993).

10. R. B. Ashman, A. Fulurija, J. M. Papadimitriou, Strain-dependent differences in host response to Candida albicans infection in mice are related to organ susceptibility and infectious load. *Infection and Immunity* **64**, 1866–1869 (1996).

11. R. B. Ashman, A gene (Carg1) that regulates tissue resistance to Candida albicans maps to chromosome 14 of the mouse. *Microb. Pathog.* **25**, 333–335 (1998).

12. R. B. Ashman, A. Fulurija, J. M. Papadimitriou, A second Candida albicans resistance gene (Carg2) regulates tissue damage, but not fungal clearance, in sub-lethal murine systemic infection. *Microb. Pathog.* **25**, 349–352 (1998).

13. C. Mora, D. P. Tittensor, S. Adl, A. G. B. Simpson, B. Worm, How many species are there on Earth and in the ocean? *Plos Biol* **9**, e1001127 (2011).

14. D. L. Hawksworth, The fungal dimension of biodiversity: magnitude, significance, and conservation. *Mycological research* (1991).

15. D. L. Hawksworth, The magnitude of fungal diversity: the 1.5 million species estimate revisited. *Mycological research* (2001).

16. M. Blackwell, The fungi: 1, 2, 3 ... 5.1 million species? *Am. J. Bot.* **98**, 426–438 (2011).

17. L. H. Taylor, S. M. Latham, M. E. Woolhouse, Risk factors for human disease emergence. *Philos. Trans. R. Soc. Lond., B, Biol. Sci.* **356**, 983–989 (2001).

18. F. L. Mayer, D. Wilson, B. Hube, Candida albicans pathogenicity mechanisms. *Virulence* **4**, 119–128 (2013).

19. F. C. Odds, *Candida and Candidosis* (W B Saunders Company, 1988).

20. R. A. Calderone, C. J. Clancy, Eds., *Candida and Candidiasis* (ASM Press, Washington, DC, USA, ed. 2, 2011).

21. P. G. Pappas, Invasive candidiasis. *Infect. Dis. Clin. North Am.* **20**, 485–506 (2006).

22. D. Diekema, S. Arbefeville, L. Boyken, J. Kroeger, M. Pfaller, The changing epidemiology of healthcare-associated candidemia over three decades. *Diagn. Microbiol. Infect. Dis.* **73**, 45–48 (2012).

23. R. E. Lewis, Overview of the changing epidemiology of candidemia. *Curr Med Res Opin* **25**, 1732–1740 (2009).

24. P. G. Rausch, T. G. Moore, Granule enzymes of polymorphonuclear neutrophils: A phylogenetic comparison. *Blood* **46**, 913–919 (1975).

25. D. Ermert *et al.*, Candida albicans escapes from mouse neutrophils. *Journal of Leukocyte Biology* **94**, 223–236 (2013).

26. Y. M. Clayton, W. C. Noble, Observations on the epidemiology of Candida albicans. *J. Clin. Pathol.* **19**, 76–78 (1966).

27. R. Hurley, J. De Louvois, Candida vaginitis. *Postgrad Med J* **55**, 645–647 (1979).

28. M.-E. Bougnoux *et al.*, Multilocus sequence typing reveals intrafamilial transmission and microevolutions of Candida albicans isolates from the human digestive tract. *Journal of Clinical Microbiology* **44**, 1810–1820 (2006).

29. J. D. Sobel, Vulvovaginal candidosis. *Lancet* **369**, 1961–1971 (2007).

30. A. Puel *et al.*, Inborn errors of human IL-17 immunity underlie chronic mucocutaneous candidiasis. *Curr Opin Allergy Clin Immunol* **12**, 616–622 (2012).

31. A. Puel *et al.*, Chronic mucocutaneous candidiasis in humans with inborn errors of interleukin-17 immunity. *Science* **332**, 65–68 (2011).

32. C. Antachopoulos, T. J. Walsh, E. Roilides, Fungal infections in primary immunodeficiencies. *Eur. J. Pediatr.* **166**, 1099–1117 (2007).

33. D. C. Vinh, Insights into human antifungal immunity from primary immunodeficiencies. *Lancet Infect Dis* **11**, 780–792 (2011).

34. G. T. Cole, A. A. Halawa, E. J. Anaissie, The role of the gastrointestinal tract in hematogenous candidiasis: from the laboratory to the bedside. *Clin Infect Dis* **22 Suppl 2**, S73–88 (1996).

35. P. G. Pappas *et al.*, A prospective observational study of candidemia: epidemiology, therapy, and influences on mortality in hospitalized adult and pediatric patients. *Clin Infect Dis* **37**,

634–643 (2003).

36. M. M. McNeil *et al.*, Trends in mortality due to invasive mycotic diseases in the United States, 1980-1997. *Clin Infect Dis* **33**, 641–647 (2001).

37. C. Lass-Flörl, The changing face of epidemiology of invasive fungal disease in Europe. *Mycoses* **52**, 197–205 (2009).

38. R. C. Spencer, Predominant pathogens found in the European Prevalence of Infection in Intensive Care Study. *Eur. J. Clin. Microbiol. Infect. Dis.* **15**, 281–285 (1996).

39. H. Wisplinghoff *et al.*, Nosocomial bloodstream infections in US hospitals: analysis of 24,179 cases from a prospective nationwide surveillance study. *Clin Infect Dis* **39**, 309–317 (2004).

40. R. P. Wenzel, C. Gennings, Bloodstream infections due to Candida species in the intensive care unit: identifying especially high-risk patients to determine prevention strategies. *Clin Infect Dis* **41 Suppl 6**, S389–93 (2005).

41. T. S. Plantinga *et al.*, Human genetic susceptibility to Candida infections. *Med. Mycol.* **50**, 785–794 (2012).

42. S. P. Smeekens, F. L. van de Veerdonk, B. J. Kullberg, M. G. Netea, Genetic susceptibility to Candida infections. *EMBO Mol Med* **5**, 805–813 (2013).

43. M. F. Parry *et al.*, Myeloperoxidase deficiency: prevalence and clinical significance. *Ann Intern Med* **95**, 293–301 (1981).

44. C. Marchetti, P. Patriarca, G. P. Solero, F. E. Baralle, M. Romano, Genetic characterization of myeloperoxidase deficiency in Italy. *Hum. Mutat.* **23**, 496–505 (2004).

45. T. K. Rudolph *et al.*, Myeloperoxidase deficiency preserves vasomotor function in humans. *Eur. Heart J.* **33**, 1625–1634 (2012).

46. W. M. Nauseef, S. Brigham, M. Cogley, Hereditary myeloperoxidase deficiency due to a missense mutation of arginine 569 to tryptophan. *J Biol Chem* **269**, 1212–1216 (1994).

47. M. Romano *et al.*, Biochemical and molecular characterization of hereditary myeloperoxidase deficiency. *Blood* **90**, 4126–4134 (1997).

48. F. R. DeLeo, M. Goedken, S. J. McCormick, W. M. Nauseef, A novel form of hereditary myeloperoxidase deficiency linked to endoplasmic reticulum/proteasome degradation. *J Clin Invest* **101**, 2900–2909 (1998).

49. A. S. Persad, Y. Kameoka, S. Kanda, Y. Niho, K. Suzuki, Arginine to cysteine mutation (R499C) found in a Japanese patient with complete myeloperoxidase deficiency. *Gene Expr.* **13**, 67–71 (2006).

50. M. Goedken *et al.*, Impact of two novel mutations on the structure and function of human myeloperoxidase. *J Biol Chem* **282**, 27994–28003 (2007).

51. Y. Y. Ohashi *et al.*, Novel missense mutation found in a Japanese patient with myeloperoxidase deficiency. *Gene* **327**, 195–200 (2004).

52. X. Wang, L. M. Johansen, H. J. Tae, E. J. Taparowsky, IFP 35 forms complexes with B-

ATF, a member of the AP1 family of transcription factors. *Biochem. Biophys. Res. Commun.* **229**, 316–322 (1996).

53. S. E. Salmon, M. J. Cline, J. Schultz, R. I. Lehrer, Myeloperoxidase Deficiency. *N. Engl. J. Med.* **282**, 250–253 (1970).

54. K. D. Metzler *et al.*, Myeloperoxidase is required for neutrophil extracellular trap formation: implications for innate immunity. *Blood* **117**, 953–959 (2011).

55. R. I. Lehrer, M. J. Cline, Interaction of Candida albicans with human leukocytes and serum. *J. Bacteriol.* **98**, 996–1004 (1969).

56. R. I. Lehrer, J. Hanifin, M. J. Cline, Defective bactericidal activity in myeloperoxidase-deficient human neutrophils. *Nature* **223**, 78–79 (1969).

57. R. I. Lehrer, M. J. Cline, Leukocyte myeloperoxidase deficiency and disseminated candidiasis: the role of myeloperoxidase in resistance to Candida infection. *J Clin Invest* **48**, 1478–1488 (1969).

58. R. I. Lehrer, Measurement of candidacidal activity of specific leukocyte types in mixed cell populations I. Normal, myeloperoxidase-deficient, and chronic granulomatous disease neutrophils. *Infection and Immunity* **2**, 42–47 (1970).

59. Y. Aratani *et al.*, Severe impairment in early host defense against Candida albicans in mice deficient in myeloperoxidase. *Infection and Immunity* **67**, 1828–1836 (1999).

60. Y. Aratani *et al.*, Critical role of myeloperoxidase and nicotinamide adenine dinucleotide phosphate-oxidase in high-burden systemic infection of mice with Candida albicans. *J. Infect. Dis.* **185**, 1833–1837 (2002).

61. P. Cech, A. Papathanassiou, G. Boreux, P. Roth, P. A. Miescher, Hereditary myeloperoxidase deficiency. *Blood* **53**, 403–411 (1979).

62. P. Cech, H. Stalder, J. J. Widmann, A. Rohner, P. A. Miescher, Leukocyte myeloperoxidase deficiency and diabetes mellitus associated with Candida albicans liver abscess. *Am. J. Med.* **66**, 149–153 (1979).

63. J. A. Winkelstein *et al.*, Chronic granulomatous disease. Report on a national registry of 368 patients. *Medicine (Baltimore)* **79**, 155–169 (2000).

64. R. A. Bridges, H. Berendes, A. H. Good, A fatal granulomatous disease of childhood; the clinical, pathological, and laboratory features of a new syndrome. *AMA J Dis Child* **97**, 387–408 (1959).

65. B. Holmes, P. G. Quie, D. B. Windhorst, R. A. GOOD, Fatal granulomatous disease of childhood. An inborn abnormality of phagocytic function. *Lancet* **1**, 1225–1228 (1966).

66. P. G. Quie, J. G. White, B. Holmes, R. A. GOOD, In vitro bactericidal capacity of human polymorphonuclear leukocytes: diminished activity in chronic granulomatous disease of childhood. *J Clin Invest* **46**, 668–679 (1967).

67. P. G. Quie, E. L. Kaplan, A. R. Page, F. L. Gruskay, S. E. Malawista, Defective polymorphonuclear-leukocyte function and chronic granulomatous disease in two female children. *N. Engl. J. Med.* **278**, 976–980 (1968).

68. R. I. Lehrer, The fungicidal mechanisms of human monocytes. I. Evidence for myeloperoxidase-linked and myeloperoxidase-independent candidacidal mechanisms. *J Clin Invest* **55**, 338–346 (1975).

69. B. H. Segal, T. L. Leto, J. I. Gallin, H. L. Malech, S. M. Holland, Genetic, biochemical, and clinical features of chronic granulomatous disease. *Medicine (Baltimore)* **79**, 170–200 (2000).

70. P. G. Heyworth, A. R. Cross, J. T. Curnutte, Chronic granulomatous disease. *Current Opinion in Immunology* **15**, 578–584 (2003).

71. C. Kannengiesser *et al.*, Molecular epidemiology of chronic granulomatous disease in a series of 80 kindreds: identification of 31 novel mutations. *Hum. Mutat.* **29**, E132–49 (2008).

72. J. D. Matute *et al.*, A new genetic subgroup of chronic granulomatous disease with autosomal recessive mutations in p40 phox and selective defects in neutrophil NADPH oxidase activity. *Blood* **114**, 3309–3315 (2009).

73. P. R. Taylor *et al.*, Dectin-1 is required for beta-glucan recognition and control of fungal infection. *Nature Publishing Group* **8**, 31–38 (2007).

74. O. Gross *et al.*, Card9 controls a non-TLR signalling pathway for innate anti-fungal immunity. *Nature* **442**, 651–656 (2006).

75. A. Drewniak *et al.*, Invasive fungal infection and impaired neutrophil killing in human CARD9 deficiency. *Blood* **121**, 2385–2392 (2013).

76. C. Gavino *et al.*, CARD9 deficiency and spontaneous central nervous system candidiasis: complete clinical remission with GM-CSF therapy. *Clin Infect Dis* (2014), doi:10.1093/cid/ciu215.

77. F. Lanternier *et al.*, Deep dermatophytosis and inherited CARD9 deficiency. *N. Engl. J. Med.* **369**, 1704–1714 (2013).

78. L. de Beaucoudrey *et al.*, Revisiting human IL-12Rβ1 deficiency: a survey of 141 patients from 30 countries. *Medicine (Baltimore)* **89**, 381–402 (2010).

79. E. van de Vosse *et al.*, IL-12Rβ1 deficiency: mutation update and description of the IL12RB1 variation database. *Hum. Mutat.* **34**, 1329–1339 (2013).

80. M. Ouederni *et al.*, Clinical Features of Candidiasis in Patients With Inherited Interleukin 12 Receptor β1 Deficiency. *Clin Infect Dis* **58**, 204–213 (2014).

81. G. Trinchieri, S. Pflanz, R. A. Kastelein, The IL-12 family of heterodimeric cytokines: new players in the regulation of T cell responses. *Immunity* **19**, 641–644 (2003).

82. C. Fieschi *et al.*, Low penetrance, broad resistance, and favorable outcome of interleukin 12 receptor beta1 deficiency: medical and immunological implications. *J Exp Med* **197**, 527–535 (2003).

83. T. Korn, E. Bettelli, M. Oukka, V. K. Kuchroo, IL-17 and Th17 Cells. *Annu. Rev. Immunol.* **27**, 485–517 (2009).

84. L. de Beaucoudrey *et al.*, Mutations in STAT3 and IL12RB1 impair the development of human IL-17-producing T cells. *Journal of Experimental Medicine* **205**, 1543–1550 (2008).

85. N. A. R. Gow, F. L. van de Veerdonk, A. J. P. Brown, M. G. Netea, Candida albicans morphogenesis and host defence: discriminating invasion from colonization. *Nat Rev Micro* **10**, 112–122 (2011).

86. J. R. Naglik, D. L. Moyes, B. Wächtler, B. Hube, Candida albicans interactions with epithelial cells and mucosal immunity. *Microbes Infect* **13**, 963–976 (2011).

87. A. J. P. Brown, G. D. Brown, M. G. Netea, N. A. R. Gow, Metabolism impacts upon Candida immunogenicity and pathogenicity at multiple levels. *Trends Microbiol.* (2014), doi:10.1016/j.tim.2014.07.001.

88. A. N. Zelensky, J. E. Gready, The C-type lectin-like domain superfamily. *FEBS J.* **272**, 6179–6217 (2005).

89. A. M. Kerrigan, G. D. Brown, C-type lectins and phagocytosis. *Immunobiology* **214**, 562–575 (2009).

90. D. Sancho, C. Reis e Sousa, Signaling by myeloid C-type lectin receptors in immunity and homeostasis. *Annu. Rev. Immunol.* **30**, 491–529 (2012).

91. K. Ariizumi *et al.*, Identification of a novel, dendritic cell-associated molecule, dectin-1, by subtractive cDNA cloning. *J Biol Chem* **275**, 20157–20167 (2000).

92. G. D. Brown, S. Gordon, Immune recognition. A new receptor for beta-glucans. *Nature* **413**, 36–37 (2001).

93. A. S. Palma *et al.*, Ligands for the beta-glucan receptor, Dectin-1, assigned using "designer" microarrays of oligosaccharide probes (neoglycolipids) generated from glucan polysaccharides. *J Biol Chem* **281**, 5771–5779 (2006).

94. M. J. Janusz, K. F. Austen, J. K. Czop, Phagocytosis of heat-killed blastospores of Candida albicans by human monocyte beta-glucan receptors. *Immunology* **65**, 181–185 (1988).

95. J. Giaimis *et al.*, Both mannose and beta-glucan receptors are involved in phagocytosis of unopsonized, heat-killed Saccharomyces cerevisiae by murine macrophages. *Journal of Leukocyte Biology* **54**, 564–571 (1993).

96. P. R. Taylor *et al.*, The beta-glucan receptor, dectin-1, is predominantly expressed on the surface of cells of the monocyte/macrophage and neutrophil lineages. *J Immunol* **169**, 3876–3882 (2002).

97. B. Martin, K. Hirota, D. J. Cua, B. Stockinger, M. Veldhoen, Interleukin-17-producing gammadelta T cells selectively expand in response to pathogen products and environmental signals. *Immunity* **31**, 321–330 (2009).

98. J. A. Willment *et al.*, The human beta-glucan receptor is widely expressed and functionally equivalent to murine Dectin-1 on primary cells. *Eur. J. Immunol.* **35**, 1539–1547 (2005).

99. J. A. Willment *et al.*, Dectin-1 expression and function are enhanced on alternatively activated and GM-CSF-treated macrophages and are negatively regulated by IL-10, dexamethasone, and lipopolysaccharide. *J Immunol* **171**, 4569–4573 (2003).

100. G. D. Brown *et al.*, Dectin-1 mediates the biological effects of beta-glucans. *J Exp Med* **197**, 1119–1124 (2003).

101. N. C. Rogers *et al.*, Syk-dependent cytokine induction by Dectin-1 reveals a novel pattern recognition pathway for C type lectins. *Immunity* **22**, 507–517 (2005).

102. B. N. Gantner, R. M. Simmons, S. J. Canavera, S. Akira, D. M. Underhill, Collaborative induction of inflammatory responses by dectin-1 and Toll-like receptor 2. *J Exp Med* **197**, 1107–1117 (2003).

103. D. M. Underhill, E. Rossnagle, C. A. Lowell, R. M. Simmons, Dectin-1 activates Syk tyrosine kinase in a dynamic subset of macrophages for reactive oxygen production. *Blood* **106**, 2543–2550 (2005).

104. A. D. Kennedy *et al.*, Dectin-1 promotes fungicidal activity of human neutrophils. *Eur. J. Immunol.* **37**, 467–478 (2007).

105. M. Donini, E. Zenaro, N. Tamassia, S. Dusi, NADPH oxidase of human dendritic cells: role in Candida albicans killing and regulation by interferons, dectin-1 and CD206. *Eur. J. Immunol.* **37**, 1194–1203 (2007).

106. S. Saijo *et al.*, Dectin-1 is required for host defense against Pneumocystis carinii but not against Candida albicans. *Nature Publishing Group* **8**, 39–46 (2007).

107. S. LeibundGut-Landmann *et al.*, Syk- and CARD9-dependent coupling of innate immunity to the induction of T helper cells that produce interleukin 17. *Nature Publishing Group* **8**, 630–638 (2007).

108. S. I. Gringhuis *et al.*, Dectin-1 directs T helper cell differentiation by controlling noncanonical NF-kappaB activation through Raf-1 and Syk. *Nat Immunol* **10**, 203–213 (2009).

109. D. Strasser *et al.*, Syk kinase-coupled C-type lectin receptors engage protein kinase C-σ to elicit Card9 adaptor-mediated innate immunity. *Immunity* **36**, 32–42 (2012).

110. H. S. Goodridge, R. M. Simmons, D. M. Underhill, Dectin-1 Stimulation by Candida albicans Yeast or Zymosan Triggers NFAT Activation in Macrophages and Dendritic Cells. *The Journal of Immunology* **178**, 3107–3115 (2007).

111. M. B. Greenblatt, A. Aliprantis, B. Hu, L. H. Glimcher, Calcineurin regulates innate antifungal immunity in neutrophils. *Journal of Experimental Medicine* **207**, 923–931 (2010).

112. O. Gross *et al.*, Syk kinase signalling couples to the Nlrp3 inflammasome for anti-fungal host defence. *Nature* **459**, 433–436 (2009).

113. A. G. Hise *et al.*, An essential role for the NLRP3 inflammasome in host defense against the human fungal pathogen Candida albicans. *Cell Host and Microbe* **5**, 487–497 (2009).

114. S. I. Gringhuis *et al.*, Dectin-1 is an extracellular pathogen sensor for the induction and processing of IL-1β via a noncanonical caspase-8 inflammasome. *Nat Immunol* **13**, 246–254 (2012).

115. M. G. Netea *et al.*, Immune sensing of Candida albicans requires cooperative recognition of mannans and glucans by lectin and Toll-like receptors. *J Clin Invest* **116**, 1642–1650 (2006).

116. G. Ferwerda, F. Meyer-Wentrup, B. J. Kullberg, M. G. Netea, G. J. Adema, Dectin-1 synergizes with TLR2 and TLR4 for cytokine production in human primary monocytes and macrophages. *Cell Microbiol* **10**, 2058–2066 (2008).

117. A. Esteban *et al.*, Fungal recognition is mediated by the association of dectin-1 and galectin-3 in macrophages. *Proc. Natl. Acad. Sci. U.S.A.* **108**, 14270–14275 (2011).

118. S. E. M. Heinsbroek *et al.*, Stage-specific sampling by pattern recognition receptors during Candida albicans phagocytosis. *PLoS Pathog* **4**, e1000218 (2008).

119. K. Strijbis *et al.*, Bruton's Tyrosine Kinase (BTK) and Vav1 contribute to Dectin1-dependent phagocytosis of Candida albicans in macrophages. *PLoS Pathog* **9**, e1003446 (2013).

120. X. Li *et al.*, The β-Glucan Receptor Dectin-1 Activates the Integrin Mac-1 in Neutrophils via Vav Protein Signaling to Promote Candida albicans Clearance. *Cell Host and Microbe* **10**, 603–615 (2011).

121. M. K. Mansour *et al.*, Dectin-1 Activation Controls Maturation of -1,3-Glucan-containing Phagosomes. *J Biol Chem* **288**, 16043–16054 (2013).

122. J. M. Tam *et al.*, Dectin-1-Dependent LC3 Recruitment to Phagosomes Enhances Fungicidal Activity in Macrophages. *Journal of Infectious Diseases* (2014), doi:10.1093/infdis/jiu290.

123. B. Ferwerda *et al.*, Human dectin-1 deficiency and mucocutaneous fungal infections. *N. Engl. J. Med.* **361**, 1760–1767 (2009).

124. K. Ariizumi *et al.*, Cloning of a second dendritic cell-associated C-type lectin (dectin-2) and its alternatively spliced isoforms. *J Biol Chem* **275**, 11957–11963 (2000).

125. P. R. Taylor *et al.*, Dectin-2 is predominantly myeloid restricted and exhibits unique activation-dependent expression on maturing inflammatory monocytes elicited in vivo. *Eur. J. Immunol.* **35**, 2163–2174 (2005).

126. E. P. McGreal *et al.*, The carbohydrate-recognition domain of Dectin-2 is a C-type lectin with specificity for high mannose. *Glycobiology* **16**, 422–430 (2006).

127. S. Saijo *et al.*, Dectin-2 recognition of alpha-mannans and induction of Th17 cell differentiation is essential for host defense against Candida albicans. *Immunity* **32**, 681–691 (2010).

128. K. Sato *et al.*, Dectin-2 is a pattern recognition receptor for fungi that couples with the Fc receptor gamma chain to induce innate immune responses. *J Biol Chem* **281**, 38854–38866 (2006).

129. M. J. Robinson *et al.*, Dectin-2 is a Syk-coupled pattern recognition receptor crucial for Th17 responses to fungal infection. *Journal of Experimental Medicine* **206**, 2037–2051 (2009).

130. L. Bi *et al.*, CARD9 mediates dectin-2-induced IkappaBalpha kinase ubiquitination leading to activation of NF-kappaB in response to stimulation by the hyphal form of Candida albicans. *J Biol Chem* **285**, 25969–25977 (2010).

131. S. Gorjestani *et al.*, Phospholipase Cγ2 (PLCγ2) is key component in Dectin-2 signaling pathway, mediating anti-fungal innate immune responses. *J Biol Chem* **286**, 43651–43659 (2011).

132. S. G. Balch, A. J. McKnight, M. F. Seldin, S. Gordon, Cloning of a novel C-type lectin expressed by murine macrophages. *J Biol Chem* **273**, 18656–18664 (1998).

133. I. Arce, L. Martínez-Muñoz, P. Roda-Navarro, E. Fernández-Ruiz, The human C-type lectin CLECSF8 is a novel monocyte/macrophage endocytic receptor. *Eur. J. Immunol.* **34**, 210–220 (2004).

134. L. M. Graham *et al.*, The C-type lectin receptor CLECSF8 (CLEC4D) is expressed by myeloid cells and triggers cellular activation through Syk kinase. *J Biol Chem* **287**, 25964–25974 (2012).

135. L.-L. Zhu *et al.*, C-type lectin receptors Dectin-3 and Dectin-2 form a heterodimeric pattern-recognition receptor for host defense against fungal infection. *Immunity* **39**, 324–334 (2013).

136. M. Matsumoto *et al.*, A novel LPS-inducible C-type lectin is a transcriptional target of NF-IL6 in macrophages. *J Immunol* **163**, 5039–5048 (1999).

137. S. Yamasaki *et al.*, Mincle is an ITAM-coupled activating receptor that senses damaged cells. *Nat Immunol* **9**, 1179–1188 (2008).

138. A. Bugarcic *et al.*, Human and mouse macrophage-inducible C-type lectin (Mincle) bind Candida albicans. *Glycobiology* **18**, 679–685 (2008).

139. C. A. Wells *et al.*, The macrophage-inducible C-type lectin, mincle, is an essential component of the innate immune response to Candida albicans. *J Immunol* **180**, 7404–7413 (2008).

140. H. M. Mora-Montes *et al.*, Recognition and blocking of innate immunity cells by Candida albicans chitin. *Infect. Immun.* **79**, 1961–1970 (2011).

141. D. Vijayan, K. J. Radford, A. G. Beckhouse, R. B. Ashman, C. A. Wells, Mincle polarizes human monocyte and neutrophil responses to Candida albicans. *Immunol Cell Biol* **90**, 889–895 (2012).

142. B. L. Largent, K. M. Walton, C. A. Hoppe, Y. C. Lee, R. L. Schnaar, Carbohydrate-specific adhesion of alveolar macrophages to mannose-derivatized surfaces. *J Biol Chem* **259**, 1764–1769 (1984).

143. M. E. Taylor, K. Bezouska, K. Drickamer, Contribution to ligand binding by multiple carbohydrate-recognition domains in the macrophage mannose receptor. *J Biol Chem* **267**, 1719–1726 (1992).

144. F. Sallusto, M. Cella, C. Danieli, A. Lanzavecchia, Dendritic cells use macropinocytosis and the mannose receptor to concentrate macromolecules in the major histocompatibility complex class II compartment: downregulation by cytokines and bacterial products. *J Exp Med* **182**, 389–400 (1995).

145. A. J. Engering *et al.*, The mannose receptor functions as a high capacity and broad specificity antigen receptor in human dendritic cells. *Eur. J. Immunol.* **27**, 2417–2425 (1997).

146. E. J. McKenzie *et al.*, Mannose receptor expression and function define a new population of murine dendritic cells. *J Immunol* **178**, 4975–4983 (2007).

147. S. A. Linehan, L. Martínez-Pomares, P. D. Stahl, S. Gordon, Mannose receptor and its putative ligands in normal murine lymphoid and nonlymphoid organs: In situ expression of mannose receptor by selected macrophages, endothelial cells, perivascular microglia, and mesangial cells, but not dendritic cells. *J Exp Med* **189**, 1961–1972 (1999).

148. M. Stein, S. Keshav, N. Harris, S. Gordon, Interleukin 4 potently enhances murine macrophage mannose receptor activity: a marker of alternative immunologic macrophage activation. *J Exp Med* **176**, 287–292 (1992).

149. A. Coste *et al.*, PPARgamma promotes mannose receptor gene expression in murine macrophages and contributes to the induction of this receptor by IL-13. *Immunity* **19**, 329–339 (2003).

150. S. J. Lee, N.-Y. Zheng, M. Clavijo, M. C. Nussenzweig, Normal host defense during systemic candidiasis in mannose receptor-deficient mice. *Infection and Immunity* **71**, 437–445 (2003).

151. S. S. Sung, R. S. Nelson, S. C. Silverstein, Yeast mannans inhibit binding and phagocytosis of zymosan by mouse peritoneal macrophages. *J. Cell Biol.* **96**, 160–166 (1983).

152. A. Karbassi, J. M. Becker, J. S. Foster, R. N. Moore, Enhanced killing of Candida albicans by murine macrophages treated with macrophage colony-stimulating factor: evidence for augmented expression of mannose receptors. *J Immunol* **139**, 417–421 (1987).

153. L. Marodi, H. M. Korchak, R. B. Johnston, Mechanisms of host defense against Candida species. I. Phagocytosis by monocytes and monocyte-derived macrophages. *J Immunol* **146**, 2783–2789 (1991).

154. L. Marodi *et al.*, Enhancement of macrophage candidacidal activity by interferon-gamma. Increased phagocytosis, killing, and calcium signal mediated by a decreased number of mannose receptors. *J Clin Invest* **91**, 2596–2601 (1993).

155. G. Gaziri, L. C. Gaziri, R. Kikuchi, J. Scanavacca, I. Felipe, Phagocytosis of Candida albicans by concanavalin-A activated peritoneal macrophages. *Med. Mycol.* **37**, 195–200 (1999).

156. A. Schweizer, P. D. Stahl, J. Rohrer, A di-aromatic motif in the cytosolic tail of the mannose receptor mediates endosomal sorting. *J Biol Chem* **275**, 29694–29700 (2000).

157. I. Porcaro, M. Vidal, S. Jouvert, P. D. Stahl, J. Giaimis, Mannose receptor contribution to Candida albicans phagocytosis by murine E-clone J774 macrophages. *Journal of Leukocyte Biology* **74**, 206–215 (2003).

158. R. A. Ezekowitz, K. Sastry, P. Bailly, A. Warner, Molecular characterization of the human macrophage mannose receptor: demonstration of multiple carbohydrate recognition-like domains and phagocytosis of yeasts in Cos-1 cells. *J Exp Med* **172**, 1785–1794 (1990).

159. A. Cambi *et al.*, Dendritic cell interaction with Candida albicans critically depends on N-linked mannan. *J Biol Chem* **283**, 20590–20599 (2008).

160. V. Le Cabec, L. J. Emorine, I. Toesca, C. Cougoule, I. Maridonneau-Parini, The human macrophage mannose receptor is not a professional phagocytic receptor. *Journal of Leukocyte Biology* **77**, 934–943 (2005).

161. A. K. Neumann, K. Jacobson, A novel pseudopodial component of the dendritic cell anti-fungal response: the fungipod. *PLoS Pathog* **6**, e1000760 (2010).

162. L. Martínez-Pomares *et al.*, A functional soluble form of the murine mannose receptor is produced by macrophages in vitro and is present in mouse serum. *J Biol Chem* **273**, 23376–23380 (1998).

163. L. Martínez-Pomares *et al.*, Fc chimeric protein containing the cysteine-rich domain of the murine mannose receptor binds to macrophages from splenic marginal zone and lymph node subcapsular sinus and to germinal centers. *J Exp Med* **184**, 1927–1937 (1996).

164. U. Gazi *et al.*, Fungal recognition enhances mannose receptor shedding through dectin-1 engagement. *J Biol Chem* **286**, 7822–7829 (2011).

165. Y. Yamamoto, T. W. Klein, H. Friedman, Involvement of mannose receptor in cytokine interleukin-1beta (IL-1beta), IL-6, and granulocyte-macrophage colony-stimulating factor responses, but not in chemokine macrophage inflammatory protein 1beta (MIP-1beta), MIP-2, and KC responses, caused by attachment of Candida albicans to macrophages. *Infection and Immunity* **65**, 1077–1082 (1997).

166. F. L. van de Veerdonk *et al.*, The macrophage mannose receptor induces IL-17 in response to Candida albicans. *Cell Host and Microbe* **5**, 329–340 (2009).

167. S. P. Smeekens *et al.*, The classical $CD14^{++}$ $CD16^{-}$ monocytes, but not the patrolling $CD14^{+}$ $CD16^{+}$ monocytes, promote Th17 responses to Candida albicans. *Eur. J. Immunol.* **41**, 2915–2924 (2011).

168. T. B. Geijtenbeek *et al.*, Identification of DC-SIGN, a novel dendritic cell-specific ICAM-3 receptor that supports primary immune responses. *Cell* **100**, 575–585 (2000).

169. D. A. Mitchell, A. J. Fadden, K. Drickamer, A novel mechanism of carbohydrate recognition by the C-type lectins DC-SIGN and DC-SIGNR. Subunit organization and binding to multivalent ligands. *J Biol Chem* **276**, 28939–28945 (2001).

170. B. J. Appelmelk *et al.*, Cutting edge: carbohydrate profiling identifies new pathogens that interact with dendritic cell-specific ICAM-3-grabbing nonintegrin on dendritic cells. *J Immunol* **170**, 1635–1639 (2003).

171. A. Cambi *et al.*, The C-type lectin DC-SIGN (CD209) is an antigen-uptake receptor for Candida albicans on dendritic cells. *Eur. J. Immunol.* **33**, 532–538 (2003).

172. A. Engering *et al.*, The dendritic cell-specific adhesion receptor DC-SIGN internalizes antigen for presentation to T cells. *J Immunol* **168**, 2118–2126 (2002).

173. E. Caparrós *et al.*, DC-SIGN ligation on dendritic cells results in ERK and PI3K activation and modulates cytokine production. *Blood* **107**, 3950–3958 (2006).

174. C. G. Park *et al.*, Five mouse homologues of the human dendritic cell C-type lectin, DC-SIGN. *Int Immunol* **13**, 1283–1290 (2001).

175. K. Takahara *et al.*, Functional comparison of the mouse DC-SIGN, SIGNR1, SIGNR3 and Langerin, C-type lectins. *Int Immunol* **16**, 819–829 (2004).

176. P. R. Taylor *et al.*, The role of SIGNR1 and the beta-glucan receptor (dectin-1) in the nonopsonic recognition of yeast by specific macrophages. *J Immunol* **172**, 1157–1162 (2004).

177. K. Takahara, S. Tokieda, K. Nagaoka, K. Inaba, Efficient capture of Candida albicans and zymosan by SIGNR1 augments TLR2-dependent TNF-α production. *Int Immunol* **24**, 89–96 (2012).

178. K. Takahara *et al.*, C-type lectin SIGNR1 enhances cellular oxidative burst response against

C. albicans in cooperation with Dectin-1. *Eur. J. Immunol.* **41**, 1435–1444 (2011).

179. C. Kato, N. Kojima, SIGNR1 ligation on murine peritoneal macrophages induces IL-12 production through NFkappaB activation. *Glycoconj. J.* **27**, 525–531 (2010).

180. U. Holmskov, S. Thiel, J. C. Jensenius, Collectins and ficolins: humoral lectins of the innate immune defense. *Annu. Rev. Immunol.* **21**, 547–578 (2003).

181. W. I. Weis, K. Drickamer, W. A. Hendrickson, Structure of a C-type mannose-binding protein complexed with an oligosaccharide. *Nature* **360**, 127–134 (1992).

182. N. Wong, R. B. Sim, Comparison of the complement system protein complexes formed by C1q and MBL. *Biochem. Soc. Trans.* **25**, 41S (1997).

183. K. Ikeda, T. Sannoh, N. Kawasaki, T. Kawasaki, I. Yamashina, Serum lectin with known structure activates complement through the classical pathway. *J Biol Chem* **262**, 7451–7454 (1987).

184. O. Neth *et al.*, Mannose-binding lectin binds to a range of clinically relevant microorganisms and promotes complement deposition. *Infection and Immunity* **68**, 688–693 (2000).

185. J. B. Lillegard, R. B. Sim, P. Thorkildson, M. A. Gates, T. R. Kozel, Recognition of Candida albicans by mannan-binding lectin in vitro and in vivo. *J. Infect. Dis.* **193**, 1589–1597 (2006).

186. N. Brouwer *et al.*, Mannose-binding lectin (MBL) facilitates opsonophagocytosis of yeasts but not of bacteria despite MBL binding. *J Immunol* **180**, 4124–4132 (2008).

187. E. C. van Asbeck, A. I. M. Hoepelman, J. Scharringa, B. L. Herpers, J. Verhoef, Mannose binding lectin plays a crucial role in innate immunity against yeast by enhanced complement activation and enhanced uptake of polymorphonuclear cells. *BMC Microbiol.* **8**, 229 (2008).

188. W. K. Ip, Y. L. Lau, Role of Mannose-Binding Lectin in the Innate Defense against Candida albicans:Enhancement of Complement Activation, but Lack of Opsonic Function, in Phagocytosis by Human Dendritic Cells. *Journal of Infectious Diseases* **190**, 632–640 (2004).

189. D. Li *et al.*, MBL-mediated opsonophagocytosis of Candida albicans by human neutrophils is coupled with intracellular Dectin-1-triggered ROS production. *PLoS ONE* **7**, e50589 (2012).

190. M. C. Ghezzi, G. Raponi, S. Angeletti, C. Mancini, Serum-mediated enhancement of TNF-alpha release by human monocytes stimulated with the yeast form of Candida albicans. *J. Infect. Dis.* **178**, 1743–1749 (1998).

191. D. J. Kitz, P. D. Stahl, J. R. Little, The effect of a mannose binding protein on macrophage interactions with Candida albicans. *Cell. Mol. Biol.* **38**, 407–412 (1992).

192. P. Tabona, A. Mellor, J. A. Summerfield, Mannose binding protein is involved in first-line host defence: evidence from transgenic mice. *Immunology* **85**, 153–159 (1995).

193. K. Held, S. Thiel, M. Loos, F. Petry, Increased susceptibility of complement factor B/C2 double knockout mice and mannan-binding lectin knockout mice to systemic infection with Candida albicans. *Mol Immunol* **45**, 3934–3941 (2008).

194. S. J. Lee, G. Gonzalez-Aseguinolaza, M. C. Nussenzweig, Disseminated Candidiasis and Hepatic Malarial Infection in Mannose-Binding-Lectin-A-Deficient Mice. *Mol Cell Biol* **22**, 8199–8203 (2002).

195. P. I. Sealy, B. Garner, E. Swiatlo, S. W. Chapman, J. D. Cleary, The interaction of mannose binding lectin (MBL) with mannose containing glycopeptides and the resultant potential impact on invasive fungal infection. *Med. Mycol.* **46**, 531–539 (2008).

196. V. Pellis *et al.*, Mannose binding lectin and C3 act as recognition molecules for infectious agents in the vagina. *Clin. Exp. Immunol.* **139**, 120–126 (2005).

197. O. Babula, G. Lazdane, J. Kroica, W. J. Ledger, S. S. Witkin, Relation between recurrent vulvovaginal candidiasis, vaginal concentrations of mannose-binding lectin, and a mannose-binding lectin gene polymorphism in Latvian women. *Clin Infect Dis* **37**, 733–737 (2003).

198. F. Liu, Q. Liao, Z. Liu, Mannose-binding lectin and vulvovaginal candidiasis. *Int J Gynaecol Obstet* **92**, 43–47 (2006).

199. S. Damiens *et al.*, Mannose-Binding Lectin Levels and Variation During Invasive Candidiasis. *J. Clin. Immunol.* **32**, 1317–1323 (2012).

200. B. Lemaitre, E. Nicolas, L. Michaut, J. M. Reichhart, J. A. Hoffmann, The dorsoventral regulatory gene cassette spätzle/Toll/cactus controls the potent antifungal response in Drosophila adults. *Cell* **86**, 973–983 (1996).

201. R. Medzhitov, P. Preston-Hurlburt, C. A. Janeway, A human homologue of the Drosophila Toll protein signals activation of adaptive immunity. *Nature* **388**, 394–397 (1997).

202. T. Kawai, S. Akira, Toll-like receptors and their crosstalk with other innate receptors in infection and immunity. *Immunity* **34**, 637–650 (2011).

203. A. L. Blasius, B. Beutler, Intracellular toll-like receptors. *Immunity* **32**, 305–315 (2010).

204. K. A. Marr *et al.*, Differential role of MyD88 in macrophage-mediated responses to opportunistic fungal pathogens. *Infection and Immunity* **71**, 5280–5286 (2003).

205. S. Bellocchio *et al.*, The contribution of the Toll-like/IL-1 receptor superfamily to innate and adaptive immunity to fungal pathogens in vivo. *J Immunol* **172**, 3059–3069 (2004).

206. E. Villamón *et al.*, Myeloid differentiation factor 88 (MyD88) is required for murine resistance to Candida albicans and is critically involved in Candida -induced production of cytokines. *Eur. Cytokine Netw.* **15**, 263–271 (2004).

207. A. Poltorak, X. He, I. Smirnova, M. Y. Liu, C. Van Huffel, Defective LPS Signaling in C3H/HeJ and C57BL/10ScCr Mice: Mutations in Tlr4 Gene. *Science* (1998).

208. K. Hoshino *et al.*, Cutting edge: Toll-like receptor 4 (TLR4)-deficient mice are hyporesponsive to lipopolysaccharide: evidence for TLR4 as the Lps gene product. *J Immunol* **162**, 3749–3752 (1999).

209. D. M. Underhill *et al.*, The Toll-like receptor 2 is recruited to macrophage phagosomes and discriminates between pathogens. *Nature* **401**, 811–815 (1999).

210. T. Jouault *et al.*, Candida albicans phospholipomannan is sensed through toll-like receptors. *J. Infect. Dis.* **188**, 165–172 (2003).

211. H. Tada *et al.*, Saccharomyces cerevisiae- and Candida albicans-derived mannan induced production of tumor necrosis factor alpha by human monocytes in a CD14- and Toll-like receptor 4-dependent manner. *Microbiol. Immunol.* **46**, 503–512 (2002).

212. M. G. Netea *et al.*, The role of toll-like receptor (TLR) 2 and TLR4 in the host defense against disseminated candidiasis. *J. Infect. Dis.* **185**, 1483–1489 (2002).

213. T. H. Gasparoto *et al.*, Absence of functional TLR4 impairs response of macrophages after Candida albicans infection. *Med. Mycol.* **48**, 1009–1017 (2010).

214. C. Murciano *et al.*, Toll-like receptor 4 defective mice carrying point or null mutations do not show increased susceptibility to Candida albicansin a model of hematogenously disseminated infection. *Med. Mycol.* **44**, 149–157 (2006).

215. M. G. Netea *et al.*, Toll-like receptor 2 suppresses immunity against Candida albicans through induction of IL-10 and regulatory T cells. *J Immunol* **172**, 3712–3718 (2004).

216. R. P. M. Sutmuller *et al.*, Toll-like receptor 2 controls expansion and function of regulatory T cells. *J Clin Invest* **116**, 485–494 (2006).

217. E. Villamón *et al.*, Toll-like receptor-2 is essential in murine defenses against Candida albicans infections. *Microbes Infect* **6**, 1–7 (2004).

218. V. Tessarolli *et al.*, Absence of TLR2 influences survival of neutrophils after infection with Candida albicans. *Med. Mycol.* **48**, 129–140 (2010).

219. A. Yáñez *et al.*, Signalling through TLR2/MyD88 induces differentiation of murine bone marrow stem and progenitor cells to functional phagocytes in response to Candida albicans. *Cell Microbiol* **12**, 114–128 (2010).

220. A. Yáñez, J. Megías, J. E. O'Connor, D. Gozalbo, M. L. Gil, Candida albicans induces selective development of macrophages and monocyte derived dendritic cells by a TLR2 dependent signalling. *PLoS ONE* **6**, e24761 (2011).

221. J. Megías, V. Maneu, P. Salvador, D. Gozalbo, M. L. Gil, Candida albicans stimulates in vivo differentiation of haematopoietic stem and progenitor cells towards macrophages by a TLR2-dependent signalling. *Cell Microbiol* **15**, 1143–1153 (2013).

222. E. Villamón *et al.*, Toll-like receptor 2 is dispensable for acquired host immune resistance to Candida albicans in a murine model of disseminated candidiasis. *Microbes Infect* **6**, 542–548 (2004).

223. S. A. Morré, L. S. Murillo, J. Spaargaren, H. S. A. Fennema, A. S. Peña, Role of the toll-like receptor 4 Asp299Gly polymorphism in susceptibility to Candida albicans infection. *J. Infect. Dis.* **186**, 1377–9– author reply 1379 (2002).

224. C. A. A. van der Graaf *et al.*, Toll-like receptor 4 Asp299Gly/Thr399Ile polymorphisms are a risk factor for Candida bloodstream infection. *Eur. Cytokine Netw.* **17**, 29–34 (2006).

225. C. A. A. van der Graaf *et al.*, Candida-specific interferon-gamma deficiency and toll-like receptor polymorphisms in patients with chronic mucocutaneous candidiasis. *Neth J Med* **61**, 365–369 (2003).

226. S. Akira, S. Uematsu, O. Takeuchi, Pathogen recognition and innate immunity. *Cell* **124**, 783–801 (2006).

227. A. Ozinsky *et al.*, The repertoire for pattern recognition of pathogens by the innate immune system is defined by cooperation between toll-like receptors. *Proc Natl Acad Sci USA* **97**, 13766–13771 (2000).

228. M. G. Netea, F. van de Veerdonk, I. Verschueren, J. W. M. Van Der Meer, B. J. Kullberg, Role of TLR1 and TLR6 in the host defense against disseminated candidiasis. *FEMS Immunology & Medical Microbiology* **52**, 118–123 (2008).

229. J. Lund, A. Sato, S. Akira, R. Medzhitov, A. Iwasaki, Toll-like receptor 9-mediated recognition of Herpes simplex virus-2 by plasmacytoid dendritic cells. *J Exp Med* **198**, 513–520 (2003).

230. F. Heil *et al.*, Species-specific recognition of single-stranded RNA via toll-like receptor 7 and 8. *Science* **303**, 1526–1529 (2004).

231. S. S. Diebold, T. Kaisho, H. Hemmi, S. Akira, C. Reis e Sousa, Innate antiviral responses by means of TLR7-mediated recognition of single-stranded RNA. *Science* **303**, 1529–1531 (2004).

232. A. Miyazato *et al.*, Toll-like receptor 9-dependent activation of myeloid dendritic cells by Deoxynucleic acids from Candida albicans. *Infect. Immun.* **77**, 3056–3064 (2009).

233. F. L. van de Veerdonk *et al.*, Redundant role of TLR9 for anti-Candida host defense. *Immunobiology* **213**, 613–620 (2008).

234. P. V. Kasperkovitz *et al.*, Toll-like receptor 9 modulates macrophage antifungal effector function during innate recognition of Candida albicans and Saccharomyces cerevisiae. *Infect. Immun.* **79**, 4858–4867 (2011).

235. C. Biondo *et al.*, Recognition of yeast nucleic acids triggers a host-protective type I interferon response. *Eur. J. Immunol.* **41**, 1969–1979 (2011).

236. C. Bourgeois *et al.*, Conventional dendritic cells mount a type I IFN response against Candida spp. requiring novel phagosomal TLR7-mediated IFN-β signaling. *The Journal of Immunology* **186**, 3104–3112 (2011).

237. C. Biondo *et al.*, Recognition of fungal RNA by TLR7 has a nonredundant role in host defense against experimental candidiasis. *Eur. J. Immunol.* **42**, 2632–2643 (2012).

238. K. Schroder, J. Tschopp, The inflammasomes. *Cell* **140**, 821–832 (2010).

239. B. K. Davis, H. Wen, J. P. Y. Ting, The Inflammasome NLRs in Immunity, Inflammation, and Associated Diseases. *Annu. Rev. Immunol.* **29**, 707–735 (2011).

240. F. Martinon, K. Burns, J. Tschopp, The inflammasome: a molecular platform triggering activation of inflammatory caspases and processing of proIL-beta. *Mol Cell* **10**, 417–426 (2002).

241. F. L. van de Veerdonk *et al.*, The inflammasome drives protective Th1 and Th17 cellular responses in disseminated candidiasis. *Eur. J. Immunol.* **41**, 2260–2268 (2011).

242. S. Joly *et al.*, Cutting edge: Candida albicans hyphae formation triggers activation of the Nlrp3 inflammasome. *The Journal of Immunology* **183**, 3578–3581 (2009).

243. H. Kumar *et al.*, Involvement of the NLRP3 Inflammasome in Innate and Humoral Adaptive

Immune Responses to Fungal -Glucan. *The Journal of Immunology* **183**, 8061–8067 (2009).

244. C. E. Zielinski *et al.*, Pathogen-induced human TH17 cells produce IFN-γ or IL-10 and are regulated by IL-1β. *Nature* **484**, 514–518 (2012).

245. S. Joly *et al.*, Cutting edge: Nlrp10 is essential for protective antifungal adaptive immunity against Candida albicans. *The Journal of Immunology* **189**, 4713–4717 (2012).

246. C. Fradin, D. Poulain, T. Jouault, beta-1,2-linked oligomannosides from Candida albicans bind to a 32-kilodalton macrophage membrane protein homologous to the mammalian lectin galectin-3. *Infection and Immunity* **68**, 4391–4398 (2000).

247. L. Kohatsu, D. K. Hsu, A. G. Jegalian, F.-T. Liu, L. G. Baum, Galectin-3 induces death of Candida species expressing specific beta-1,2-linked mannans. *J Immunol* **177**, 4718–4726 (2006).

248. T. Jouault *et al.*, Specific recognition of Candida albicans by macrophages requires galectin-3 to discriminate Saccharomyces cerevisiae and needs association with TLR2 for signaling. *J Immunol* **177**, 4679–4687 (2006).

249. J. R. Linden, M. E. De Paepe, S. S. Laforce-Nesbitt, J. M. Bliss, Galectin-3 plays an important role in protection against disseminated candidiasis. *Med. Mycol.* **51**, 641–651 (2013).

250. S. Jawhara *et al.*, Colonization of mice by Candida albicans is promoted by chemically induced colitis and augments inflammatory responses through galectin-3. *J. Infect. Dis.* **197**, 972–980 (2008).

251. L. Romani *et al.*, The exploitation of distinct recognition receptors in dendritic cells determines the full range of host immune relationships with Candida albicans. *Int Immunol* **16**, 149–161 (2004).

252. T. K. Means *et al.*, Evolutionarily conserved recognition and innate immunity to fungal pathogens by the scavenger receptors SCARF1 and CD36. *Journal of Experimental Medicine* **206**, 637–653 (2009).

253. J. O. Sunyer, I. K. Zarkadis, J. D. Lambris, Complement diversity: a mechanism for generating immune diversity? *Immunol. Today* **19**, 519–523 (1998).

254. P. F. Zipfel, Complement and immune defense: from innate immunity to human diseases. *Immunol Lett* **126**, 1–7 (2009).

255. D. Ricklin, G. Hajishengallis, K. Yang, J. D. Lambris, Complement: a key system for immune surveillance and homeostasis. *Nat Immunol* **11**, 785–797 (2010).

256. M. Kolev, G. Le Friec, C. Kemper, Complement [mdash] tapping into new sites and effector systems. *Nat. Rev. Immunol.* **14**, 811–820 (2014).

257. C. Gaboriaud *et al.*, Structure and activation of the C1 complex of complement: unraveling the puzzle. *Trends in Immunology* **25**, 368–373 (2004).

258. M. Kojouharova, K. Reid, M. Gadjeva, New insights into the molecular mechanisms of classical complement activation. *Mol Immunol* **47**, 2154–2160 (2010).

259. M. Matsumoto *et al.*, Probing the C4-binding site on C1s with monoclonal antibodies.

Evidence for a C4/C4b-binding site on the gamma-domain. *J Immunol* **142**, 2743–2750 (1989).

260. S. Nagasawa, R. M. Stroud, Cleavage of C2 by C1s into the antigenically distinct fragments C2a and C2b: demonstration of binding of C2b to C4b. *Proc Natl Acad Sci USA* **74**, 2998–3001 (1977).

261. C. Suankratay, X. H. Zhang, Y. Zhang, T. F. Lint, H. Gewurz, Requirement for the alternative pathway as well as C4 and C2 in complement-dependent hemolysis via the lectin pathway. *J Immunol* **160**, 3006–3013 (1998).

262. Y. J. Ma, M.-O. Skjoedt, P. Garred, Collectin-11/MASP complex formation triggers activation of the lectin complement pathway--the fifth lectin pathway initiation complex. *J Innate Immun* **5**, 242–250 (2013).

263. Y. Liu *et al.*, Human M-ficolin is a secretory protein that activates the lectin complement pathway. *J Immunol* **175**, 3150–3156 (2005).

264. M. Matsushita, Y. Endo, T. Fujita, Cutting edge: complement-activating complex of ficolin and mannose-binding lectin-associated serine protease. *J Immunol* **164**, 2281–2284 (2000).

265. M. Matsushita *et al.*, Activation of the lectin complement pathway by H-ficolin (Hakata antigen). *J Immunol* **168**, 3502–3506 (2002).

266. P. Garred, C. Honoré, Y. J. Ma, L. Munthe-Fog, T. Hummelshøj, MBL2, FCN1, FCN2 and FCN3-The genes behind the initiation of the lectin pathway of complement. *Mol Immunol* **46**, 2737–2744 (2009).

267. T. Vorup-Jensen *et al.*, Distinct pathways of mannan-binding lectin (MBL)- and C1-complex autoactivation revealed by reconstitution of MBL with recombinant MBL-associated serine protease-2. *J Immunol* **165**, 2093–2100 (2000).

268. V. Rossi *et al.*, Substrate specificities of recombinant mannan-binding lectin-associated serine proteases-1 and -2. *J Biol Chem* **276**, 40880–40887 (2001).

269. C.-B. Chen, R. Wallis, Two mechanisms for mannose-binding protein modulation of the activity of its associated serine proteases. *J Biol Chem* **279**, 26058–26065 (2004).

270. M. K. Pangburn, R. D. Schreiber, H. J. Müller-Eberhard, Formation of the initial C3 convertase of the alternative complement pathway. Acquisition of C3b-like activities by spontaneous hydrolysis of the putative thioester in native C3. *J Exp Med* **154**, 856–867 (1981).

271. F. Bexborn, P. O. Andersson, H. Chen, B. Nilsson, K. N. Ekdahl, The tick-over theory revisited: formation and regulation of the soluble alternative complement C3 convertase (C3(H2O)Bb). *Mol Immunol* **45**, 2370–2379 (2008).

272. D. T. Fearon, K. F. Austen, S. Ruddy, Formation of a hemolytically active cellular intermediate by the interaction between properdin factors B and D and the activated third component of complement. *J Exp Med* **138**, 1305–1313 (1973).

273. D. Spitzer, L. M. Mitchell, J. P. Atkinson, D. E. Hourcade, Properdin can initiate complement activation by binding specific target surfaces and providing a platform for de novo convertase assembly. *J Immunol* **179**, 2600–2608 (2007).

274. D. T. Fearon, K. F. Austen, Properdin: binding to C3b and stabilization of the C3b-dependent C3 convertase. *J Exp Med* **142**, 856–863 (1975).

275. M. Harboe, G. Ulvund, L. Vien, M. Fung, T. E. Mollnes, The quantitative role of alternative pathway amplification in classical pathway induced terminal complement activation. *Clin. Exp. Immunol.* **138**, 439–446 (2004).

276. M. K. Pangburn, N. Rawal, Structure and function of complement C5 convertase enzymes. *Biochem. Soc. Trans.* **30**, 1006–1010 (2002).

277. H. J. Müller-Eberhard, The killer molecule of complement. *J. Invest. Dermatol.* **85**, 47s–52s (1985).

278. D. S. Cole, B. P. Morgan, Beyond lysis: how complement influences cell fate. *Clin. Sci.* **104**, 455–466 (2003).

279. R. Morelli, L. T. Rosenberg, The role of complement in the phagocytosis of Candida albicans by mouse peripheral blood leukocytes. *J Immunol* **107**, 476–480 (1971).

280. K. Kagaya, Y. Fukazawa, Murine defense mechanism against Candida albicans infection. II. Opsonization, phagocytosis, and intracellular killing of C. albicans. *Microbiol. Immunol.* **25**, 807–818 (1981).

281. R. R. Davies, T. J. Denning, Candida albicans and the fungicidal activity of the blood. *Sabouraudia* **10**, 301–312 (1972).

282. P. C. Leijh, M. T. van den Barselaar, R. van Furth, Kinetics of phagocytosis and intracellular killing of Candida albicans by human granulocytes and monocytes. *Infection and Immunity* **17**, 313–318 (1977).

283. J. S. Solomkin *et al.*, Phagocytosis of Candida albicans by human leukocytes: opsonic requirements. *J. Infect. Dis.* **137**, 30–37 (1978).

284. H. A. Pereira, C. S. Hosking, The role of complement and antibody in opsonization and intracellular killing of Candida albicans. *Clin. Exp. Immunol.* **57**, 307–314 (1984).

285. P. Robinson, D. Wakefield, S. N. Breit, J. F. Easter, R. Penny, Chemiluminescent response to pathogenic organisms: normal human polymorphonuclear leukocytes. *Infection and Immunity* **43**, 744–752 (1984).

286. M. W. Turner, C. Grant, N. D. Seymour, B. Harvey, R. J. Levinsky, Evaluation of C3b/C3bi opsonization and chemiluminescence with selected yeasts and bacteria using sera of different opsonic potential. *Immunology* **58**, 111–115 (1986).

287. M. X. Zhang, D. M. Lupan, T. R. Kozel, Mannan-specific immunoglobulin G antibodies in normal human serum mediate classical pathway initiation of C3 binding to Candida albicans. *Infection and Immunity* **65**, 3822–3827 (1997).

288. M. X. Zhang, T. R. Kozel, Mannan-specific immunoglobulin G antibodies in normal human serum accelerate binding of C3 to Candida albicans via the alternative complement pathway. *Infection and Immunity* **66**, 4845–4850 (1998).

289. T. R. Kozel, Activation of the complement system by pathogenic fungi. *Clin. Microbiol. Rev.* **9**, 34–46 (1996).

290. I. Rubin-Bejerano, C. Abeijon, P. Magnelli, P. Grisafi, G. R. Fink, Phagocytosis by human neutrophils is stimulated by a unique fungal cell wall component. *Cell Host and Microbe* **2**, 55–67 (2007).

291. M. X. Zhang *et al.*, Human recombinant antimannan immunoglobulin G1 antibody confers resistance to hematogenously disseminated candidiasis in mice. *Infection and Immunity* **74**, 362–369 (2006).

292. G. Peltz *et al.*, Next-generation computational genetic analysis: multiple complement alleles control survival after Candida albicans infection. *Infect. Immun.* **79**, 4472–4479 (2011).

293. T. L. Ray, A. Hanson, L. F. Ray, K. D. Wuepper, Purification of a mannan from Candida albicans which activates serum complement. *J. Invest. Dermatol.* **73**, 269–274 (1979).

294. Y. J. Ma *et al.*, Heterocomplexes of Mannose-binding Lectin and the Pentraxins PTX3 or Serum Amyloid P Component Trigger Cross-activation of the Complement System. *J Biol Chem* **286**, 3405–3417 (2011).

295. R. Morelli, L. T. Rosenberg, Role of complement during experimental Candida infection in mice. *Infection and Immunity* **3**, 521–523 (1971).

296. F. L. Lyon, R. F. Hector, J. E. Domer, Innate and acquired immune responses against Candida albicansin congenic B10.D2 mice with deficiency of the C5 complement component. *Med. Mycol.* **24**, 359–367 (1986).

297. R. F. Hector, J. E. Domer, E. W. Carrow, Immune responses to Candida albicans in genetically distinct mice. *Infection and Immunity* **38**, 1020–1028 (1982).

298. A. Mullick *et al.*, Dysregulated inflammatory response to Candida albicans in a C5-deficient mouse strain. *Infection and Immunity* **72**, 5868–5876 (2004).

299. A. Mullick *et al.*, Cardiac Failure in C5-Deficient A/J Mice after Candida albicans Infection. *Infection and Immunity* **74**, 4439–4451 (2006).

300. A. Fulurija, R. B. Ashman, J. M. Papadimitriou, Early inflammatory responses to Candida albicans infection in inbred and complement-deficient mice. *FEMS Immunology & Medical Microbiology* **14**, 83–94 (1996).

301. R. B. Ashman *et al.*, Role of complement C5 and T lymphocytes in pathogenesis of disseminated and mucosal candidiasis in susceptible DBA/2 mice. *Microb. Pathog.* **34**, 103–113 (2003).

302. S. I. Rosenfeld, J. Baum, R. T. Steigbigel, J. P. Leddy, Hereditary deficiency of the fifth component of complement in man. II. Biological properties of C5-deficient human serum. *J Clin Invest* **57**, 1635–1643 (1976).

303. K. T. Lappegård *et al.*, Human genetic deficiencies reveal the roles of complement in the inflammatory network: lessons from nature. *Proc. Natl. Acad. Sci. U.S.A.* **106**, 15861–15866 (2009).

304. S.-C. Cheng *et al.*, Complement plays a central role in Candida albicans-induced cytokine production by human PBMCs. *Eur. J. Immunol.* **42**, 993–1004 (2012).

305. J. A. Gelfand, D. L. Hurley, A. S. Fauci, M. M. Frank, Role of complement in host defense against experimental disseminated candidiasis. *J. Infect. Dis.* **138**, 9–16 (1978).

306. G. M. Naked *et al.*, Deficiency of human complement factor I associated with lowered factor H. *Clin. Immunol.* **96**, 162–167 (2000).

307. J. Losse, P. F. Zipfel, M. Józsi, Factor H and factor H-related protein 1 bind to human neutrophils via complement receptor 3, mediate attachment to Candida albicans, and enhance neutrophil antimicrobial activity. *The Journal of Immunology* **184**, 912–921 (2010).

308. T. Triebel *et al.*, Importance of the terminal complement components for immune defence against Candida. *Int. J. Med. Microbiol.* **292**, 527–536 (2003).

309. E. Lukasser-Vogl *et al.*, Membrane attack complex formation on yeast as trigger of selective release of terminal complement proteins from human polymorphonuclear leukocytes. *FEMS Immunology & Medical Microbiology* **28**, 15–23 (2000).

310. E. M. Hersh, G. P. Bodey, B. A. Nies, E. J. Freireich, Causes of Death in Acute Leukemia: a Ten-Year Study of 414 Patients From 1954-1963. *JAMA* **193**, 105–109 (1965).

311. R. I. Lehrer, Functional aspects of a second mechanism of candidacidal activity by human neutrophils. *J Clin Invest* **51**, 2566–2572 (1972).

312. A. Ferrante, Y. H. Thong, Requirement of heat-labile opsonins for maximal phagocytosis of Candida albicans. *Sabouraudia* **17**, 293–297 (1979).

313. J. M. Wilton, H. H. Renggli, T. Lehner, The role of Fc and C3b receptors in phagocytosis by inflammatory polymorphonuclear leucocytes in man. *Immunology* **32**, 955–961 (1977).

314. L. M. Lavigne, J. E. Albina, J. S. Reichner, Beta-glucan is a fungal determinant for adhesion-dependent human neutrophil functions. *J Immunol* **177**, 8667–8675 (2006).

315. G. Marquis, S. Garzon, S. Montplaisir, H. Strykowski, N. Benhamou, Histochemical and immunochemical study of the fate of Candida albicans inside human neutrophil phagolysosomes. *Journal of Leukocyte Biology* **50**, 587–599 (1991).

316. S. J. Klebanoff, A. J. Kettle, H. Rosen, C. C. Winterbourn, W. M. Nauseef, Myeloperoxidase: a front-line defender against phagocytosed microorganisms. *Journal of Leukocyte Biology* **93**, 185–198 (2013).

317. K. M. Rigby, F. R. DeLeo, Neutrophils in innate host defense against Staphylococcus aureus infections. *Semin Immunopathol* **34**, 237–259 (2012).

318. K. M. Brothers, Z. R. Newman, R. T. Wheeler, Live imaging of disseminated candidiasis in zebrafish reveals role of phagocyte oxidase in limiting filamentous growth. *Eukaryotic Cell* **10**, 932–944 (2011).

319. R. I. Lehrer, K. M. Ladra, R. B. Hake, Nonoxidative fungicidal mechanisms of mammalian granulocytes: demonstration of components with candidacidal activity in human, rabbit, and guinea pig leukocytes. *Infection and Immunity* **11**, 1226–1234 (1975).

320. E. W. Odell, A. W. Segal, Killing of pathogens associated with chronic granulomatous disease by the non-oxidative microbicidal mechanisms of human neutrophils. *J. Med. Microbiol.* **34**, 129–135 (1991).

321. A. Risso, Leukocyte antimicrobial peptides: multifunctional effector molecules of innate immunity. *Journal of Leukocyte Biology* **68**, 785–792 (2000).

322. M. P. Kolotila, R. D. Diamond, Stimulation of neutrophil actin polymerization and degranulation by opsonized and unopsonized Candida albicans hyphae and zymosan. *Infection and Immunity* **56**, 2016–2022 (1988).

323. A. R. Murthy, R. I. Lehrer, S. S. Harwig, K. T. Miyasaki, In vitro candidastatic properties of the human neutrophil calprotectin complex. *J Immunol* **151**, 6291–6301 (1993).

324. C. F. Urban *et al.*, Neutrophil extracellular traps contain calprotectin, a cytosolic protein complex involved in host defense against Candida albicans. *PLoS Pathog* **5**, e1000639 (2009).

325. R. I. Lehrer, T. Ganz, D. Szklarek, M. E. Selsted, Modulation of the in vitro candidacidal activity of human neutrophil defensins by target cell metabolism and divalent cations. *J Clin Invest* **81**, 1829–1835 (1988).

326. T. Tanida, F. Rao, T. Hamada, E. Ueta, T. Osaki, Lactoferrin peptide increases the survival of Candida albicans-inoculated mice by upregulating neutrophil and macrophage functions, especially in combination with amphotericin B and granulocyte-macrophage colony-stimulating factor. *Infection and Immunity* **69**, 3883–3890 (2001).

327. J. Y. Djeu, K. Matsushima, J. J. Oppenheim, K. Shiotsuki, D. K. Blanchard, Functional activation of human neutrophils by recombinant monocyte-derived neutrophil chemotactic factor/IL-8. *J Immunol* **144**, 2205–2210 (1990).

328. C. Palma, A. Cassone, D. Serbousek, C. A. Pearson, J. Y. Djeu, Lactoferrin release and interleukin-1, interleukin-6, and tumor necrosis factor production by human polymorphonuclear cells stimulated by various lipopolysaccharides: relationship to growth inhibition of Candida albicans. *Infection and Immunity* **60**, 4604–4611 (1992).

329. M. P. McNamara, J. H. Wiessner, C. Collins-Lech, B. L. Hahn, P. G. Sohnle, Neutrophil death as a defence mechanism against Candida albicans infections. *Lancet* **2**, 1163–1165 (1988).

330. V. Brinkmann *et al.*, Neutrophil extracellular traps kill bacteria. *Science* **303**, 1532–1535 (2004).

331. C. F. Urban, U. Reichard, V. Brinkmann, A. Zychlinsky, Neutrophil extracellular traps capture and kill Candida albicans yeast and hyphal forms. *Cell Microbiol* **8**, 668–676 (2006).

332. R. Menegazzi, E. Decleva, P. Dri, Killing by neutrophil extracellular traps: fact or folklore? *Blood* **119**, 1214–1216 (2012).

333. T. A. Fuchs *et al.*, Novel cell death program leads to neutrophil extracellular traps. *J. Cell Biol.* **176**, 231–241 (2007).

334. D. Ermert *et al.*, Mouse neutrophil extracellular traps in microbial infections. *J Innate Immun* **1**, 181–193 (2009).

335. J. Y. Djeu, D. Serbousek, D. K. Blanchard, Release of tumor necrosis factor by human polymorphonuclear leukocytes. *Blood* **76**, 1405–1409 (1990).

336. J. F. Sweeney, P. K. Nguyen, G. M. Omann, D. B. Hinshaw, Autocrine/paracrine modulation of polymorphonuclear leukocyte survival after exposure to Candida albicans. *Shock* **9**, 146–152 (1998).

337. A. M. Megiovanni *et al.*, Polymorphonuclear neutrophils deliver activation signals and antigenic molecules to dendritic cells: a new link between leukocytes upstream of T lymphocytes. *Journal of Leukocyte Biology* **79**, 977–988 (2006).

338. J. Voigt *et al.*, Human Natural Killer Cells Acting as Phagocytes Against Candida albicans and Mounting an Inflammatory Response That Modulates Neutrophil Antifungal Activity. *Journal of Infectious Diseases* **209**, 616–626 (2014).

339. M. S. Gresnigt *et al.*, Neutrophil-mediated inhibition of proinflammatory cytokine responses. *The Journal of Immunology* **189**, 4806–4815 (2012).

340. J. Y. Djeu, D. K. Blanchard, D. Halkias, H. Friedman, Growth inhibition of Candida albicans by human polymorphonuclear neutrophils: activation by interferon-gamma and tumor necrosis factor. *J Immunol* **137**, 2980–2984 (1986).

341. A. Ferrante, Tumor necrosis factor alpha potentiates neutrophil antimicrobial activity: increased fungicidal activity against Torulopsis glabrata and Candida albicans and associated increases in oxygen radical production and lysosomal enzyme release. *Infection and Immunity* **57**, 2115–2122 (1989).

342. E. Roilides, K. Uhlig, D. Venzon, P. A. Pizzo, T. J. Walsh, Neutrophil oxidative burst in response to blastoconidia and pseudohyphae of Candida albicans: augmentation by granulocyte colony-stimulating factor and interferon-gamma. *J. Infect. Dis.* **166**, 668–673 (1992).

343. E. Roilides, A. Holmes, C. Blake, P. A. Pizzo, T. J. Walsh, Effects of granulocyte colony-stimulating factor and interferon-gamma on antifungal activity of human polymorphonuclear neutrophils against pseudohyphae of different medically important Candida species. *Journal of Leukocyte Biology* **57**, 651–656 (1995).

344. T. Musso *et al.*, Interleukin-15 activates proinflammatory and antimicrobial functions in polymorphonuclear cells. *Infection and Immunity* **66**, 2640–2647 (1998).

345. H. T. Le *et al.*, IL-33 priming regulates multiple steps of the neutrophil-mediated anti-Candida albicans response by modulating TLR and dectin-1 signals. *The Journal of Immunology* **189**, 287–295 (2012).

346. S. Wei, J. H. Liu, D. K. Blanchard, J. Y. Djeu, Induction of IL-8 gene expression in human polymorphonuclear neutrophils by recombinant IL-2. *J Immunol* **152**, 3630–3636 (1994).

347. B. J. Kullberg, J. W. van t Wout, C. Hoogstraten, R. van Furth, Recombinant interferon-gamma enhances resistance to acute disseminated Candida albicans infection in mice. *J. Infect. Dis.* **168**, 436–443 (1993).

348. E. Roilides *et al.*, Interleukin 10 suppresses phagocytic and antihyphal activities of human neutrophils. *Cytokine* **12**, 379–387 (2000).

349. F. Bistoni *et al.*, Correlation between in vivo and in vitro studies of modulation of resistance to experimental Candida albicans infection by cyclophosphamide in mice. *Infection and Immunity* **40**, 46–55 (1983).

350. J. Jensen, T. Warner, E. Balish, Resistance of SCID mice to Candida albicans administered intravenously or colonizing the gut: role of polymorphonuclear leukocytes and macrophages. *J. Infect. Dis.* **167**, 912–919 (1993).

351. A. Fulurija, R. B. Ashman, J. M. Papadimitriou, Neutrophil depletion increases susceptibility to systemic and vaginal candidiasis in mice, and reveals differences between brain and kidney in mechanisms of host resistance. *Microbiology (Reading, Engl.)* **142 (Pt 12)**, 3487–3496 (1996).

352. L. Romani *et al.*, An immunoregulatory role for neutrophils in CD4+ T helper subset selection in mice with candidiasis. *J Immunol* **158**, 2356–2362 (1997).

353. B. J. Spellberg *et al.*, A phagocytic cell line markedly improves survival of infected neutropenic mice. *Journal of Leukocyte Biology* **78**, 338–344 (2005).

354. M. G. Manz, S. Boettcher, Emergency granulopoiesis. *Nat. Rev. Immunol.* **14**, 302–314 (2014).

355. G. Morstyn *et al.*, Effect of granulocyte colony stimulating factor on neutropenia induced by cytotoxic chemotherapy. *Lancet* **1**, 667–672 (1988).

356. W. C. Liles, J. E. Huang, J. A. van Burik, R. A. Bowden, D. C. Dale, Granulocyte colony-stimulating factor administered in vivo augments neutrophil-mediated activity against opportunistic fungal pathogens. *J. Infect. Dis.* **175**, 1012–1015 (1997).

357. Y. Yamamoto, T. W. Klein, H. Friedman, S. Kimura, H. Yamaguchi, Granulocyte colony-stimulating factor potentiates anti-Candida albicans growth inhibitory activity of polymorphonuclear cells. *FEMS Immunology & Medical Microbiology* **7**, 15–22 (1993).

358. J. M. Gaviria, J. A. van Burik, D. C. Dale, R. K. Root, W. C. Liles, Modulation of neutrophil-mediated activity against the pseudohyphal form of Candida albicans by granulocyte colony-stimulating factor (G-CSF) administered in vivo. *J. Infect. Dis.* **179**, 1301–1304 (1999).

359. E. Roilides, T. J. Walsh, P. A. Pizzo, M. Rubin, Granulocyte colony-stimulating factor enhances the phagocytic and bactericidal activity of normal and defective human neutrophils. *J. Infect. Dis.* **163**, 579–583 (1991).

360. M. Matsumoto *et al.*, Protective effect of human granulocyte colony-stimulating factor on microbial infection in neutropenic mice. *Infection and Immunity* **55**, 2715–2720 (1987).

361. K. Uchida, Y. Yamamoto, T. W. Klein, H. Friedman, H. Yamaguchi, Granulocyte-colony stimulating factor facilitates the restoration of resistance to opportunistic fungi in leukopenic mice. *J. Med. Vet. Mycol.* **30**, 293–300 (1992).

362. S. Steinshamn, K. Bergh, A. Waage, Effects of stem cell factor and granulocyte colony-stimulating factor on granulocyte recovery and Candida albicans infection in granulocytopenic mice. *J. Infect. Dis.* **168**, 1444–1448 (1993).

363. M. D. Richardson, C. E. Brownlie, G. S. Shankland, Enhanced phagocytosis and intracellular killing of Candida albicans by GM-CSF-activated human neutrophils. *J. Med. Vet. Mycol.* **30**, 433–441 (1992).

364. S. Basu *et al.*, "Emergency" granulopoiesis in G-CSF-deficient mice in response to Candida albicans infection. *Blood* **95**, 3725–3733 (2000).

365. S. Basu, C. Quilici, H.-H. Zhang, D. Grail, A. R. Dunn, Mice lacking both G-CSF and IL-6 are more susceptible to Candida albicans infection: critical role of neutrophils in defense against Candida albicans. *Growth Factors* **26**, 23–34 (2008).

366. M. S. Lionakis, J. K. Lim, C.-C. R. Lee, P. M. Murphy, Organ-Specific Innate Immune Responses in a Mouse Model of Invasive Candidiasis. **3**, 180–199 (2011).

367. M. G. Netea *et al.*, Increased susceptibility of TNF-alpha lymphotoxin-alpha double knockout mice to systemic candidiasis through impaired recruitment of neutrophils and phagocytosis of Candida albicans. *J Immunol* **163**, 1498–1505 (1999).

368. E. E. Balish *et al.*, Mucosal and systemic candidiasis in IL-8Rh-/- BALB/c mice. *Journal of Leukocyte Biology* **66**, 144–150 (1999).

369. W. Huang, L. Na, P. L. Fidel, P. Schwarzenberger, Requirement of interleukin-17A for systemic anti-Candida albicans host defense in mice. *J. Infect. Dis.* **190**, 624–631 (2004).

370. M. G. Netea, J. W. van der Meer, J. F. Meis, B. J. Kullberg, Fas-FasL interactions modulate host defense against systemic Candida albicans infection. *J. Infect. Dis.* **180**, 1648–1655 (1999).

371. H.-A. Kim *et al.*, Nitric oxide plays a key role in the platelet-activating factor-induced enhancement of resistance against systemic candidiasis. *Immunology* **124**, 428–435 (2008).

372. E. Kolaczkowska, P. Kubes, Neutrophil recruitment and function in health and inflammation. *Nat. Rev. Immunol.* **13**, 159–175 (2013).

373. S. L. Davis, E. P. Hawkins, E. O. Mason, C. W. Smith, S. L. Kaplan, Host defenses against disseminated candidiasis are impaired in intercellular adhesion molecule 1-deficient mice. *J. Infect. Dis.* **174**, 435–439 (1996).

374. M. S. Lionakis *et al.*, Chemokine receptor Ccr1 drives neutrophil-mediated kidney immunopathology and mortality in invasive candidiasis. *PLoS Pathog* **8**, e1002865 (2012).

375. O. Majer *et al.*, Type I interferons promote fatal immunopathology by regulating inflammatory monocytes and neutrophils during Candida infections. *PLoS Pathog* **8**, e1002811 (2012).

376. C. del Fresno *et al.*, Interferon-β production via Dectin-1-Syk-IRF5 signaling in dendritic cells is crucial for immunity to C. albicans. *Immunity* **38**, 1176–1186 (2013).

377. K. Maruyama *et al.*, The transcription factor Jdp2 controls bone homeostasis and antibacterial immunity by regulating osteoclast and neutrophil differentiation. *Immunity* **37**, 1024–1036 (2012).

378. Z. Liu, R. Petersen, L. Devireddy, Impaired neutrophil function in 24p3 null mice contributes to enhanced susceptibility to bacterial infections. *The Journal of Immunology* **190**, 4692–4706 (2013).

379. G. Wirnsberger *et al.*, Jagunal homolog 1 is a critical regulator of neutrophil function in fungal host defense. *Nat Genet* **46**, 1028–1033 (2014).

380. K. E. Schuit, Phagocytosis and intracellular killing of pathogenic yeasts by human monocytes and neutrophils. *Infection and Immunity* **24**, 932–938 (1979).

381. R. D. Nelson, E. L. Mills, R. L. Simmons, P. G. Quie, Chemiluminescence response of phagocytizing human monocytes. *Infection and Immunity* **14**, 129–134 (1976).

382. M. Sasada *et al.*, Candidacidal activity of monocyte-derived human macrophages:

relationship between Candida killing and oxygen radical generation by human macrophages. *Journal of Leukocyte Biology* **41**, 289–294 (1987).

383. L. Marodi, J. R. Forehand, R. B. Johnston, Mechanisms of host defense against Candida species. II. Biochemical basis for the killing of Candida by mononuclear phagocytes. *J Immunol* **146**, 2790–2794 (1991).

384. T. Decker, M. L. Lohmann-Matthes, M. Baccarini, Heterogeneous activity of immature and mature cells of the murine monocyte-macrophage lineage derived from different anatomical districts against yeast-phase Candida albicans. *Infection and Immunity* **54**, 477–486 (1986).

385. R. D. Diamond, C. C. Haudenschild, Monocyte-mediated Serum-independent Damage to Hyphal and Pseudohyphal Forms of Candida albicans In Vitro. *J Clin Invest* **67**, 173–182 (1981).

386. W. A. Pryor, G. L. Squadrito, The chemistry of peroxynitrite: a product from the reaction of nitric oxide with superoxide. *Am. J. Physiol.* **268**, L699–722 (1995).

387. M. G. Netea, J. W. M. V. D. Meer, I. Verschueren, B. J. Kullberg, CD40/CD40 ligand interactions in the host defense against disseminated Candida albicans infection: the role of macrophage-derived nitric oxide. *Eur. J. Immunol.* **32**, 1455–1463 (2002).

388. A. Vazquez-Torres, J. Jones-Carson, E. Balish, Peroxynitrite contributes to the candidacidal activity of nitric oxide-producing macrophages. *Infection and Immunity* **64**, 3127–3133 (1996).

389. E. Brummer, C. J. Morrison, D. A. Stevens, Recombinant and natural gamma-interferon activation of macrophages in vitro: different dose requirements for induction of killing activity against phagocytizable and nonphagocytizable fungi. *Infection and Immunity* **49**, 724–730 (1985).

390. C. F. Nathan, H. W. Murray, M. E. Wiebe, B. Y. Rubin, Identification of interferon-gamma as the lymphokine that activates human macrophage oxidative metabolism and antimicrobial activity. *J Exp Med* **158**, 670–689 (1983).

391. K. Watanabe, K. Kagaya, T. Yamada, Y. Fukazawa, Mechanism for candidacidal activity in macrophages activated by recombinant gamma interferon. *Infection and Immunity* **59**, 521–528 (1991).

392. N. Vazquez, T. J. Walsh, D. Friedman, S. J. Chanock, C. A. Lyman, Interleukin-15 augments superoxide production and microbicidal activity of human monocytes against Candida albicans. *Infection and Immunity* **66**, 145–150 (1998).

393. P. D. Smith *et al.*, Granulocyte-macrophage colony-stimulating factor augments human monocyte fungicidal activity for Candida albicans. *J. Infect. Dis.* **161**, 999–1005 (1990).

394. E. Roilides *et al.*, Ex vivo effects of macrophage colony-stimulating factor on human monocyte activity against fungal and bacterial pathogens. *Cytokine* **8**, 42–48 (1996).

395. E. Roilides *et al.*, Interleukin-4 suppresses antifungal activity of human mononuclear phagocytes against Candida albicans in association with decreased uptake of blastoconidia. *FEMS Immunology & Medical Microbiology* **19**, 169–180 (1997).

396. E. Roilides *et al.*, Suppressive effects of interleukin-10 on human mononuclear phagocyte function against Candida albicans and Staphylococcus aureus. *J. Infect. Dis.* **178**, 1734–1742

(1998).

397. E. Cenci *et al.*, Interleukin-4 and interleukin-10 inhibit nitric oxide-dependent macrophage killing of Candida albicans. *Eur. J. Immunol.* **23**, 1034–1038 (1993).

398. M. Castro, J. A. Bjoraker, M. S. Rohrbach, A. H. Limper, Candida albicans induces the release of inflammatory mediators from human peripheral blood monocytes. *Inflammation* **20**, 107–122 (1996).

399. J. Y. Djeu, D. K. Blanchard, A. L. Richards, H. Friedman, Tumor necrosis factor induction by Candida albicans from human natural killer cells and monocytes. *J Immunol* **141**, 4047–4052 (1988).

400. M. A. Vadas *et al.*, Mononuclear cell-mediated enhancement of granulocyte function in man. *J Immunol* **133**, 202–207 (1984).

401. Q. Qian, M. A. Jutila, N. Van Rooijen, J. E. Cutler, Elimination of mouse splenic macrophages correlates with increased susceptibility to experimental disseminated candidiasis. *J Immunol* **152**, 5000–5008 (1994).

402. J. W. van t Wout, I. Linde, P. C. Leijh, R. van Furth, Contribution of granulocytes and monocytes to resistance against experimental disseminated Candida albicans infection. *Eur. J. Clin. Microbiol. Infect. Dis.* **7**, 736–741 (1988).

403. F. Geissmann, S. Jung, D. R. Littman, Blood monocytes consist of two principal subsets with distinct migratory properties. *Immunity* **19**, 71–82 (2003).

404. M. A. Ingersoll *et al.*, Comparison of gene expression profiles between human and mouse monocyte subsets. *Blood* **115**, e10–9 (2010).

405. L. Y. Ngo *et al.*, Inflammatory monocytes mediate early and organ-specific innate defense during systemic candidiasis. *J. Infect. Dis.* **209**, 109–119 (2014).

406. M. S. Lionakis *et al.*, CX3CR1-dependent renal macrophage survival promotes Candida control and host survival. *J Clin Invest* **123**, 5035–5051 (2013).

407. D. C. Vinh *et al.*, Autosomal dominant and sporadic monocytopenia with susceptibility to mycobacteria, fungi, papillomaviruses, and myelodysplasia. *Blood* **115**, 1519–1529 (2010).

408. A. P. Hsu *et al.*, Mutations in GATA2 are associated with the autosomal dominant and sporadic monocytopenia and mycobacterial infection (MonoMAC) syndrome. *Blood* **118**, 2653–2655 (2011).

409. S. Hambleton *et al.*, IRF8 mutations and human dendritic-cell immunodeficiency. *N. Engl. J. Med.* **365**, 127–138 (2011).

410. W. C. Van Voorhis *et al.*, Relative efficacy of human monocytes and dendritic cells as accessory cells for T cell replication. *J Exp Med* **158**, 174–191 (1983).

411. Q. Huang *et al.*, The plasticity of dendritic cell responses to pathogens and their components. *Science* **294**, 870–875 (2001).

412. Z. G. Ramirez-Ortiz, T. K. Means, The role of dendritic cells in the innate recognition of pathogenic fungi (A. fumigatus, C. neoformans and C. albicans). *Virulence* **3**, 635–646 (2012).

413. C. F. d'Ostiani *et al.*, Dendritic cells discriminate between yeasts and hyphae of the fungus Candida albicans. Implications for initiation of T helper cell immunity in vitro and in vivo. *J Exp Med* **191**, 1661–1674 (2000).

414. S. L. Newman, A. Holly, Candida albicans is phagocytosed, killed, and processed for antigen presentation by human dendritic cells. *Infection and Immunity* **69**, 6813–6822 (2001).

415. G. Romagnoli *et al.*, The interaction of human dendritic cells with yeast and germ-tube forms of Candida albicans leads to efficient fungal processing, dendritic cell maturation, and acquisition of a Th1 response-promoting function. *Journal of Leukocyte Biology* **75**, 117–126 (2004).

416. M. G. Netea *et al.*, Human dendritic cells are less potent at killing Candida albicans than both monocytes and macrophages. *Microbes Infect* **6**, 985–989 (2004).

417. N. Pöntynen *et al.*, Critical immunological pathways are downregulated in APECED patient dendritic cells. *J. Mol. Med.* **86**, 1139–1152 (2008).

418. K. R. Ryan *et al.*, Impaired dendritic cell maturation and cytokine production in patients with chronic mucocutanous candidiasis with or without APECED. *Clin. Exp. Immunol.* **154**, 406–414 (2008).

419. J. Roder, A. Duwe, The beige mutation in the mouse selectively impairs natural killer cell function. *Nature* **278**, 451–453 (1979).

420. A. Baghian, K. W. Lee, Systemic candidosis in beige mice. *J. Med. Vet. Mycol.* **27**, 51–55 (1989).

421. E. Balish, T. Warner, C. J. Pierson, D. M. Bock, R. D. Wagner, Oroesophageal candidiasis is lethal for transgenic mice with combined natural killer and T-cell defects. *Med. Mycol.* **39**, 261–268 (2001).

422. J. J. Gaforio, E. Ortega, I. Algarra, M. J. Serrano, G. Alvarez de Cienfuegos, NK cells mediate increase of phagocytic activity but not of proinflammatory cytokine (interleukin-6 [IL-6], tumor necrosis factor alpha, and IL-12) production elicited in splenic macrophages by tilorone treatment of mice during acute systemic candidiasis. *Clin. Diagn. Lab. Immunol.* **9**, 1282–1294 (2002).

423. E. Ortega *et al.*, Enhanced resistance to experimental systemic candidiasis in tilorone-treated mice. *FEMS Immunology & Medical Microbiology* **28**, 283–289 (2000).

424. I. Algarra, E. Ortega, M. J. Serrano, G. Alvarez de Cienfuegos, J. J. Gaforio, Suppression of splenic macrophage Candida albicans phagocytosis following in vivo depletion of natural killer cells in immunocompetent BALB/c mice and T-cell-deficient nude mice. *FEMS Immunology & Medical Microbiology* **33**, 159–163 (2002).

425. H. L. Mathews, L. Witek-Janusek, Antifungal activity of interleukin-2-activated natural killer (NK1.1+) lymphocytes against Candida albicans. *J. Med. Microbiol.* **47**, 1007–1014 (1998).

426. S. J. Zunino, D. Hudig, Interactions between human natural killer (NK) lymphocytes and yeast cells: human NK cells do not kill Candida albicans, although C. albicans blocks NK lysis of K562 cells. *Infection and Immunity* **56**, 564–569 (1988).

427. G. Arancia *et al.*, Noninhibitory binding of human interleukin-2-activated natural killer cells

to the germ tube forms of Candida albicans. *Infection and Immunity* **63**, 280–288 (1995).

428. L. Scaringi *et al.*, Local and systemic immune response to inactivated Candida albicans in mice. *Nat Immun* **14**, 234–249 (1995).

429. S. M. Levitz, E. A. North, gamma Interferon gene expression and release in human lymphocytes directly activated by Cryptococcus neoformans and Candida albicans. *Infection and Immunity* **64**, 1595–1599 (1996).

430. J. Y. Djeu, D. K. Blanchard, Regulation of human polymorphonuclear neutrophil (PMN) activity against Candida albicans by large granular lymphocytes via release of a PMN-activating factor. *J Immunol* **139**, 2761–2767 (1987).

431. J. E. Cutler, Acute systemic candidiasis in normal and congenitally thymic-deficient (nude) mice. *J Reticuloendothel Soc* **19**, 121–124 (1976).

432. T. J. Rogers, E. Balish, D. D. Manning, The role of thymus-dependent cell-mediated immunity in resistance to experimental disseminated candidiasis. *J Reticuloendothel Soc* **20**, 291–298 (1976).

433. A. Fulurija, R. B. Ashman, J. M. Papadimitriou, Increased tissue resistance in the nude mouse against Candida albicans without altering strain-dependent differences in susceptibility. *J. Med. Vet. Mycol.* **35**, 197–203 (1997).

434. D. Tavares, P. Ferreira, M. Arala-Chaves, Increased resistance to systemic candidiasis in athymic or interleukin-10-depleted mice. *J. Infect. Dis.* **182**, 266–273 (2000).

435. S. P. Saville, A. L. Lazzell, A. K. Chaturvedi, C. Monteagudo, J. L. Lopez-Ribot, Use of a genetically engineered strain to evaluate the pathogenic potential of yeast cell and filamentous forms during Candida albicans systemic infection in immunodeficient mice. *Infect. Immun.* **76**, 97–102 (2008).

436. D. K. Giger, J. E. Domer, S. A. Moser, J. T. McQuitty, Experimental murine candidiasis: pathological and immune responses in T-lymphocyte-depleted mice. *Infection and Immunity* **21**, 729–737 (1978).

437. S. Mahanty, R. A. Greenfield, W. A. Joyce, P. W. Kincade, Inoculation candidiasis in a murine model of severe combined immunodeficiency syndrome. *Infection and Immunity* **56**, 3162–3166 (1988).

438. E. Balish, J. Jensen, T. Warner, J. Brekke, B. Leonard, Mucosal and disseminated candidiasis in gnotobiotic SCID mice. *J. Med. Vet. Mycol.* **31**, 143–154 (1993).

439. L. A. Coker, C. M. Mercadal, B. T. Rouse, R. N. Moore, Differential effects of CD4+ and CD8+ cells in acute, systemic murine candidosis. *Journal of Leukocyte Biology* **51**, 305–306 (1992).

440. L. Romani *et al.*, Course of primary candidiasis in T cell-depleted mice infected with attenuated variant cells. *J. Infect. Dis.* **166**, 1384–1392 (1992).

441. R. B. Ashman, A. Fulurija, J. M. Papadimitriou, Both CD4+ and CD8+ lymphocytes reduce the severity of tissue lesions in murine systemic cadidiasis, and CD4+ cells also demonstrate strain-specific immunopathological effects. *Microbiology (Reading, Engl.)* **145 (Pt 7)**, 1631–1640 (1999).

442. E. Balish, F. A. Vazquez-Torres, J. Jones-Carson, R. D. Wagner, T. Warner, Importance of beta2-microglobulin in murine resistance to mucosal and systemic candidiasis. *Infection and Immunity* **64**, 5092–5097 (1996).

443. J. Jones-Carson, A. Vazquez-Torres, T. Warner, E. Balish, Disparate requirement for T cells in resistance to mucosal and acute systemic candidiasis. *Infection and Immunity* **68**, 2363–2365 (2000).

444. E. W. Carrow, R. F. Hector, J. E. Domer, Immunodeficient CBA/N mice respond effectively to Candida albicans. *Clin. Immunol. Immunopathol.* **33**, 371–380 (1984).

445. U. Kuruganti *et al.*, Nonspecific and Candida-specific immune responses in mice suppressed by chronic administration of anti-mu. *Journal of Leukocyte Biology* **44**, 422–433 (1988).

446. C. Montagnoli *et al.*, A role for antibodies in the generation of memory antifungal immunity. *Eur. J. Immunol.* **33**, 1193–1204 (2003).

447. A. B. van Spriel *et al.*, The tetraspanin protein CD37 regulates IgA responses and anti-fungal immunity. *PLoS Pathog* **5**, e1000338 (2009).

448. R. D. Diamond, C. A. Lyman, D. R. Wysong, Disparate effects of interferon-gamma and tumor necrosis factor-alpha on early neutrophil respiratory burst and fungicidal responses to Candida albicans hyphae in vitro. *J Clin Invest* **87**, 711–720 (1991).

449. A. Stevenhagen, R. van Furth, Interferon-gamma activates the oxidative killing of Candida albicans by human granulocytes. *Clin. Exp. Immunol.* **91**, 170–175 (1993).

450. S. Tansho, S. Abe, H. Yamaguchi, Inhibition of Candida albicans growth by murine peritoneal neutrophils and augmentation of the inhibitory activity by bacterial lipopolysaccharide and cytokines. *Microbiol. Immunol.* **38**, 379–383 (1994).

451. J. M. Gaviria, J. A. van Burik, D. C. Dale, R. K. Root, W. C. Liles, Comparison of interferon-gamma, granulocyte colony-stimulating factor, and granulocyte-macrophage colony-stimulating factor for priming leukocyte-mediated hyphal damage of opportunistic fungal pathogens. *J. Infect. Dis.* **179**, 1038–1041 (1999).

452. E. Blasi, S. Farinelli, L. Varesio, F. Bistoni, Augmentation of GG2EE macrophage cell line-mediated anti-Candida activity by gamma interferon, tumor necrosis factor, and interleukin-1. *Infection and Immunity* **58**, 1073–1077 (1990).

453. H. P. Redmond, J. Shou, H. J. Gallagher, C. J. Kelly, J. M. Daly, Macrophage-dependent candidacidal mechanisms in the murine system. Comparison of murine Kupffer cell and peritoneal macrophage candidacidal mechanisms. *J Immunol* **150**, 3427–3433 (1993).

454. R. Káposzta, P. Tree, L. Marodi, S. Gordon, Characteristics of invasive candidiasis in gamma interferon- and interleukin-4-deficient mice: role of macrophages in host defense against Candida albicans. *Infection and Immunity* **66**, 1708–1717 (1998).

455. E. Balish, R. D. Wagner, A. Vazquez-Torres, C. Pierson, T. Warner, Candidiasis in interferon-gamma knockout (IFN-gamma-/-) mice. *J. Infect. Dis.* **178**, 478–487 (1998).

456. E. Cenci *et al.*, IFN-gamma is required for IL-12 responsiveness in mice with Candida albicans infection. *J Immunol* **161**, 3543–3550 (1998).

457. D. A. A. Vignali, V. K. Kuchroo, IL-12 family cytokines: immunological playmakers. *Nat*

Immunol **13**, 722–728 (2012).

458. M. G. Netea *et al.*, Differential role of IL-18 and IL-12 in the host defense against disseminated Candida albicans infection. *Eur. J. Immunol.* **33**, 3409–3417 (2003).

459. L. M. Lavigne, L. R. Schopf, C. L. Chung, R. Maylor, J. P. Sypek, The role of recombinant murine IL-12 and IFN-gamma in the pathogenesis of a murine systemic Candida albicans infection. *J Immunol* **160**, 284–292 (1998).

460. A. Mencacci *et al.*, IL-10 is required for development of protective Th1 responses in IL-12-deficient mice upon Candida albicans infection. *J Immunol* **161**, 6228–6237 (1998).

461. H. Okamura *et al.*, Cloning of a new cytokine that induces IFN-gamma production by T cells. *Nature* **378**, 88–91 (1995).

462. D. Robinson *et al.*, IGIF does not drive Th1 development but synergizes with IL-12 for interferon-gamma production and activates IRAK and NFkappaB. *Immunity* **7**, 571–581 (1997).

463. G. Fantuzzi, D. A. Reed, C. A. Dinarello, IL-12-induced IFN-gamma is dependent on caspase-1 processing of the IL-18 precursor. *J Clin Invest* **104**, 761–767 (1999).

464. R. J. L. Stuyt *et al.*, Role of interleukin-18 in host defense against disseminated Candida albicans infection. *Infection and Immunity* **70**, 3284–3286 (2002).

465. R. J. L. Stuyt, M. G. Netea, J. H. Van Krieken, J. W. M. Van Der Meer, B. J. Kullberg, Recombinant interleukin-18 protects against disseminated Candida albicans infection in mice. *J. Infect. Dis.* **189**, 1524–1527 (2004).

466. M. G. Netea *et al.*, The role of endogenous interleukin (IL)-18, IL-12, IL-1beta, and tumor necrosis factor-alpha in the production of interferon-gamma induced by Candida albicans in human whole-blood cultures. *J. Infect. Dis.* **185**, 963–970 (2002).

467. M. G. Netea, B. J. Kullberg, J. W. M. van der Meer, Severely impaired IL-12/IL-18/IFNgamma axis in patients with hyper IgE syndrome. *Eur. J. Clin. Invest.* **35**, 718–721 (2005).

468. L. Romani *et al.*, Neutralizing antibody to interleukin 4 induces systemic protection and T helper type 1-associated immunity in murine candidiasis. *J Exp Med* **176**, 19–25 (1992).

469. L. Tonnetti *et al.*, Interleukin-4 and -10 exacerbate candidiasis in mice. *Eur. J. Immunol.* **25**, 1559–1565 (1995).

470. E. Roilides *et al.*, Suppressive Effects of Interleukin-10 on Human Mononuclear Phagocyte Function against Candida albicansand Staphylococcus aureus. *Journal of Infectious Diseases* **178**, 1734–1742 (1998).

471. S. M. Levitz, A. Tabuni, S. H. Nong, D. T. Golenbock, Effects of interleukin-10 on human peripheral blood mononuclear cell responses to Cryptococcus neoformans, Candida albicans, and lipopolysaccharide. *Infection and Immunity* **64**, 945–951 (1996).

472. L. Romani *et al.*, Neutralization of IL-10 up-regulates nitric oxide production and protects susceptible mice from challenge with Candida albicans. *J Immunol* **152**, 3514–3521 (1994).

473. A. Vazquez-Torres, J. Jones-Carson, R. D. Wagner, T. Warner, E. Balish, Early resistance of

interleukin-10 knockout mice to acute systemic candidiasis. *Infection and Immunity* **67**, 670–674 (1999).

474. S. Naundorf *et al.*, IL-10 interferes directly with TCR-induced IFN-gamma but not IL-17 production in memory T cells. *Eur. J. Immunol.* **39**, 1066–1077 (2009).

475. A. Mencacci *et al.*, Endogenous interleukin 4 is required for development of protective CD4+ T helper type 1 cell responses to Candida albicans. *J Exp Med* **187**, 307–317 (1998).

476. C. Montagnoli *et al.*, B7/CD28-dependent CD4+CD25+ regulatory T cells are essential components of the memory-protective immunity to Candida albicans. *J Immunol* **169**, 6298–6308 (2002).

477. L. E. Harrington *et al.*, Interleukin 17-producing CD4+ effector T cells develop via a lineage distinct from the T helper type 1 and 2 lineages. *Nature Publishing Group* **6**, 1123–1132 (2005).

478. B. Stockinger, M. Veldhoen, B. Martin, Th17 T cells: linking innate and adaptive immunity. *Semin. Immunol.* **19**, 353–361 (2007).

479. P. Schwarzenberger *et al.*, IL-17 stimulates granulopoiesis in mice: use of an alternate, novel gene therapy-derived method for in vivo evaluation of cytokines. *J Immunol* **161**, 6383–6389 (1998).

480. M. A. Stark *et al.*, Phagocytosis of apoptotic neutrophils regulates granulopoiesis via IL-23 and IL-17. *Immunity* **22**, 285–294 (2005).

481. T. Dejima *et al.*, Protective Role of Naturally Occurring Interleukin-17A-Producing T Cells in the Lung at the Early Stage of Systemic Candidiasis in Mice. *Infection and Immunity* **79**, 4503–4510 (2011).

482. H. R. Conti *et al.*, Th17 cells and IL-17 receptor signaling are essential for mucosal host defense against oral candidiasis. *Journal of Experimental Medicine* **206**, 299–311 (2009).

483. A. Gladiator, N. Wangler, K. Trautwein-Weidner, S. LeibundGut-Landmann, Cutting edge: IL-17-secreting innate lymphoid cells are essential for host defense against fungal infection. *The Journal of Immunology* **190**, 521–525 (2013).

484. H. R. Conti *et al.*, Oral-resident natural Th17 cells and γδ T cells control opportunistic Candida albicans infections. *Journal of Experimental Medicine* **211**, 2075–2084 (2014).

485. J. D. Milner *et al.*, Impaired T(H)17 cell differentiation in subjects with autosomal dominant hyper-IgE syndrome. *Nature* **452**, 773–U11 (2008).

486. C. S. Ma *et al.*, Deficiency of Th17 cells in hyper IgE syndrome due to mutations in STAT3. *Journal of Experimental Medicine* **205**, 1551–1557 (2008).

487. F. L. van de Veerdonk *et al.*, Milder clinical hyperimmunoglobulin E syndrome phenotype is associated with partial interleukin-17 deficiency. *Clin. Exp. Immunol.* **159**, 57–64 (2010).

488. K. Kisand *et al.*, Chronic mucocutaneous candidiasis in APECED or thymoma patients correlates with autoimmunity to Th17-associated cytokines. *Journal of Experimental Medicine* **207**, 299–308 (2010).

489. A. Puel *et al.*, Autoantibodies against IL-17A, IL-17F, and IL-22 in patients with chronic

mucocutaneous candidiasis and autoimmune polyendocrine syndrome type I. *Journal of Experimental Medicine* **207**, 291–297 (2010).

490. F. L. van de Veerdonk *et al.*, STAT1 mutations in autosomal dominant chronic mucocutaneous candidiasis. *N. Engl. J. Med.* **365**, 54–61 (2011).

491. L. Liu *et al.*, Gain-of-function human STAT1 mutations impair IL-17 immunity and underlie chronic mucocutaneous candidiasis. *Journal of Experimental Medicine* **208**, 1635–1648 (2011).

492. S. G. Filler, D. C. Sheppard, Fungal invasion of normally non-phagocytic host cells. *PLoS Pathog* **2**, e129 (2006).

493. M. G. Netea, G. D. Brown, B. J. Kullberg, N. A. R. Gow, An integrated model of the recognition of Candida albicans by the innate immune system. *Nat Rev Micro* **6**, 67–78 (2008).

494. G. Chamilos, M. S. Lionakis, R. E. Lewis, D. P. Kontoyiannis, Role of mini-host models in the study of medically important fungi. *Lancet Infect Dis* **7**, 42–55 (2007).

495. D. M. Maccallum, Candida infections and modelling disease. 41–67 (2010).

496. A.-M. Alarco *et al.*, Immune-deficient Drosophila melanogaster: a model for the innate immune response to human fungal pathogens. *J Immunol* **172**, 5622–5628 (2004).

497. S. L. Stroschein-Stevenson, E. Foley, P. H. O'Farrell, A. D. Johnson, Identification of Drosophila gene products required for phagocytosis of Candida albicans. *Plos Biol* **4**, e4 (2006).

498. G. Chamilos *et al.*, Drosophila melanogaster as a facile model for large-scale studies of virulence mechanisms and antifungal drug efficacy in Candida species. *J. Infect. Dis.* **193**, 1014–1022 (2006).

499. M. Gottar *et al.*, Dual detection of fungal infections in Drosophila via recognition of glucans and sensing of virulence factors. *Cell* **127**, 1425–1437 (2006).

500. A. Levitin *et al.*, Drosophila melanogaster Thor and response to Candida albicans infection. *Eukaryotic Cell* **6**, 658–663 (2007).

501. M. B. Lohse, A. D. Johnson, Differential phagocytosis of white versus opaque Candida albicans by Drosophila and mouse phagocytes. *PLoS ONE* **3**, e1473 (2008).

502. G. Chamilos *et al.*, Candida albicans Cas5, a regulator of cell wall integrity, is required for virulence in murine and toll mutant fly models. *J. Infect. Dis.* **200**, 152–157 (2009).

503. R. A. Hall *et al.*, CO(2) acts as a signalling molecule in populations of the fungal pathogen Candida albicans. *PLoS Pathog* **6**, e1001193 (2010).

504. R. I. Clark *et al.*, MEF2 Is an In Vivo Immune-Metabolic Switch. *Cell* **155**, 435–447 (2013).

505. G. Cotter, S. Doyle, K. Kavanagh, Development of an insect model for the in vivo pathogenicity testing of yeasts. *FEMS Immunology & Medical Microbiology* **27**, 163–169 (2000).

506. M. Brennan, D. Y. Thomas, M. Whiteway, K. Kavanagh, Correlation between virulence of

Candida albicans mutants in mice and Galleria mellonella larvae. *FEMS Immunology & Medical Microbiology* **34**, 153–157 (2002).

507. G. B. Dunphy, U. Oberholzer, M. Whiteway, R. J. Zakarian, I. Boomer, Virulence of Candida albicans mutants toward larval Galleria mellonella (Insecta, Lepidoptera, Galleridae). *Can. J. Microbiol.* **49**, 514–524 (2003).

508. D. Bergin, L. Murphy, J. Keenan, M. Clynes, K. Kavanagh, Pre-exposure to yeast protects larvae of Galleria mellonella from a subsequent lethal infection by Candida albicans and is mediated by the increased expression of antimicrobial peptides. *Microbes Infect* **8**, 2105–2112 (2006).

509. L. E. Cowen *et al.*, Harnessing Hsp90 function as a powerful, broadly effective therapeutic strategy for fungal infectious disease. *Proc. Natl. Acad. Sci. U.S.A.* **106**, 2818–2823 (2009).

510. C. H. Kim *et al.*, An insect multiligand recognition protein functions as an opsonin for the phagocytosis of microorganisms. *J Biol Chem* **285**, 25243–25250 (2010).

511. D.-D. Li *et al.*, Using Galleria mellonella-Candida albicans infection model to evaluate antifungal agents. *Biol. Pharm. Bull.* **36**, 1482–1487 (2013).

512. E. Borghi *et al.*, Correlation between Candida albicans biofilm formation and invasion of the invertebrate host Galleria mellonella. *Future Microbiol* **9**, 163–173 (2014).

513. J. Breger *et al.*, Antifungal chemical compounds identified using a C. elegans pathogenicity assay. *PLoS Pathog* **3**, e18 (2007).

514. A. Y. Peleg *et al.*, Prokaryote-eukaryote interactions identified by using Caenorhabditis elegans. *Proc. Natl. Acad. Sci. U.S.A.* **105**, 14585–14590 (2008).

515. R. Pukkila-Worley, A. Y. Peleg, E. Tampakakis, E. Mylonakis, Candida albicans hyphal formation and virulence assessed using a Caenorhabditis elegans infection model. *Eukaryotic Cell* **8**, 1750–1758 (2009).

516. R. Pukkila-Worley, F. M. Ausubel, E. Mylonakis, Candida albicans infection of Caenorhabditis elegans induces antifungal immune defenses. *PLoS Pathog* **7**, e1002074 (2011).

517. C. Jain, K. Pastor, A. Y. Gonzalez, M. C. Lorenz, R. P. Rao, The role of Candida albicans AP-1 protein against host derived ROS in in vivo models of infection. **4**, 67–76 (2013).

518. E. K. Szabo, D. M. Maccallum, The contribution of mouse models to our understanding of systemic candidiasis. *FEMS Microbiol. Lett.* **320**, 1–8 (2011).

519. D. B. Louria, R. G. Brayton, G. Finkel, Studies on the pathogenesis of experimental Candida albicansinfections in mice. *Med. Mycol.* **2**, 271–283 (1963).

520. J. M. Papadimitriou, R. B. Ashman, The pathogenesis of acute systemic candidiasis in a susceptible inbred mouse strain. *J. Pathol.* **150**, 257–265 (1986).

521. D. M. Maccallum, F. C. Odds, Temporal events in the intravenous challenge model for experimental Candida albicans infections in female mice. *Mycoses* **48**, 151–161 (2005).

522. L. de Repentigny, M. Phaneuf, L. G. Mathieu, Gastrointestinal colonization and systemic dissemination by Candida albicans and Candida tropicalis in intact and

immunocompromised mice. *Infection and Immunity* **60**, 4907–4914 (1992).

523. L. de Repentigny, Animal models in the analysis of Candida host-pathogen interactions. *Curr. Opin. Microbiol.* **7**, 324–329 (2004).

524. F. C. Odds, L. Van Nuffel, N. A. Gow, Survival in experimental Candida albicans infections depends on inoculum growth conditions as well as animal host. *Microbiology (Reading, Engl.)* **146 (Pt 8)**, 1881–1889 (2000).

525. A. Baghian, K. W. Lee, Elimination of Candida albicans from kidneys of mice during short-term systemic infections. *Kidney Int* **40**, 400–405 (1991).

526. M. Richardson, R. Rautemaa, How the host fights against Candida infections. *Front Biosci* **14**, 4363–4375 (2009).

527. R. B. Ashman, Protective and pathologic immune responses against Candida albicans infection. *Front Biosci* **13**, 3334–3351 (2008).

528. B. Spellberg, A. S. Ibrahim, J. E. Edwards, S. G. Filler, Mice with disseminated candidiasis die of progressive sepsis. *J. Infect. Dis.* **192**, 336–343 (2005).

529. R. B. Ashman, Candida albicans: pathogenesis, immunity and host defence. *Res Immunol* **149**, 281–8; discussion 494–6 (1998).

530. L. M. Pope, G. T. Cole, M. N. Guentzel, L. J. Berry, Systemic and gastrointestinal candidiasis of infant mice after intragastric challenge. *Infection and Immunity* **25**, 702–707 (1979).

531. L. H. Field, L. M. Pope, G. T. Cole, M. N. Guentzel, L. J. Berry, Persistence and spread of Candida albicans after intragastric inoculation of infant mice. *Infection and Immunity* **31**, 783–791 (1981).

532. G. T. Cole, K. T. Lynn, K. R. Seshan, L. M. Pope, Gastrointestinal and systemic candidosis in immunocompromised mice. *J. Med. Vet. Mycol.* **27**, 363–380 (1989).

533. H. Sandovsky-Losica, L. Barr-Nea, E. Segal, Fatal systemic candidiasis of gastrointestinal origin: an experimental model in mice compromised by anti-cancer treatment. *J. Med. Vet. Mycol.* **30**, 219–231 (1992).

534. K. V. Clemons *et al.*, Development of an orogastrointestinal mucosal model of candidiasis with dissemination to visceral organs. *Antimicrobial Agents and Chemotherapy* **50**, 2650–2657 (2006).

535. E. Mellado *et al.*, Sustained gastrointestinal colonization and systemic dissemination by Candida albicans, Candida tropicalis and Candida parapsilosis in adult mice. *Diagn. Microbiol. Infect. Dis.* **38**, 21–28 (2000).

536. A. Y. Koh, J. R. Köhler, K. T. Coggshall, N. van Rooijen, G. B. Pier, Mucosal damage and neutropenia are required for Candida albicans dissemination. *PLoS Pathog* **4**, e35 (2008).

537. G. T. Cole, K. R. Seshan, L. M. Pope, R. J. Yancey, Morphological aspects of gastrointestinal tract invasion by Candida albicans in the infant mouse. *J. Med. Vet. Mycol.* **26**, 173–185 (1988).

538. L. M. Silver, *Mouse Genetics: Concepts and Applications* (Oxford University Press, 1995).

539. M. J. Corbel, S. M. Eades, The relative susceptibility of New Zealand black and CBA mice to infection with opportunistic fungal pathogens. *Sabouraudia* **14**, 17–32 (1976).

540. F. Bistoni, P. Marconi, L. Frati, E. Bonmassar, E. Garaci, Increase of mouse resistance to Candida albicans infection by thymosin alpha 1. *Infection and Immunity* **36**, 609–614 (1982).

541. S. B. Salvin, R. Neta, Resistance and susceptibility to infection in inbred murine strains. I. Variations in the response to thymic hormones in mice infected with Candida albicans. *Cell Immunol* **75**, 160–172 (1983).

542. A. Tuite, A. Mullick, P. Gros, Genetic analysis of innate immunity in resistance to Candida albicans. *Genes Immun* **5**, 576–587 (2004).

543. R. A. Wetsel, D. T. Fleischer, D. L. Haviland, Deficiency of the murine fifth complement component (C5). A 2-base pair gene deletion in a 5'-exon. *J Biol Chem* **265**, 2435–2440 (1990).

544. Y. M. Ooi, H. R. Colten, Genetic defect in secretion of complement C5 in mice. *Nature* **282**, 207–208 (1979).

545. G. Marquis, S. Montplaisir, M. Pelletier, S. Mousseau, P. Auger, Strain-dependent differences in susceptibility of mice to experimental candidosis. *J. Infect. Dis.* **154**, 906–909 (1986).

546. P. Démant, A. A. Hart, Recombinant congenic strains--a new tool for analyzing genetic traits determined by more than one gene. *Immunogenetics* **24**, 416–422 (1986).

547. A. Fortin *et al.*, Recombinant congenic strains derived from A/J and C57BL/6J: a tool for genetic dissection of complex traits. *Genomics* **74**, 21–35 (2001).

548. E. Diez *et al.*, Birc1e is the gene within the Lgn1 locus associated with resistance to Legionella pneumophila. *Nat Genet* **33**, 55–60 (2003).

549. G. Min-Oo *et al.*, Pyruvate kinase deficiency in mice protects against malaria. *Nat Genet* **35**, 357–362 (2003).

550. M.-F. Roy *et al.*, Pyruvate kinase deficiency confers susceptibility to Salmonella typhimurium infection in mice. *Journal of Experimental Medicine* **204**, 2949–2961 (2007).

551. G. A. Boivin *et al.*, Mapping of clinical and expression quantitative trait loci in a sex-dependent effect of host susceptibility to mouse-adapted influenza H3N2/HK/1/68. *The Journal of Immunology* **188**, 3949–3960 (2012).

552. C. Meunier *et al.*, Characterization of a major colon cancer susceptibility locus (Ccs3) on mouse chromosome 3. *Oncogene* **29**, 647–661 (2010).

553. A.-M. Lemay, C. K. Haston, Radiation-induced lung response of AcB/BcA recombinant congenic mice. *Radiat. Res.* **170**, 299–306 (2008).

554. P. Camateros *et al.*, Identification of novel chromosomal regions associated with airway hyperresponsiveness in recombinant congenic strains of mice. *Mamm Genome* **21**, 28–38 (2010).

555. R. B. Ashman, J. M. Papadimitriou, Murine candidiasis. Pathogenesis and host responses in genetically distinct inbred mice. *Immunol Cell Biol* **65 (Pt 2)**, 163–171 (1987).

556. R. B. Ashman, J. M. Papadimitriou, Genetic resistance to Candida albicans infection is conferred by cells derived from the bone marrow. *J. Infect. Dis.* **166**, 947–948 (1992).

557. R. B. Ashman, A. Fulurija, J. M. Papadimitriou, Evidence that two independent host genes influence the severity of tissue damage and susceptibility to acute pyelonephritis in murine systemic candidiasis. *Microb. Pathog.* **22**, 187–192 (1997).

558. H. L. Mathews, L. Witek-Janusek, in *Candida and candidiasis*, C. R. ed, Ed. (ASM Press, Washington, DC., 2002), pp. 179–192.

559. B. J. Spellberg, S. G. Filler, J. E. Edwards, Current treatment strategies for disseminated candidiasis. *Clin Infect Dis* **42**, 244–251 (2006).

560. J. Morgan, Global trends in candidemia: review of reports from 1995-2005. *Curr Infect Dis Rep* **7**, 429–439 (2005).

561. O. Gudlaugsson *et al.*, Attributable mortality of nosocomial candidemia, revisited. *Clin Infect Dis* **37**, 1172–1177 (2003).

562. M. G. Shepherd, R. T. Poulter, P. A. Sullivan, Candida albicans: biology, genetics, and pathogenicity. *Annu Rev Microbiol* **39**, 579–614 (1985).

563. F. Lanza, Clinical manifestation of myeloperoxidase deficiency. *J. Mol. Med.* **76**, 676–681 (1998).

564. S. M. Holland *et al.*, STAT3 mutations in the hyper-IgE syndrome. *N. Engl. J. Med.* **357**, 1608–1619 (2007).

565. J. C. Rhodes, L. S. Wicker, W. J. Urba, Genetic control of susceptibility to Cryptococcus neoformans in mice. *Infection and Immunity* **29**, 494–499 (1980).

566. E. Brummer, D. A. Stevens, Anticryptococcal activity of macrophages: role of mouse strain, C5, contact, phagocytosis, and L-arginine. *Cell Immunol* **157**, 1–10 (1994).

567. J. D. Lambris, D. Ricklin, B. V. Geisbrecht, Complement evasion by human pathogens. *Nat Rev Micro* **6**, 132–142 (2008).

568. R. Zeller, Fixation, embedding, and sectioning of tissues, embryos, and single cells. *Curr Protoc Mol Biol* **Chapter 14**, Unit 14.1 (2001).

569. C. S. Haley, S. A. Knott, A simple regression method for mapping quantitative trait loci in line crosses using flanking markers. *Heredity* **69**, 315–324 (1992).

570. E. S. Lander, D. Botstein, Mapping mendelian factors underlying quantitative traits using RFLP linkage maps. *Genetics* **121**, 185–199 (1989).

571. K. W. Broman, H. Wu, S. Sen, G. A. Churchill, R/qtl: QTL mapping in experimental crosses. *Bioinformatics* **19**, 889–890 (2003).

572. H. M. Kang *et al.*, Efficient Control of Population Structure in Model Organism Association Mapping. *Genetics* **178**, 1709–1723 (2008).

573. J. M. Cheverud, A simple correction for multiple comparisons in interval mapping genome scans. *Heredity* **87**, 52–58 (2001).

574. K. A. Frazer *et al.*, A sequence-based variation map of 8.27 million SNPs in inbred mouse strains. *Nature* **448**, 1050–1053 (2007).

575. D. M. Maccallum, L. Castillo, A. J. P. Brown, N. A. R. Gow, F. C. Odds, Early-Expressed Chemokines Predict Kidney Immunopathology in Experimental Disseminated Candida albicans Infections. *PLoS ONE* **4**, e6420 (2009).

576. G. D. Kitsios, N. Tangri, P. J. Castaldi, J. P. Ioannidis, Laboratory mouse models for the human genome-wide associations. *PLoS ONE* **5**, e13782 (2010).

577. A. Kirby *et al.*, Fine mapping in 94 inbred mouse strains using a high-density haplotype resource. *Genetics* **185**, 1081–1095 (2010).

578. W.-L. Su *et al.*, Assessing the prospects of genome-wide association studies performed in inbred mice. *Mamm Genome* **21**, 143–152 (2010).

579. P. McClurg, M. T. Pletcher, T. Wiltshire, A. I. Su, Comparative analysis of haplotype association mapping algorithms. *BMC Bioinformatics* **7**, 61 (2006).

580. G. Manenti *et al.*, Mouse genome-wide association mapping needs linkage analysis to avoid false-positive Loci. *PLoS Genet* **5**, e1000331 (2009).

581. M. S. Cohen *et al.*, Fungal infection in chronic granulomatous disease. The importance of the phagocyte in defense against fungi. *Am. J. Med.* **71**, 59–66 (1981).

582. K. Schroder, P. J. Hertzog, T. Ravasi, D. A. Hume, Interferon-gamma: an overview of signals, mechanisms and functions. *Journal of Leukocyte Biology* **75**, 163–189 (2004).

583. M. M. Brierley, E. N. Fish, Stats: multifaceted regulators of transcription. *J Interferon Cytokine Res* **25**, 733–744 (2005).

584. G. Robertson *et al.*, Genome-wide profiles of STAT1 DNA association using chromatin immunoprecipitation and massively parallel sequencing. *Nat Methods* **4**, 651–657 (2007).

585. U. Seifert *et al.*, Immunoproteasomes preserve protein homeostasis upon interferon-induced oxidative stress. *Cell* **142**, 613–624 (2010).

586. B. Duan *et al.*, Distinct Roles of Adenylyl Cyclase VII in Regulating the Immune Responses in Mice. *The Journal of Immunology* **185**, 335–344 (2010).

587. P. A. Watson, J. Krupinski, A. M. Kempinski, C. D. Frankenfield, Molecular cloning and characterization of the type VII isoform of mammalian adenylyl cyclase expressed widely in mouse tissues and in S49 mouse lymphoma cells. *J Biol Chem* **269**, 28893–28898 (1994).

588. P. B. Ernst, J. C. Garrison, L. F. Thompson, Much ado about adenosine: adenosine synthesis and function in regulatory T cell biology. *The Journal of Immunology* **185**, 1993–1998 (2010).

589. A. L. Hertz *et al.*, Elevated cyclic AMP and PDE4 inhibition induce chemokine expression in human monocyte-derived macrophages. *Proc. Natl. Acad. Sci. U.S.A.* **106**, 21978–21983 (2009).

590. M. Peters-Golden, Putting on the brakes: cyclic AMP as a multipronged controller of macrophage function. *Science Signaling* **2**, pe37 (2009).

591. A. M. Buhl, N. Avdi, G. S. Worthen, G. L. Johnson, Mapping of the C5a receptor signal transduction network in human neutrophils. *Proc Natl Acad Sci USA* **91**, 9190–9194 (1994).

592. D. Choubey, R. Panchanathan, Interferon-inducible Ifi200-family genes in systemic lupus erythematosus. *Immunol Lett* **119**, 32–41 (2008).

593. S. E. Johnatty *et al.*, Evaluation of candidate stromal epithelial cross-talk genes identifies association between risk of serous ovarian cancer and TERT, a cancer susceptibility "hot-spot." *PLoS Genet* **6**, e1001016 (2010).

594. J. Tan *et al.*, IFP35 is involved in the antiviral function of interferon by association with the viral tas transactivator of bovine foamy virus. *J Virol* **82**, 4275–4283 (2008).

595. F. C. Bange *et al.*, IFP 35 is an interferon-induced leucine zipper protein that undergoes interferon-regulated cellular redistribution. *J Biol Chem* **269**, 1091–1098 (1994).

596. L. Zhang *et al.*, The PH domain containing protein CKIP-1 binds to IFP35 and Nmi and is involved in cytokine signaling. *Cell Signal* **19**, 932–944 (2007).

597. B. U. Schraml *et al.*, The AP-1 transcription factor Batf controls T(H)17 differentiation. *Nature* **460**, 405–409 (2009).

598. K. Eyerich *et al.*, Patients with chronic mucocutaneous candidiasis exhibit reduced production of Th17-associated cytokines IL-17 and IL-22. *J. Invest. Dermatol.* **128**, 2640–2645 (2008).

599. J. C. Rodriguez-Gallego *et al.*, Clinical Features of Candidiasis in Patients with Interleukin-12 Receptor B1 Deficiency. *J. Clin. Immunol.* **32**, 305–305 (2012).

600. F. Lanternier *et al.*, Human Invasive Dermatophytic Disease Is Caused by Inborn Errors of Card9. *J. Clin. Immunol.* **32**, 94–94 (2012).

601. D. Neofytos *et al.*, Epidemiology, outcomes, and risk factors of invasive fungal infections in adult patients with acute myelogenous leukemia after induction chemotherapy. *Diagn. Microbiol. Infect. Dis.* **75**, 144–149 (2013).

602. I. Radovanovic, A. Mullick, P. Gros, Genetic Control of Susceptibility to Infection with Candida albicans in Mice. *PLoS ONE* **6**, e18957 (2011).

603. K. W. Broman, Mapping quantitative trait loci in the case of a spike in the phenotype distribution. *Genetics* **163**, 1169–1175 (2003).

604. A. Mocsai *et al.*, G-protein-coupled receptor signaling in Syk-deficient neutrophils and mast cells. *Blood* **101**, 4155–4163 (2003).

605. S.-L. Ng *et al.*, IκB kinase epsilon (IKK(epsilon)) regulates the balance between type I and type II interferon responses. *Proc. Natl. Acad. Sci. U.S.A.* **108**, 21170–21175 (2011).

606. G. D. Barish *et al.*, Bcl-6 and NF-kappaB cistromes mediate opposing regulation of the innate immune response. *Genes Dev.* **24**, 2760–2765 (2010).

607. T. J. Fleming, M. L. Fleming, T. R. Malek, Selective expression of Ly-6G on myeloid lineage cells in mouse bone marrow. RB6-8C5 mAb to granulocyte-differentiation antigen (Gr-1) detects members of the Ly-6 family. *J Immunol* **151**, 2399–2408 (1993).

608. J. M. Daley, A. A. Thomay, M. D. Connolly, J. S. Reichner, J. E. Albina, Use of Ly6G-specific monoclonal antibody to deplete neutrophils in mice. *Journal of Leukocyte Biology* **83**, 64–70 (2008).

609. K. Hestdal *et al.*, Characterization and regulation of RB6-8C5 antigen expression on murine bone marrow cells. *J Immunol* **147**, 22–28 (1991).

610. J.-X. Wang *et al.*, Ly6G ligation blocks recruitment of neutrophils via a β2-integrin-dependent mechanism. *Blood* **120**, 1489–1498 (2012).

611. C. Auffray, M. H. Sieweke, F. Geissmann, Blood Monocytes: Development, Heterogeneity, and Relationship with Dendritic Cells. *Annu. Rev. Immunol.* **27**, 669–692 (2009).

612. N. V. Serbina, E. G. Pamer, Monocyte emigration from bone marrow during bacterial infection requires signals mediated by chemokine receptor CCR2. *Nature Publishing Group* **7**, 311–317 (2006).

613. D. Rifkind, J. A. Frey, Sex difference in antibody response of CFW mice to Candida albicans. *Infection and Immunity* **5**, 695–698 (1972).

614. A. Baba, T. Fujita, N. Tamura, Sexual dimorphism of the fifth component of mouse complement. *J Exp Med* **160**, 411–419 (1984).

615. R. B. Ashman, P. H. Kay, D. M. Lynch, J. M. Papadimitriou, Murine candidiasis: sex differences in the severity of tissue lesions are not associated with levels of serum C3 and C5. *Immunol Cell Biol* **69 (Pt 1)**, 7–10 (1991).

616. K.-P. Chuang *et al.*, Ligation of lymphocyte function-associated antigen-1 on monocytes decreases very late antigen-4-mediated adhesion through a reactive oxygen species-dependent pathway. *Blood* **104**, 4046–4053 (2004).

617. R. Sun *et al.*, Identification of neutrophil granule protein cathepsin G as a novel chemotactic agonist for the G protein-coupled formyl peptide receptor. *J Immunol* **173**, 428–436 (2004).

618. O. Soehnlein *et al.*, Neutrophil secretion products pave the way for inflammatory monocytes. *Blood* **112**, 1461–1471 (2008).

619. O. Soehnlein, E. Kenne, P. Rotzius, E. E. Eriksson, L. Lindbom, Neutrophil secretion products regulate anti-bacterial activity in monocytes and macrophages. *Clin. Exp. Immunol.* **151**, 139–145 (2008).

620. J. J. Osterholzer *et al.*, Chemokine receptor 2-mediated accumulation of fungicidal exudate macrophages in mice that clear cryptococcal lung infection. *Am. J. Pathol.* **178**, 198–211 (2011).

621. V. Espinosa *et al.*, Inflammatory monocytes orchestrate innate antifungal immunity in the lung. *PLoS Pathog* **10**, e1003940 (2014).

622. L. Boring *et al.*, Impaired monocyte migration and reduced type 1 (Th1) cytokine responses in C-C chemokine receptor 2 knockout mice. *J Clin Invest* **100**, 2552–2561 (1997).

623. A. Laroque *et al.*, Genetic control of susceptibility to infection with Plasmodium chabaudi chabaudi AS in inbred mouse strains. *Genes Immun* **13**, 155–163 (2012).

624. E. P. Blankenhorn *et al.*, Genetic loci that regulate healing and regeneration in LG/J and

SM/J mice. *Mamm Genome* **20**, 720–733 (2009).

625. T. Tamura, H. Yanai, D. Savitsky, T. Taniguchi, The IRF family transcription factors in immunity and oncogenesis. *Annu. Rev. Immunol.* **26**, 535–584 (2008).

626. Q. Xu, J. C. Reed, Bax inhibitor-1, a mammalian apoptosis suppressor identified by functional screening in yeast. *Mol Cell* **1**, 337–346 (1998).

627. G.-H. Lee *et al.*, Bax inhibitor-1 regulates endoplasmic reticulum stress-associated reactive oxygen species and heme oxygenase-1 expression. *J Biol Chem* **282**, 21618–21628 (2007).

628. H.-R. Kim *et al.*, Bax inhibitor 1 regulates ER-stress-induced ROS accumulation through the regulation of cytochrome P450 2E1. *J. Cell. Sci.* **122**, 1126–1133 (2009).

629. H.-J. Chae *et al.*, BI-1 regulates an apoptosis pathway linked to endoplasmic reticulum stress. *Mol Cell* **15**, 355–366 (2004).

630. B. Dibbert *et al.*, Cytokine-mediated Bax deficiency and consequent delayed neutrophil apoptosis: a general mechanism to accumulate effector cells in inflammation. *Proc Natl Acad Sci USA* **96**, 13330–13335 (1999).

631. K. Lauber *et al.*, Apoptotic cells induce migration of phagocytes via caspase-3-mediated release of a lipid attraction signal. *Cell* **113**, 717–730 (2003).

632. G.-H. Lee *et al.*, Bax inhibitor 1 increases cell adhesion through actin polymerization: involvement of calcium and actin binding. *Mol Cell Biol* **30**, 1800–1813 (2010).

633. W. Weninger, M. Biro, R. Jain, Leukocyte migration in the interstitial space of non-lymphoid organs. *Nat. Rev. Immunol.* (2014), doi:10.1038/nri3641.

634. V. M. Holers *et al.*, Molecular cloning of a murine fibronectin receptor and its expression during inflammation. Expression of VLA-5 is increased in activated peritoneal macrophages in a manner discordant from major histocompatibility complex class II. *J Exp Med* **169**, 1589–1605 (1989).

635. S. Johansson, G. Svineng, K. Wennerberg, A. Armulik, L. Lohikangas, Fibronectin-integrin interactions. *Front Biosci* **2**, d126–46 (1997).

636. J. A. Burns, T. B. Issekutz, H. Yagita, A. C. Issekutz, The alpha 4 beta 1 (very late antigen (VLA)-4, CD49d/CD29) and alpha 5 beta 1 (VLA-5, CD49e/CD29) integrins mediate beta 2 (CD11/CD18) integrin-independent neutrophil recruitment to endotoxin-induced lung inflammation. *J Immunol* **166**, 4644–4649 (2001).

637. A. L. F. Sampaio *et al.*, Inflammation-dependent alpha 5 beta 1 (very late antigen-5) expression on leukocytes reveals a functional role for this integrin in acute peritonitis. *Journal of Leukocyte Biology* **87**, 877–884 (2010).

638. L. M. Lavigne *et al.*, Integrin engagement mediates the human polymorphonuclear leukocyte response to a fungal pathogen-associated molecular pattern. *J Immunol* **178**, 7276–7282 (2007).

639. C. Berlin *et al.*, Alpha 4 beta 7 integrin mediates lymphocyte binding to the mucosal vascular addressin MAdCAM-1. *Cell* **74**, 185–195 (1993).

640. K. L. Cepek *et al.*, Adhesion between epithelial cells and T lymphocytes mediated by E-

cadherin and the alpha E beta 7 integrin. *Nature* **372**, 190–193 (1994).

641. R. D. Wagner, A. Vazquez-Torres, J. Jones-Carson, T. Warner, E. Balish, B cell knockout mice are resistant to mucosal and systemic candidiasis of endogenous origin but susceptible to experimental systemic candidiasis. *J. Infect. Dis.* **174**, 589–597 (1996).

642. S. Tiisala, T. Paavonen, R. Renkonen, Alpha E beta 7 and alpha 4 beta 7 integrins associated with intraepithelial and mucosal homing, are expressed on macrophages. *Eur. J. Immunol.* **25**, 411–417 (1995).

643. G. Bungartz *et al.*, Adult murine hematopoiesis can proceed without beta1 and beta7 integrins. *Blood* **108**, 1857–1864 (2006).

644. D. A. Calderwood *et al.*, Increased filamin binding to beta-integrin cytoplasmic domains inhibits cell migration. *Nat. Cell Biol.* **3**, 1060–1068 (2001).

645. H. H. Garcia, A. E. Gonzalez, C. A. W. Evans, R. H. Gilman, Cysticercosis Working Group in Peru, Taenia solium cysticercosis. *Lancet* **362**, 547–556 (2003).

646. E. Sciutto *et al.*, Taenia solium disease in humans and pigs: an ancient parasitosis disease rooted in developing countries and emerging as a major health problem of global dimensions. *Microbes Infect* **2**, 1875–1890 (2000).

647. A. Fleury *et al.*, An epidemiological study of familial neurocysticercosis in an endemic Mexican community. *Trans. R. Soc. Trop. Med. Hyg.* **100**, 551–558 (2006).

648. O. H. Del Brutto, G. Granados, O. Talamas, J. Sotelo, C. Gorodezky, Genetic pattern of the HLA system: HLA A, B, C, DR, and DQ antigens in Mexican patients with parenchymal brain cysticercosis. *Hum. Biol.* **63**, 85–93 (1991).

649. M. Huerta *et al.*, Vaccination against Taenia solium cysticercosis in underfed rustic pigs of México: roles of age, genetic background and antibody response. *Vet. Parasitol.* **90**, 209–219 (2000).

650. K. Heldwein *et al.*, Subcutaneous Taenia crassiceps infection in a patient with non-Hodgkin's lymphoma. *Am. J. Trop. Med. Hyg.* **75**, 108–111 (2006).

651. R. Freeman, Studies on the biology of Taenia crassiceps (Zeder, 1800) Rudolphi, 1810 (Cestoda). *Canadian Journal of Zoology* **40**, 969–990 (1962).

652. F. J. Dorais, G. W. Esch, Growth rate of two Taenia crassiceps strains. *Exp. Parasitol.* **25**, 395–398 (1969).

653. K. Willms, R. Zurabian, Taenia crassiceps: in vivo and in vitro models. *Parasitology* **137**, 335–346 (2010).

654. E. Sciutto *et al.*, Cysticercosis vaccine: cross protecting immunity with T. solium antigens against experimental murine T. crassiceps cysticercosis. *Parasite Immunol.* **12**, 687–696 (1990).

655. E. Sciutto *et al.*, Murine Taenia crassiceps cysticercosis: H-2 complex and sex influence on susceptibility. *Parasitol. Res.* **77**, 243–246 (1991).

656. G. Fragoso *et al.*, Increased resistance to Taenia crassiceps murine cysticercosis in Qa-2 transgenic mice. *Infection and Immunity* **66**, 760–764 (1998).

657. G. Meneses *et al.*, Taenia crassiceps cysticercosis: variations in its parasite growth permissiveness that encounter with local immune features in BALB/c substrains. *Exp. Parasitol.* **123**, 362–368 (2009).

658. J. L. Reyes, C. A. Terrazas, L. Vera-Arias, L. I. Terrazas, Differential response of antigen presenting cells from susceptible and resistant strains of mice to Taenia crassiceps infection. *Infect. Genet. Evol.* **9**, 1115–1127 (2009).

659. G. Fragoso *et al.*, Genetic control of susceptibility to Taenia crassiceps cysticercosis. *Parasitology* **112 (Pt 1)**, 119–124 (1996).

660. G. Fragoso, G. Meneses, E. Sciutto, A. Fleury, C. Larralde, Preferential growth of Taenia crassiceps cysticerci in female mice holds across several laboratory mice strains and parasite lines. *J. Parasitol.* **94**, 551–553 (2008).

661. J. A. Vargas-Villavicencio, C. Larralde, M. A. De León-Nava, G. Escobedo, J. Morales-Montor, Tamoxifen treatment induces protection in murine cysticercosis. *J. Parasitol.* **93**, 1512–1517 (2007).

662. E. G. Ibarra-Coronado *et al.*, A helminth cestode parasite express an estrogen-binding protein resembling a classic nuclear estrogen receptor. *Steroids* **76**, 1149–1159 (2011).

663. E. Sciutto *et al.*, Depressed T-cell proliferation associated with susceptibility to experimental Taenia crassiceps infection. *Infection and Immunity* **63**, 2277–2281 (1995).

664. G. Min-Oo *et al.*, Complex genetic control of susceptibility to malaria: positional cloning of the Char9 locus. *J Exp Med* **204**, 511–524 (2007).

665. A. Fortin *et al.*, The AcB/BcA recombinant congenic strains of mice: strategies for phenotype dissection, mapping and cloning of quantitative trait genes. *Novartis Found. Symp.* **281**, 141–53; discussion 153–5, 208–9 (2007).

666. M. F. Roy, N. Riendeau, J. C. Loredo-Osti, D. Malo, Complexity in the host response to Salmonella Typhimurium infection in AcB and BcA recombinant congenic strains. *Genes Immun* **7**, 655–666 (2006).

667. A. E. Siebert, A. H. Good, J. E. Simmons, Ultrastructural aspects of early immune damage to Taenia crassiceps metacestodes. *Int. J. Parasitol.* **8**, 45–53 (1978).

668. S. W. Davis, B. Hammerberg, Activation of the alternative pathway of complement by larval Taenia taeniaeformis in resistant and susceptible strains of mice. *Int. J. Parasitol.* **18**, 591–597 (1988).

669. T. Letonja, B. Hammerberg, Third component of complement, immunoglobulin deposition, and leucocyte attachment related to surface sulfate on larval Taenia taeniaeformis. *J. Parasitol.* **69**, 637–644 (1983).

670. A. M. Ferreira, M. Breijo, R. B. Sim, A. Nieto, Contribution of C5-mediated mechanisms to host defence against Echinococcus granulosus hydatid infection. *Parasite Immunol.* **22**, 445–453 (2000).

671. L. I. Terrazas, R. Bojalil, T. Govezensky, C. Larralde, Shift from an early protective Th1-type immune response to a late permissive Th2-type response in murine cysticercosis (Taenia crassiceps). *J. Parasitol.* **84**, 74–81 (1998).

672. L. I. Terrazas *et al.*, Th1-type cytokines improve resistance to murine cysticercosis caused by Taenia crassiceps. *Parasitol. Res.* **85**, 135–141 (1999).

673. S. A. Toenjes, R. E. Kuhn, The initial immune response during experimental cysticercosis is of the mixed Th1/Th2 type. *Parasitol. Res.* **89**, 407–413 (2003).

674. A. Chavarria *et al.*, TH2 profile in asymptomatic Taenia solium human neurocysticercosis. *Microbes Infect* **5**, 1109–1115 (2003).

675. B. I. Restrepo *et al.*, Brain granulomas in neurocysticercosis patients are associated with a Th1 and Th2 profile. *Infection and Immunity* **69**, 4554–4560 (2001).

676. J. P. Laclette *et al.*, Paramyosin inhibits complement C1. *J Immunol* **148**, 124–128 (1992).

677. M. Rodriguez-Sosa, J. R. David, R. Bojalil, A. R. Satoskar, L. I. Terrazas, Cutting edge: susceptibility to the larval stage of the helminth parasite Taenia crassiceps is mediated by Th2 response induced via STAT6 signaling. *J Immunol* **168**, 3135–3139 (2002).

678. M. Rodriguez-Sosa *et al.*, A STAT4-dependent Th1 response is required for resistance to the helminth parasite Taenia crassiceps. *Infection and Immunity* **72**, 4552–4560 (2004).

679. J. Alonso-Trujillo, I. Rivera-Montoya, M. Rodriguez-Sosa, L. I. Terrazas, Nitric oxide contributes to host resistance against experimental Taenia crassiceps cysticercosis. *Parasitol. Res.* **100**, 1341–1350 (2007).

680. D. C. Savage, R. J. Dubos, Localization of indigenous yeast in the murine stomach. *J. Bacteriol.* **94**, 1811–1816 (1967).

681. A. J. Scupham *et al.*, Abundant and diverse fungal microbiota in the murine intestine. *Appl. Environ. Microbiol.* **72**, 793–801 (2006).

682. I. D. Iliev *et al.*, Interactions between commensal fungi and the C-type lectin receptor Dectin-1 influence colitis. *Science* **336**, 1314–1317 (2012).

683. H. J. Lo *et al.*, Nonfilamentous C. albicans mutants are avirulent. *Cell* **90**, 939–949 (1997).

684. C. A. Gale *et al.*, Linkage of adhesion, filamentous growth, and virulence in Candida albicans to a single gene, INT1. *Science* **279**, 1355–1358 (1998).

685. M. Arendrup, T. Horn, N. Frimodt-Møller, In vivo pathogenicity of eight medically relevant Candida species in an animal model. *Infection* **30**, 286–291 (2002).

686. T. Gumbo, C. M. Isada, G. Hall, M. T. Karafa, S. M. Gordon, Candida glabrata Fungemia. Clinical features of 139 patients. *Medicine (Baltimore)* **78**, 220–227 (1999).

687. J. R. Wingard *et al.*, Increase in Candida krusei infection among patients with bone marrow transplantation and neutropenia treated prophylactically with fluconazole. *N. Engl. J. Med.* **325**, 1274–1277 (1991).

688. J. Mestas, C. C. W. Hughes, Of mice and not men: differences between mouse and human immunology. *J Immunol* **172**, 2731–2738 (2004).

689. D. C. Doeing, J. L. Borowicz, E. T. Crockett, Gender dimorphism in differential peripheral blood leukocyte counts in mice using cardiac, tail, foot, and saphenous vein puncture methods. *BMC Clin Pathol* **3**, 3 (2003).

690. P. B. Eisenhauer, R. I. Lehrer, Mouse neutrophils lack defensins. *Infection and Immunity* **60**, 3446–3447 (1992).

691. S. N. Patel *et al.*, C5 deficiency and C5a or C5aR blockade protects against cerebral malaria. *Journal of Experimental Medicine* **205**, 1133–1143 (2008).

692. Y. Okada *et al.*, Common variations in PSMD3-CSF3 and PLCB4 are associated with neutrophil count. *Hum Mol Genet* **19**, 2079–2085 (2010).

693. M. A. Nalls *et al.*, Multiple loci are associated with white blood cell phenotypes. *PLoS Genet* **7**, e1002113 (2011).

694. A. P. Reiner *et al.*, Genome-wide association study of white blood cell count in 16,388 African Americans: the continental origins and genetic epidemiology network (COGENT). *PLoS Genet* **7**, e1002108 (2011).

695. M. F. Keller *et al.*, Trans-ethnic meta-analysis of white blood cell phenotypes. *Hum Mol Genet* **23**, 6944–6960 (2014).

696. J. M. van den Berg, S. Weyer, J. J. Weening, D. Roos, T. W. Kuijpers, Divergent effects of tumor necrosis factor alpha on apoptosis of human neutrophils. *Journal of Leukocyte Biology* **69**, 467–473 (2001).

697. A. Cross, R. J. Moots, S. W. Edwards, The dual effects of TNFalpha on neutrophil apoptosis are mediated via differential effects on expression of Mcl-1 and Bfl-1. *Blood* **111**, 878–884 (2008).

698. S. Fox, A. E. Leitch, R. Duffin, C. Haslett, A. G. Rossi, Neutrophil apoptosis: relevance to the innate immune response and inflammatory disease. *J Innate Immun* **2**, 216–227 (2010).

699. B. Geering, H. U. Simon, Peculiarities of cell death mechanisms in neutrophils. *Cell Death Differ.* **18**, 1457–1469 (2011).

700. A. Ortega-Gómez, M. Perretti, O. Soehnlein, Resolution of inflammation: an integrated view. *EMBO Mol Med* **5**, 661–674 (2013).

701. B. Geering, U. Gurzeler, E. Federzoni, T. Kaufmann, H.-U. Simon, A novel TNFR1-triggered apoptosis pathway mediated by class IA PI3Ks in neutrophils. *Blood* **117**, 5953–5962 (2011).

702. O. Soehnlein, L. Lindbom, Phagocyte partnership during the onset and resolution of inflammation. *Nat. Rev. Immunol.* **10**, 427–439 (2010).

703. I. Radovanovic *et al.*, Genetic Control of Susceptibility to Candida albicans in SM/J Mice. *The Journal of Immunology* **193**, 1290–1300 (2014).

704. F. K. Swirski *et al.*, Identification of splenic reservoir monocytes and their deployment to inflammatory sites. *Science* **325**, 612–616 (2009).

705. Z. A. Wood, L. B. Poole, P. A. Karplus, Peroxiredoxin evolution and the regulation of hydrogen peroxide signaling. *Science* **300**, 650–653 (2003).

706. J. P. Conway, M. Kinter, Dual role of peroxiredoxin I in macrophage-derived foam cells. *J Biol Chem* **281**, 27991–28001 (2006).

707. S. W. Kang *et al.*, Mammalian peroxiredoxin isoforms can reduce hydrogen peroxide generated in response to growth factors and tumor necrosis factor-alpha. *J Biol Chem* **273**, 6297–6302 (1998).

708. M. C. Sobotta *et al.*, Peroxiredoxin-2 and STAT3 form a redox relay for H2O2 signaling. *Nat. Chem. Biol.* (2014), doi:10.1038/nchembio.1695.

709. S. Salzano *et al.*, Linkage of inflammation and oxidative stress via release of glutathionylated peroxiredoxin-2, which acts as a danger signal. *Proc. Natl. Acad. Sci. U.S.A.* **111**, 12157–12162 (2014).

710. K. H. Grabstein *et al.*, Cloning of a T cell growth factor that interacts with the beta chain of the interleukin-2 receptor. *Science* **264**, 965–968 (1994).

711. M. A. Cooper *et al.*, In vivo evidence for a dependence on interleukin 15 for survival of natural killer cells. *Blood* **100**, 3633–3638 (2002).

712. C.-L. Tsou *et al.*, Critical roles for CCR2 and MCP-3 in monocyte mobilization from bone marrow and recruitment to inflammatory sites. *J Clin Invest* **117**, 902–909 (2007).

713. T. Jia *et al.*, Additive roles for MCP-1 and MCP-3 in CCR2-mediated recruitment of inflammatory monocytes during Listeria monocytogenes infection. *J Immunol* **180**, 6846–6853 (2008).

714. Y. Qiu *et al.*, Early induction of CCL7 downstream of TLR9 signaling promotes the development of robust immunity to cryptococcal infection. *The Journal of Immunology* **188**, 3940–3948 (2012).

715. R. Ramirez-Aquino *et al.*, Identification of loci controlling restriction of parasite growth in experimental Taenia crassiceps cysticercosis. *PLoS Negl Trop Dis* **5**, e1435 (2011).

716. A. A. Freitas *et al.*, Kinetics of the inflammatory response in subcutaneous cysticercosis induced in mice by Taenia crassiceps. *J. Comp. Pathol.* **147**, 267–274 (2012).

717. A. E. Cardona, B. I. Restrepo, J. M. Jaramillo, J. M. Teale, Development of an animal model for neurocysticercosis: immune response in the central nervous system is characterized by a predominance of gamma delta T cells. *J Immunol* **162**, 995–1002 (1999).

718. Y.-H. Chien, C. Meyer, M. Bonneville, γδ T cells: first line of defense and beyond. *Annu. Rev. Immunol.* **32**, 121–155 (2014).

719. A. E. Cardona, J. M. Teale, Gamma/delta T cell-deficient mice exhibit reduced disease severity and decreased inflammatory response in the brain in murine neurocysticercosis. *J Immunol* **169**, 3163–3171 (2002).

720. M. Hashimoto *et al.*, Complement drives Th17 cell differentiation and triggers autoimmune arthritis. *Journal of Experimental Medicine* **207**, 1135–1143 (2010).

721. J. Liu *et al.*, IFN-gamma and IL-17 production in experimental autoimmune encephalomyelitis depends on local APC-T cell complement production. *J Immunol* **180**, 5882–5889 (2008).

722. M. G. Strainic *et al.*, Locally produced complement fragments C5a and C3a provide both costimulatory and survival signals to naive CD4+ T cells. *Immunity* **28**, 425–435 (2008).

723. M. G. Strainic, E. M. Shevach, F. An, F. Lin, M. E. Medof, Absence of signaling into $CD4^+$ cells via C3aR and C5aR enables autoinductive TGF-β1 signaling and induction of $Foxp3^+$ regulatory T cells. *Nat Immunol* **14**, 162–171 (2013).

Appendix

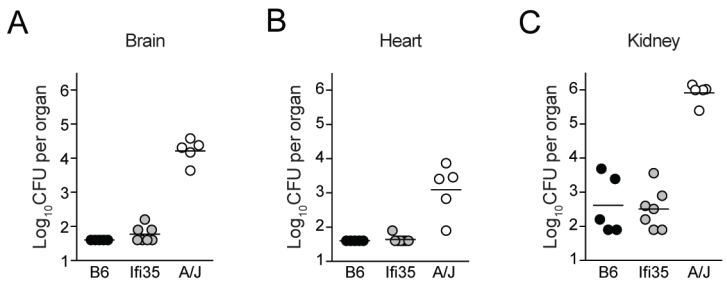

Figure A1. Phenotypic response of Ifi35 mutants upon *C. albicans* infection.

Ifi35 mutant mice, along with B6 and A/J controls, were infected intravenously with $5x10^4$ *C. albicans* blastospores and sacrificed 48h post-infection. Fungal burden was assessed in the brain (A), heart (B), and kidney (C).

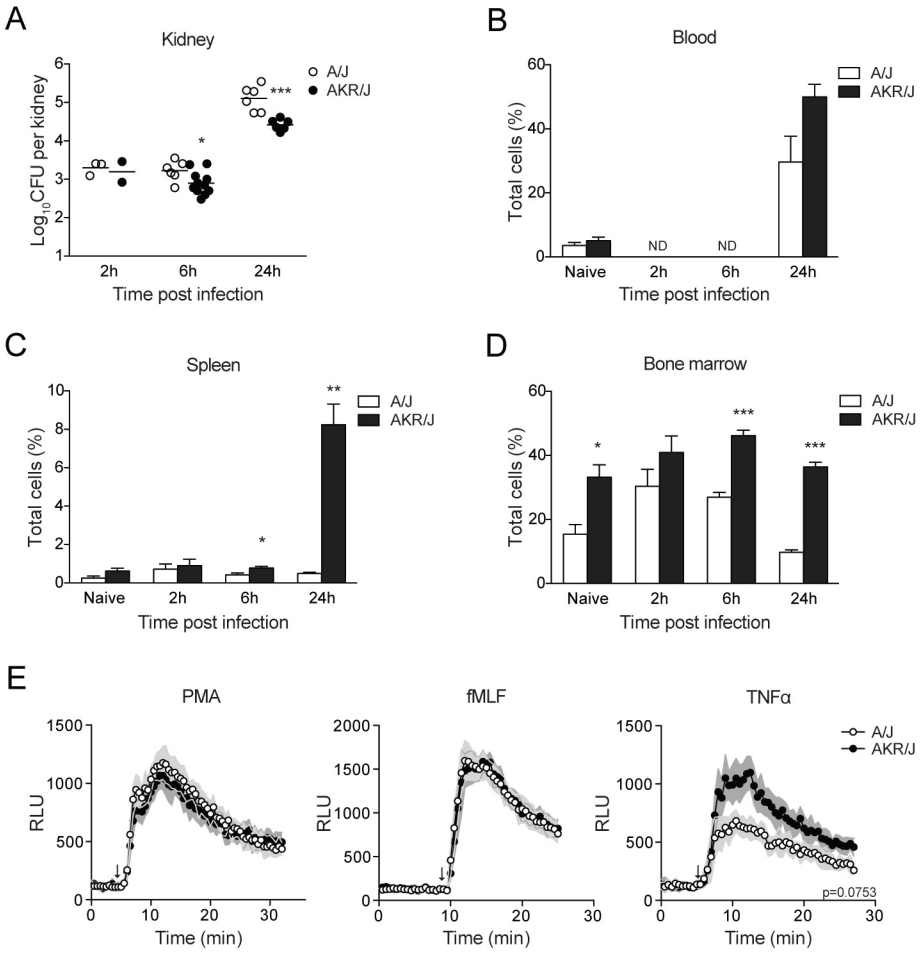

Figure A2. Examination of granulopoiesis during invasive candidiasis and neutrophil function in A/J and AKR/J mice.

A/J and AKR/J mice were infected intravenously with $5x10^4$ *C. albicans* yeasts and sacrificed at 2h, 6h, or 24h, along with naïve controls. Fungal burden was assessed in the kidney (A), whereas neutrophil proportions were determined by flow cytometry in the blood (B), spleen (C), and bone marrow (D). The capacity of bone marrow neutrophils to generate ROS (E) was probed with 200nM PMA, 3μM fMLF, or 20ng/ml TNFα. The arrows indicate the injection of the stimulus. ND, Not done.

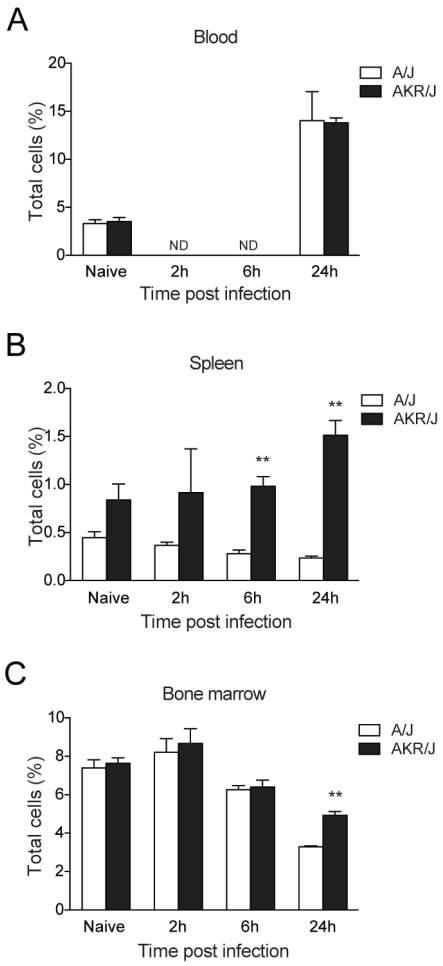

Figure A3. Examination of inflammatory monocyte recruitment during invasive candidiasis in A/J and AKR/J mice.

A/J and AKR/J mice were infected intravenously with $5x10^4$ *C. albicans* yeasts and sacrificed at 2h, 6h, or 24h, along with naïve controls. Inflammatory monocyte proportions were determined by flow cytometry in the blood (A), spleen (B), and bone marrow (C). ND, Not done.

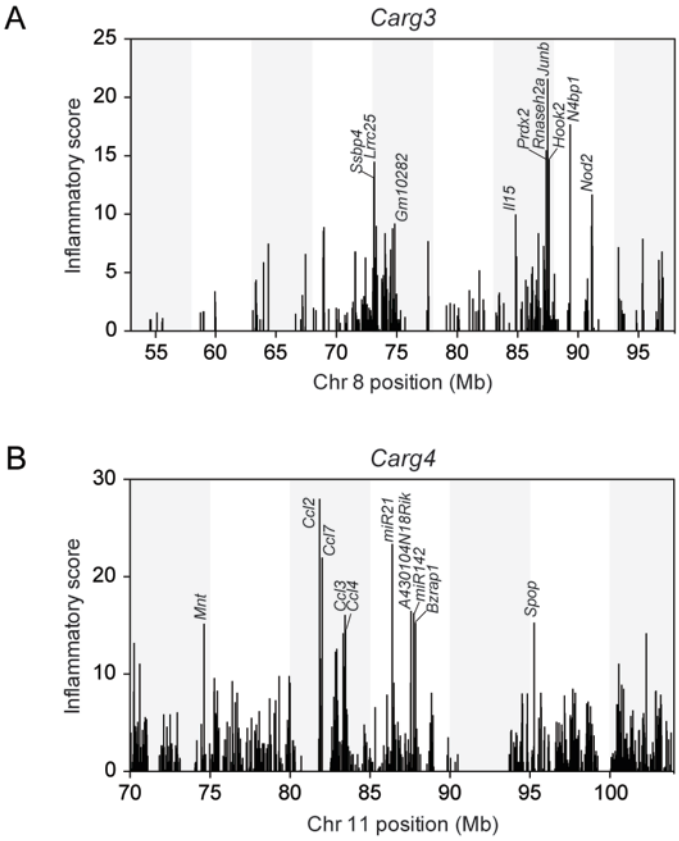

Figure A4. Computation of the myeloid inflammatory score for genes under *Carg3* and *Carg4*.

The minimal *Carg3* (A) and *Carg4* (B) genetic intervals were revisited and the myeloid inflammatory score calculated for 516 and 1118 genes, respectively, based on the the formula described in Chapter 3. The 10 highest scoring genes are identified for each locus.

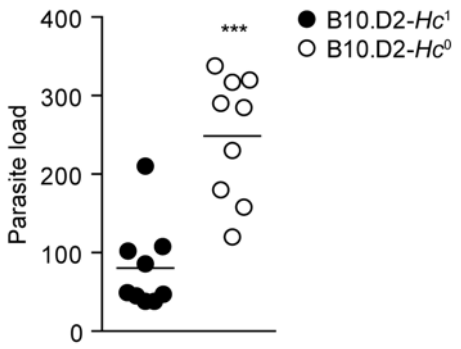

Figure A5. Effect of C5 on parasite burden in B10.D2 congenic mice.

C5-sufficient and C5-deficient B10.D2 congenic mice (n=9) were infected intraperitoneally with 10 non-budding *T. crassiceps* larvae and parasite number was determined 30 days post-infection. C5 plays a highly significant role in restriction of parasite replication ($p<0.0001$).